Department of Bioproducts and Biosystems

Characterisation of lignocellulose components by analytical pyrolysis gas chromatography mass spectrometry

Taina Ohra-aho

Aalto University

DOCTORAL DISSERTATIONS

Aalto University publication series
DOCTORAL DISSERTATIONS 230/2017
VTT SCIENCE 168

Characterisation of lignocellulose components by analytical pyrolysis gas chromatography mass spectrometry

Taina Ohra-aho

A doctoral dissertation completed for the degree of Doctor of Science (Technology) to be defended, with the permission of the Aalto University School of Chemical Engineering, at a public examination held at the lecture hall Ke2 of the school on 20th of December 2017 at 12.

Aalto University
School of Chemical Engineering
Department of Bioproducts and Biosystems

Supervising professor
Professor Tapani Vuorinen, Aalto University, Finland

Thesis advisors
Doctor Tarja Tamminen, VTT Technical Research Centre of Finland Ltd, Finland

Preliminary examiners
Associate Professor Dmitry Evtyugin, University of Aveiro, Portugal
Associate Professor Elisabeth Sjöholm, KTH, Sweden

Opponent
Professor Jalel Labidi, University of the Basque Country, Spain

Aalto University publication series
DOCTORAL DISSERTATIONS 230/2017

VTT SCIENCE 168

ISBN 978-952-60-7733-8 (printed)
ISBN 978-952-60-7734-5 (pdf)
ISSN-L 1799-4934
ISSN 1799-4934 (printed)
ISSN 1799-4942 (pdf)
http://urn.fi/URN:ISBN:978-952-60-7734-5

ISBN 978-951-38-8595-3 (printed)
ISBN 978-951-38-8594-6 (pdf)
ISSN-L 2242-119X
ISSN 2242-119X (printed)
ISSN 2242-1203 (pdf)
http://urn.fi/URN:ISBN:978-951-38-8594-6

Unigrafia Oy
Helsinki 2017

Finland

441 697
Printed matter

Aalto University

Abstract

Aalto University, P.O. Box 11000, FI-00076 Aalto www.aalto.fi

Author
Taina Ohra-aho

Name of the doctoral dissertation
Characterisation of lignocellulose components by analytical pyrolysis gas chromatography mass spectrometry

Publisher School of Chemical Engineering

Unit Department of Bioproducts and Biosystems

Series Aalto University publication series DOCTORAL DISSERTATIONS 230/2017

Field of research Bioproduct technology

Manuscript submitted 23 August 2017 **Date of the defence** 20 December 2017

Permission to publish granted (date) 1 November 2017 **Language** English

☐ **Monograph** ☒ **Article dissertation** ☐ **Essay dissertation**

Abstract

Analytical pyrolysis combined with gas chromatography mass spectrometry (Py-GC/MS) is a technique that can be used for the analysis of lignocellulose materials in situ. Pyrolysis degradation products provide information concerning the nature and origin of the initial sample. The main aim of this thesis was to apply analytical pyrolysis for lignin and carbohydrate characterisation from various lignocellulosic plant materials. Isothermal pyrolysis was the main technique utilised. In addition, thermochemolysis, thermal desorption and fractionated pyrolysis were applied in order to provide better understanding of the changes observed in lignin structure and carbohydrate composition in various materials and processes. In pyrolysis, hardwood lignin is degraded to guaiacyl and syringyl type pyrolysis degradation products with similar side chain structures, whereas carbohydrates form stable anhydrosugars. Lignin degradation products can be used to define the lignin composition and S/G ratio of the wood feedstocks. However, Py-GC/MS cannot be recommended for the comparison of carbohydrate composition between different wood species. Information on lignin structure and quantity was obtained directly from pulps by Py-GC/MS. Decrease of oxygenated lignin pyrolysis products and increase of short side chain structures were associated with beta-ether bond cleavage. Decrease of the short side chain structures as a function of delignification was interpreted to indicate leaching of the lignin products formed in cooking, and thus enrichment of native lignin in the residual pulp lignin.

Due to the more complex chemical structure of brewers spent grain than of wood, its lignin composition was characterised by Py-GC/MS and thermochemolysis. Thermochemolysis results demonstrated that Py-GC/MS leads to underestimation of native type syringyl structures and S/G ratios. In addition, thermochemolysis with TMAAc and TMAH reagents was applied as a means to differentiate between free fatty acids and esters, respectively. The results showed that thermochemolysis with alkaline TMAH can be used to determine total fatty acid contents from the aliphatic and aromatic esters. TMAAc can be used to distinguish between free acids and aliphatic esters, but not between aromatic esters and free acids.

In addition a thermal desorption method was developed to provide information on the odorous volatile organic compounds released from lignin. The method is applicable to the comparison of different lignin samples below their thermal degradation temperatures.

Keywords Py-GC/MS, analysis, lignocellulose, lignin, carbohydrates

ISBN (printed) 978-952-60-7733-8 **ISBN (pdf)** 978-952-60-7734-5

ISSN-L 1799-4934 **ISSN (printed)** 1799-4934 **ISSN (pdf)** 1799-4942

Location of publisher Helsinki **Location of printing** Helsinki **Year** 2017

Pages 154 **urn** http://urn.fi/URN:ISBN:978-952-60-7734-5

Tekijä
Taina Ohra-aho

Väitöskirjan nimi
Lignoselluloosan komponenttien luonnehtiminen analyyttisellä pyrolyysi-kaasukromatografia-massaspektrometrialla

Julkaisija Kemian tekniikan korkeakoulu

Yksikkö Biotuotteiden ja biotekniikan laitos

Sarja Aalto University publication series DOCTORAL DISSERTATIONS 230/2017

Tutkimusala Biotuotetekniikka

Käsikirjoituksen pvm 23.08.2017 **Väitöspäivä** 20.12.2017

Julkaisuluvan myöntämispäivä 01.11.2017 **Kieli** Englanti

☐ **Monografia** ☒ **Artikkeliväitöskirja** ☐ **Esseeväitöskirja**

Tiivistelmä

Pyrolyysi-kaasukromatografia-massaspektrometrialla (Py-GC/MS) voidaan analysoida lignoselluloosamateriaaleja ilman tarvetta eristää niiden komponentteja. Pyrolyysituotteet antavat tietoa tutkittavan näytteen luonteesta ja alkuperästä. Tässä väitöskirjassa tutkittiin laajasti analyyttisen pyrolyysin soveltuvuutta ligniinin ja hiilihydraattien karakterisointiin erilaisista lignoselluloosamateriaaleista. Pääasiallisena menetelmänä käytettiin isotermistä pyrolyysiä. Sen lisäksi hyödynnettiin termokemolyysi-, termodesorptio- ja fraktiopyrolyysitekniikoita, jotta voitiin paremmin ymmärtää muutoksia ligniinin rakenteessa ja hiilihydraattien koostumuksessa eri materiaaleissa ja prosesseissa. Pyrolyysissä hiilihydraatit muodostavat stabiileja anhydrosokereita, kun taas lehtipuun ligniini hajoaa sivuketjurakenteeltaan analogisiksi guajasyyli- ja syringyylityyppisiksi yhdisteiksi. Näiden pyrolyysituotteiden avulla voidaan lignoselluloosaraaka-aineista määrittää ligniinin koostumus ja syringyyli-guajasyylisuhde (S/G). Työssä saatujen tulosten perusteella Py-GC/MS-tekniikkaa ei kuitenkaan voida suositella hiilihydraattikoostumuksen vertaamiseen eri puulajien välillä. Kemiallisten massojen Py-GC/MS antoi tietoa ligniinin pitoisuudesta ja rakenteesta ilman edeltävää ligniinin eristystä. Työssä havaittiin, että happea sisältävien ligniinin pyrolyysin hajoamistuotteiden väheneminen ja lyhyen sivuketjun omaavien rakenteiden lisääntyminen ovat yhteydessä keiton aikana tapahtuneeseen beta-eetterisidosten katkeamiseen. Vastaavasti lyhyen sivuketjun omaavien pyrolyysituotteiden väheneminen massaa valkaistaessa osoitti keittoprosessissa syntyneiden kemiallisten rakenteiden poistuvan ja natiivin kaltaisen ligniinin rikastuvan massan jäännösligniiniin.

Koska panimomäskillä on monimutkaisempi kemiallinen koostumus kuin puulla, sen ligniinin rakennetta luonnehdittiin sekä Py-GC/MS- että termokemolyysitekniikoilla. Termokemolyysin antamat tulokset osoittivat, että Py-GC/MS aliarvioi luonnollisten syringyylirakenteiden osuuden ja S/G-suhteen. Termokemolyysiä sovellettiin myös erottamaan vapaat rasvahapot niiden estereistä käyttämällä TMAAc- ja TMAH-reagensseja. Tulokset osoittivat, että alkalista TMAH-reagenssia voidaan käyttää kokonaisrasvahappopitoisuuden määrittämiseen sekä alifaattisista että aromaattisista estereistä. TMAAc-reagenssia voidaan puolestaan käyttää erottamaan vapaat hapot ja alifaattiset esterit, mutta ei aromaattisia estereitä ja vapaita happoja.

Lisäksi kehitettiin termodesorptioon perustuva menetelmä ligniinistä haihtuvien haisevien orgaanisten yhdisteiden määrittämiseksi. Menetelmä soveltuu erilaisten ligniininäytteiden vertailuun lämpötiloissa, jotka ovat alle niiden termisen hajoamislämpötilan.

Avainsanat Py-GC/MS, analyysi, lignoselluloosa, ligniini, hiilihydraatit

ISBN (painettu) 978-952-60-7733-8 **ISBN (pdf)** 978-952-60-7734-5

ISSN-L 1799-4934 **ISSN (painettu)** 1799-4934 **ISSN (pdf)** 1799-4942

Julkaisupaikka Helsinki **Painopaikka** Helsinki **Vuosi** 2017

Sivumäärä 154 **urn** http://urn.fi/URN:ISBN:978-952-60-7734-5

Acknowledgements

This thesis work is based on experimental work carried out at Oy Keskuslaboratorio, KCL and VTT Technical Research Centre of Finland during the years 2003-2017. Financial support from the Academy of Finland (projects “Effect of fibre wall chemistry on energy demand in wood defibration, Defibre” no 133276 and “Lignin Fiber” no 133091), Tekes- the Finnish Funding Agency for Innovation (project “VOC reduction of lignin-containing materials” in the ERA-IB program), KCL and VTT is gratefully acknowledged.

I express my deepest gratitude to my supervisor, Dr. Tarja Tamminen, for encouraging me to continue towards a doctoral degree, and for her constant support and valuable advice during these years. I want to thank Prof. Tapani Vuorinen for the supervision and guidance during doctoral studies. Assoc. Prof. Dmitry Evtyugin and Assoc. Prof. Elisabeth Sjöholm are acknowledged for their comments as the pre-examiners of this thesis.

Warm thanks are extended to my co-autors Prof. Maija Tenkanen, Dr. Anna Kalliola, Dr. Jarmo Ropponen, Prof. Jorge Colodette, Prof. Borges Gomes, Dr. Piritta Niemi, Dr. Anna-Marja Aura, Prof. Kaisa Poutanen, Prof. Marco Orlandi, Prof. Johanne Buchert, Dr. Greta Faccio and Dr. Anne Savolainen for their advice and pleasant collaboration.

I also thank the skilful technical staff at KCL and VTT. Special thanks go to Petteri Vihra and Eila Turunen for their help in sample pretreatments and in Py-GC/MS analyses. I am grateful to my colleagues at VTT for inspiring discussion on the research and other topics, and for creating a pleasant and relaxing working atmosphere.

Thanks to my parents and sister and my friends for their support. Finally, my warmest thanks to my family Timo, Leevi and Vilppu for their love and encouragement.

Espoo, November 13, 2017

Taina Ohra-aho

Contents

List of Abbreviations

AL	acidolysis
AoSOX1	*Aspergillus* oryzae sulfhydryl oxidase
AQ	antraquinone
BSG	brewer's spent grain
BSTFA	N,O-bis(trimethylsilyl)trifluoroacetamide
D	chlorine dioxide
2D NMR	two-dimensional nuclear magnetic resonance spectroscopy
ECF	elemental chlorine free
EMAL	enzymatic mild acidolysis
FA	ferulic acid
FID	flame ionization detector
FPD	flame photometric detector
FTIR	fourier transform infrared spectroscopy
G	guaiacyl
H	*p*-hydroxyphenyl
HexA	hexenuronic acid
HPLC	high performance liquid chromatography
INS	insoluble residue after hydrolysis
IR	infrared spectroscopy
MaL	*Melanocarpus albomyces* laccase
MWL	milled wood lignin
NIR	near-infrared spectrometry
NMR	nuclear magnetic resonance spectroscopy
O	oxygen

P-AEF	protease-alkali extracted fraction
p-CA	*para*-coumaric acid
PC	principal component
PCA	principal component analysis
^{31}P NMR	phosphorus nuclear magnetic resonance spectroscopy
PO	pressurized alkaline hydrogen peroxide
Py-GC/MS	pyrolysis coupled with gas chromatography mass spectrometry
Q	chelation
S	syringyl
SE	softwood Kraft lignin provided by Stora Enso
SEC	size-exclusion chromatography
TBAH	tetrabutylammonium hydroxide
TD	thermal desorption
TEAAc	tetraethylammonium acetate
TFPTAH	trimethyl-3-trifluoromethylphenylammonium hydroxide
TG	thermogravimetry
THM	thermally assisted hydrolysis and methylation
TIC	total ion current
TMAAc	tetramethyl ammonium acetate
TMAH	tetramethyl ammonium hydroxide
TMPAH	trimethylphenylamine hydroxide
TMSH	trimethylsulfonium hydroxide
UB	unbleached
UV	ultraviolet spectroscopy
VOC	volatile organic compound

List of Publications

This doctoral dissertation consists of a summary and of the following publications which are referred to in the text by their numerals

I Ohra-aho, T., Tenkanen, M., Tamminen, T. (2005). Direct analysis of lignin and lignin-like components from softwood kraft pulp by Py-GC/MS techniques. *Journal of Analytical and Applied Pyrolysis* 74, 123–128. DOI: 10.1016/j.jaap.2004.11.010

II Kalliola, A., Savolainen, A., Ohra-aho, T., Faccio, G., Tamminen, T. (2012). Reducing the content of VOCs of softwood kraft lignins for material applications. *BioResources* 7, 2871–2882.

III Ohra-aho, T., Ropponen, J., Tamminen, T. (2013). Thermochemolysis using TMAAc and TMAH reagents as means to differentiate between free acids and esters. *Journal of Analytical and Applied Pyrolysis* 103, 31–35. DOI: 10.1016/j.jaap.2012.09.015.

IV Ohra-aho, T., Gomes, F.J.B., Colodette, J.L., Tamminen, T. (2013). S/G ratio and lignin structure among Eucalyptus hybrids determined by Py-GC/MS and nitrobenzene oxidation. *Journal of Analytical and Applied Pyrolysis* 101, 166–171. DOI: 10.1016/j.jaap.2013.01.015.

V Ohra-aho, T., Niemi, P., Aura, A.-M., Orlandi, M., Poutanen, K., Buchert, J., Tamminen, T. (2016). Structure of brewer's spent grain lignin and its interactions with gut microbiota *in vitro*. *Journal of Agricultural and Food Chemistry* 64, 812–820. DOI: 10.1021/acs.jafc.5b05535.

VI Ohra-aho, T., Gomes, F.J.B., Colodette, J.L., Tamminen, T. Carbohydrate composition in Eucalyptus wood and pulps – comparison between Py-GC/MS and acid hydrolysis. Accepted for publication to *Journal of Analytical and Applied Pyrolysis*.

Author's Contribution

Publication I: The author planned the analysis work and interpreted the results together with Dr. Tarja Tamminen and Prof. Maija Tenkanen; the author supervised the Py-GC/MS measurements and performed the Py-GC/MS data handling. Prof. Maija Tenkanen was responsible for the cooking and bleaching experiments. The author wrote the publication together with the supervisor Dr. Tarja Tamminen.

Publication II: The author planned the TD-GC/MS measurements with Dr. Tarja Tamminen and Dr Anna Kalliola and supervised the TD-GC/MS measurements and evaluated its data. Dr. Anna Kalliola supervised oxidation experiments and wrote the publication. Dr. Anne Savolainen performed the laccase treatments and Dr. Greta Faccio the Sulfuryl oxidase treatments.

Publication III: The author designed the work plan together with Dr. Tarja Tamminen and Dr. Jarmo Ropponen, supervised the Py-GC/MS measurements and interpreted the Py-GC/MS data. Dr. Jarmo Ropponen synthetized the lignin model compounds and carried out the NMR measurements. The author had main responsibility for writing the publication.

Publication IV: The author designed the work plan together with Dr. Tarja Tamminen and Prof. Jorge Luiz Colodette. Prof. Fernando José Borges Gomes was responsible for the alkaline nitrobenzene oxidation measurements. The author supervised the Py-GC/MS measurements, evaluated the measurement data and had main responsibility for writing the publication.

Publication V: The author planned the Py-GC/MS measurements together with Dr. Piritta Niemi, Dr. Anna-Marja Aura and Dr. Tarja Tamminen. The author supervised the BSG and lignin Py-GC/MS measurements and carried out Py-GC/MS measurements after the *in vitro* Colona experiments. Dr. Piritta Niemi performed the lignin isolations under the supervision of Prof. Johanna Buchert for the enzymatic treatments and Prof. Marco Orlandi for the chemical treatments. Dr. Anna-Marja Aura carried out the *in vitro* colona fermentations and interpreted the results together with Prof. Kaisa Poutanen. The author interpreted the Py-GC/MS data and had main responsibility for writing the publication.

Publication VI: The author designed the work plan together with Dr. Tarja Tamminen and Prof. Jorge Luiz Colodette. The author supervised the isothermal pyrolysis measurements, carried out the fractionated pyrolysis measurements and interpreted the Py-GC/MS data. Prof. Fernando José Borges Gomes was responsible for the carbohydrate analyses carried out by HPLC after acid hydrolysis. The author had main responsibility for writing the publication.

1. Introduction

Chemical components of lignocellulosic biomasses are divided into macromolecular substances and low molecular weight compounds. Macromolecular cell wall components, lignin and polysaccharides i.e. cellulose and hemicelluloses, are present in all plant species. The chemical composition of lignin and hemicelluloses varies depending on the plant species, whereas cellulose is a uniform component in all. The amount and type of low molecular weight compounds, extractives and minerals also varies between different plant species.

As a linear, high molecular weight polymer, cellulose is built up exclusively of glucose. Hemicelluloses are variously composed of five neutral sugars: glucose, mannose, galactose, xylose and arabinose, which are in close association with cellulose in the cell wall. The molecular chains of hemicelluloses are much shorter and more branched due to side groups in comparison to cellulose. During development of the cells, lignin is the last component formed in the cell walls, interpenetrating the polysaccharide fibrils and thus strengthening the cell walls. The structure of lignin is different from that of polysaccharides. It is an amorphous substance, composed of aromatic phenylpropanes including *p*-hydroxypehnyl (H), guaiacyl (G) and syringyl (S) units with different numbers of methoxyl groups. Lignin units are linked together with carbon-oxygen and carbon-carbon bonds, but also with polysaccharides. Minor polymeric carbohydrates in lignocellulosic biomasses are starch and pectin, which are more abundant in annual plants than in wood species (Fengel and Wegener, 1989).

Analysis of biomass components is complex because the components are highly associated with each other. It is difficult to separate lignocellulosic components without degrading the polymers or changing the molecular properties. Analysis of lignocellulosic components can be carried out by determining only the main cell wall components together with extractives and ash. On the other hand, very detailed analyses including the determination of functional groups and individual polysaccharide and lignin units are also carried out. Composition analyses are made for the extractive-free samples. Thus the analyses are always started by removing extractives. For studying the detailed structures and polymer properties of the lignocellulosic constituents, their isolation is first necessary (Fengel and Wegener, 1989).

An approximate estimate of the total content of polysaccharides can be obtained by subjecting the sample to an oxidative delignification, after which the polysaccharide material (holocellulose) remains as a solid residue. However, a more reliable analysis is based on separate determination of the polysaccharide constituents using chromatographic methods (gas chromatography, high-performance anion-exchange chromatography or capillary electrophoresis). Before the analysis, cell wall polysaccharides are depolymerized to sugar units, which is most commonly effected by acid hydrolysis of glycoside bonds. Other advantageous depolymerisation techniques are acid methanolysis and enzymatic hydrolysis. Methanolysis is suitable for the neutral monosaccharides and acidic sugars, but cellulose is not depolymer-

ized totally due to its high crystallinity. Enzymatic hydrolysis can be performed to determine the uronic and hexenuronic acid contents of pulp samples (Sjöström and Alen 1999).

Lignin content can be determined using either direct or indirect methods. Most commonly, lignin is determined gravimetrically as Klason lignin after hydrolysis of polysaccharides with strong acid. However, part of the lignin is soluble in acid. This acid soluble lignin can be determined by UV spectroscopy from the hydrolysate and be included in Klason lignin in order to obtain a value for total lignin. Lignin content can also be determined without isolation from wood and pulp samples by Fourier transform infrared spectroscopy (FTIR) and near-infrared spectrometry (NIR). For these methods, a specific calibration model is needed in order to determine the lignin content. In the acetyl bromide method, lignin content can be determined by UV spectroscopy at 280 nm after solubilisation of lignin-containing samples in a mixture of acetyl bromide and glacial acetic acid. For spectroscopic methods, the adsorption coefficients of various types of lignins are needed. The content of methoxyl groups can be used to determine the lignin content indirectly. From the pulp samples, residual lignin can be measured by the kappa number, based on oxidant consumption. Kappa number can be converted to Klason lignin by using specific conversion factors (Fengel and Wegener, 1989).

Structural information of lignin *in situ* can be obtained for biomass samples using several spectroscopic techniques, UV, FTIR and nuclear magnetic resonance (NMR) and oxidative degradation methods. In the case of lignocellulosic materials, however, spectroscopic methods suffer from poor sensitivity and overlapping signals of lignin and polysaccharides. Oxidative degradation methods in alkaline media that preserve the aromatic ring include oxidation with potassium permanganate followed by hydrolysis and methylation, nitrobenzene oxidation, and oxidation with metal oxides such as cupric oxide (CuO). Degradation products can be used to determine the H, G and S unit ratios, but also the etherified and free phenolic hydroxyl group of lignin.

For more detailed structural analysis, lignin must first be isolated. This cannot be done without altering the structure of lignin. However, relatively unchanged lignin can be obtained from ball milled biomass by dioxane-water extraction (Björkman's procedure) or enzymatic hydrolysis. A third isolation method that has been used is mild enzymatic hydrolysis followed by an acid hydrolysis stage. Isolated lignin samples can be characterized with several techniques, including the previously mentioned oxidative degradation methods, but molar-mass distribution by size-exclusion chromatography (SEC) can also be carried out. More detailed information concerning lignin functional groups together with substructures can be determined with UV, IR and ^{13}C-NMR spectroscopy from isolated lignins without interfering polysaccharides. Free phenolic hydroxyl groups after phosphitylation can be determined by ^{31}P NMR and interunit linkages by 2D-NMR. The average composition of the C_9-units in lignin can be calculated based on the elemental composition and methoxyl group content.

The previously mentioned methods are widely used to determine the composition of lignocellulosic materials either separately or in combinations of several methods. Most of the direct methods are time consuming, and determination of lignin and carbohydrates must be performed separately. One potential method to determine the composition of lignocellulosic materials is analytical pyrolysis combined with gas chromatography mass spectrometry (Py-GC/MS). Py-GC/MS enables simultaneous determination of lignin and carbohydrates from fibre-based materials in a micro scale without the need for tedious isolation. Other advantages are that pretreatments such as extractives removal or refining are not always necessarily required prior to the analysis of lignocellulose materials. Due to extensive studies of

various lignocellulosic materials, the phenolic lignin pyrolysis products and degradation products of polysaccharides have been well identified and reported (Faix et al. 1990b; Faix et al. 1991a; Ralph and Hatfield 1991). Isothermal pyrolysis is widely used for materials comparison. However, there are various techniques, including thermochemolysis, thermal desorption, fractionated pyrolysis and sequential pyrolysis, which can be applied in conjunction with isothermal pyrolysis in order to better understand the lignocellulose structure of feedstocks and products.

1.1 Aims and approaches of the study

The main aim of this thesis was to study how analytical pyrolysis can be applied for the lignin and carbohydrate characterisation of various lignocellulosic plant materials and products. In a broader framework, the aim is to understand more deeply the changes observed in lignin structure and carbohydrate composition in various processes, and whether these changes can be detected not only by isothermal pyrolysis, but by applying several different Py-GC/MS techniques. More specifically, different Py-GC/MS techniques were applied:

- to evaluate differences between lignocellulosic feedstocks
- to monitor structural changes in lignin together with its quantity during pulp delignification and bleaching
- to determine volatile organic compounds released from treated Kraft lignins
- to differentiate aromatic and aliphatic ester bonds together with their corresponding free acids

2. Analytical pyrolysis

Analytical pyrolysis is a method in which chemical bonds between molecules are degraded in an inert atmosphere using thermal energy. The original large molecules are degraded to low molecular weight fragments, i.e. volatiles, that can be more easily analysed. The strength of the bonds between molecules influences the energy needed to break the bonds. The pyrolysis conditions (time, temperature and heating rate) and the nature of the sample material affect the type and distribution of the formed degradation products. Samples of the same material pyrolysed under identical conditions are degraded repeatedly in a similar manner to the same degradation products, whereas samples from other origins behave differently. The volatile degradation products retain the structural information of the initial sample. Thus analysis of the degradation products and the process used for the thermal degradation provides information about the nature and origin of the initial sample material (Ericsson, 1985; Wampler, 1995).

Analytical pyrolysis is designed for the analysis of solid and high molecular weight material. The samples may thus be insoluble, or they may include both synthetic and natural polymers as well as volatiles. The pyrolysis is a pretreatment method, and must be connected with an analytical instrument for the analysis of degradation products.

2.1 Instrumentation

There are several analytical pyrolysis instruments available. The three most commonly used pyrolysis instruments are isothermal furnace (micro furnace), inductively heated Curie-point and resistively heated filament (Sobeih et al., 2008). The way the sample is heated depends on the instrument type. In each of the techniques the aim is to heat the sample rapidly to the final temperature, thus avoiding secondary reactions of the products. The sample size must be kept low (recommended 10-100 μg) in order to reach the desired temperature quickly enough (Andersson and Ericsson, 1979; Wampler, 1995).

The furnace pyrolyser is kept isothermally at the desired pyrolysis temperature and the sample is injected into a hot interface. The degradation starts immediately when the sample meets the hot zone and the degradation products are led simultaneously into a gas chromatography. In this system the temperature is kept constant, but the heating rate of the sample is dependent on the sample material itself together with the composition of the sample introduction device. In Curie-point instruments, electric current is induced into the pyrolysis filament inductively with the aid of a high frequency coil. The filament is made from ferromagnetic metal or alloy. Pyrolysis temperature is dependent on the Curie-point of the ferromagnetic alloy or metal. Only one temperature can be used at a time. It is necessary to change a filament made from a different alloy if a different temperature is required. In a Curie-point pyrolyser the sample is placed into a cold interface, heated briefly and cooled again. That is

also the case in the resistively heated filaments, but the heating source is different from that in the Curie-point pyrolyser (Wampler, 1999, 1995). Resistively heated filament is heated using a high voltage, which produces a current through the filament made from resistive metal (platinum). The first high voltage pulse heats the filament until it reaches the desired temperature. The second low voltage pulse maintains the pyrolysis temperature for the selected time. The advantage of the resistively heated pyrolysers is that sample can be heated to a variety of temperatures without the need to change the filament for each temperature. Pyrolysis can be performed at any temperature over the filament's usable range (Andersson and Ericsson, 1979; Ericsson, 1985; Tydén-Ericsson, 1973).

For the analysis of degradation products, the pyrolyser is connected with an analysis device. Most commonly, the pyrolyser is directly connected to the gas chromatograph injection port. Column carrier gas passes through the pyrolysis instrument, leading degradation products to the injector and thereafter into the capillary column for separation. Separation of compounds is based on their polarity or boiling point differences. These factors are dependent on the selected stationary phase of the capillary column. Detection of degradation products is usually carried out by mass spectrometry, because this enables the identification of compounds based on the formed mass spectra. There are several commercial mass spectra libraries, which help in the identification of compounds (Wampler, 1995). Other types of detectors, such as a flame ionisation detector (FID), a flame photometric detector (FPD), which is selective for sulphur (Selsbo et al., 1997), and FTIR have been used. Compound identification without model compounds is not possible if FID is used as a detector. However, pyrolysis profiles i.e. fingerprints are distinct among polymers determined under the same conditions. Therefore is also possible to identify polymers based on their pyrolysis profiles. Gas chromatography separates only the volatile and semi-volatile degradation products. The high molecular weight fragments may leave and condense into the injector. Direct installation of the pyrolysis instrument into mass spectrometry or IR also enables analysis of the high molecular weight fragments (Wampler, 1995).

2.2 Sample preparation

Pyrolysis is a degradative pretreatment method for high molecular weight material. However, optimization of sample size, homogeneity, removal of contaminants and sample dosage are also important parts of the analyses. It is necessary to keep the sample size constant and rather low (10-100 μg), because pyrolysis instruments are designed to heat low sample amounts rapidly to high temperatures. Overload of sample changes the heating rate and causes contamination of both the pyrolysis unit and the analytical instrument. The homogeneity and sample size together with dosage can be controlled more easily for soluble than for insoluble material. The sample volume can be kept constant when sample solution is transferred with a syringe to the pyrolysis instrument. Solvent is evaporated before the sample is transferred to the pyrolysis unit. This enables better contact between the sample and the sample holder. In the case of insoluble samples, which most natural materials are, homogenization and sample size optimization are necessary. The smaller the particles are the better, and the higher surface area of sample is in contact with the sample holder (Wampler, 1995). Pretreatments such as milling, however, may change the nature of the sample and the results are no longer representative (Syverud et al., 2003). Samples may contain natural or external-

ly added inorganic species, which may change the decomposition behaviour of the polymer either by lowering the pyrolysis temperature or changing the product distribution (Müller-Hagedorn et al., 2003; Patwardhan et al., 2010). Inorganic species can be removed by extracting samples with acid or tap water (Kleen and Gellerstedt, 1995).

2.3 Pyrolysis techniques

Isothermal pyrolysis
The commonest way to analyse various sample materials is isothermal pyrolysis in which the temperature, time and heating rates are kept constant. The used instrument type defines the temperature and time needed for the efficient degradation of material. Isothermal pyrolysis is used for both qualitative and quantitative analyses of sample materials (Wampler, 1995). Depending on the instrument type, the pyrolysis unit can be utilized for thermal desorption, sequential pyrolysis, fractionated pyrolysis and thermochemolysis analyses.

Thermal desorption
The principle in thermal desorption (TD) is that volatile organic compounds (VOCs) are collected into an adsorbent. The adsorbent is heated in a gas flow, and the VOCs thus released pass directly into gas chromatography (Woolfenden, 2012). Thermal desorption temperatures are lower in comparison to those used in pyrolysis, because degradation of the sample material needs to be avoided. Thermal desorption can be used prior to pyrolysis in order to separate non-polymeric compounds from the polymeric material. In this case sample material is heated in a pyrolysis unit at constant temperature until all the volatile compounds have been released (Kleen et al., 2003). Volatiles are directly led by the carrier gas into the gas chromatography column for separation and detection. External adsorbent is not used.

Fractionated pyrolysis
Fractionated pyrolysis measurements can be performed directly after thermal desorption analysis. The principle of fractionated pyrolysis is that the same original sample is analysed at increasing temperatures for different times. The method makes it possible to study particular fractions of a sample. The pyrolysis time is sufficient when all the degradation products have been released at the adjusted temperature (Selsbo et al., 1997). In general, at lower temperatures longer times are needed to release all the compounds. Pyrolysis time is set using sequential pyrolysis, in which sample pyrolysis is performed under identical conditions (temperature and time) several times until all the degradation products have been released (Ericsson, 1978; Ericsson and Lattimer, 1995).

Thermochemolysis
After isothermal pyrolysis, thermochemolysis is the second most utilized technique in pyrolysis. In thermochemolysis, organic substance is degraded into smaller fragments by means of a chemical reagent and heat. Thermally assisted hydrolysis and methylation (THM) in the presence of tetramethyl ammonium hydroxide (TMAH) is one such reaction and it was established for a pyrolysis instrument by Challinor (1989). In this procedure, a mixture of sample material and reagent solution are subjected to heat in a pyrolysis unit. As a consequence, hydrolytic scission of ester and ether bonds takes place. This is followed by salt formation and finally the salts undergo pyrolysis to form corresponding methyl derivatives. The THM reac-

tion scheme suggested by Challinor (2001) is shown in Figure 1. As a strong base, TMAH cleaves ether and ester bonds, leading to methylation of etherified and esterified functional groups together with release of free alcohol and acid groups, as well as salts (Challinor, 1996; Drechsel et al., 2003; Hardell and Nilvebrant, 1999) Other similar types of reagents that have been used for the thermochemolysis are trimethylsulfonium hydroxide (TMSH), tetrabutylammonium hydroxide (TBAH), trimethylphenylamine hydroxide (TMPAH) and trimethyl-3-trifluoromethylphenylammonium hydroxide (TFPTAH) (Shadkami and Helleur, 2010).

Neutral derivatization reagents, e.g. tetramethylammonium acetate (TMAAc), tetraethylammonium acetate (TEAAc) and N,O-bis(trimethylsilyl)trifluoroacetamide (BSTFA), have been used to determine free acids and hydroxyl groups (Grasset et al., 2002; Hardell and Nilvebrant, 1999; Kuroda, 2000a). The use of neutral reagents with more basic reagents makes it possible to distinguish bound fatty acids from free acids. Instead of methylation, an ethylation reaction takes place with TEAAc. This phenomenon can be utilized when naturally existing methyl esters or ethers are differentiated from the free acids and alcohols.

1) Hydrolysis

$OH^- + \mathbf{A–B} \rightarrow A^- + B–OH$

2) Formation of TAA salt

$A^- + R_4N^+OH^- \rightarrow R_4N^+A^- + OH^-$

$B–OH + R_4N^+OH^- \rightarrow R_4N^+OB^- + H_2O$

3) Thermal dissociation to alkyl derivatives

$R_4N^+A^- \rightarrow AR + R_3N$

$R_4N^+OB^- \rightarrow BOR + R_3N$

A-B = hydrolysable analyte molecule

Figure 1. Reaction mechanisms in thermochemolysis (Challinor, 2001).

3. Thermal degradation of the main lignocellulose components

3.1 Lignin

Lignin is the most abundant aromatic substance in the living world, giving mechanical strength to plant species (S.Y. Lin and Dence 1992). Lignin originates from phenylpropanoid precursors such as *p*-coumaryl alcohol, coniferyl alcohol and sinapyl alcohol (Figure 2). The phenylpropanoid units are linked with ether (β-O-4, 4-O-5) or carbon-carbon bonds (β-β, β-1, 5-5, β-5) in the lignin network as shown in Figure 3 (Ralph et al., 2007). The structure of lignin and the ratios of different hydroxycinnamyl alcohols vary depending on the plant species, cell type and environmental factors, but also between different parts of the plant (Sarkanen and Hergert, 1971). Lignin in softwood is enriched with guaiacyl substructures, whereas hardwood lignin contains about equal amounts of guaiacyl and syringyl substructures. Both softwood and hardwood contain minor amounts of *p*-hydroxyphenyl substructures. Annual plants contain all three substructures, but significantly more *p*-hydroxyphenyl substructures than wood species. However, the main linkage between phenylpropanoid units in all plant species is β-O-4.

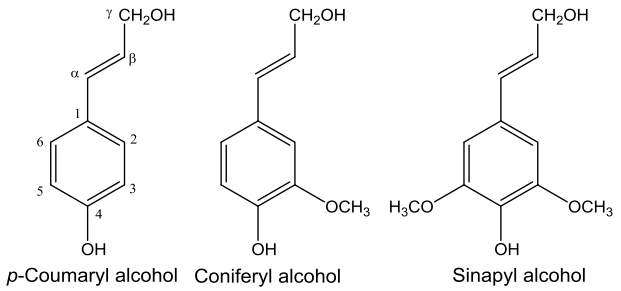

Figure 2. Primary lignin monomers, the monolignols *p*-coumaryl, coniferyl and sinapyl alcohol.

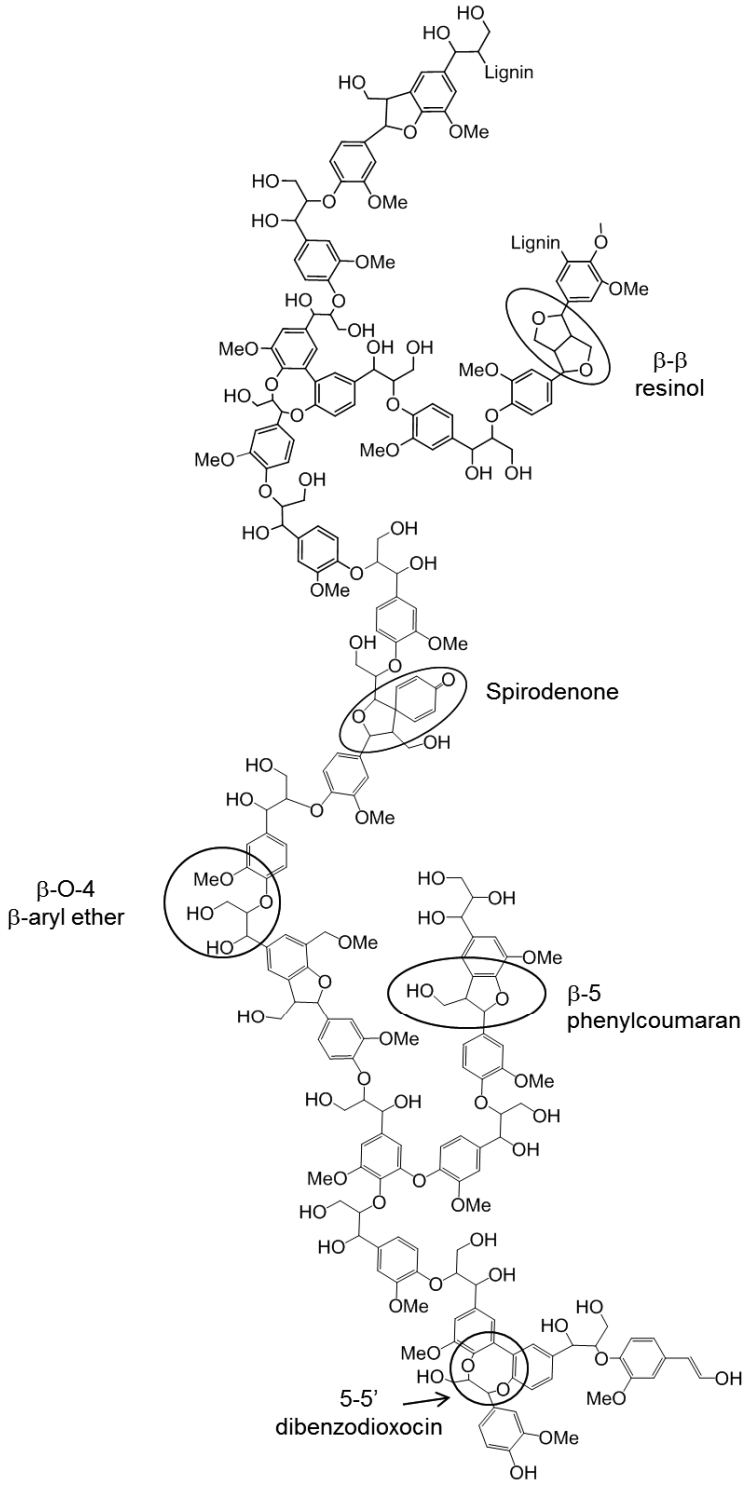

Figure 3. Schematic structure of softwood lignin and the common linkages of softwood (Ralph et al., 2007)

In pyrolysis, lignin is thermally degraded to a mixture of phenols including *p*-hydroxyphenyl, guaiacyl and syringyl type degradation products with side chains of from one to three carbon atoms. Side chains contain both saturated and unsaturated alkyl groups including oxygenated functionalities (C=O, C-OH), as shown in Table 1. These monomeric degradation products are formed mainly as a result of the cleavage of ether linkages. Based on extensive model compound studies, some of the condensed linkages, such as β-5 (Kuroda & Nakagawa-izumi 2006) and β-1 (Kuroda & Ashitani 2007; Jiang et al. 2016) are also known to be cleaved to monomers. Degradation of ether linkages both in free and non-phenolic form has been verified in several studies (Akazawa et al., 2016; Amen-Chen et al., 2001; Brezny et al., 1983; Faix et al., 1988; Kuroda, 2000b; Y. Liu et al., 2016; Zhang et al., 2016). It has been found that the free phenolic ether and β-aryl bonds are thermally less stable than non-phenolic bonds (Akazawa et al., 2016; Nakamura et al., 2008; Watanabe et al., 2009). In addition the absence of hydroxyl groups from the α and γ position of the propyl chain reduces the reactivity of β-O-4 bond cleavage to the same level as that of non-phenolic structures (Kawamoto et al., 2007). The release of hydroxyl group or cleavage of the α-ether linkage is the rate determining step for the cleavage of β-ether bonds (Kawamoto et al., 2008). The condensed structures present in lignin affect the yield of the monomeric pyrolysis products. (Böttcher, 1993; Gardner et al., 1985; Izumi et al., 1995a; Izumi and Kuroda, 1997; Kuroda et al., 1994). Syringyl substructures are less condensed than guaiacyl substructures. Thus syringyl units are overestimated in comparison to guaiacyl units in Py-GC/MS analysis. A correction equation has been developed that reduces the yield of syringyl units with relation to guaiacyl units and compensates for the effect of condensation (Böttcher, 1993).

Degradation mechanisms for β-ether bond cleavage

Even after extensive studies, the degradation mechanisms of lignin in pyrolysis are not yet fully understood. Molecular mechanisms of lignin degradation in pyrolysis and gasification were summarised in the recent review by Kawamoto (2017). In analytical pyrolysis the focus is on primary pyrolysis reactions, although the temperatures used in analytical pyrolysis are in most cases in the range in which secondary pyrolysis reactions may also occur (> 400 °C).

It has been proposed that both homolytic and heterolytic reactions take place, even though there is no actual evidence of pyrolytic cleavage mechanisms. However, both mechanisms lead to the same degradation products. The heterolytic reaction is possible only for free phenolic lignin structures. In the heterolytic reaction pathway, a para substituted phenolate anion is formed as a result of the cleavage of ether linkages. In the homolysis reaction pathways, *a* phenoxy radical is formed from the cleavage of ether bonds. Formation of stable radical improves the efficient cleavage of the ether linkages and reduces the bond dissociation energy of the aromatic O-C bond.

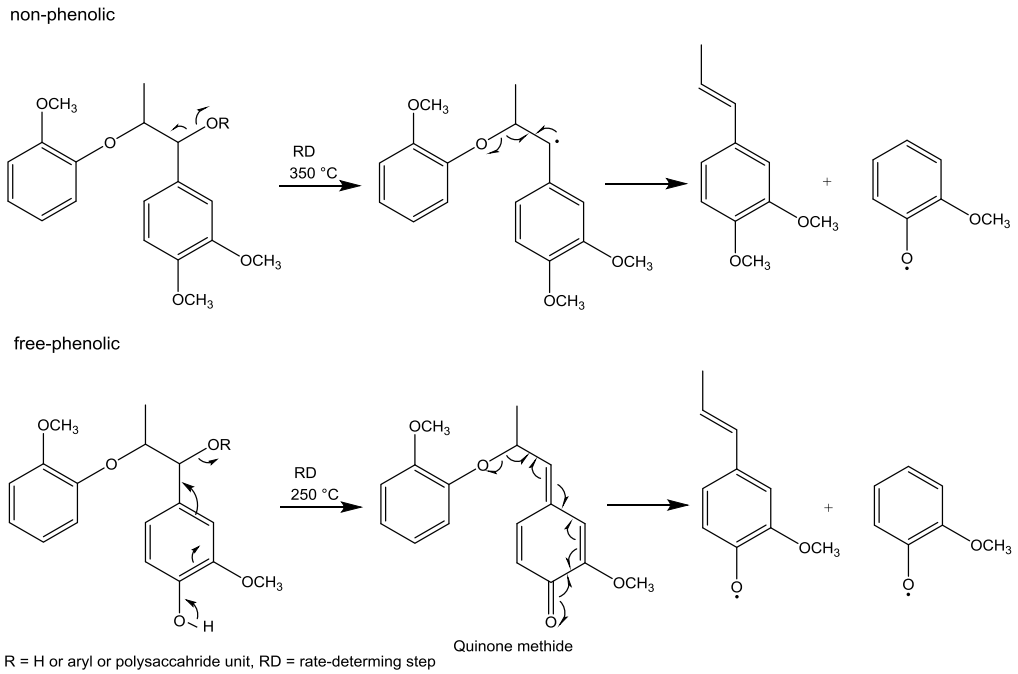

Figure 4. Supposed cleavage mechanisms of non-phenolic and free phenolic β-ether bonds of lignin. Figure modified from Kawamoto et al. (2008).

Homolytic and heterolytic reaction mechanisms have been widely studied by using model compounds with phenolic or non-phenolic end groups (Figure 4). The release of hydroxyl functional groups or degradation of ether-linked polysaccharides or lignin units from the α-position has been explained to be the rate determining step for the cleavage of β-ether bonds (Kawamoto et al., 2008). It is important to note that the presence of α,β-diaryl ether linkages in plant lignin are in general either undetectable or present at very low levels (Ralph et al., 1998), although α,β-diaryl ether linkages have been detected from tobacco lignin (Ralph et al., 1998) and wheat straw lignin (del Río et al., 2012). In the case of free phenolic units, the heterolysis reaction is thought to take place via a quinone methide intermediate. The reaction will be continued via the homolytic pathway, which is thought to be followed when non-phenolic groups exist in lignin. The temperature needed for the bond cleavage is lower in heterolysis than in homolysis reactions (Kawamoto et al., 2008).

Two types of radical chain mechanism have been supposed to cleave the β-ether bond in lignin networks (Kawamoto, 2017). The reactions taking place for the non-phenolic structures (A) and for the free phenolic structures (B) are shown in Figure 5. The reaction rate for the free phenolic structures is greater than that for the non-phenolic structures. The reaction products that are formed via radical degradation mechanisms of the β-ether bond are C=O and C_α=C_β type monomers (Figure 5).

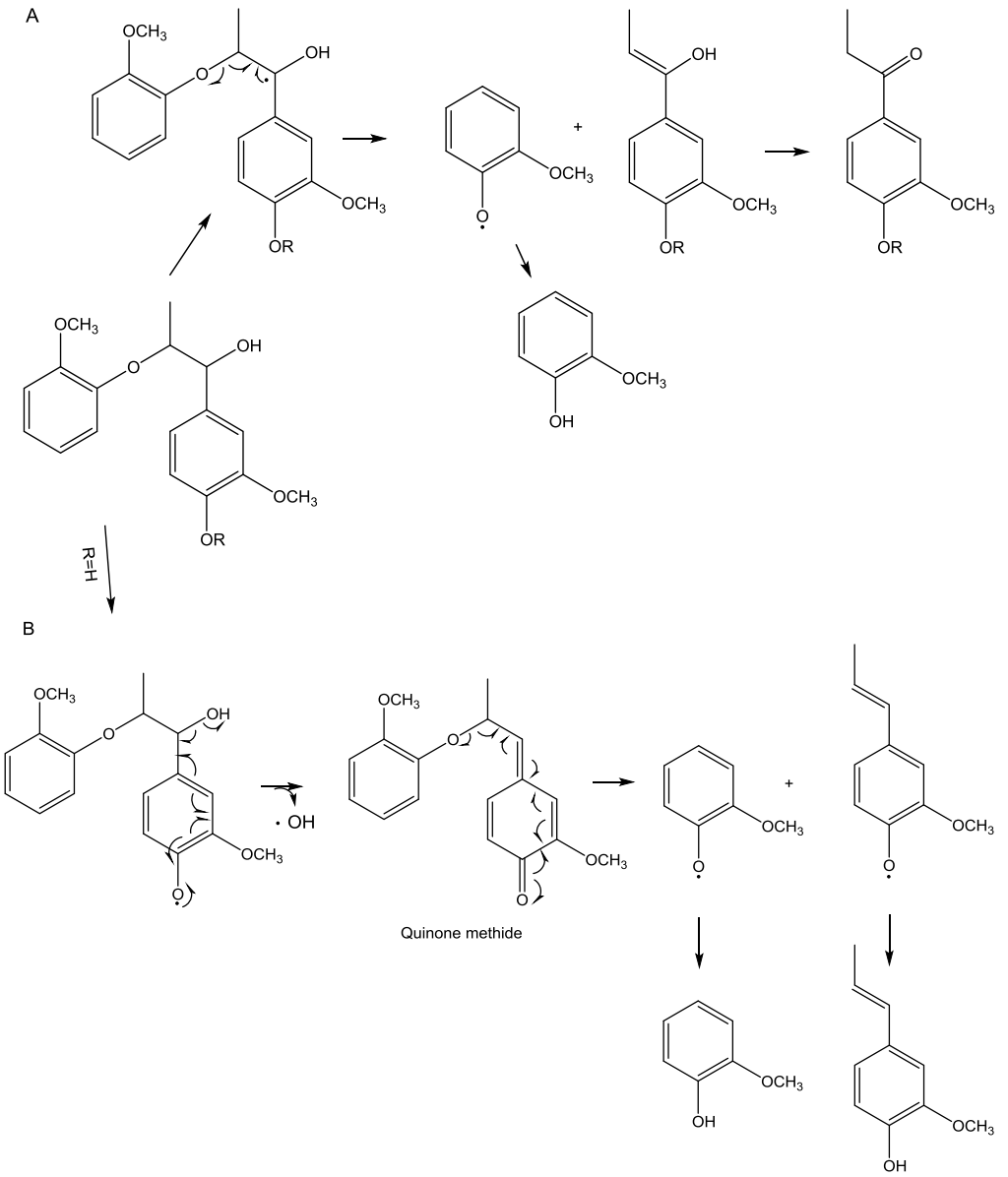

Figure 5. Proposed radical chain reaction mechanisms for the cleavage of lignin ether bonds in dimers representing non-phenolic (A) and free phenolic (B) structures (Kawamoto, 2017).

Based on the model compound studies and the formed degradation products it has been observed that both condensation and side-chain conversion occur already during primary pyrolysis at low temperatures (Kawamoto, 2017). The condensation reactions are promoted by the formation of side-chain double bonds in primary pyrolysis reactions, via quinone methide mechanisms. The side-chain conversion products have been explained to be formed both via radical and quinone methide mechanisms. This is because both oxidation (coniferylaldehyde) and reduction degradation products (dihydroconiferyl alcohol, isoeugenol) are formed from the coniferyl alcohol thought to be the most abundant primary pyrolysis product of guaiacyl type lignin. Evaporation is the key process used to determine primary

pyrolysis products during heat treatment of lignin, and also in analytical pyrolysis measurements. Evaporation prevents the formation of secondary products.

Table 1. Lignin pyrolysis degradation products and main side chain structures.

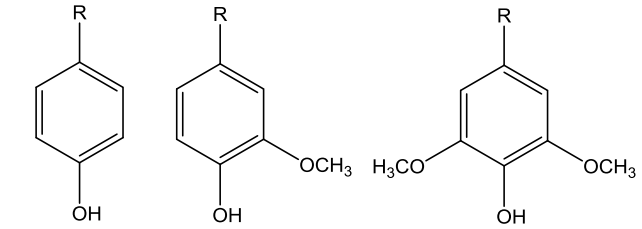

p-Hydroxyphenyl unit (H) | Guaiacyl unit (G) | Syringyl unit (S)

H units		**Side chain structure, R**
Phenol		H
4-Methylphenol		CH3
4-Vinylphenol		CH=CH2
G units	**S units**	
Guaiacol	Syringol	H
4-Methylguaiacol	Methylsyringol	CH3
4-Ethylguaiacol	Ethylsyringol	CH2-CH3
Vinylguaiacol	4-Vinylsyringol	CH=CH2
Eugenol	4-Allylsyringol	CH2-CH=CH2
cis-Isoeugenol	*cis*-Propenylsyringol	CH=CH-CH3 (cis)
trans-Isoeugenol	*trans*-Propenylsyringol	CH=CH-CH3 (trans)
Vanillin	Syringaldehyde	CHO
Acetoguaiacone	Acetosyringone	CO-CH3
Guaiacyl vinyl ketone	Syringyl vinyl ketone	CO-CH=CH2
Homovanillin	Homosyringaldehyde	CH2-CHO
Guaiacylacetone	Syringylacetone	CH2-CO-CH3
4-(1-Hydroxyprop-2-enyl)guaiacol	4-(1-Hydroxy-prop-2-enyl)syringol	CHOH-CH=CH2
Dihydroconiferyl alcohol	Dihydrosinapyl alcohol	CH2-CH2-CH2OH
cis-Coniferyl alcohol	*cis*-Sinapyl alcohol	CH=CH-CHOH
trans-Coniferyl alcohol	*trans*-Sinapyl alcohol	CH=CH-CHOH
Coniferaldehyde	Sinapaldehyde	CH=CH-CHO

3.2 Cellulose

Cellulose is a linear high molecular weight polymer with a uniform chain structure of D-glucose units (Figure 6). The units are bound by β-(1-4)-glucoside linkages with a repeating cellobiose unit (Fengel and Wegener, 1989). Thermal degradation of cellulose begins by water evolution and rearrangement of interchain and intrachain hydrogen bonds. Dehydration initiates the cellulose degradation, which involves the cleavage of β-(1-4)-glycosidic linkages and the formation of levoglucosan. Non-reducing chain ends, higher molecular weight and

the crystallinity of cellulose promote levoglucosan formation in high yield. Oppositely reducing chain-ends as well as amorphous regions of cellulose have lower thermal stability, being thus the initiation points for the thermal degradation. At lower temperatures, a high yield of char is formed, whereas higher temperatures support the formation of levoglucosan as well as non-condensable gases. Carbon monoxide and carbon dioxide follow closely the weight loss of cellulose, but carbon monoxide is also formed at higher temperatures as a result of supposed secondary reactions.

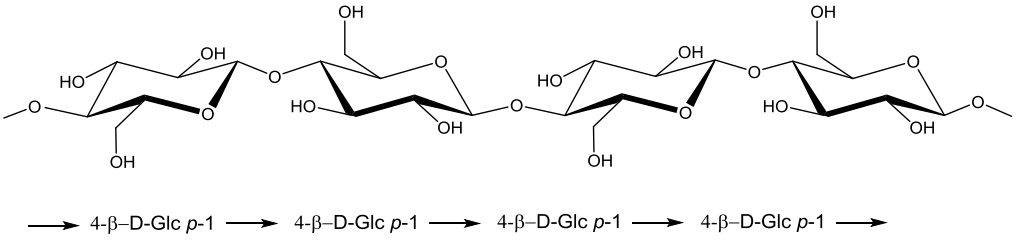

Figure 6. Structure of cellulose (Fengel and Wegener, 1989).

There are several theories of cellulose thermal degradation mechanisms and the formation of levoglucosan as the main degradation product. Several studies have suggested that cellulose degradation occurs via two main competitive transglycosylation reactions (Choi et al., 2011; Mamleev et al., 2009, 2006; Sheirs et al., 2001). The initial pathway is via an intermolecular transglycosylation reaction within the glucose monomer of cellulose. This is followed by two different reactions to form anhydrosaccharides after a second transglycosylation reaction and *β*-elimination (acid catalysed) to form liquid tar (Mamleev et al., 2006; Zhang et al., 2013). The acids (Bronsted acid) formed via *β*-elimination are able to attack the remaining cellulose, thus catalysing further reactions (Shaik et al., 2013). Two continuous transglycosylation steps are included for the cellulose degradation by transglycosylation reactions. In the first transglycosylation step a cellulose chain is depolymerized into a levoglucosan chain-end intermediate and a short cellulose chain. In the second transglycosylation step the levoglucosan chain-end intermediate is converted into levoglucosan and another levoglucosan chain-end intermediate is formed (Mamleev et al., 2006; Zhang et al., 2013). It has also been proposed that cellulose can be degraded to form levoglucosan via a glucose intermediate, free radical mechanisms or ionic mechanisms. Based on the theoretical studies of Zhang et al. (2013), it was concluded that levoglucosan formation via the levoglucosan chain-end intermediate in the transglycosylation reaction is the most reasonable pathway.

The levoglucosan yield can be as high as 60 w%, but other anhydrosugars are also formed, together with pyrans, furans, light oxygenate gases and char. Levoglucosan and the other most abundant products of cellulose degradation in the temperature range of 350 -550 °C are presented in Table 2.

Table 2. Main degradation products formed in cellulose pyrolysis in the temperature range of 350-550 °C (Mettler et al., 2012; Paulsen et al., 2013; Wu et al., 2016).

Compounds	
Anhydrosugar	**Light oxygenates**
Levoglucosan	Methyl glyoxal
1,6-Anhydroglucofuranose	Glucolaldehyde
1,4:3,6-Dianhydroglucopyranose	Formaldehyde
Levoglucosanone	Hydroxyacetone
Pyrans	Acetic acid
1,5-Anhydro-4-deoxy-D-glycero-hex-1-en-3-ulose	Formic acid
2,3-Dihydro-3,5-dihydro-6-methyl-4H-pyran-4-one	Puryvic acid
3,5-Dihydroxy-2-methyl-4H-pyran-4-one	2,3-butanedione
Furans	Glyoxal
Hydroxymethylfurfural	**Permanent gases**
Furfural	Carbon monoxide
5-Methylfurfural	Carbon dioxide
2-Furanmethanol	**Other**
2,5-Dimethyfuran	2-Hydroxy-3-methyl-2-cyclopenten-one
2-Methyl furan	1,2-Cyclopentanedione
Furan	Char
2,5-Dimethyl-4-hydroxy-3(2H)-furanone	
2(5H) Furanone	

3.3 Hemicelluloses

Hemicelluloses are heteropolysaccharides composed of various sugar units and with a much shorter, and branched, molecular chain than that of cellulose. Sugar units (anhydrosugars) making up the polyoses can be subdivided into groups such as pentoses, hexoses, hexuronic acids and deoxy-hexoses. The main hemicellulose of softwood is galactoglucomannan, but low quantities of xylan (arabinoglucuronoxylan) are also present. Hardwood is composed mainly of glucuronoxylan and minor amounts of glucomannan (Fengel and Wegener, 1989; Sjöström and Alen, 1999). In herbaceous crops, xylan is the most abundant hemicellulose. Partial chemical structures of hardwood hemicelluloses are shown in Table 7. Pectins, composed mainly of galacturonans, are present at less than 1% in both softwoods and hardwoods (Fengel and Wegener, 1989).

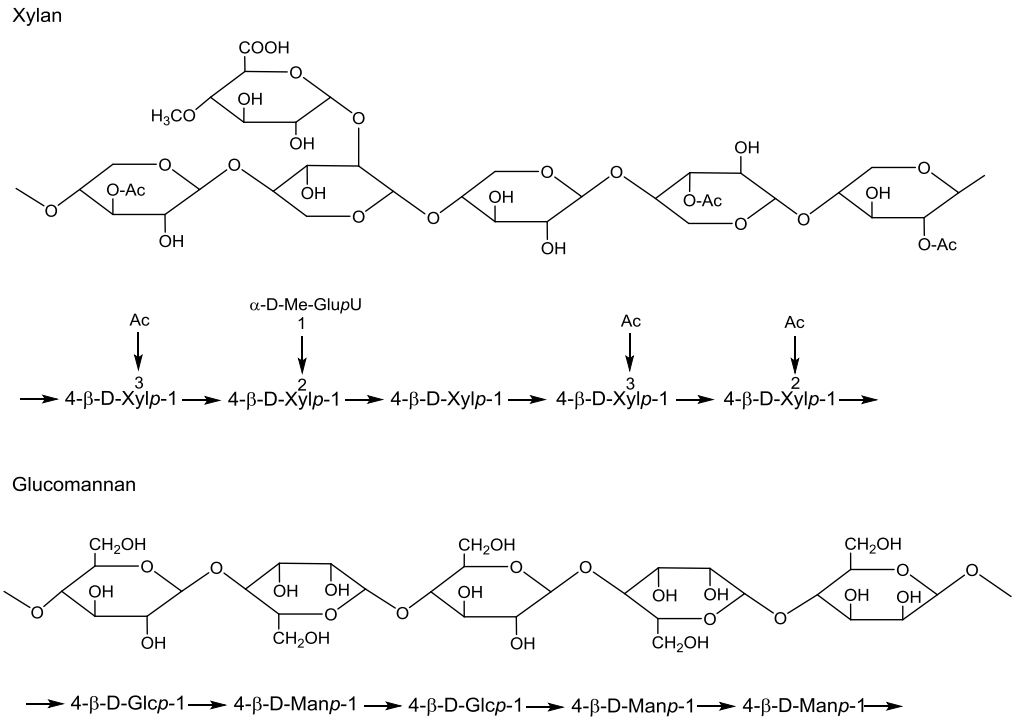

Figure 7. Partial chemical structure of (above) O-acetyl-4-O-methylglucuronoxylan (Fengel and Wegener, 1989) and (below) glucomannan from hardwood (Sjöström and Alen, 1999).

In thermal analysis, thermal degradation of hemicelluloses occurs clearly at lower temperatures (220-315 C) than cellulose (315-400 C) (Yang et al., 2007) and in a sharper range than the degradation of lignin. Acetylated hemicellulose fragments are more susceptible to thermal degradation than non-acetylated fragments. Hardwood xylan, that contains more acetylated units than softwood galactoglucomannan, is thus thermally less stable than xylan in hardwood (Fengel and Wegener, 1989). Under the fast pyrolysis conditions the glyosidic bond is cleaved among sugar units, forming stable anhydrosugars that retain the stereoconfiguration of the sugar unit (Helleur, 1987), but also several other small molecular weight fragments including carbonyl compounds, acids and methyl esters, furans and pyrans (Faix et al., 1991a, 1991b). However, pentose and hexose degradation products have mainly been used to determine the hemicellulose composition of lignocellulose feedstocks and products due to their unique formulae. Arabinan and xylan are degraded to pentoses, 1,5-anhydroarabinofuranose (1,5-Anhydro-β-D-xylofuranose) and 1,4-anhydroxylopyranose (1,4-anhydro-α-D-xylopyranose), but the most abundant degradation product of xylose is 1,5-anhydro-4-deoxypent-1-en-3-ulose (Kleen et al., 1993; Kleen and Gellerstedt, 1991). Pyrolysis degradation products of glucan, galactan and mannan are 1,6-anhydroglucopyranose, 1,6-anhydrogalactopyranose and 1,6-anhydromannopyranose, respectively. Chemical structures of the main hemicellulose pyrolysis derivatives are presented in Figure 8 (Faix et al., 1991a).

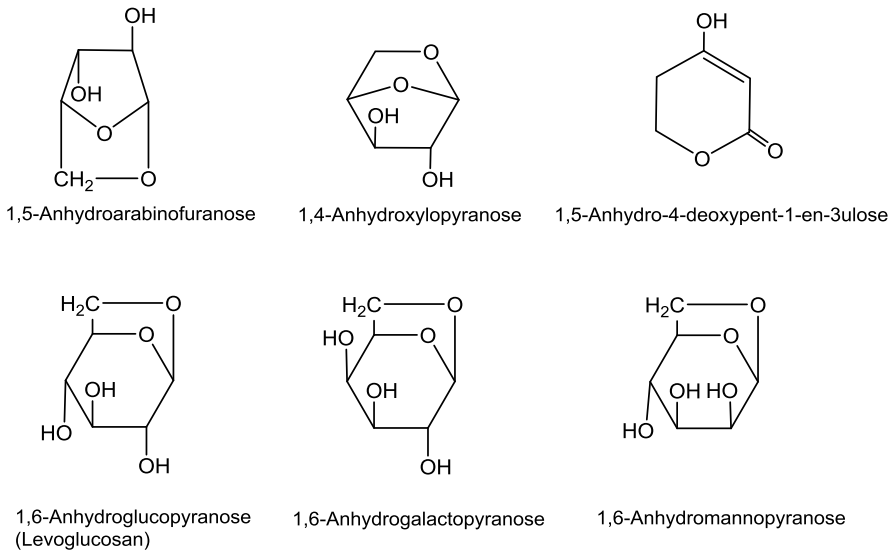

Figure 8. Pentose and hexose pyrolysis derivatives of cellulose and hemicelluloses (Faix et al., 1991a).

4. Applications of analytical pyrolysis in lignocellulosic processing

4.1 Macromolecular biomass components

4.1.1 Wood fibres

Analytical pyrolysis combined with gas chromatography mass spectrometry (Py-GC/MS) has widely been used to determine lignin and carbohydrate composition from various lignocellulose feedstocks and products directly, especially from wood fibres. Both softwood and hardwood species have been classified based on their pyrolysis degradation products with (Challinor, 1995; Clifford et al., 1995) and without derivatisation (Kuroda and Yamaguchi, 1995; Saiz-Jimenez and De Leeuw, 1986). Pyrolysis degradation products of lignin have been used to distinguish between pine, spruce and larch softwood species and the location inside the species, but also to identify different tissue types (Alves et al., 2009). Degradation products of both lignin and polysaccharides formed from oak species have been found to classify oaks based on their origin (Nonier et al., 2006). Lignin content has been determined by Py-GC/MS directly from softwoods, without the need for external or internal calibration. Lignin content has been determined by dividing the sum of peak areas of lignin degradation products by the sum of all degradation products present in chromatograms (Alves et al., 2008, 2006).

The Py-GC/MS technique has increasingly been used to determine the S/G/H ratio from different wood species, but especially the S/G ratio from hardwood species. G/H ratios determined by Py-GC/MS have been found to distinguish between compression and native young *Pinus radiata* wood (Nanayakkara et al., 2016). S/G ratios have been found to vary within a single tree (Yokoi et al., 1999), but the wood provenance (Rodrigues et al., 1999), eccentric growth (Rodrigues et al., 2001), and seeds of different origin (Yokoi et al., 2001) may also have an effect. S/G ratios have been determined from wood feedstocks meant for pulp production, such as various *Eucalyptus spp*. (del Río et al., 2005; Lima et al., 2008) and *Eucalyptus spp*. wood clones cultivated in four regions in Brazil (Barbosa et al., 2008; Nunes et al., 2010; Yokoi et al., 2001). Selected lignin pyrolysis degradation products have been used to distinguish between different eucalypt species and geographical origins, but also to predict the ease of delignification of the resulting pulps measured as active alkali consumption (Galetta et al., 2014). Lignin pyrolysis derivatives as well as S/G ratios of various *Eucalyptus spp*. with (González-Vila et al., 1999) and without derivatisation (Reina et al., 2014) have been used to estimate ease of delignification and alkali consumption.

Py-GC/MS has been used to characterise lignin structure and S/G/H ratios together with other techniques (2D-NMR, thioacidolysis and derivatisation followed by reductive cleavage) after lignin isolation from different eucalypt species (Rencoret et al., 2008) and hybrids

(Prinsen et al., 2012) and tissues of *Quercus suber* (Lourenço et al., 2016). Changes in lignin and carbohydrate composition and yield after the isolation of lignin carbohydrate complexes from spruce wood has been monitored by Py-GC/MS together with 2D-NMR (Du et al., 2014).

Thermochemolysis with various reagents has been utilised to obtain more detailed information on lignin structure and functional groups. Thermochemolysis with TMAH has been used to determine lignin composition from different species such as spruce (Hardell and Nilvebrant, 1996), beech leaf litter (Hermosin and Saiz-Jimenez, 1999) and eucalypt (González-Vila et al., 1999). Free and etherified phenolic lignin units have been distinguished by Py-GC/MS by analysing pre-methylated samples (Camarero et al., 1999). Thermochemolysis with trimethylsilylation reagent has been found to provide useful information concerning the cinnamyl alcohol and cinnamyl aldehyde end-groups, whereas thermochemolysis with TMAH provides information only on cinnamyl alcohol end-groups (Kuroda, 2000a; Nakagawa-Izumi and Kuroda, 2003).

Changes in both carbohydrate and lignin composition have been determined by Py-GC/MS from surface and inner layers of pulp fibres after different alkaline cooking processes (Sjöberg et al., 2002; Tanaka et al., 1997) and from pulp fibres in cooking (Kleen et al., 1993; Lourenço et al., 2013, 2012), but also from wood fibres after fungal degradation (del Río et al., 2002, 2001a; Martínez et al., 2005), hydrothermal treatment (Grinins et al., 2013), hydrothermal carbonisation (Wikberg et al., 2016), genetic modification (Meier et al., 2005) and from archaeological wood (Łucejko et al., 2012). Lignin structure has been followed extensively directly from pulps or isolated lignin fractions after various alkaline cooking processes (Choi et al., 2001; Prinsen et al., 2013), oxygen delignification (Akim et al., 2001; Ibarra et al., 2005; Lima et al., 2015), bleaching (del Río et al., 2001b; Ibarra et al., 2007), and mediator-laccase delignification (Oudia et al., 2009, 2007; Tamminen et al., 2003a). Changes in S/G ratios of eucalypt species have been followed directly from wood and pulps after cooking, oxygen delignification and bleaching (Hasumi et al., 2009; Lima et al., 2015). Delignification kinetics of syringyl and guaiacyl units in heartwood and sapwood of *Eucalyptus globulus* have been investigated by Py-GC-MS/FID and modelled as double first-order reactions (Lourenço et al., 2012). Lignins dissolved during alkaline cooking (Prinsen et al., 2013) and organosolv cooking (Kangas et al., 2015) have been characterised by Py-GC/MS together with other techniques (2D-NMR, ^{31}P NMR, SEC) in order to obtain more information on delignification mechanisms. Py-GC/MS analysis of non-hydrolysed residues from different bioethanol production methods from softwood provided useful information concerning fermentation processes, i.e. the efficiency of cellulose hydrolysis (Dizhbite et al., 2011).

Lignin pyrolysis degradation products together with some other chemical experiments and chemometric methods have been used to quantitatively characterize lignin structure-antioxidant activity relationships from lignins of various industrial side streams (Ponomarenko et al., 2015).

Recently, analytical pyrolysis has been increasingly utilized to simulate applied pyrolysis reactions and to obtain understanding on bio-oil composition; especially catalytic upgrading is being studied (Adam et al., 2005; Mullen and Boateng, 2010). Different zeolite catalysts have been studied for upgrading lignin-based bio-oils from Kraft lignin (Shen et al., 2015), from various industrial side streams (Mullen and Boateng, 2010), milled wood lignins and organosolv lignin from hardwood, softwood and herbaceous biomasses (Zhou et al., 2016),

but also from bio-oils from wood feedstocks (Ohra-aho and Linnekoski, 2015). In addition to zeolite catalyst, various Al/SBA-15 catalysts for the cracking of pyrolysis vapours of sawdust have also been studied (Qiang et al., 2009). The effect of the chemical structure of lignin on the phenolic composition of bio-oil at various temperatures has been studied by Py-GC/MS (C. Liu et al., 2016). The effects of hydrolysis pretreatment temperature and washing pH on the pyrolysis liquid product yield and quality of birch wood have been investigated. Based on the results, neutral washing pH and low hydrolysis temperature favoured the formation of lignin derivatives, anhydrosugars and especially levoglucosan (Zhurinsh et al., 2013). Catalytic effects of different alkali metals, alkali earth metals and switchgrass ash on primary cellulose pyrolysis reactions at various temperatures showed that mineral salts and high temperature accelerated the reaction. These parameters led to the formation of low molecular weight compounds instead of levoglucosan from pure cellulose (Patwardhan et al., 2010), as well as from different hardwood and softwood species (Müller-Hagedorn et al., 2003).

4.1.2 Alternative biomass sources (non-wood)

The structure of non-wood plant biomass differs from wood structure, containing significantly more *p*-hydroxypenyl substructures than wood and also having *p*-hydroxycinnamates among lignin and polysaccharides. Corresponding acids of hydroxycinnamates are *p*-coumarylic acid and ferulic acid, the structures of which are shown in Figure 9. In pyrolysis, the carboxylic acid groups present in *p*-coumarates and ferulates are released. As a result of decarboxylation, 4-vinylphenol and 4-vinylguaiacol are formed. Those degradation products are the same that are formed from lignin (Blokker et al., 2006; del Río et al., 2007a; Kuroda and Yamaguchi, 1995). In the case of non-wood plants, thermochemolysis with tetramethylammonium hydroxide has been utilized to distinguish between lignin derivatives from the *p*-coumarates and ferulates (del Río et al., 1996). Protein present in non-wood plants complicates the determination of *p*-hydroxyphenyl type lignin derivatives by Py-GC/MS. In pyrolysis, proteins have been found to release phenol, 4-methylphenol, and 4-vinylphenol, which are the same degradation products as formed from the *p*-hydroxyphenyl-type lignin substructure (Kleen et al., 2003; Rencoret et al., 2015).

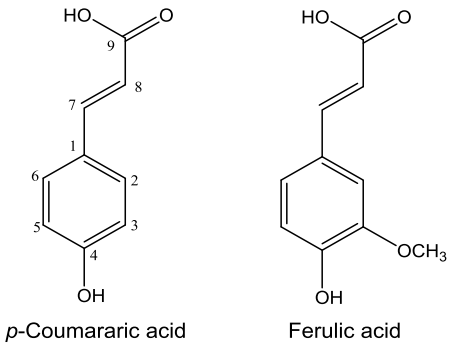

Figure 9. The hydroxycinnamic acids *p*-coumaric acid and ferulic acid.

One advantage of the Py-GC/MS method for the determination of S/G/H ratio from non-wood plants is that extractives removal is not needed (Lopes et al., 2011). Pyrolysis with and without TMAH has been used to determine lignin composition, S/G ratio and cinnamyl acids

directly from non-wood biomasses such as sago palm, jute, hemp, flax, sisal and abaca (del Río et al., 2007a; Gutiérrez et al., 2006; Kuroda et al., 2001), core and bast fibres of kenaf (Kuroda et al., 2005, 2002), but also lignins isolated from wheat straw (del Río et al., 2012), coconut (Rencoret et al., 2013) and brewer's spent grain (Rencoret et al., 2015). Lignin from sugarcane bagasse and wheat straw has been characterized by Py-GC/MS directly and after isolation (del Río et al., 2015). The effect of harvesting time on kenaf bast lignin S/G ratio was evaluated by Py-GC/MS. Based on the results, a harvesting time of 5 months provided a raw material that was most suitable for the delignification (Mazumder et al., 2005). For the optimisation of bio-oil production from palm kernel shell its phenolic lignin units have been determined by Py-GC/MS (Chang et al., 2016). 5-hydroxyguaiacyl lignin unit has been identified by Py-GC/MS from non-wood plants (del Río et al., 2007b).

In addition to structural analysis, wheat straw lignin has been quantified by Py-GC/MS using 1,3,5-trimethoxybenzene as an internal standard (Bocchini et al., 1997). A linear relationship between lignin pyrolysis degradation products and the Klason lignin content of various grasses was observed (Fahmi et al., 2007). Thermochemolysis with TMAH has been used to determine the *p*-coumaric and ferulic acid ratio and quantity from different fossil plant materials (Blokker et al., 2006).

Pre-methylation prior to Py-GC/MS has been used to evaluate changes in free phenolic lignin structures and S/G/H ratios during fungal treatment of wheat straw (Camarero et al., 2001; Martínez et al., 2001). Changes in lignin in angiosperm and woody plants after genetic modification (Rencoret et al., 2016) and in bamboo lignin after organosolv treatment (Bai et al., 2013) have also been evaluated by Py-GC/MS. Py-GC/MS together with thermogravimetric analysis has been used to evaluate the thermal behaviour of wheat straw lignin in order to provide data and kinetic information necessary for the evaluation of the pyrolysis process and products formed as a means to use wheat straw lignin for energy and chemicals (Yang et al., 2010).

4.2 Low molecular weight compounds

4.2.1 Extractives

The lignocellulosic biomasses contain small amounts of low molecular weight extractives that have also been analysed by Py-GC/MS, mainly using thermochemolysis technique (Challinor, 2001; Shadkami and Helleur, 2010). Derivatisation has been used in order to avoid decarboxylation of acid groups present in the extractives. Extractives composition can be determined from natural materials directly (Niemi et al., 2012) and after solvent extraction (Challinor, 1996). Thermochemolysis with TMAH and TMAAc reagents together have been used to determine wood resin acids and fatty acids (Hardell and Nilvebrant, 1999; Mizumoto et al., 2010), and the composition of natural waxes (Asperger et al., 2001). TMAH is used to define total fatty acids, whereas TMAAc defines only the free fatty acids. Thermochemolysis with TMAAc has been used to determine fatty acids, phenolic acids and gallocatechin compounds directly from *Eucalyptus camaldulensis* wood. Similar results were obtained by the conventional standard method including off-line transmethylation of acetone extracts and GC analysis (Yokoi et al., 2003). The main disadvantage of TMAH is that polyunsaturated fatty acids are isomerized and partly degraded at high concentrations of this strong base. Dilution of TMAH has been found to diminish the isomerisation (Jun-kai et al., 1997). TMSH is

another alkaline reagent which does not isomerize polyunsaturated fatty acid. Therefore its reactivity to determine fatty acids containing saturated, monounsaturated and polyunsaturated fatty acid from triglycerides, phospholipids, free fatty acids and cholesteryl esters has been evaluated together with TMAH. The results showed that TMAH allowed almost quantitative methylation of saturated and mono-unsaturated fatty acid components independently of the classes of lipids, but polyunsaturated fatty acids were isomerized and partly degraded. TMSH was effective in determining quantitatively all types of fatty acids including polyunsaturated fatty acids from triglycerides, free fatty acids and phospholipids, the exception being cholesteryl ester. TMSH was unable to react with cholesteryl ester due to steric hindrance (Ishida et al., 2009). In addition to TMAAc, TEAAc has been used together with more basic thermochemolysis reagents (TMAH and TBAH) for the analysis of lipids from natural materials (Guignard et al., 2005; Válková et al., 2009). The advantage of TEAAc is that naturally occurring methyl esters can be distinguished from the free acids. Phenolic extractives have been determined directly from wood by thermochemolysis with TBAH. TBAH reacts only with free acids and hydroxyl groups and thus phenolic extractives can be distinguished from lignin derivatives (Ishida et al., 2009). Derivatisation of sample with trimethylsilyl diazomethane (TMS- diazomethane) prior to thermochemolysis with TMSH enables analysis of catechins and condensed tannins from plants (Shadkami et al., 2009). Thermochemolysis with ^{13}C-labeled TMAH has been used to distinguish between tannin and lignin phenolic degradation products from soil samples (Nierop and Filley, 2008). Based on the pyrolysis degradation products of monomeric and dimeric flavanols, different types of condensed tannins can be distinguished from bark extracts of *Salix species* and *Acacia mearnsii* (Ohara et al., 2003).

5. Experimental

5.1 Materials and methods

All materials and methods, including the analytical pyrolysis methods used in Publications I-VI, are summarized in Table 3. More detailed descriptions of the materials and methods are presented in the original Publications.

5.1.1 Material preparation

Synthesis of guaiacyl palmitate and 2-nonylpalmitate

The structures of esters for the thermochemolysis study presented in Publication III are shown in Figure 10. The syntheses of the products are here described briefly. Palmitic acid and guaiacol or 2-nonanol together with 4-dimethylaminopyridine were dissolved in dichloromethane and cooled to 0°C. This was followed by addition of dicyclohexanecarbodiimide portion-wise in a dichloromethane solution. The reaction was left at room temperature overnight and was then filtered to remove solids. The filtrate was evaporated and the crude product was purified by flash chromatography from heptane, increasing the polarity with ethanol. The yields of guaiacyl palmitate and 2-nonylplmitate were 83 % and 72 %, respectively.

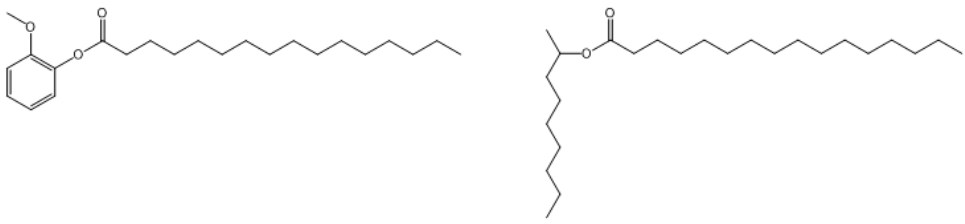

Figure 10. The model compounds guaiacyl palmitate and 2-nonylpalmitate synthesized for the thermochemolysis study reported in Publication III.

Table 3. Materials, pyrolysis conditions and standard analysis methods used for the study

Materials	Thermal desorption	Isothermal pyrolysis	Fractionated pyrolysis	Thermochemolysis	Other methods	Publication
Laboratory ECF-light bleached pine (Pinus silvestris) Kraft pulps		580 °C, 2 s		TMAH 400 °C, 4 s	Kappa number according to SCAN-C1 and hexenuronic acid content was determined by HPLC after enzymatic hydrolysis according to method by Tenkanen et al., (1999)	I
Laboratory oxygen delignified ECF bleached spruce (*Picea abies*) Kraft pulps			320 °C, 40 s 480 °C, 12 s 620 °C, 4 s 800 °C, 2 s			I
Eighteen 7-year-old eucalypt hybrids, including a number of double/triple/fourth crossings among E. *grandis*, E. *urophylla*, E. *globulus*, E. *dunnii* and E. *camaldulensis* species		580 °C, 2 s	320 °C, 44 s 450 °C, 16 s 580 °C, 4 s 800 °C, 2 s		S/G ratio with nitrobenzene oxidation followed by HPLC (Lin and Dence, 1992) Carbohydrate composition using acid hydrolysis followed by HPLC (Wallis et al., 1996)	IV VI
Laboratory-prepared soda-O_2 and soda-AQ pulps of Eucalypt hybrid G1xUGL (*E. grandis* (Coffs Harbour) x [*E. urophylla* (R) x *E. globulus* (R)]) at different degrees of delignification (κ = 50, 35 and 15)		580 °C, 2 s	320 °C, 44 s 450 °C, 16 s 580 °C, 4 s 800 °C, 2 s		Carbohydrate composition using acid hydrolysis followed by HPLC (Wallis et al., 1996)	VI
Softwood Kraft lignins treated with and without laccase (and sulfhydryl oxidase, Aspergillus oryzae) at pH 8 and oxidation at pH 10	150 °C, 5 min and 190 °C, 5 min					II
Guaiacyl palmitate and 2-nonyl palmitate				TMAAc: 280 °C, 2 s TMAH: 600 °C, 700 °C, 800 °C each 2 s	^{1}H NMR	III
BSG and its lignin fractions P-AEF (Niemi et al., 2012), INS (Aura et al., 2013), AL and EMAL		600 °C, 2 s		TMAH: 600 °C, 2 s		V

Isolation of lignin-rich fractions from BSG

Lignin isolation from the BSG by enzymatic hydrolysis to soluble (P-AEF) and insoluble (INS) lignin-rich fractions was described in more detailed publications by Aura et al. (2013) and Niemi et al. (2012). However, the scheme of the isolation is shown in Figure 11 a. Fractionations of BSG by acidolysis (AL) and enzymatic mild acidolysis (EMAL) are also shown in Figure 11. Prior to lignin isolation by AL and EMAL, BSG was dried and milled with a Retch S100 ball mill (Figure 11, Publication VI). After the milling, extractives were removed with hexane in a Soxhlet apparatus. Reduction of protein content was carried out with Alcalase 2.4 L (20 μl/g of dry material). Acidolysis was performed according to the method of Gellerstedt et al., (1994) The conditions used in acidolysis are shown in Figure 11. Dissolved lignin was precipitated with 0.01 M HCl at 4 °C overnight. Isolation of EMAL was performed according to Guerra et al., (2006), with some modifications. BSG material after the protease treatment was subjected to carbohydrate digestion with Depol740 and Celluclast 1.5 treatment at pH 4.5 and 50 °C for 48 h. This was followed by mild acidolysis with 0.01 M HCl and lignin precipitation from the solution similarly to the procedure used after the acidolysis (Figure 11).

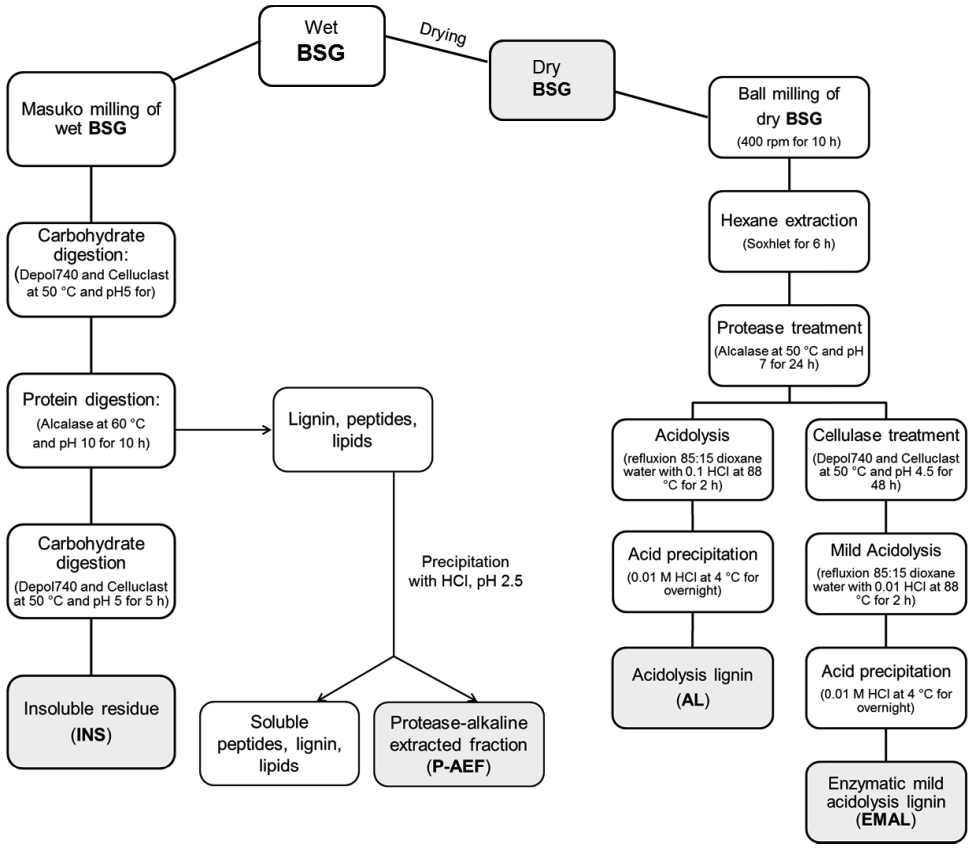

Figure 11. Scheme for the BSG fractionation by enzymatic hydrolysis (left) (Aura et al., 2013; Niemi et al., 2012) and acidolysis and enzymatic mild acidolysis (right).

5.1.2 Pyrolysis techniques

Instrument

All pyrolysis measurements in the Publications I-VI were performed with a platinum foil pulse pyrolyser (Pyrola2000®, Pyrol AB, Lund, Sweden), which was connected to a GC/MS instrument (Varian 3800 GC/2000 MS, Walnut Creek, USA). Figure 12 shows the pyrolysis unit. For the separation of degradation products, a mid-polar capillary column coated with a stationary phase of 14% cyanopropyl-phenyl 86% dimethyl polysiloxane (J&W, DB-1701, 30 m x 0.25 mm, film 1 µm) was used. The mass spectra of the products were obtained using ion trap mass spectrometry (EI 70 eV). The detector mass range was selected based on the material studied. In the cases of isothermal pyrolysis results, peak identifications were carried out according to the literature (Faix et al., 1991a, 1991b, 1990a, 1990b; Ralph and Hatfield, 1991) and commercial mass spectra Nist92 and Nist05 libraries.

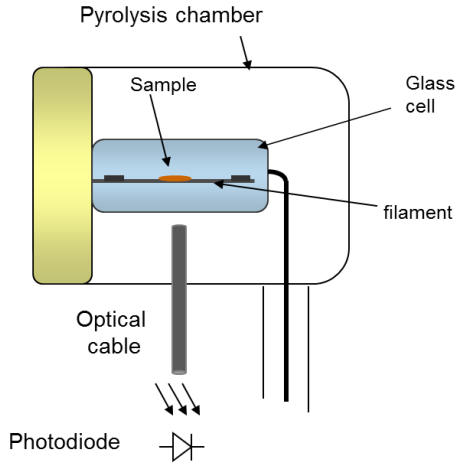

Figure 12. Resistively heated filament pyrolyzer

Isothermal and fractionated pyrolysis

Isothermal pyrolysis of wood and pulp samples was carried out at 580 °C. The pyrolysis time was 2 s. The temperature was selected because it gave the best yield for the lignin degradation products. Short pyrolysis time was favoured in order to avoid secondary reactions in pyrolysis. Pyrolysis of brewer's spent grain and its lignin fractions was carried out at 600 °C, a slightly higher temperature than used for wood and pulp samples. A temperature of 600 °C was selected because thermochemolysis in the presence of TMAH was carried out at that temperature. Fractionated pyrolysis results were reported in two different Publications, I and VI. The conditions used for the fractionated pyrolysis were slightly different in Publications I and VI (Table 3). This was due to the different aims of the fractionation pyrolysis. Publication I focused on lignin and Publication VI on carbohydrate thermal behaviour.

Thermal desorption

Thermal desorption measurements were carried out in a pyrolyser unit. A more detailed description of the GC/MS conditions is described in Publication II. The measurements were carried out utilizing the chamber temperature only. This was possible because the temperatures used for the study, 150 and 190 °C, were lower than the maximum allowed chamber temperature of 225 °C. The samples were placed in special glass boats made for thermal de-

sorption purposes. Therefore it was also possible to use higher amounts of sample, about 2.5 mg for the thermal desorption analysis in comparison to 100 μg used for pyrolysis measurements. For the quantitative analysis, standard solutions of guaiacol in amounts of 1.5-6 μg were prepared (R^2 = 0.96). A pyrolysis probe for the liquid injections was used for guaiacol standard.

Thermochemolysis

Thermochemolysis technique was utilized in Publications I, III and V. All thermochemolysis measurements were performed on-line in Py-GC/MS instruments. Depending on the material studied, slightly different conditions were used as shown in Table 3. In Publications I and V, thermochemolysis was carried out using TMAH, aiming at obtaining structural information concerning lignin. Thermochemolysis results were compared in these studies with isothermal pyrolysis results.

Publication III reported the results obtained when two model compounds, guaiacyl palmitate and 2-nonyl palmitate (Figure 10), which contained both aromatic and aliphatic ester bonds, were analysed with two methylation reagents TMAH and TMAAc, aiming at determining the total fatty and free fatty acids contents, respectively. A short reaction time of 2 seconds was favoured with both reagents. TMAH thermochemolysis was performed at 600°C, whereas a lower temperature of 280 °C was used for TMAAc thermochemolysis in order to prevent thermal degradation of the ester bond. A thermochemolysis temperature of 600°C was selected because at that temperature the highest recovery for the fatty acids with TMAH has been obtained (Drechsel et al., 2003). Overloading of the detector was avoided by diluting both model compounds as well as the internal standard heneicosanoic acid to solvent (methanol or dichloromethane) before transferring to the filament. In TMAH thermochemolysis, sample together with internal standard was added to the filament prior to the TMAH reagent. In the case of TMAAc thermochemolysis, reagent was mixed with sample either before or after the addition of sample and internal standard. The results were similar. Therefore, average values were calculated for all the measurements.

Data analysis

The peak areas of lignin and carbohydrate degradation products were integrated as a total ion current (TIC) or using selected main ions (m/z). The selected peak ions were used in case of the peak intensities were low or there existed co-eluted peaks in the total ion current gas chromatogram. The ions that were used for the integration are listed in Table 4. The peak areas that were calculated with selected ions were converted to the corresponding total peak areas using factors calculated from the pure mass spectrum of each compound as was reported by Sjöberg (Sjöberg et al., 2002). Monosaccharide content was calculated, including 1,4-anhydroxylopyranose, 4-hydroxy-5,6-dihydro-(2H)-pyran-2-one, 1,5-anhydroarabinofuranose, 1,6-anhydrogalactopyranose, 1,6-anhydroglucopyranose and 5-hydroxymethyl-2-tetrahydofuraldehyde-3-one, 5-hydroxymethyl-2-furaldehyde and 1.4-dideoxy-D-*glycero*-hex-1-enopyranos-3-ulose to determine xylose (two first compounds), arabinose, galactose and glucose (four last compounds), respectively. Two methods for the calculation of monosaccharide content were used. In method A cellulose derivative, 1,6-anhydroglucopyranose (levoglucosan) was used for the calculation of glucose, whereas in method B the four main degradation products of cellulose, 1,6-anhydroglucopyranose, 5-hydroxymethyl-2-

tetrahydofuraldehyde-3-one, 5-hydroxymethyl-2-furaldehyde and 1.4-dideoxy-D-*glycero*-hex-1-enopyranos-3-ulose were included.

For the lignin structure evaluation peak areas of lignin degradation products were divided by the weight of the sample and peak areas were normalized to 100 %. For the lignin quantitative analysis from alkaline softwood pulps (Publication I), a one point external standard calibration using Kraft lignin as a standard was used.

Principal component analysis

All guaiacyl and syringyl type lignin pyrolysis products integrated from pyrograms of eucalypt hybrids were normalized to 100% separately (Publication IV). Thereafter the data was subjected to multivariate data analysis SIMCA-P 8.1 (Umetrics AB, Umeå, Sweden). Principal component analysis (PCA) is designed for visualization of similarities and differences among samples. It presents the data in two- or three-dimension so that the major trends and dominant patterns can be overviewed. Principal components that are obtained describe the variance of the data. The first principal component (PC1) describes the largest variance in the data set. A second component (PC2) is orthogonal to PC1 and it reflects the second largest source of variation in the data. Two principal components were calculated for the data set in Publication IV, because the third component did not improve the model.

Table 4. Pyrolysis degradation products of lignocellulosic materials in isothermal pyrolysis and the origin of degradation products. Ions listed were used to integrate degradation products when intensities of degradation products were low or co-eluted peaks existed. Multiplication factors were used to convert peak the selective ion peak areas to corresponding total ion current (TIC) areas.

Compound	Origin	Ions (m/z)	Factor
Phenol	Lg/prot	65, 66, 94	1.5
2-Methylphenol	Lg/prot	77, 107, 108	2.2
4-Methylphenol	Lg/prot	77, 107, 108	2.2
4-Vinylphenol	Lg/prot/FA	TIC	1.0
Guaiacol	Lg	81, 109, 124	1.6
4-Methylguaiacol	Lg	67, 123, 138	2.0
4-Ethylguaiacol	Lg	122, 137, 152	2.2
4-Vinylguaiacol	Lg/*p*CA	135, 107, 150	2.1
Eugenol	Lg	77, 149, 164	3.8
cis-Isoeugenol	Lg	77, 149, 164	3.9
trans-Isoeugenol	Lg	77, 149, 164	3.5
Vanillin	Lg	123, 151, 152	2.4
Homovanillin	Lg	122, 137, 166	2.0
Acetoguaiacone	Lg	123, 151, 166	2.1
Guaiacylacetone	Lg	122, 137, 180	2.7
4-(Oxy-allyl)guaiacol	Lg	123, 151, 178	2.7
4-(1-Hydroxyprop-2-enyl)guaiacol	Lg	124, 137, 180	3.1
Dihydroconiferyl alcohol	Lg	122, 137, 182	2.9
cis-Coniferyl alcohol	Lg	124, 137, 180	4.0
trans-Coniferyl alcohol	Lg	137, 163, 180	2.7
Coniferaldehyde	Lg	135, 147, 178	5.5
Syringol	Lg	139, 154	2.9
4-Methylsyringol	Lg	153, 168	3.3
4-Ethylsyringol	Lg	167, 182	2.5
4-Vinylsyringol	Lg	165, 180	3.0
4-Allylsyringol	Lg	179, 194	5.3
cis-Propenylsyringol	Lg	179, 194	6.8
trans-Propenylsyringol	Lg	179, 194	4.5
Syringaldehyde	Lg	167, 181, 182	3.0
Homosyringaldehyde	Lg	167, 196	2,7
Acetosyringone	Lg	181, 196	2.8
Syringylacetone	Lg	167, 210	2.3
Propiosyringol	Lg	181, 210	2.4
4-(Oxy-allyl)syringol	Lg	181, 208	4.5
4-(1-Hydroxy-prop-2-enyl)syringol	Lg	167, 210	5.3
Dihydrosinapyl alcohol	Lg	167, 168, 212	2.9
cis-Sinapyl alcohol	Lg	167, 210	4.5
trans-Sinapyl alcohol	Lg	167, 210	7.5
Sinapaldehyde	Lg	208	8.1
4-Hydroxy-5,6-dihydro-(2H)-pyran-2-one	Ch	TIC	1
1,4-Anhydroxylopyranose	Ch	TIC	1
1,5-Anhydroarabinofuranose	Ch	TIC	1
1,6-Anhydrogalactopyranose	Ch	60	4,2
5-Hydroxymethyl-2-furaldehyde	Ch	TIC	1
5-Hydroxymethyl-2-tetrahydofuraldehyde-3-one	Ch	TIC	1
1.4-Dideoxy-D-*glycero*-hex-1-enopyranos-3-ulose	Ch	TIC	1
1,6-Anhydroglucopyranose (levoglucosan)	Ch	TIC	1

Lg = lignin, Prot=protein, FA = Ferulic acid, pCA = *p*-Coumaric acid, Ch = carbohydrate, TIC=total ion current

6. Results and discussion

6.1 Applications in pulping chemistry

Wood raw materials for alkaline pulping and pulps after cooking and bleaching were characterized by Py-GC/MS. Observed differences in lignin structure between different wood species and clones based on pyrolysis degradation products were evaluated (Publications I and IV). The structure and quantity of aromatic fibre components were followed during alkaline pulping (Publications I and VI). Carbohydrate composition in eucalypt wood and pulps were determined by Py-GC/MS and the results were compared with those obtained by acid hydrolysis followed by HPLC (Publication VI).

6.1.1 Lignin structure in different wood types (I, IV)

The Py-GC/MS technique makes lignin analysis possible without prior isolation from wood. Lignin degradation products are well separated from the carbohydrate degradation products. This can be seen from pyrograms (Figure 13) of softwood pine (*Pinus silvestris*) (Publication I) and hardwood eucalypt hybrid G1xUGL (*E. grandis* (Coffs Harbour) x [*E. urophylla* (R) x *E. globulus* (R)]), which is one of the eighteen 7-year-old eucalypt hybrids studied as a raw material for pulping (Publications IV and VI). The result in Figure 13 shows that the pyrolysis degradation products of lignin from the softwood pine were mainly guaiacyl type, whereas hardwood eucalyptus lignin produced both syringyl and guaiacyl type degradation products. A few *p*-hydroxyphenyl type degradation products were also detected from both wood types. The side chain structures of guaiacyl type degradation products in both wood types and with syringyl type degradation products were similar. Both wood raw materials showed high contents of oxygen-rich pyrolysis degradation products, referred to as peak numbers 13, 15-16, 18, 20-21, 24-37 in Figure 13. This is due to the high content of phenolic β-O-4 linkages together with cinnamyl and sinapyl alcohol-end groups present in native wood lignin (Akazawa et al., 2016; Brezny et al., 1983; Kuroda, 2000b).

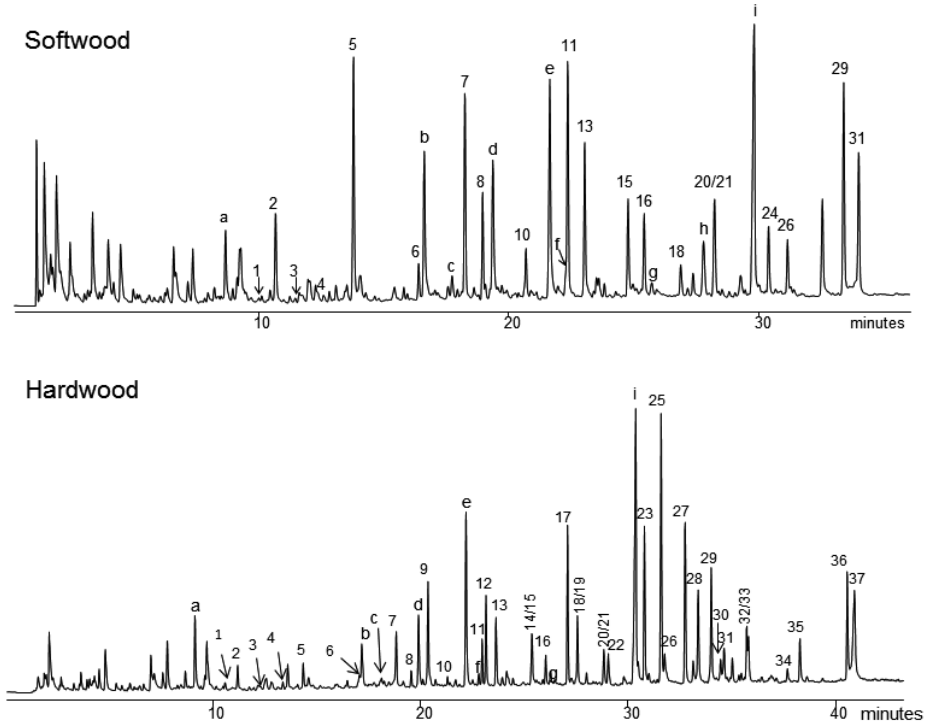

Figure 13. Pyrograms of softwood pine and hardwood eucalypt hybrid G1xUGL (*E. grandis* (Coffs Harbour) x [*E. urophylla* (R) x *E. globulus* (R)]) obtained at 580 °C.

Peak identities of carbohydrate derivatives: a 1,5-Anhydro-4-deoxypent-1-en-3-ulose (xyl); b 5-Hydroxymethyl-2-tetrahydrofuraldehyde-3-one (glc); c 1,5-Anhydroarabinofuranose (ara); d 5-Hydroxymethyl-2-furaldehyde (glc); e 1.4-Dideoxy-D-glycero-hex-1-enopyranose-3-ulose (glc); f 1,5-Anhydroxylopyranose (xyl); g 1,6-Anhydrogalactopyranose (gal); h 1,6-Anhydromannopyranose (man); i 1,6-Anhydroglucopyranose (glc)

Peak identities of lignin derivatives: 1 Phenol (H); 2 Guaiacol (G); 3 2-Methylphenol (H); 4 4-Methylphenol (H); 5 4-Methylguaiacol (G); 6 4-Ethylguaiacol (G); 7 Vinylguaiacol (G); 8 Eugenol (G); 9 Syringol (S); 10 cis-Isoeugenol (G); 11 trans-Isoeugenol (G); 12 4-Methylsyringol (S); 13 Vanillin (V); 14 4-Ethylsyringol (S); 15 Homovanillin (G); 16 Acetoguaiacone (G); 17 4-Vinylsyringol (S); 18 Guaiacylacetone (G); 19 4-Allylsyringol (S); 20 4-(oxy-allyl)guaiacol (G); 21 4-(1-Hydroxyprop-2-enyl)guaiacol (G); 22 cis-Propenylsyringol (S); 23 trans-Propenylsyringol (S); 24 Dihydroconiferyl alcohol (G); 25 Syringaldehyde (S); 26 cis-Coniferyl alcohol (G); 27 Homosyringaldehyde (S); 28 Acetosyringone (S); 29 trans-Coniferyl alcohol (G); 30 Syringylacetone (S); 31 Coniferaldehyde (G); 32 4-(oxy-allyl)syringol (S); 33 4-(1-Hydroxy-prop-2-enyl)syringol (S); 34 Dihydrosinapyl alcohol (S); 35 cis-Sinapyl alcohol (S); 36 trans-Sinapyl alcohol (S); 37 Sinapaldehyde (S)

Hardwood and softwood can easily be distinguished based on the Py-GC/MS results, because the degradation products are different. In this study, the effect of the change of the species in eucalypt hybrids on lignin structure and thereafter lignin degradation products in Py-GC/MS was evaluated. Although the same guaiacyl and syringyl type lignin pyrolysis degradation products were formed, their intensities were changed when one crossing was replaced by another. By subjecting the data (Publication IV, Tables 3 and 4) to principal component analysis (PCA), a clearer indication of the structural variations of lignins between different species was observed. Eucalypt crossings were well separated from each other (a score plot, Figure 14) based on the Py-GC/MS data shown in the loading plot (Figure 15). This supports

the interpretation that original lignin structure varies between eucalypt hybrids. A similar phenomenon has been reported earlier (Prinsen et al., 2012; Rencoret et al., 2008; Yokoi et al., 2001).

Lignin degradation products were divided into four different sides in the loading plot, altering the distribution of eucalypt hybrids in the score plot. In the first principal component direction, lignin degradation products with a carbonyl group (C=O) in the side chain were placed opposite to the degradation product with reduced short side chain (C6-C1 and C6-C2) structures. Potential sources of degradation products with a carbonyl group in the side chain and reduced short side chain structures are expected to be β-O-4 and β-5 substructures, respectively (Brezny et al., 1983; Kuroda and Nakagawa-izumi, 2006; Kuroda, 2000b; Ohra-aho et al., 2000). In the second component direction, eucalypt hybrids were divided based on the frequency of degradation products with and without a hydroxyl group in the propenyl side chain (C6-C3). Coniferyl alcohol and sinapyl alcohol degradation products reflect the presence of cinnamyl and sinapyl alcohol end groups in lignin, but also β-O-4 bond cleavage (Kuroda, 2000b). Formation of propenylphenols in Py-GC/MS has also been linked to cleavage of β-O-4 bonds (Kuroda, 2000b; Watanabe et al., 2009) as a result of water loss from the hydroxyl group present in the α-position of the propenyl chain (Choi et al., 2001; Kawamoto et al., 2008). Propenylphenols have been minor components detected in the pyrolysis of β-O-4 ether type trimeric model compound (Ohra-aho et al., 2000), but present in lignins containing less β-O-4 substructures, such as Kraft lignin (Ohra-aho and Linnekoski, 2015). This indicates that propenylphenols have another origin.

Guaiacyl and syringyl pyrolysis degradation products with equal side chains were correlated (loading plot in Figure 15). This indicates that they have originated from similar substructures present in lignin. The result emphasized the importance of using all the main degradation products for the calculation of S/G ratios, rather than only selected degradation products. Selected guaiacyl and syringyl degradation products with different side chains have been used in previous studies to determine S/G ratios (Lima et al., 2008; Nunes et al., 2010).

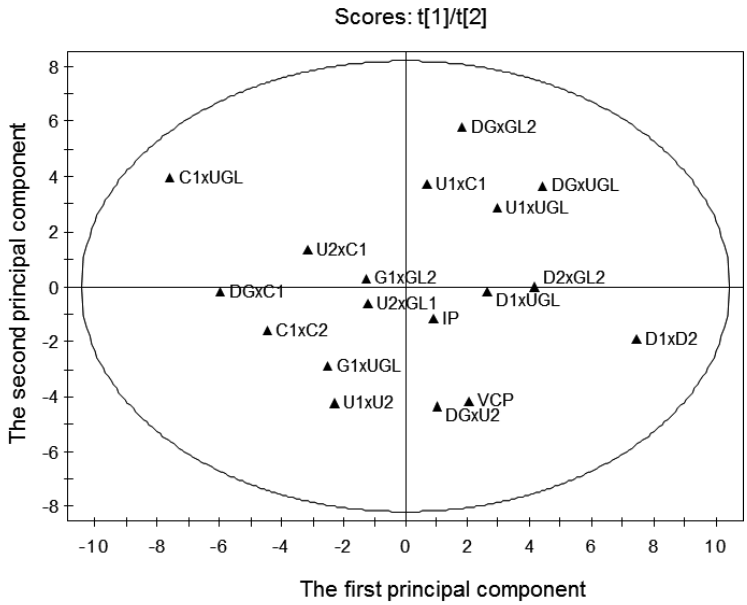

Figure 14. PCA of the pyrolysis data for eucalypt hybrids. The score plot of the two principal components shows how the samples are related to each other. The first principal component described the highest variance (44 %) and the second component the second highest variance (27 %) of the data (Publication VI).

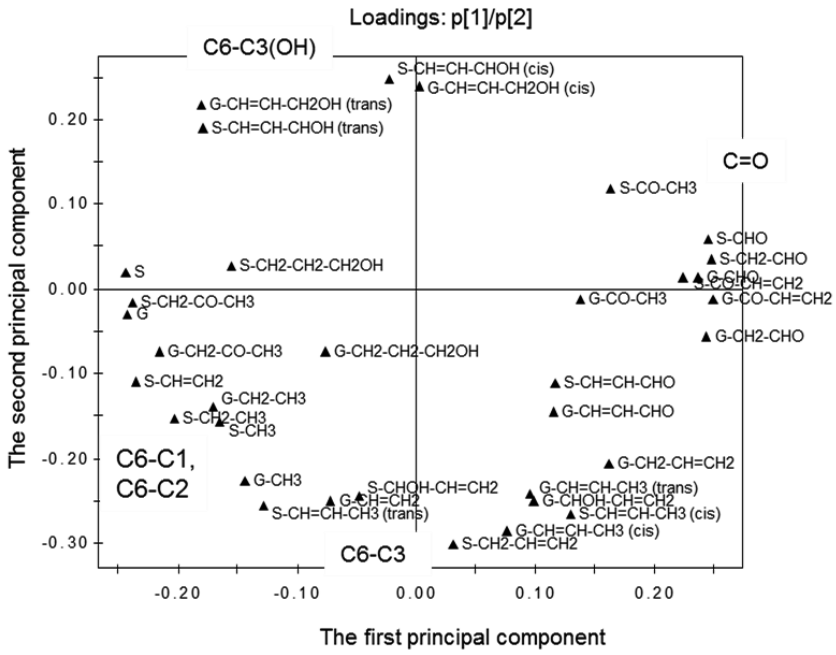

Figure 15. Loading plot describing which guaiacyl (G) and syringyl (S) lignin structural units are important for the classification of samples seen in the Score plot in Figure 14.

6.1.2 Lignin structure in alkaline pulps (I, V)

Eucalypt hybrid E. grandis × [E. urophylla × E. globulus], G1xUGL was used as a feedstock for the production of pulps by soda-AQ and soda-O_2 cooking processes aimed at bioethanol and/or biogas production. In order to better understand the cooking performance, pulps at kappa 50, 35 and 15 were studied in more detail. Residual lignin structure from these pulps was characterised previously after isolation by acidolysis (Prinsen et al., 2013). The aim of this study was to demonstrate the possibility to determine residual lignin from alkaline pulps directly, without lignin isolation by Py-GC/MS. The results of direct analysis of residual lignin from soda-AQ and soda-O_2 pulps have not been published earlier, but the carbohydrate compositions of the same pulps are presented in Publication VI. Due to the decreased lignin content in cooking, degradation products were integrated using selected ions as described in the method section (section 5.1.2).

The main change during cooking was the decrease of the oxygenated pyrolysis degradation products that are typical for native wood lignin (Table 5). The phenomenon was observed already at the early stage of both alkaline cooks of eucalypt wood (k=50). This means that part of the β-O-4 substructures are cleaved already in the early stage, but the degradation reaction continues throughout the cooking time. At the same time, degradation products with short side chains were increased, reflecting the cleavage of lignin side chains in cooking (Fengel and Wegener, 1989). Similar behaviour has been observed from lignins isolated from eucalypt pulps (Prinsen et al., 2013). The proportion of phenylpropenyls increased abundantly in the impregnation stage, but by the final stage the structures were reduced to the same level as in the wood. The total proportion of carbonyl type structures was rather stable during cooking, although some changes were observed inside the carbonyl type structures. As a result of added oxygen at higher kappa values, a slightly higher proportion of carbonyl type structures was observed in soda-O2 than in soda-AQ pulps. Otherwise the changes in lignin structure were similar with both cooking types.

The result for unbleached softwood Kraft pulp (result in Publication I, and section 6.1.3) was compared with that for both unbleached alkaline hardwood pulps. Similar changes in guaiacyl type lignin degradation products were observed in unbleached softwood Kraft pulp as in both alkaline hardwood pulps in the final cooking stage (Table 5). This indicates that similar types of reaction are taking place in all types of cooking processes.

Table 5. Distribution of guaiacyl and syringyl type lignin pyrolysis degradation products (after normalization to 100 %) in eucalypt wood (G1xUGL) and soda-AQ and soda-O_2 alkaline pulps, at kappa 50, 35 and 15.

	Wood	Soda-AQ			Soda-O2		
Peak Name	G1xUGL	k=50	k=35	k=15	k=50	k=35	k=15
Phenol	0.2	0.7	1.2	2.6	0.8	1.3	2.4
2-Methylphenol	0.1	0.3	0.5	1.0	0.4	0.6	1.1
4-Methylphenol	0.2	0.6	0.9	1.6	0.7	1.0	1.8
Guaiacol	1.1	1.6	3.1	2.0	1.8	2.0	2.1
4-Methylguaiacol	1.0	1.5	1.7	1.8	1.7	1.9	2.0
4-Ethylguaiacol	0.1	0.4	0.4	0.5	0.4	0.5	0.5
4-Vinylguaiacol	2.8	3.5	3.7	4.2	4.2	4.7	4.8
Eugenol	0.6	1.0	0.9	0.8	1.0	1.0	0.9
cis-Isoeugenol	0.4	0.6	0.6	0.0	0.6	0.6	0.4
trans-Isoeugenol	2.2	2.8	2.6	1.7	2.7	2.7	1.8
Vanillin	2.8	2.5	2.1	2.1	2.6	2.5	1.9
Homovanillin	2.5	2.9	2.7	5.4	4.1	4.4	5.8
Acetoguaiacone	1.1	1.4	1.3	1.1	1.5	1.4	1.1
Guaiacylacetone	0.4	0.9	1.0	1.6	1.6	1.8	2.0
4-(Oxy-allyl)guaiacol	1.4	0.6	0.5	0.0	0.5	0.4	0.0
4-(1-Hydroxyprop-2-enyl)guaiacol	0.7	0.6	0.6	0.0	0.6	0.6	0.0
Dihydroconiferyl alcohol	0.4	0.4	0.4	0.0	0.4	0.4	0.0
cis-Coniferyl alcohol	0.8	0.5	0.4	0.0	0.4	0.3	0.0
trans-Coniferyl alcohol	6.4	0.6	0.3	0.0	0.4	0.3	0.0
Coniferaldehyde	2.5	1.0	0.9	0.0	1.0	1.1	0.0
Syringol	5.4	6.2	7.6	9.9	6.0	6.9	8.6
4-Methylsyringol	3.7	5.2	5.8	6.1	5.0	5.4	6.0
4-Ethylsyringol	1.0	1.0	1.2	1.5	1.1	1.2	1.6
4-Vinylsyringol	7.6	9.6	10.3	10.2	9.3	9.8	9.9
4-Allylsyringol	2.9	4.3	3.9	2.5	3.7	3.3	2.7
cis-Propenylsyringol	1.6	3.1	2.9	1.5	2.6	2.2	1.7
trans-Propenylsyringol	6.3	10.9	10.3	5.3	8.8	7.8	5.3
Syringaldehyde	10.9	8.4	7.5	7.9	7.2	6.3	6.4
Homosyringaldehyde	6.5	11.6	10.8	18.9	14.7	14.7	18.7
Acetosyringone	3.8	4.7	4.6	4.8	4.3	4.2	4.7
Syringylacetone	1.5	3.1	3.4	4.0	4.3	4.8	4.8
Propiosyringol	0.3	0.4	0.5	0.0	0.4	0.4	0.0
4-(Oxy-allyl)syringol	2.8	1.2	0.9	0.0	0.8	0.5	0.0
4-(1-Hydroxy-prop-2-enyl)syringol	3.1	1.5	1.4	1.0	1.3	1.1	1.1
Dihydrosinapyl alcohol	0.7	0.4	0.2	0.0	0.3	0.0	0.0
cis-Sinapyl alcohol	2.2	0.5	0.4	0.0	0.3	0.0	0.0
trans-Sinapyl alcohol	6.1	0.0	0.0	0.0	0.0	0.0	0.0
Sinapaldehyde	5.9	3.7	2.6	0.0	2.9	2.1	0.0

6.1.3 Lignin structure in bleached pulps (I)

Residual lignin structure in a light ECF bleaching of pine pulps was monitored directly from pulps by Py-GC/MS without lignin isolation. As in the case of unbleached hardwood pulps, method sensitivity was increased using selected mass fragments for the integration of lignin degradation products instead of TIC (Publication I, section 5.1.2). Changes in softwood lignin structure along with delignification and bleaching were followed using guaiacyl type degradation products.

Figure 16 shows distributions of guaiacyl type degradation products after the normalization to 100 % after cooking and at different stages of delignification. The proportion of propenylphenols (eugenol, *cis*-isoeugenol and *trans*-isoeugenol), which was slightly increased at the beginning of cooking (section 6.1.2), was constant throughout the whole bleaching sequence. The main change after the cooking was an increase of carbonyl-type degradation products (vanillin, homovanillin, acetoguaiacone), whereas the proportion of short side chain structures (guaiacol, 4-methylguaiacol and 4-vinylguaiacol), which were abundant in unbleached pulp, was decreased during delignification and bleaching. This indicates that the bleaching chemicals readily leached the lignin structures which had reacted during cooking, leaving the native type lignin structures present in pulp residual lignin intact. Thus, bleaching enriches the proportion of native type lignin. The results of the residual lignin isolated from a fully bleached eucalypt pulp supported this finding (Ibarra et al., 2005).

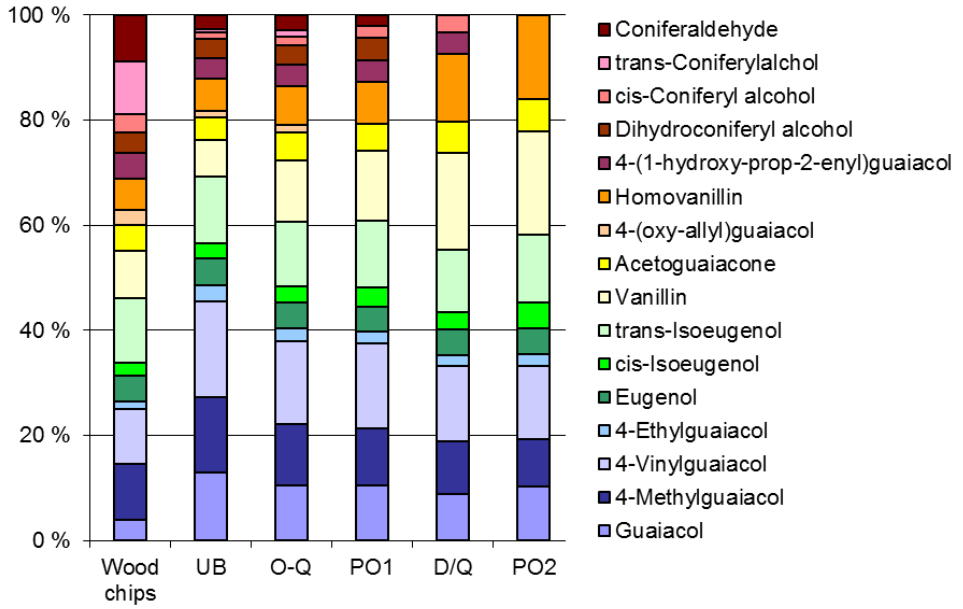

Figure 16. Distribution of guaiacyl-type lignin pyrolysis degradation products (after normalization to 100%) in pine wood chips and pulps after cooking (UB) and different ECF bleaching stages.

6.1.4 Determination of lignin substructures (S/G/H) (I, IV)

The S/G/H ratio is an important parameter to be measured from wood feedstocks intended for pulping, due to the different reactivities of substructures. The syringyl substructures have higher reactivity in alkaline pulping conditions than guaiacyl substructures (Tsutsumi et al., 1995). An increased pulp yield has been obtained for eucalypt wood with higher S/G ratios

(del Río et al., 2005). The S/G ratio also affects the alkali charge necessary to obtain the required lignin content in Kraft pulping (Reina et al., 2014). The reactivity of *p*-hydroxyphenyl type substructures in wood has been found to be lower in comparison to guaiacyl type units (Akim et al., 2001). The high enrichment of *p*-hydroxyphenyl type units has been evident in both softwood and hardwood pulps after alkaline cooking stages (Poppius-Levlin et al., 2001; Prinsen et al., 2013; Tamminen et al., 2003a).

The lignin substructures were followed in greater detail in two Publications I and IV. Publication IV reports the S/G/H ratio, particularly the S/G ratio determination from the various eucalypt hybrids used as feedstocks for pulp production. The aim was to evaluate the suitability of Py-GC/MS to determine S/G ratios from wood feedstocks in comparison to the most commonly used alkaline nitrobenzene oxidation method. Publication I reports results according to which high enrichment of *p*-hydroxyphenyl substructures was observed in comparison to the guaiacyl substructures during cooking and especially delignification of pine wood pulp. For a deeper analysis of the possible origin of *p*-hydroxyphenyl substructures, thermochemolysis with TMAH and fractionated pyrolysis were applied.

Eucalypt raw materials

Lignin substructures (S/G/H) have been determined most commonly by the oxidative degradation of lignin followed by analysis of the products. Suitable methods in alkaline media are nitrobenzene oxidation, oxidation with metal oxides such as cupric oxide, or with potassium permanganate followed by hydrolysis and methylation (Schultz and Templeton, 1986; Sun et al., 1995; Xie, 2004). Degradation products are aldehydes and aromatic acids that can be determined by chromatographic methods. A disadvantage of these methods is long and laborious sample preparation. An alternative method used for the determination of lignin substructures is Py-GC/MS, because time-consuming sample preparation is not needed (Izumi et al., 1995a; Izumi and Kuroda, 1997).

The lignin substructures (S/G/H) from the hardwood were in general determined as the S/G ratio, as also reported in Publication IV. The proportion of *p*-hydoxyphenyl structures in the studied eucalypt hybrids were low, varying from 0.3 to 0.5 %. This was one reason why only guaiacyl and syringyl type degradation products were used for the determination of lignin substructures, but also because part of the *p*-hydroxyphenyl structures may originate from other structures than lignin (Publication I, Böttcher 1993). Based on the result obtained in the principal component analysis (Figure 15), all the guaiacyl and syringyl type degradation products were used to determine S/G ratios.

Figure 17 shows that the S/G ratios determined by Py-GC/MS varied from 1.9 to 3.1 among eucalypt hybrids. Rather higher S/G ratios from 2.7 to 4.0 were determined by alkaline nitrobenzene oxidation. Similar results obtained by Py-GC/MS and alkaline nitrobenzene oxidation have been reported earlier (Izumi et al., 1995a; Nunes et al., 2010). The differences between these two methods are related to different degradation mechanisms of lignin by Py-GC/MS and alkaline nitrobenzene oxidation. In alkaline nitrobenzene oxidation, lignin is oxidatively cleaved to form mainly syringylaldehyde and vanillin from syringyl and guaiacyl β-O-4 substructures, respectively. Thus the method is indicative for the non-condensed lignin units that are more prevalent among syringyl than guaiacyl type substructures (Xie 2004). In pyrolysis, mixtures of phenols are formed as a result of cleavage of β-O-4 and some condensed linkages using thermal energy. Degradation of non-condensed lignin units is favoured in alkaline nitrobenzene oxidation methods, but also in Py-GC/MS. Thus both methods over-

estimate the actual S/G ratios, especially the syringyl substructures present in lignin. However, in Py-GC/MS the overestimation is smaller due to the cleavage of some condensed linkages present mainly in guaiacyl type lignin substructures.

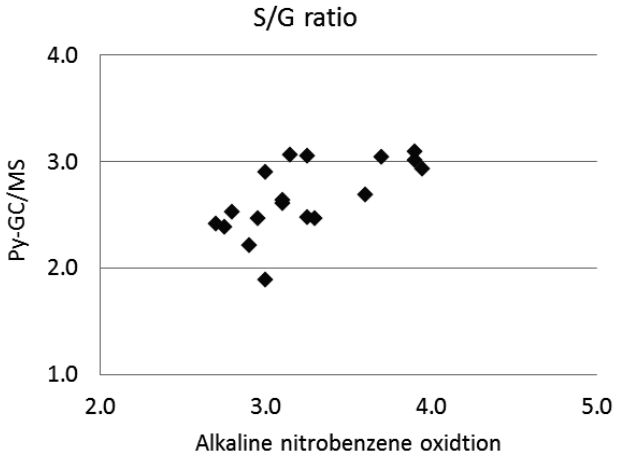

Figure 17. S/G ratios determined by Py-GC/MS and alkaline nitrobenzene oxidation methods for 18 Eucalypt crossings.

Pulps after cooking and delignification

The number of *p*-hydroxyphenyl type degradation products detected from both wood raw materials and pulps was lower in comparison to the guaiacyl and syringyl type degradation products, as shown in Table 5 and Figure 18. The proportion of *p*-hydroxyphenyl substructures was also minor (< 1 %) in wood feedstocks in comparison to the guaiacyl or guaiacyl and syringyl type substructures. However, after the soda-AQ and soda-O2 cooking series of eucalypt wood, p-hydroxyphenyl type degradation products were enriched to 5% (Table 5). In unbleached softwood Kraft pulp, the enrichment was to 10% and was even more striking in fully bleached pulp at over 35 % (Figure 18). The result in Figure 18 shows that all three *p*-hydroxyphenyl structures (phenol, 2-methylphenol and 4-methylphenol) were enriched in delignification. However, the proportions of the corresponding guaiacyl structures (guaiacol and 4-methylguaiacol) were simultaneously decreased. The distinctive behaviour of *p*-hydroxyphenyl structures in comparison to guaiacyl structres during cooking and bleaching support the interpretation that the *p*-hydroxypenyl structure may also have other sources than lignin. Other wood components that have been reported to form phenols and methylphenols in pyrolysis are polysaccharides after alkaline pulping (Ziobro, 1990) and at high temperature (Higman et al., 1970), proteins and amino acids (Choi et al., 2001; Higman et al., 1970; Kleen et al., 2003). Phenolic extractives also form phenol (Ohara et al., 2003).

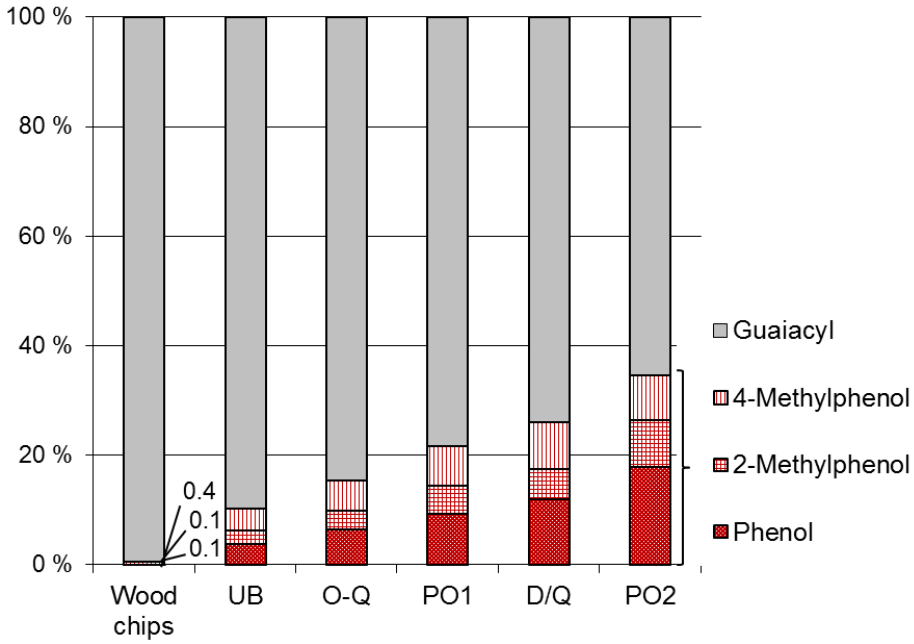

Figure 18. Distribution of lignin substructures (H and G) during a light ECF bleaching of pine pulp (Publication I).

Thermochemolysis in the presence of TMAH was used to evaluate whether the *p*-hydroxyphenyl structures originate in existing aromatic substructures or non-aromatic structures (Publication I). As a result of derivatisation with TMAH, degradation products formed in conventional pyrolysis are converted to their methylated counterparts (Challinor, 1995; del Río et al., 1996). *p*-Hydroxyphenyl and guaiacyl type methylated derivatives 4-methoxy benzoic acid methyl ester and 3,4-dimethoxy benzoic acid methyl ester were detected, respectively. These methylated derivatives were detected from both unbleached and fully bleached pulps, as presented in Figure 19. The yield (peak area) of the 4-methoxybenzoic acid methyl ester was the same in unbleached and fully bleached pulp, whereas the yield of 3,4-dimethoxy benzoic acid methyl ester was decreased. This result is in accordance with Py-GC/MS results obtained without derivatisation (Figure 18). Similar behaviour of *p*-hydroxyphenyl and guaiacyl type degradation products with and without derivatisation supports the interpretation that *p*-hydroxyphenyl substructures have aromatic origin, and are not secondary pyrolysis products.

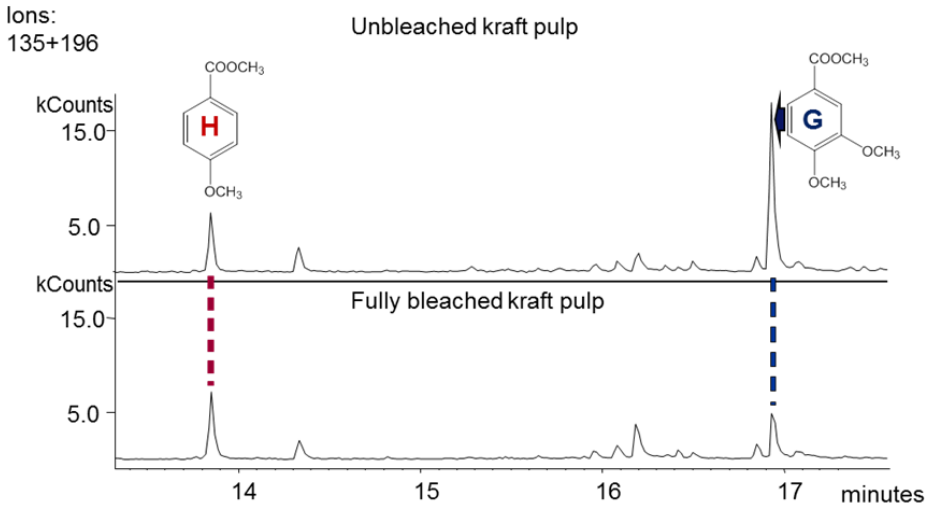

Figure 19. Pyrolysis degradation products obtained from an unbleached and a fully bleached pulp using thermochemolysis with TMAH at 400 °C. Thermochemolysis products with TMAH were methoxybenzoic acid methyl ester and dimethoxybenzoic acid methyl ester (Publication III).

Fractionated pyrolysis, which was used in Publication I, is one potential method to study lignin substructures (S/G/H). The method makes it possible to study the degradation behaviour of sample components as a function of temperature (Selsbo et al., 1997). It has been used to study the possible bonds formed during pulping among the added chemicals and pulp components (Kleen et al., 2003; Selsbo et al., 1997). In Publication I, fractionated pyrolysis was applied to clarify the origin of the *p*-hydroxyphenyl type substructures. Fully bleached pulp was subjected to fractionated pyrolysis due to its observed highest proportion of *p*-hydroxyphenyl type degradation products of aromatic structures (34 %).

The degradation of *p*-hydroxyphenyl and guaiacyl type substructures together with degradation of cellulose and hemicelluloses in fully bleached pulp as a function of temperature is presented in Figure 20. Formation of guaiacyl and *p*-hydroxyphenyl substructures as a function of temperature clearly differed from each other, but also from the degradation of cellulose and hemicelluloses (not previously reported). Release of guaiacyl type degradation products started and ended at lower temperatures than the *p*-hydroxyphenyl type degradation products. High levels of *p*-hydroxyphenyl type degradation products were released at a temperature of 620 °C, at which only a small quantity of guaiacol was detected of the guaiacyl type degradation products, but also at the highest temperature (800 °C), at which no guaiacyl type degradation products were released. In fully bleached pulps, degradation of cellulose and hemicelluloses follow each other closely up to 620 °C. At that temperature, no degradation products of hemicelluloses were detected, whereas some degradation products of cellulose were still present. Degradation of cellulose continued up to highest temperature (800 °C), as did the formation of *p*-hydroxyphenyl type degradation products. A small quantity of phenol, but not of other aromatics, has been detected from Avicel, pure microcrystalline cellulose, in Py-GC/MS (Tamminen, Ohra-aho, et al. 2003). However, under pulping conditions other phenolic structures are also known to be formed from polysaccharides (Ziobro 1990). Higher enrichment of *p*-hydroxyphenyl structures in pulps, as in the corresponding isolated residual lignin, also supports this phenomenon (Tamminen et al., 2003a). Other possible

sources than polysaccharides for *p*-hydroxypehnyl type degradation products could be plant proteins, which degrade to the same *p*-hydroxyphenyl structures as have been detected from the studied pulps, but also to other nitrogenous compounds (1H-pyrrole-2,5-dione, indole and 2-methylindole). Thermal degradation of these protein-based nitrogenous compounds determined by fractionated pyrolysis is similar to that of *p*-hydroxyphenyl type degradation products in pulps (Kleen et al., 2003). However, nitrogenous compounds were not detected from the fully bleached pulps subjected to fractionated pyrolysis. Based on this result, protein as a source of *p*-hydroxyphenyl structures in pulps can be excluded.

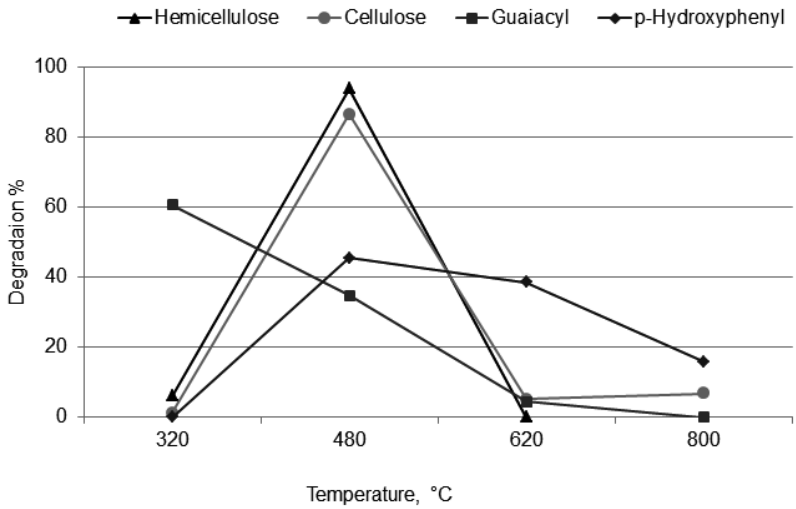

Figure 20. Degradation of guaiacyl and *p*-hydroxyphenyl type substructures as well as cellulose and hemicelluloses of fully bleached pulp as a function of temperature after laboratory oxygen delignification and ECF bleaching of spruce Kraft pulp.

6.1.5 Quantity of lignin in pulps after cooking and bleaching (I, IV)

Quantitative analysis of lignin or other natural polymers by Py-GC/MS is more complex in comparison to synthetic polymers, due to the difficulties in finding suitable standards for calibration. Quantitative methods have been reported in the literature in which the amount of each degradation product is calculated separately using the corresponding pure compounds for calibration (Izumi et al., 1995b) or using one monomeric compound as an internal standard (Bocchini et al., 1997). However, this underestimates the lignin content, due to the formation of compounds not detectable by GC/MS. Other approaches to the quantification of lignin from softwood and pulps have been to divide lignin degradation products by all the degradation products (lignin and carbohydrates) present in the pyrogram (Alves et al., 2006) and to predict the lignin content from pyrolysis data with aid of a multivariate calibration model (Kleen et al., 1993). The approach of the study presented in Publication I was to use a standard for lignin calibration that behaved similarly to the studied material. The distribution of degradation products formed from softwood Kraft lignin was closest to that for pulp lignin (Poppius-Levlin et al., 2001). Milled wood lignin was rejected due to its high content of native type structures present in lignin. In order to obtain information concerning the possible applicability of the Py-GC/MS method, comparison of the results with lignin contents calculated from lignin kappa values was performed. In the kappa number analysis the con-

sumption of potassium permanganate during oxidation of pulp under standardised conditions is measured. Lignin can be calculated from the kappa number using an earlier defined constant (Fengel and Wegener, 1989). In addition to lignin, hexenuronic acid formed from hemicelluloses during pulping also contribute to the kappa number. As a result the hexenuronic acids content must be reduced from the kappa number before its conversion to lignin content (Li and Gellerstedt, 1997).

Lignin quantitation was based on the one point external standard calibration method, assuming that the sum of peak areas of lignin degradation products of the external standard is 100 %. *p*-Hydroxyphenyl and guaiacyl type degradation products (Figure 16 and Figure 18) were integrated and the sum of the peak area was normalized to the weight of the sample. Thereafter the lignin contents of the unbleached pulp and a light ECF delignified softwood pulp were calculated and compared with lignin values calculated from lignin kappa number. Good correlation among the methods was obtained (Figure 21), although in unbleached pulp the quantity of pyrolysis lignin was lower and in fully bleached pulp samples higher than lignin kappa. In Py-GC/MS, known aromatic pyrolysis degradation products are used to determine the lignin content. However, all components that are oxidized by potassium permanganate, not only lignin, will increase the Kappa number (Li et al., 2002; Li and Gellerstedt, 2002). Pulps after cooking and the first delignification stage may contain higher levels of non-lignin structures, which may increase the lignin value estimated from the kappa number more than after further delignification stages. For the fully bleached pulps, a higher lignin content was obtained by Py-GC/MS than from the kappa number. This is probably due to the fact that *p*-hydroxyphenyl type units originating from other sources than lignin increase the apparent lignin content as determined by Py-GC/MS, but also because all lignin fragments in pulps do not react in kappa number determination, thus lowering the lignin content estimated from the kappa number (Tamminen et al., 2003b).

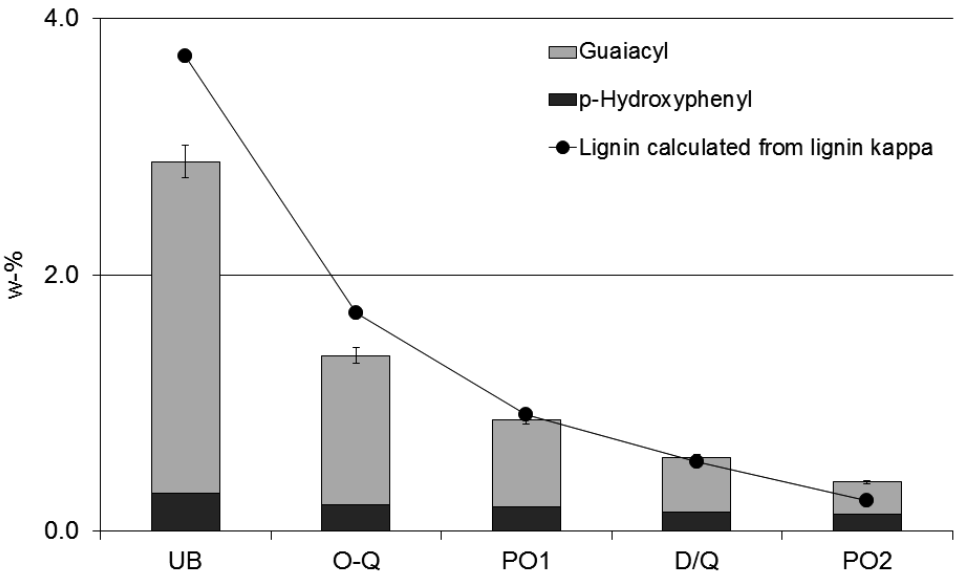

Figure 21. Quantity of *p*-hydroxyphenyl and guaiacyl type pyrolysis degradation products in pulps measured by Py-GC/MS. Lignin content in pulp was calculated from the lignin kappa value, multiplying lignin kappa by 0.15 % (Publication I).

6.1.6 Carbohydrate composition in wood and pulps (VI)

Acid hydrolysis followed by high performance anion exchange chromatography with pulsed amperometric detection (HPAEC-PAD) is the commonest method to determine carbohydrate composition as monosaccharides from fibre materials. Py-GC/MS is an alternative method to determine carbohydrate composition. In pyrolysis, cellulose and hemicelluloses are degraded to stable anhydrosugars, such as 1,6-anhydromannopyranose, 1,6-anhydrogalactopyranose, 1,6-anhydroglucopyranose, 1,5-anhydroarabinofuranose and 1,4-anhydroxylopyranose, but furans, pyrans, light oxygenates and gases are also formed. Even incomplete formation of anhydrosugars has successfully been used to determine carbohydrate composition from pulp fibres via multivariate calibration against reference data (Kleen et al., 1993) and also direct comparison of peak areas (Syverud et al., 2003). The advantage of Py-GC/MS in comparison to acid hydrolysis is that fibre-based materials can be analysed without milling (Syverud et al., 2003) and extractives removal (Barbosa et al., 2008).

In the study presented in Publication VI, the relative carbohydrate compositions of various eucalypt species were determined by Py-GC/MS. In addition, pulps produced from the same species by soda-AQ and soda-O_2 processes were analysed similarly. The results were compared with those obtained by acid hydrolysis followed by HPLC. As described in the experimental part (section 5.1.2), carbohydrate composition was calculated in two ways both in the wood and pulp samples. In the method A, glucose content was calculated including only 1,6-anhydroglucopyranose, as has been done earlier for pulp samples (Kleen et al., 1993; Syverud et al., 2003) and in method B the glucose content was calculated including 1,6-anhydroglucopyranose and three other main cellulose degradation products 5-hydroxymethyl-2-tetrahydofuraldehyde-3-one, 5-hydroxymethyl-2-furaldehyde and 1.4-dideoxy-D-*glycero*-hex-1-enopyranos-3-ulose. For the wood samples the method A gave values 51.3–64.1 % for glucose and 33.0–46.5 % for xylose, whereas the method B gave values 67.9–78.2% for glucose and 19.4–30.6% for xylose. The absolute values determined by method B were closer to the values obtained by acid hydrolysis (74.1–78.6 % for glucose and 16.7–22.6 % for xylose). In the case of pulp samples the method A gave closer values (85.5 - 91.2 % for glucose and 8.8 – 14.5 % for xylose) than method B (91.2 – 94.3 % for glucose and 5.7 – 8.8 % for xylose) to those obtained with acid hydrolysis (84.4 – 88.7 % for glucose and 11.3 – 15.6 % for xylose). This was opposite to the results obtained for the wood samples, but well in accordance with the results presented for the pulp samples in earlier Publications (Kleen et al., 1993; Syverud et al., 2003).

Figure 22 shows that the linear relationship between the relative glucose and xylose contents among the Py-GC/MS results calculated by method A or method B and acid hydrolysis in the whole sample set was poor for the wood samples. A similar phenomenon was observed for the arabinose and galactose that were present in lower amounts in wood (not shown). For the pulp samples the correlation between the two methods was good. Py-GC/MS methods A and B gave similar correlation results, as shown in Figure 23. This is consistent with earlier reports (Kleen et al., 1993; Syverud et al., 2003). The correlation among the methods was improved when different types of cooks (soda-AQ and soda-O_2) were followed separately as shown in Figure 23. These results indicate that the degradation behaviour of cellulose and hemicelluloses in pyrolysis are different in wood than in pulp. The lignin content is much higher in wood than in pulp samples, which may affect the thermal behaviour of carbohydrates, especially of xylan, that is partly linked with lignin (Pinto et al., 2002). Additionally, cooking changes the xylan structure, releasing the acetyl and uronic acid groups of xylan.

These changes have been proposed to make xylan thermally more stable in pulp than in wood (Oudia et al., 2007).

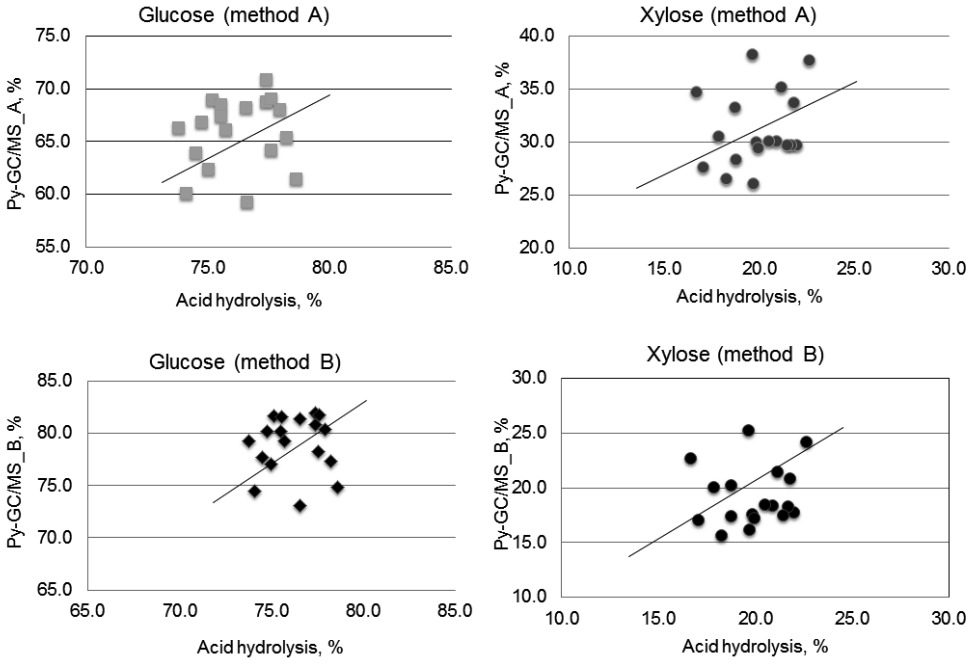

Figure 22. Comparison of relative glucose and xylose contents between Py-GC/MS and acid hydrolysis followed by HPLC from eucalypt hybrids. In method A, carbohydrate composition was calculated from Py-GC/MS data including only 1,6-anhydroglucopyranose for the glucose content. In method B (Publication VI), relative carbohydrate composition was calculated from Py-GC/MS data including 1,6-anhydroglucopyranose; 5-hydroxymethyl-2-tetrahydofuraldehyde-3-one; 5-hydroxymethyl-2-furaldehyde and 1.4-Dideoxy-D-glycero-hex-1-enopyranos-3-ulose for the glucose content

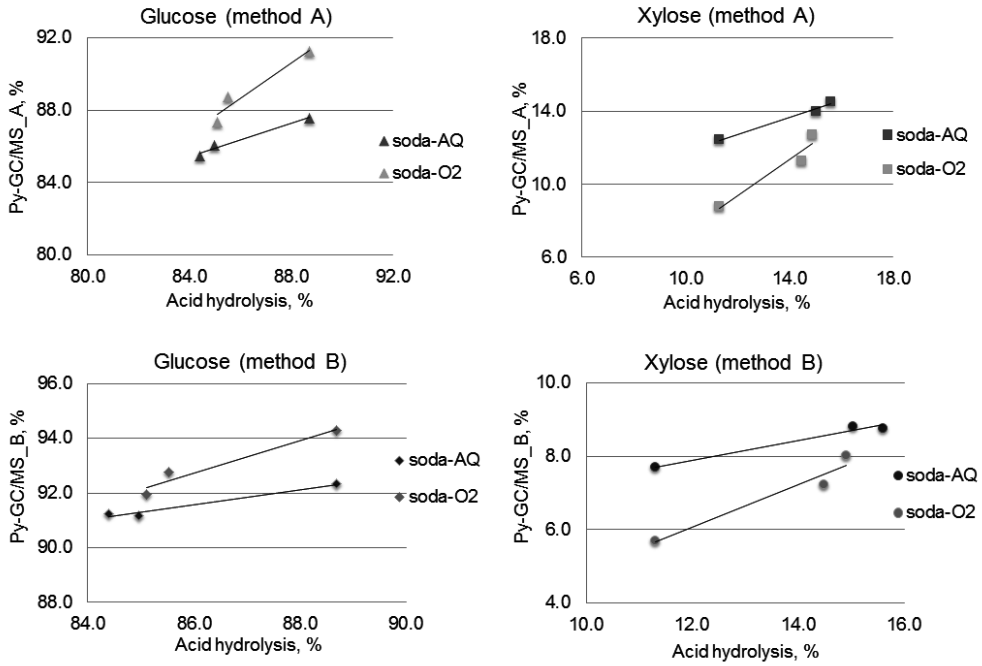

Figure 23. Comparison of relative glucose and xylose contents between Py-GC/MS and acid hydrolysis followed by HPLC from different cooking stages of soda-AQ and soda-O2 pulps. Raw material was the same for both pulps (E. grandis (Coffs Harbour) x [E. urophylla (R) x E. globulus (R)]. In method A, carbohydrate composition was calculated from Py-GC/MS data including only 1,6-anhydroglucopyranose for the glucose content. In method B, relative carbohydrate composition was calculated from Py-GC/MS data including 1,6-anhydroglucopyranose; 5-hydroxymethyl-2-tetrahydofuraldehyde-3-one; 5-hydroxymethyl-2-furaldehyde and 1.4-Dideoxy-D-glycero-hex-1-enopyranos-3-ulose for the glucose content (Publication VI).

In this study, fractionated pyrolysis was applied in order to find an explanation for the observed difference in the degradation behaviours of carbohydrates in wood and pulp samples. Two eucalypt hybrids, G1xUGL and C1xUGL, as well as soda-O2 pulp cooked from G1xUGL (kappa 15), were selected for the fractionated pyrolysis. Degradation behaviour of the carbohydrates and lignin was followed. Thermal stability of hemicelluloses was lower in comparison to lignin and cellulose in the wood samples (G1xUGL and C1xUGL), as shown in Table 6. This is in accordance with earlier results reported in the literature (Shen et al., 2010; Yang et al., 2007). The thermal behaviour of cellulose was similar both in wood and pulp samples, whereas cooking clearly increased the thermal stability of lignin and especially of xylan (Table 6). Release of acetyl and methylglucuronic acid side groups has been reported to occur at a lower temperature than degradation of the xylan chain (Shen et al., 2010). Cooking releases side groups of xylan (Pinto et al., 2002), which increases the thermal stability of xylan in pulp. This has earlier been verified by thermogravimetry (Oudia et al., 2007). In conclusion, in the pulp sample xylan, lignin and cellulose were degraded mainly at one temperature (450 °C), whereas in wood samples the degradation of xylan and lignin occurred more clearly at a lower temperature than cellulose. Thermal degradation of all fibre components was closer to each other in pulp than in wood samples.

Table 6. Thermal behaviour of carbohydrates and lignin in eucalypt hybrids (C1xUGL and G1xUGL) and soda-O2 pulp (k=15) of G1xUGL, determined by fractionated pyrolysis (Publication VI).

	C1xUGL				G1xUGL				soda-O_2 pulp of G1xUGL			
Temp., °C	320	450	580	800	320	450	580	800	320	450	580	800
Time, s	44	16	4	2	44	16	4	2	44	16	4	2
Xylose	42.9	57.1	0.0	0.0	44.1	55.9	0.0	0.0	1.3	98.7	0.0	0.0
Arabinose	100.0	0.0	0.0	0.0	100.0	0.0	0.0	0.0	0.0	0.0	0.0	0.0
Galactose	55.4	44.6	0.0	0.0	43.3	56.7	0.0	0.0	0.0	0.0	0.0	0.0
Glucose	2.2	97.1	0.6	0.1	2.3	97.4	0.3	<0.1	0.1	99.4	0.4	0.1
Lignin	28.2	71.1	0.7	0.1	24.2	74.7	1.0	0.1	5.9	89.8	4.2	0.2

6.2 Lignin utilization

Concern due to increasing greenhouse gas emissions and diminishing fossil resources has increased the impetus towards using renewable resources. Lignin, as the largest natural source of aromatics, has been seen as a promising resource for renewable materials, chemicals and fuels. However, its complex structure has made its utilisation difficult without any modification. In this study, the structures of Kraft lignins from different sources were characterised with various analytical pyrolysis techniques with the aim of using the lignin for composites and barriers. The main problem that has been encountered in applying Kraft lignin as such, or in the processing of Kraft lignin at high temperatures, is the release of odorous volatile organic compounds (VOCs). A thermal desorption method was utilised for the evaluation of Kraft lignin quality intended for composites (Publication II). Esterification is one potential way to modify lignin and especially improve its film forming ability (Hult et al., 2013). The potential of the use of thermochemolysis to determine the degree of esterification of fatty acid modified lignins was evaluated in Publication III. The method evaluation was carried out with model compounds representing aliphatic and aromatic esters of modified lignin.

Brewers Spent Grain (BSG), a by-product generated in the brewing industry, is one new alternative lignin source. However, the structure of non-wood plant biomass such as BSG differs from wood structure, containing ferulic and *p*-coumaric acid units among lignin and cellulose, together with protein. Thus its composition is more complex, which makes lignin isolation and characterisation more challenging. Py-GC/MS with and without methylation was utilized as a direct method to obtain structural information concerning BSG and its lignin-rich fractions (VI).

6.2.1 Thermal desorption method for lignin quality control (II)

The thermal desorption method has been utilized as a part of fractionated pyrolysis to separate volatiles from the polymeric material (Kleen et al., 2003). In the current study, thermal desorption was used as an individual method for the analysis of volatile organic compounds (VOCs) released from the Kraft lignins in conditions simulating the temperature in thermoplastic processing. The pyrolysis unit was selected for thermal desorption analyses because it was possible to use a much wider and higher temperature range than is possible in other methods (static headspace, dynamic headspace) generally used to determine VOCs (Koning et al., 2009). Two classes of odorous compounds with low odour threshold values have been

defined from Kraft lignins: phenolic structures of lignin and other aliphatic thiols formed in cooking (Karnofski, 1975).

Two softwood Kraft lignins (StoraEnso = SE and Indulin AT) from different sources were treated under oxidative conditions with and without enzymes (Laccase MaL from *Melanocarpus albomyces (Ma)* and sulfhydryl oxidase AoSOX1 from *Aspergillus oryzae (Ao)*) in order to reduce VOCs. The conditions used for the oxidative treatments are presented in Publication II in more detail. After the treatments, VOCs were measured at two separate temperatures, 150 °C and 190 °C. The lower temperature was selected because it is close to the softening temperature of Kraft lignin (Ropponen et al., 2011), whereas the higher temperature was closer to the thermoplastic processing temperature. Two heating times, 5 and 10 minutes, were tested prior to selection of the final thermal desorption temperature. At the lower temperature, the longer heating time did not increase VOC formation, whereas at the higher temperature the average increase of VOCs was 17 %. The shorter time was selected in order to avoid secondary reactions during heating. Figure 24 shows the main VOCs released from references and treated Kraft lignins at 150 °C and 190 °C. More VOCs were released at the higher temperature, especially lignin-related monomers. It is obvious that at 190 °C, lignin degradation may already be taking place (Kawamoto, 2017; Ropponen et al., 2011). Sulphur compounds and lignin-related monomers were the main volatiles released at both temperatures from SE lignins, but at 190 °C the odorous carbohydrate derivative 2-cyclopenten-1-one-3-ethy-2-hydroxy was also detected (Niemelä, 1988). There was some variation in VOC formation between different treatments of SE lignin, but only oxygen treatment without enzyme at pH 10.7 clearly reduced VOC formation. Lower amounts of odorous sulphur compounds and only a few lignin-based compounds were released from Indulin AT in comparison to SE lignin.

The amount of guaiacol was determined quantitatively, due to the facts that it was present in the highest amount and has a low odour threshold value (3-21 ppb). The result showed that the treatments clearly reduced guaiacol formation from both lignins (Figure 25). However, the amount of guaiacol released from the lignins remained far above its odour threshold value. The difference in odour values evaluated for the untreated and treated samples was minor (Publication II, Figure 21). However, the obtained odour values decreased simultaneously with decreasing VOCs released from the sample.

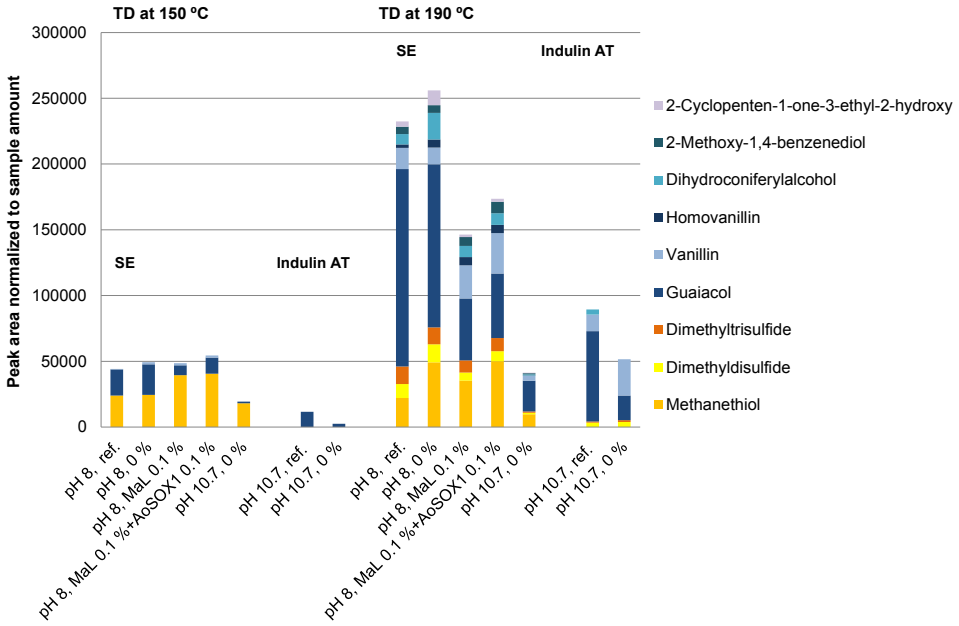

Figure 24. Main volatiles released from freeze-dried SE lignin and Indulin AT samples at 150 °C and 190 °C after oxidative treatments with and without enzymes (*Laccase MaL from Melanocarpus albomyces (Ma) and sulfhydryl oxidase AoSOX1 from Aspergillus oryzae (Ao)*). Reference sample (ref.) was not O_2 boosted and all other samples are O_2 boosted with laccase dose (0.1%) or without (0%).

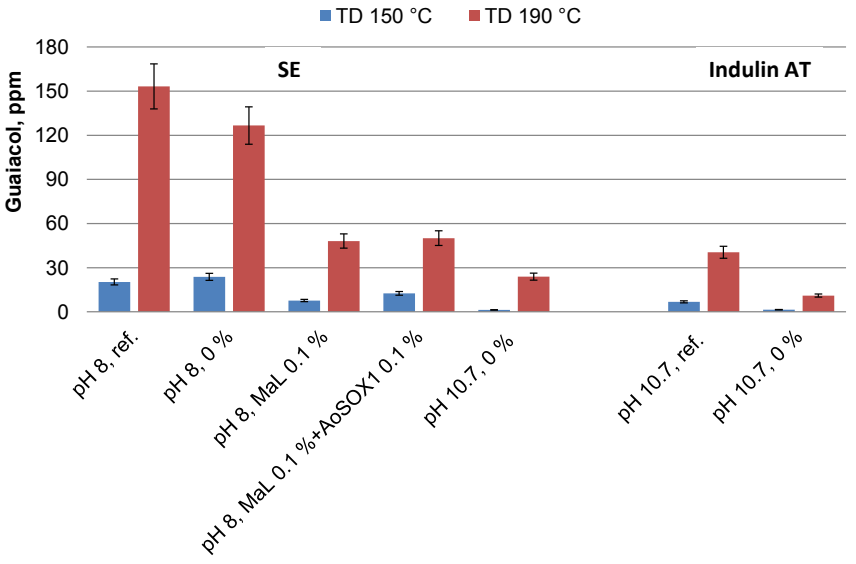

Figure 25. Amount of guaiacol released from the freeze-dried SE lignin and Indulin AT samples at 150 °C and 190 °C after oxidative treatments with and without enzymes (*Laccase MaL from Melanocarpus albomyces (Ma) and sulfhydryl oxidase AoSOX1 from Aspergillus oryzae (Ao)*). Reference sample (ref.) was not O_2 boosted and all other samples are O_2 boosted with laccase dose (0.1 %) or without (0 %).

6.2.2 Thermochemolysis as a tool for the analysis of esterified lignin substrucures (III)

Lignin as such has poor thermoplastic properties due to its three-dimensional molecular structure. However, esterification of technical lignins with fatty acids has been found to lower the glass transition point of lignin (Funakoshi et al., 1979; Thiebaud et al., 1997). As a result, the thermoplasticity and film forming properties of lignin are improved. This enables the use of lignin as a coating material on paperboard. Lignin functionalization with tall oil fatty acid (TOFA), consisting of a mixture of oleic, linoleic and linolenic acids, has been presented in a recent Publication (Hult et al., 2013). Lignin hydroxyl groups were esterified with fatty acids to different degrees of substitution, aiming to develop aqueous lignin ester dispersion formulations for coatings. In the study presented in Publication III, model compounds (guaiacyl palmitate and 2-nonyl palmitate) representing both aliphatic and aromatic ester bonds among lignin and fatty acids were used to evaluate the existing thermochemolysis method for the analysis of degree of esterification from the novel lignin material.

Thermochemolysis in the presence of TMAH and TMAAc was applied in Publication III. TMAH has been used to determine total acid contents in both natural and synthetic materials (Challinor, 1996; Drechsel et al., 2003; Hardell and Nilvebrant, 1999), whereas TMAAc has been used to determine free fatty acids in wood extractives (Hardell and Nilvebrant, 1999). It has been reported that degradation and methylation of ester bonds may take place especially in high temperature thermochemolysis with TMAAc (Drechsel et al., 2003). Another proposed explanation for the high degree of free acids has been possible transesterification in TMAAc thermochemolysis in the presence of methanol (Joll et al. 2004). In this study, guaiacyl palmitate and 2-nonyl palmitate were analysed by thermochemolysis using TMAH and TMAAc reagents as a means to differentiate between free acids and esters. Additionally, the possible transesterification reaction during on-line thermochemolysis using TMAAc in the presence of methanol was evaluated. Thus all the measurements were carried out using two solvents, methanol and dichloromethane.

The results in Figure 26 and Figure 27 show that aromatic ester reacted completely with TMAH, whereas part of the aliphatic ester was intact in the presence of TMAH. As a result, a small amount of the original 2-nonyl palmitate was detected. The yields of palmitic acid from the theoretical value in the case of guaiacyl palmitate were 100 % and 88 % when methanol and dichloromethane were used as a solvent, respectively. Correspondingly, the yields of palmitic acid in the case of 2-nonyl palmitate were 79 % and 78 % in methanol and dichlormethane media (Figure 28). Due to the incomplete hydrolysis of 2-nonyl palmitate at 600 °C, thermochemolysis with TMAH was also performed at 700 °C and 800 °C, which gave yields of 76 % and 82 %, respectively. This showed that increase of thermochemolysis temperature did not have an influence on the hydrolysis of 2-nonylpalmitate with TMAH.

The palmitic acid contents released from guaiacyl palmitate and 2-nonyl palmitate in TMAAc thermochemolysis were partly unexpected. A high amount of palmitic acid was detected from the guaiacyl palmitate with TMAAc, corresponding to about one third of the theoretical content (Figure 28). The measured value was abundant, as any unreacted palmitic acid after the synthesis was shown to be removed during the purification, further verified by NMR analysis of the product. A small amount of nonmethylated guaiacol was also detected after TMAAc thermochemolysis, indicating thermal degradation of guaiacyl palmitate already at 280 °C (Figure 26). However, thermal degradation cannot explain the high content of released palmitic acid, because hydrolysis and salt formation were expected to occur prior to

thermal degradation (Challinor, 2001). Thus it was assumed that palmitic acid is released and methylated from the aromatic esters in the presence of TMAAc. Significantly less palmitic acid was released from the 2-nonyl palmitate than from guaiacyl palmitate in the presence of TMAAc (Figure 28). This indicates that aliphatic ester is more stable in the presence of TMAAc than aromatic ester in low temperature thermochemolysis. In the case of 2-nonyl palmitate, TMAAc appears to react mainly with the free acid group, and not with the ester group as originally expected.

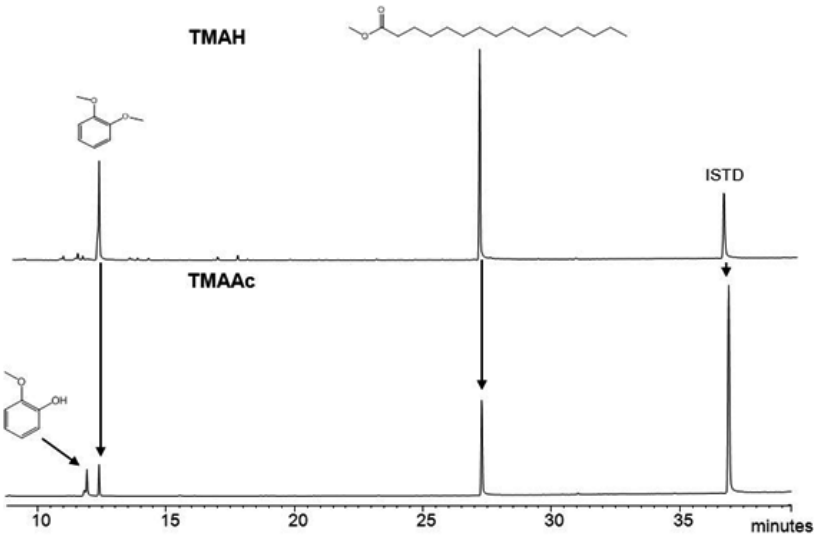

Figure 26. Products formed from guaiacyl palmitate by TMAH thermochemolysis (above) and TMAAc thermochemolysis (below) (Publication III).

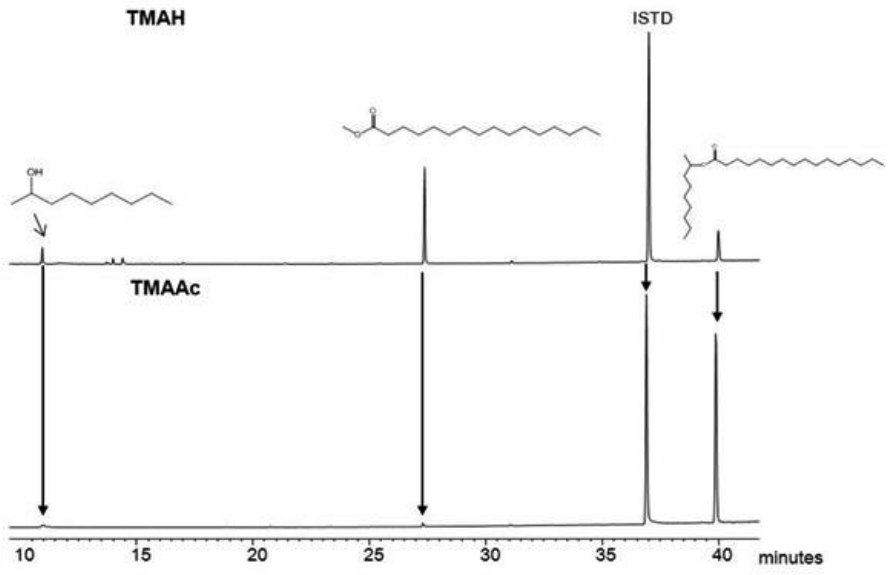

Figure 27. Products formed from 2-nonyl palmitate by TMAH thermochemolysis (above) and TMAAc thermochemolysis (below) (Publication III).

Two solvents, methanol and dichloromethane, were used in order to gain better understanding of the effect of the solvents on the methylation reaction, i.e. transesterification. If transesterification of the ester groups in the sample takes place via methoxide ion formation from methanol, a higher proportion of methylated products would be formed with methanol than with dichloromethane. The palmitic acid content was slightly higher when the samples were diluted in methanol rather than in dichloromethane in the presence of TMAAc. However, taking into account the standard deviation, similar values were obtained with both solvents. Thus it is proposed that transesterification with TMAAc is an insignificant reaction in on-line thermochemolysis, supporting the earlier results of (Joll et al., 2004).

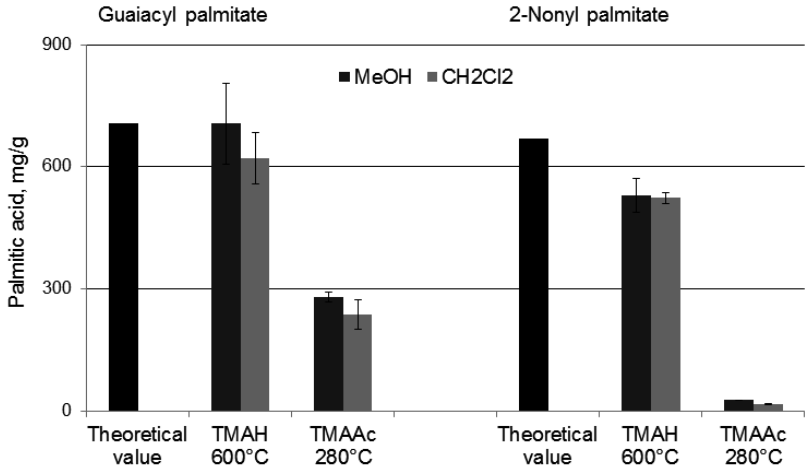

Figure 28. Theoretical and measured palmitic acid contents determined from guaiacyl palmitate and 2-nonyl palmitate using TMAH and TMAAc.

6.2.3 BSG as a potential novel source of lignin material (V)

Brewers spent grain (BSG) is an abundant by-product generated in the brewing of beer from barley grain (Xiros and Christakopoulos, 2012). It is a food grade material, which is rich in cell wall polysaccharides (arabinoxylan and cellulose), protein and lignin (Robertson et al., 2010). BSG is currently used as a ruminant feed (Mussatto et al., 2006), but other potential applications are also being investigated due to its low price, good availability and valuable composition (Mussatto, 2014). As BSG is rich in protein and dietary fibre, it could also be used in more valuable applications, e.g. as a dietary component in human food. It has been suggested that lignin as part of dietary fibre may help to protect against cancer and cardiovascular diseases (Mussatto, 2014). A recent study by Rencoret et al. (2015) showed that lignin in BSG consists of guaiacyl and syringyl type units, but also contains significant amounts of *p*-coumarates and ferulates. *p*-Coumarates have been supposed to acylate the lignin γ-OH group, and ferulates to form crosslinks between lignin and polysaccharides. These structural features together with high protein content have made isolation and also characterisation of lignin from BSG challenging. The aim of the work presented in Publication V was to obtain structural information on BSG lignin fractions by Py-GC/MS methods after the isolation by enzymatic and chemical methods. Original BSG fibres were measured as well, due to the possible modification of lignin during isolation.

Lignin isolation from BSG using enzymatic hydrolysis to two lignin-rich fractions, soluble (P-AEF) and insoluble fraction (INS), has been reported in Publications by Niemi et al. (2012) and Aura et al. (2013), but the scheme of BSG fractionation by enzymatic hydrolysis is shown in Figure 11. The composition analysis determined by traditional wet-chemical methods for P-AEF and INS fractions was also reported earlier (Aura et al., 2013; Niemi et al., 2012). Two other lignin fractions were isolated by acidolysis (AL) and enzymatic mild acidolysis (EMAL), and detailed description of the isolations are presented in section 5.1.1. Py-GC/MS analysis results of all four lignin-rich fractions together with the original BSG was only presented in Publication V.

Composition analysis by Py-GC/MS showed that separation of lignin from protein and carbohydrates by enzymatic hydrolysis was incomplete (Figure 29). This result is in accordance with earlier reported results (Aura et al., 2013; Niemi et al., 2012). The yield of P-AEF and INS fractions also remained low, at 14 and 39 %, respectively. More pure lignin fractions were obtained with two other isolation methods, acidolysis (AL) and enzymatic mild acidolysis (EMAL) including a protease pretreatment (Figure 29). However, the yields of AL and EMAL fractions were 21 % and 5.8 %, being thus rather low. The reason for the low yield of the EMAL fraction was the poor solubility of lignin in mild acid. In P-AEF and AL the lignin was solubilized, but was poorly precipitable. This was observed as dark colour of the residual liquid.

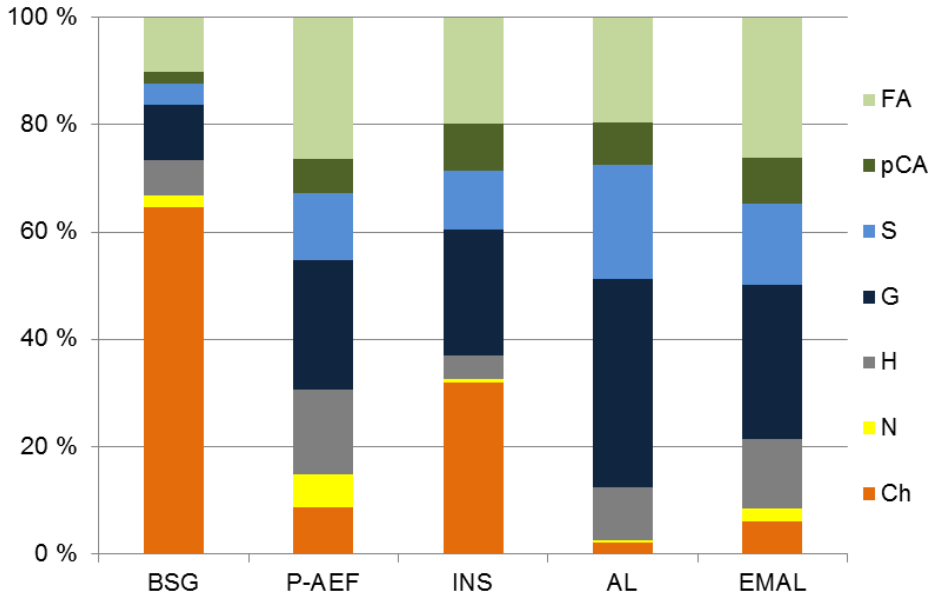

Figure 29. Composition of original BSG and its lignin-rich fractions determined by Py-GC/MS. Isolation processes of lignin-rich fractions from BSG are presented in Figure 11. Brewers spent grain (BSG), protease-alkaline extracted fraction (P-AEF) and insoluble residue (INS) after enzymatic hydrolysis, acidolysis lignin (AL) and enzymatic mild acidolysis lignin (EMAL). Carbohydrates (Ch), nitrogen-containing aromatic structures from protein (N), *p*-hydroxyphenyl substructures from protein and lignin (H), guaiacyl (G) and syringyl (S) substructures from lignin, 4-vinylphenol from lignin, protein and *p*-coumarate (pCA) and 4-vinylguaiacol from lignin and ferulate (FA) (Publication V).

The next Py-GC/MS and thermochemolysis results of hydroxycinnamates and lignin are presented in more detail from the original BSG and its lignin fractions. At higher temperature, hydroxycinnamates are degraded to 4-vinylphenol and 4-vinylguaiacol, and therefore these degradation products were excluded from the lignin structure evaluation in Py-GC/MS. Thermochemolysis with TMAH enables separation of hydroxycinnamates from lignin derivatives (Blokker et al., 2006; del Río et al., 2007a; Kuroda et al., 1995). *p*-Hydroxyphenyl type pyrolysis degradation products originate from protein, lignin and *p*-coumarate, which are all present in BSG (Kleen et al., 2003; Rencoret et al., 2015). *p*-Hydroxyphenyl type degradation products were excluded, because they cannot be specified as lignin degradation products.

The content of ferulic and *p*-coumaric acids in the original BSG and its lignin-rich fractions was highest of all the aromatic degradation products (Table 8). The result showed that high ferulic acid contents in the original BSG and in the lignin-rich fractions INS and P-AEF were related to a high polysaccharide content of samples (Figure 29). It has been reported that ferulic acid binds polysaccharides and lignin together, forming ester bonds with polysaccharides and ether bonds with lignin (Jacquet et al., 1995; Ralph, 2010). Acidolysis treatment releases ferulate-linked polysaccharides. Thus the yield of ferulic acid and polysaccharides was low in AL and EMAL fractions. Due to the milder acidolysis conditions, carbohydrates and ferulic acid were released to a lesser extent after the EMAL than AL treatment, as has been reported by Jacquet et al., (1995). The proportion of *p*-coumaric acid was the same in BSG, P-AEF and EMAL, but lower than in INS and AL (Table 8). *p*-Coumaric acid has been reported to acylate the γ-carbon of the lignin side chain (Ralph, 2010), especially in con-

densed lignin structures (Rencoret et al., 2015). Based on this, it appears that lignin in INS and AL is enriched with condensed lignin.

Degradation of the β-*O*-4 bond results in a high yield of oxygen-containing side chain structures in pyrolysis with (Kuroda, 2002; Kuroda and Nakagawa-Izumi, 2006) and without TMAH (Kuroda, 2000b). The results showed that oxygenated syringyl units were less abundant in all samples from Py-GC/MS than from Py/TMAH (Table 7, Table 8). Recently it has been reported that a small amount of γ-OH is acylated in BSG lignin mainly in syringyl units (Rencoret et al., 2015). In pyrolysis, acetyl groups have been reported to be eliminated together with the attached hydroxyl group, leading to the formation of double bond structures in the side chains (Moldoveanu, 2010). This also occurs in the case of acylation by *p*-coumaric acid (Ralph, 2010; Rencoret et al., 2015). The total absence of sinapyl alcohol type degradation products in the BSG samples thus suggests that the γ-OH groups in syringyl units are more acylated than in guaiacyl units. This was observed especially for P-AEF, AL and EMAL samples.

The TMAH/py analysis confirmed that acylation of γ-OH groups in the syringyl structures leads to underestimation of the content of native type syringyl structures in Py-GC/MS. As a result, higher S/G ratios (0.8-1.2) were obtained by Py/TMAH in comparison to Py-GC/MS (0.5-0.7), especially in the case of BSG and AL. Thus, thermochemolysis with TMAH should be used for the determination of S/G-ratios of acylated lignins.

Table 7. Relative proportion of aromatic degradation products of guaiacyl (G) and syringyl (S) type lignin units, *p*-coumaric and ferulic acid formed in Py-GC/MS from the original BSG and from lignin-rich enzymatically and chemically isolated fractions of BSG (Publication V).

Compound	M_w	orig.	BSG	P-AEF	INS	AL	EMAL
4-Vinylphenol	120	H/*p*-CA	8.0	8.8	13.8	8.5	10.0
Guaiacol	124	G	4.4	5.0	5.8	7.0	5.3
4-Methylguaiacol	138	G	4.9	7.6	3.6	9.1	6.1
4-Ethylguaiacol	152	G	1.2	1.7	0.8	2.1	2.2
4-Vinylguaiacol	150	G/FA	36.6	36.2	30.3	20.8	31.4
Eugenol	164	G	1.8	2.3	1.4	2.0	2.5
cis-Isoeugenol	164	G	1.1	1.4	0.8	1.5	1.8
trans-Isoeugenol	164	G	4.9	7.7	4.1	6.6	9.0
Vanillin	152	G	7.2	1.0	4.1	2.0	1.5
Homovanillin	166	G	1.5	0.0	2.2	2.5	0.7
Acetoguaiacone	166	G	1.6	0.7	1.3	0.8	0.6
Guaiacylacetone	180	G	0.6	1.0	0.8	3.2	3.1
4-(Oxy-allyl)guaiacol	178	G	0.7	0.1	0.6	0.6	0.4
4-(1-Hydroxyprop-2-enyl)guaiacol	180	G	0.3	0.0	0.6	0.5	0.1
cis-Coniferyl alcohol	180	G	1.6	0.8	1.9	0.6	0.3
trans-Coniferyl alcohol	180	G	4.1	3.8	5.8	1.6	0.9
Coniferaldehyde	178	G	1.7	0.0	2.0	1.3	0.0
Syringol	154	S	2.1	2.3	2.9	3.5	2.2
4-Methylsyringol	168	S	2.3	3.7	1.8	4.8	3.0
4-Ethylsyringol	182	S	0.1	0.5	0.2	0.9	0.7
4-Vinylsyringol	180	S	3.2	4.7	3.1	6.6	6.1
4-Allylsyringol	194	S	1.5	2.0	1.2	1.8	1.9
cis-Propenylsyringol	194	S	1.0	1.5	0.7	1.4	1.5
trans-Propenylsyringol	194	S	3.4	5.7	2.9	4.8	5.3
Syringaldehyde	182	S	2.3	0.3	1.5	1.1	0.6
Homosyringaldehyde	196	S	0.2	0.0	0.6	0.5	0.0
Acetosyringone	196	S	1.5	1.0	1.3	1.4	0.9
Syringylacetone	210	S	0.2	0.4	0.3	2.0	1.6
4-(Oxy-allyl)syringol	208	S	0.0	0.0	0.2	0.4	0.4
4-(1-Hydroxy-prop-2-enyl)syringol	210	S	0.0	0.0	0.2	0.1	0.0
cis-Sinapyl alcohol	210	S	0.0	0.0	0.2	0.0	0.0
trans-Sinapyl alcohol	210	S	0.0	0.0	1.7	0.0	0.0
Sinapaldehyde	208	S	0.0	0.0	1.1	0.0	0.0
S/G			0.5	0.7	0.6	0.7	0.7

Table 8. Relative proportion of aromatic degradation products of guaiacyl (G) and syringyl (S) type lignin units, *p*-coumaric and ferulic acid formed in Py/TMAH from the original BSG and lignin-rich enzymatically and chemically isolated fractions of BSG (Publication V).

Compound	orig.	M_W	BSG	P-AEF	INS	AL	EMAL
1,2-Dimethoxybenzene	G	138	0.0	0.0	0.0	0.2	0.0
3,4-Dimethoxytoluene	G	152	0.0	0.0	0.0	0.2	0.7
3,4-Dimethoxybenzeneethylene	G	164	0.0	1.0	0.3	0.6	1.2
3,4-Dimethoxybenzene methanol methyl ether	G	182	0.0	0.0	0.0	0.5	0.0
1,2-Dimethoxy-4-propenylbenzene	G	178	0.0	0.0	0.0	0.4	0.3
3,4-Dimethoxybenzaldehyde	G	166	0.0	1.5	0.7	0.9	1.2
3,4-Dimethoxy benzoic acid methyl ester	G	196	4.5	4.6	4.5	4.6	5.3
3,4-Dimethoxybenzeneacetic acid methyl ester	G	210	0.0	0.4	0.5	0.6	0.3
cis-1-(3,4-Trimethoxyphenyl)-2-methoxyethene	G	194	8.6	8.7	8.4	5.6	10.3
trans-1-(3,4-Trimethoxyphenyl)-2-methoxyethene	G	194	5.9	4.7	4.7	3.1	5.3
cis-1-(3,4-Dimethoxyphenyl)-2-methoxyprop-1-ene	G	208	0.0	1.0	1.0	0.9	1.4
trans-1-(3,4-Dimethoxyphenyl)-2-methoxyprop-1-ene	G	208	0.0	0.6	0.9	0.7	0.6
1-(3,4-Dimethoxyphenyl)-1-methoxyprop-1-ene	G	208	0.0	1.0	1.2	0.9	1.5
erythro 4-(1,2,3-Trimethoxypropyl)-1,2-dimethoxybenzene	G	270	3.7	3.7	4.0	5.1	6.1
threo 4-(1,2,3-Trimethoxypropyl)-1,2-dimethoxybenzene	G	270	5.8	4.0	3.9	4.7	5.1
1,2,3-Trimethoxybenzene	S	168	0.0	2.7	0.6	0.5	4.0
3,4,5-Trimethoxybenzaldehyde	S	196	0.0	0.6	0.4	0.8	0.6
3,4,5-Trimethoxybenzoic acid methyl ester	S	226	5.3	5.8	4.1	8.0	6.1
cis-1-(3,4,5-Trimethoxyphenyl)-2-methoxyethene	S	224	17.1	6.6	6.8	7.3	10.1
trans-1-(3,4,5-Trimethoxyphenyl)-2-methoxyethene	S	224	0.0	3.7	3.5	3.3	0.0
erythro 4-(1,2,3-Trimethoxypropyl)-1,2,3-trimethoxybenzene	S	300	4.0	5.0	3.7	5.2	5.1
threo 4-(1,2,3-Trimethoxypropyl)-1,2,3-trimethoxybenzene	S	300	6.8	4.4	3.6	4.3	4.5
trans-3-(4-Methoxypenyl)-3-propenoic acid methyl ester	*p*-CA	192	11.4	11.1	20.1	24.1	11.1
cis-3-(3,4-Dimethoxyphenyl)-3-propenoic acid methyl ester	FA	222	1.5	0.8	1.6	0.5	0.6
trans-3-(3,4-Dimethoxyphenyl)-3-propenoic acid methyl ester	FA	222	25.5	28.1	25.5	17.0	18.6
S/G			1.2	0.9	0.8	1.1	0.8
p-CA/FA			0.4	0.4	0.4	0.7	1.4

7. Conclusions

In this thesis, different analytical pyrolysis techniques were applied for the characterisation of lignin and carbohydrates from various lignocellulosic plant materials. Based on the results of the study, Py-GC/MS is better suitable for the characterisation and quantitation of lignin than carbohydrates. The results were supported by other methods used in the study. Isothermal pyrolysis can be well used for the analysis of woody feedstocs, however, in the case of non-woody materials thermochemolysis method give more precise information. Thermal desorption technique is applicable for the determination of volatiles from the lignocellulose materials without breaking the macromolecular structure. Fractionated pyrolysis can be applied together with other pyrolysis techniques to understand more deeply the lignocellulose structure and its effect on thermal degradation behaviour.

Variation in lignin composition between softwood and hardwood feedstocks, but also in non-woody material (agro-industrial residue) such BSG, was observed directly from the degradation product profiles. In addition, the change of species in eucalypt hybrids altered the pyrolysis degradation products formed from lignin and S/G ratios, confirming that there are differences in the original lignin structure in all the studied eucalypt hybrids. Py-GC/MS showed lower S/G ratios in comparison to alkaline nitrobenzene oxidation, due to the different degradation mechanisms of these two methods. Py-GC/MS is a potential method for the determination of S/G ratios from the feedstocks intended for pulping. In addition to lignin, Py-GC/MS provides information on the carbohydrate composition of eucalypt hybrids. However, based on the results of this study, Py-GC/MS cannot be recommended for the comparison of carbohydrate composition among different wood species. Fractionated pyrolysis demonstrated that the thermal behaviour of cellulose and xylose, together with the minor components arabinose and galactose, varies between different eucalypt wood species. Similar thermal behaviour between studied components is a prerequisite for reliable Py-GC/MS analysis.

Characterisation of lignin from BSG by Py-GC/MS was more challenging than from wood. BSG contains significant amounts of protein and hydroxycinnamates that interfere with the analysis of lignin structure, even from the isolated lignin fractions. Comparison of the isothermal pyrolysis and thermochemolysis results of BSG and its lignin fractions showed that more detailed information on lignin structure can be obtained with these methods together than with either method separately. Thermochemolysis results demonstrated that isothermal pyrolysis leads to underestimation of native type syringyl structures and S/G ratios due to the acylation. More precise information on lignin structure and S/G ratio can therefore be obtained by thermochemolysis than by isothermal pyrolysis.

Py-GC/MS provided information on lignin structure and quantity directly from pulps in cooking, oxygen delignification and bleaching stages. For that purpose, the sensitivity of the method was improved by integrating the compounds with selected mass fragments (m/z)

instead of using total ion current. The main key features of pyrolysis degradation products in different stages are described in the following. Decrease of oxygenated lignin pyrolysis degradation products was reflected in the β-ether bond cleavage and in increased degradation of short chain structures of the side chains during cooking. As a result of the oxygen delignification stage, the proportion of lignin pyrolysis degradation products with oxygenated side chain structures increased. Delignification leached the lignin products that were formed in cooking. As a result, lignin pyrolysis degradation products with short side chains were decreased to the same level that has been found in native lignin. The result demonstrated that the residual lignin structure in fully bleached pulps is close to the native lignin structure.

In addition striking enrichment of *p*-hydroxyphenyl structures was observed during cooking and delignification that was opposite phenomenon in comparison to the behaviour of guaiacyl type structures. Thermochemolysis and fractionated pyrolysis were applied in order to obtain more information on the phenomena. The thermochemolysis method demonstrated that *p*-hydroxyphenyl substructures are formed from aromatic substructures, and are not secondary pyrolysis products. The distinct thermal behaviour of *p*-hydroxyphenyl type degradation products in comparison to guaiacyl type degradation products in fractionated pyrolysis suggested that they are derived not only from lignin but also from other pulp components. Analysis of *p*-hydroxyphenyl type degradation products is complex, due to the several possible sources. This phenomenon does not apply only to wood based material, but to all types of lignocelluloses, including BSG. In BSG the origin of *p*-hydroxyphenyl type degradation products were lignin, hydroxycinnamates and protein.

A new external standard calibration method was developed for the quantitative analysis of lignin directly from pulps after the cooking and different delignification stages up to fully bleached pulps. The method is well applicable to the pulps because the degradation products used for the quantitation can be well defined, which is not possible in the case of traditional methods.

The thermal desorption method provided information on odorous volatile organic compounds released from treated Kraft lignins intended for composite processes. The method is applicable in the comparison of odorous compounds released from various samples below 225 °C. Quantitative analysis enables comparison of results with the odour threshold values of the compounds.

Thermochemolysis with TMAAc and TMAH reagents was applied as means to differentiate between free acids and esters, respectively. The reactivity of aromatic and aliphatic esters was evaluated in thermochemolysis as the release of palmitic acid from model compounds. The result demonstrated that thermochemolysis with alkaline TMAH can be used to determine total fatty acid content from both aliphatic and aromatic esters. Aliphatic ester was stable with neutral TMAAc, whereas aromatic ester was partially degraded. Thus TMAAc can be used to distinguish between free acids and aliphatic esters in matrices such as wood extractives, containing only aliphatic esters. However, it cannot be used to determine free acids from samples which contain aromatic and aliphatic ester linkages, or only aromatic ester linkages.

8. Future prospects

In this study lignin structure was mainly characterized by isothermal pyrolysis, the exception being non-woody BSG that was determined with isothermal pyrolysis and thermochemolysis. In the future, it would be advantageous to utilize the thermochemolysis method to determine lignin structure, and also S/G/H ratios from the various types of lignocellulosic materials. It would be informative to use other thermochemolysis reagents than TMAH for the lignin structural characterisation, especially of the free functional groups from various lignocellulose materials and products. Thermochemolysis has not widely been applied for the determination of carbohydrate composition from wood species. Thermochemolysis or pre-sialylation followed by Py-GC/MS could probably provide more stable carbohydrate degradation products. Quantitative analysis of lignin from non-woody materials with traditional methods is complicated due to the presence of protein and hydroxycinnamates that interfere with the analysis. Development of an *in situ* Py-GC/MS method for lignin quantitation from non-woody materials would increase the applicability of the method in the future.

Thermochemolysis with TMAAc for the determination of free acid from the aromatic esters was not acceptable. However, it was suitable for determining free acids from aliphatic esters. For the purpose of differentiating free acids from esters, different thermochemolysis reagents need to be tested. The reagent would be more applicable if it could be used to distinguish free acids from both aliphatic and aromatic esters.

The utilization of thermal desorption, sequential and fractionated pyrolysis techniques is advantageous in studies in which more information concerning the thermal behaviour of materials is needed. The method could be used to simulate various thermal processes with different types of biomasses.

References

Adam, J., Blazso, M., Meszaros, E., Stöcker, M., Nilsen, M.H., Bouzga, A., Hustad, J.E., Grronli, M., Oye, G., 2005. Pyrolysis of biomass in the presence of Al-MCM-41 type catalysts. Fuel 1494–1502. doi:10.1016/j.fuel.2005.02.006

Akazawa, M., Kojima, Y., Kato, Y., 2016. Effect of pyrolysis temperature on the pyrolytic degradation mechanism of β-aryl ether linkages. J. Anal. Appl. Pyrolysis 118, 164–174. doi:10.1016/j.jaap.2016.02.001

Akim, L.G., Colodette, J.L., Argyropoulos, D.S., 2001. Factors limiting oxygen delignification of kraft pulp. Can. J. Chem. 79, 201–210. doi:10.1139/cjc-79-2-201

Alves, A., Gierlinger, N., Schwanninger, M., Rodrigues, J., 2009. Analytical pyrolysis as a direct method to determine the lignin content in wood Part 3 . Evaluation of species-specific and tissue-specific differences in softwood lignin composition using principal component analysis. J. Anal. Appl. Pyrolysis 85, 30–37. doi:10.1016/j.jaap.2008.09.006

Alves, A., Rodrigues, J., Wimmer, R., Schwanninger, M., 2008. Analytical pyrolysis as a direct method to determine the lignin content in wood Part 2: Evaluation of the common model and the influence of compression wood. J. Anal. Appl. Pyrolysis 81, 167–172. doi:10.1016/j.jaap.2007.11.001

Alves, A., Schwanninger, M., Pereira, H., Rodrigues, J., 2006. Analytical pyrolysis as a direct method to determine the lignin content in wood Part 1: Comparison of pyrolysis lignin with Klason lignin. J. Anal. Appl. Pyrolysis 76, 209–213. doi:10.1016/j.jaap.2005.11.004

Amen-Chen, C., Pakdel, H., Roy, C., 2001. Production of monomeric phenols by thermochemical conversion of biomass: A review. Bioresour. Technol. 79, 277–299. doi:10.1016/S0960-8524(00)00180-2

Andersson, E.M., Ericsson, I., 1979. Determination of the temperature—time profile of the sample in pyrolysis—gas chromatography. J. Anal. Appl. Pyrolysis 1, 27–38. doi:10.1016/0165-2370(79)80003-0

Asperger, A., Engewald, W., Fabian, G., 2001. Thermally assisted hydrolysis and methylation - A simple and rapid online derivatization method for the gas chromatographic analysis of natural waxes. J. Anal. Appl. Pyrolysis 61, 91–109. doi:10.1016/S0165-2370(01)00116-4

Aura, A.M., Niemi, P., Mattila, I., Niemelä, K., Smeds, A., Tamminen, T., Faulds, C., Buchert, J., Poutanen, K., 2013. Release of small phenolic compounds from Brewer's spent grain and its lignin fractions by human intestinal microbiota in vitro. J. Agric. Food Chem. 61, 9744–9753. doi:10.1021/jf4024195

Bai, Y.Y., Xiao, L.P., Shi, Z.J., Sun, R.C., 2013. Structural variation of bamboo lignin before and after ethanol organosolv pretreatment. Int. J. Mol. Sci. 14, 21394–21413. doi:10.3390/ijms141121394

Barbosa, L.C.A., Maltha, C.R., Silva, V.L., Colodette, J.L., 2008. Determination of the syringyl/guaiacyl ratio in eucalyptus wood by pyrolysis-gas chromatography/mass spectrometry (Py-GC/MS). Quim. Nova 31, 2035–2041. doi:10.1590/S0100-40422008000800023

Blokker, P., Boelen, P., Broekman, R., Rozema, J., 2006. The occurrence of p-coumaric acid and ferulic acid in fossil plant materials and their use as UV-proxy. Plant Ecol. 182, 197–207. doi:10.1007/s11258-005-9026-y

Bocchini, P., Galletti, G.C., Camarero, S., Martinez, A.T., 1997. Absolute quantitation of lignin pyrolysis products using an internal standard. J. Chromatogr. A 773, 227–232.

Brezny, R., Mihalov, V., Kovasick, V., 1983. Low temperature thermolysis of lignins. Holzforschung 37, 199–204.

Böttcher, J.H., 1993. Untersuchungen zur Charakterisierung von Holz und Holzkomponenten mittels konventioneller Analysentechniken und der FTIR- Spekroskopie unter Anwendung von multivariaten statistischen Verfahren. University of Hamburg.

Camarero, S., Bocchini, P., Galletti, G.C., Martínez, A.T., 1999. Pyrolysis-gas chromatography/mass spectrometry analysis of phenolic and etherified units in natural and industrial lignins. Rapid Commun. Mass Spectrom. 13, 630–636. doi:10.1002/(SICI)1097-0231(19990415)13:7<630::AID-RCM535>3.0.CO;2-5

Camarero, S., Bocchini, P., Galletti, G.C., Martinez, M.J., Martinez, A.T., 2001. Compositional changes of weat lignin by a funagal peroxidase analysed by pyrolysis-GC-MS. J. Anal. Appl. Pyrolysis 58–59, 413–423.

Challinor, J.M., 2001. Review: The development and applications of thermally assisted hydrolysis and methylation reactions. J. Anal. Appl. Pyrolysis 61, 3–34. doi:10.1016/S0165-2370(01)00146-2

Challinor, J.M., 1996. Characterisation of wood extractives by pyrolysis-gas chromatography/mass spectrometry of quaternary ammonium hydroxide extracts. J. Anal. Appl. Pyrolysis 37, 1–13.

Challinor, J.M., 1995. Characterisation of wood by pyrolysis derivatisation gas chromatography–mass spectrometry. J. Anal. Appl. Pyrolysis 35, 93–107.

Challinor, J.M., 1989. A Pyrolysis-derivatisation-gas chromatography technique for the structural elucidation of some synthetic polymers. J. Anal. Appl. Pyrolysis 16, 323–333.

Chang, G., Huang, Y., Xie, J., Yang, H., Liu, H., Yin, X., Wu, C., 2016. The lignin pyrolysis composition and pyrolysis products of palm kernel shell, wheat straw, and pine sawdust. Energy Convers. Manag. 124, 587–597. doi:10.1016/j.enconman.2016.07.038

Choi, B.J., Faix, O., Meier, D., 2001. Characterization of Residual Lignins from Chemical Pulps of Spruce (Picea abies L.) and Beech (Fagus sylvatica L.) by Analytical Pyrolysis – Gas Chromatography/Mass Spectrometry. Holzforschung 55, 185–192.

Choi, S.S., Kim, M.C., Kim, Y.K., 2011. Influence of silica on formation of levoglucosan from carbohydrates by pyrolysis. J. Anal. Appl. Pyrolysis 90, 56–62. doi:10.1016/j.jaap.2010.10.009

Clifford, D.J., Carson, D.M., McKinney, D.E., Bortiatynski, J.M., Hatcher, P.G., 1995. A new rapid technique for the characterization of lignin in vascular plants: thermochemolysis with tetramethylammonium hydroxide (TMAH). Org. Geochem. 23, 169–175. doi:10.1016/0146-6380(94)00109-E

del Río, J.C., Gutiérrez, A., Hernando, M., Landín, P., Romero, J., Martínez, Á.T., 2005. Determining the influence of eucalypt lignin composition in paper pulp yield using Py-GC/MS. J. Anal. Appl. Pyrolysis 74, 110–115. doi:10.1016/j.jaap.2004.10.010

del Río, J.C., Gutiérrez, A., Martínez, M.J., Martínez, A.T., 2001a. Py-GC/MS study of Eucalyptus globulus wood treated with different fungi. J. Anal. Appl. Pyrolysis 58–59, 441–452. doi:10.1016/S0165-2370(00)00184-4

del Río, J.C., Gutiérrez, A., Rodríguez, I.M., Ibarra, D., Martínez, Á.T., 2007a. Composition of non-woody plant lignins and cinnamic acids by Py-GC/MS, Py/TMAH and FT-IR. J. Anal. Appl. Pyrolysis 79, 39–46. doi:10.1016/j.jaap.2006.09.003

del Río, J.C., Gutiérrez, A., Romero, J., Martínez, M.J., Martínez, A.T., 2001b. Identification of residual lignin markers in eucalypt kraft pulps by Py-GC/MS. J. Anal. Appl. Pyrolysis 58–59, 425–439. doi:10.1016/S0165-2370(00)00126-1

del Río, J.C., Lino, A.G., Colodette, J.L., Lima, C.F., Gutiérrez, A., Martínez, Á.T., Lu, F., Ralph, J., Rencoret, J., 2015. Differences in the chemical structure of the lignins from sugarcane bagasse

and straw. Biomass and Bioenergy 81, 322–338. doi:10.1016/j.biombioe.2015.07.006

del Río, J.C., Marques, G., Rencoret, J., Martínez, Á.T., Gutiérrez, A., 2007b. Occurrence of naturally acetylated lignin units. J. Agric. Food Chem. 55, 5461–5468. doi:10.1021/jf0705264

del Río, J.C., Martin, F., Gonzalez-Vila, F.J., 1996. Thermally assisted hydrolysis and alkylation as a novel pyrolytic approach for the structural characterization of natural biopolymers and geomacromolecules. TrAC - Trends Anal. Chem. 15, 70–79. doi:10.1016/0165-9936(96)80763-1

del Río, J.C., Rencoret, J., Prinsen, P., Martínez, Á.T., Ralph, J., Gutiérrez, A., 2012. Structural characterization of wheat straw lignin as revealed by analytical pyrolysis, 2D-NMR, and reductive cleavage methods. J. Agric. Food Chem. 60, 5922–5935. doi:10.1021/jf301002n

del Río, J.C., Speranza, M., Gutiérrez, A., Martínez, M.J., Martínez, A.T., 2002. Lignin attack during eucalypt wood decay by selected basidiomycetes: A Py-GC/MS study. J. Anal. Appl. Pyrolysis 64, 421–431. doi:10.1016/S0165-2370(02)00043-8

Dizhbite, T., Telysheva, G., Dobele, G., Arshanitsa, A., Bikovens, O., Andersone, A., Kampars, V., 2011. Py-GC/MS for characterization of non-hydrolyzed residues from bioethanol production from softwood. J. Anal. Appl. Pyrolysis 90, 126–132. doi:10.1016/j.jaap.2010.11.004

Drechsel, D., Dettmer, K., Engewald, W., 2003. Studies of thermally assisted hydrolysis and methylation - GC-MS of fatty acids and triglycerides using different reagents and injection systems. Chromatographia 57, S-283-S-289. doi:10.1007/BF02492117

Du, X., Pérez-Boada, M., Fernández, C., Rencoret, J., del Río, J.C., Jiménez-Barbero, J., Li, J., Gutiérrez, A., Martínez, A.T., 2014. Analysis of lignin–carbohydrate and lignin–lignin linkages after hydrolase treatment of xylan–lignin, glucomannan–lignin and glucan–lignin complexes from spruce wood. Planta 239, 1079–1090. doi:10.1007/s00425-014-2037-y

Ericsson, I., 1985. Influence of pyrolysis parameters on results in pyrolysis-gas chromatography. J. Anal. Appl. Pyrolysis 8, 73–86. doi:10.1016/0165-2370(85)80016-4

Ericsson, I., 1978. Sequential Pyrolysis Gas Chromatographic Study of the Decomposition Kinetics of Cis-1,4-Polybutadiene. J. Chromatogr. Sci. 16, 340–344. doi:10.1093/chromsci/16.8.340

Ericsson, I., Lattimer, R.P., 1995. Nomenclature and terminology for analytical pyrolysis. J. Anal. Appl. Pyrolysis 31, 251–256.

Fahmi, R., Bridgwater, A. V., Thain, S.C., Donnison, I.S., Morris, P.M., Yates, N., 2007. Prediction of Klason lignin and lignin thermal degradation products by Py-GC/MS in a collection of Lolium and Festuca grasses. J. Anal. Appl. Pyrolysis 80, 16–23. doi:10.1016/j.jaap.2006.12.018

Faix, O., Fortmann, I., Bremer, J., Meier, D., 1991a. Thermal degradation products of wood: A collection of electron-impact (EI) mass spectra of polysaccharide derived products. Holz als Roh- und Werkst. 49, 299–304.

Faix, O., Fortmann, I., Bremer, J., Meier, D., 1991b. Thermal degradation products of wood: Gas chromatographic separation and mass spectrometric characterization of polysaccharide derived products. Holz als Roh- und Werkst. 49, 213–219.

Faix, O., Meier, D., Fortmann, I., 1990a. Thermal degradation products of wood: Gas chromatographic separation and mass spectrometric characterization of monomeric lignin derived products. Holz als Roh- und Werkst. 48, 281–285.

Faix, O., Meier, D., Fortmann, I., 1990b. Thermal degradation products of wood: A collection of electron-impact (EI) mass spectra of monomeric lignin derived products. Holz als Roh- und Werkst. 48, 351–354.

Faix, O., Meier, D., Fortmann, I., 1988. Pyrolysis-gas chromatography-mass spectrometry of two trimeric lignin model compounds with alkyl-aryl ether structure. J. Anal. Appl. Pyrolysis 14, 135–148.

Fengel, D., Wegener, G., 1989. Wood: Chemistry, Ultrastructure, Reactions. Walter de Gruyter, Berlin, Germany.

Funakoshi, H., Shiraishi, N., Norimoto, M., Aoki, T., Hayashi, H., Yokota, T., 1979. Studies on the thermoplasticization of wood. Holzforschung 33, 159–166.

Galetta, M.A., Reina, L., Resquin, F., Mantero, C., González-Pérez, J.A., Almendros, G., Menéndez, M.P., González-Vila, F.J., 2014. Chemometric appraisal of lignin pyrolytic assemblages from Eucalyptus woods relevant for pulping in Uruguay. J. Anal. Appl. Pyrolysis 109, 296–303. doi:10.1016/j.jaap.2014.08.001

Gardner, D.J., Schultz, T.P., McGinnis, G.D., 1985. The pyrolytic behaviour of selected lignin preparations. J. Wood Chem. Technol. 5, 85–110.

Gellerstedt, G., Pranda, J., Lindfors, E.-L., 1994. Structural and molecular properties of residual birch kraft lignins. J. Wood Chem. Technol. 14, 467–482.

González-Vila, F.J., Almendros, G., del Río, J.C., Martín, F., Gutiérrez, A., Romero, J., 1999. Ease of delignification assessment of wood from different Eucalyptus species by pyrolysis (TMAH)-GC/MS and CP/MAS 13C-NMR spectrometry. J. Anal. Appl. Pyrolysis 49, 295–305. doi:10.1016/S0165-2370(98)00097-7

Grasset, L., Guignard, C., Amblès, A., 2002. Free and esterified aliphatic carboxylic acids in humin and humic acids from a peat sample as revealed by pyrolysis with tetramethylammonium hydroxide or tetraethylammonium acetate. Org. Geochem. 33, 181–188. doi:10.1016/S0146-6380(01)00150-4

Grinins, J., Andersons, B., Biziks, V., Andersone, I., Dobele, G., 2013. Analytical pyrolysis as an instrument to study the chemical transformations of hydrothermally modified wood. J. Anal. Appl. Pyrolysis 103, 36–41. doi:10.1016/j.jaap.2012.10.016

Guerra, A., Filpponen, I., Lucia, L.A., Saquing, C., Baumberger, S., Argyropoulos, D.S., 2006. Toward a Better Understanding of the Lignin Isolation Process from Wood. J. Agric. Food Chem. 54, 5939–5947.

Guignard, C., Lemée, L., Amblès, A., 2005. Lipid constituents of peat humic acids and humin. Distinction from directly extractable bitumen components using TMAH and TEAAc thermochemolysis. Org. Geochem. 36, 287–297. doi:10.1016/j.orggeochem.2004.07.016

Gutiérrez, A., Rodríguez, I.M., del Río, J.C., 2006. Chemical characterization of lignin and lipid fractions in industrial hemp bast fibers used for manufacturing high-quality paper pulps. J. Agric. Food Chem. 54, 2138–2144. doi:10.1021/jf052935a

Hardell, H.-L., Nilvebrant, N.-O., 1999. A rapid method to discriminate between free and esterified fatty acids by pyrolytic methylation using tetramethylammonium acetate or hydroxide. J. Anal. Appl. Pyrolysis 52, 1–14. doi:10.1016/S0165-2370(99)00035-2

Hardell, H.-L., Nilvebrant, N.-O., 1996. Analytical pyrolysis of spruce milled wood lignins in the presence of tetramethylammonium hydroxide. Nord. Pulp Pap. Res. J. 11, 121–126.

Hasumi, A., Nakagawa-Izumi, A., Homma, M., Ohi, H., Nakamata, K., 2009. Structural Micro-analysis of Residual Lignin in Pulp by Pyrolysis-GC Mass spectrometry. Japan Tappi J. 63, 81–88.

Helleur, R.J., 1987. Characterization of the saccharide composition of heteropolysaccharides by pyrolysis-capillary gas chromatography-mass spectrometry. J. Anal. Appl. Pyrolysis 11, 297–311.

Hermosin, B., Saiz-Jimenez, C., 1999. Thermally assisted hydrolysis and methylation of milled beech leaf litter. J. Anal. Appl. Pyrolysis 49, 417–424. doi:10.1016/S0165-2370(98)00111-9

Higman, E.B., Schmeeltz, I., Schlotzhauer, W.S., 1970. Products from the Thermal Degradation of Some Naturally Occuring Materials. J. Agric. Food Chem. 18, 636–639.

Hult, E.-L., Ropponen, J., Poppius-Levlin, K., Ohra-aho, T., Tamminen, T., 2013. Enhancing the

barrier properties of paper board by a novel lignin coating. Ind. Crops Prod. 50, 694–700. doi:10.1016/j.indcrop.2013.08.013

Ibarra, D., Chávez, M.I., Rencoret, J., del Río, J.C., Gutiérrez, A., Romero, J., Camarero, S., Martínez, M.J., Jiménez-Barbero, J., Martínez, A.T., 2007. Lignin Modification during Eucalyptus globulus Kraft Pulping Followed by Totally Chlorine-Free Bleaching: A Two-Dimensional Nuclear Magnetic Resonance, Fourier Transform Infrared, and Pyrolysis–Gas Chromatography/Mass Spectrometry Study. J. Agric. Food Chem. 55, 3477–3490. doi:10.1021/jf063728t

Ibarra, D., del Río, J.C., Gutiérrez, A., Rodríguez, I.M., Romero, J., Martínez, M.J., Martínez, Á.T., 2005. Chemical characterization of residual lignins from eucalypt paper pulps. J. Anal. Appl. Pyrolysis 74, 116–122. doi:10.1016/j.jaap.2004.12.009

Ishida, Y., Katagiri, M., Ohtani, H., 2009. Reaction efficiency of organic alkalis with various classes of lipids during thermally assisted hydrolysis and methylation. J. Chromatogr. A 1216, 3296–3299. doi:10.1016/j.chroma.2009.01.071

Izumi, A., Kuroda, K., Ohi, H., Yamaguchi, A., 1995a. Strucutral Analysis of Lignin by Pyrolysis-Gas Chromatography (III) -Comparative studues of pyrolysis-gas chromatography and nitrobenzene oxidation for the determination method of lignin composition in hardwood. Japan TAPPI J. 49, 1339–1346.

Izumi, A., Kuroda, K., Ohi, H., Yamaguchi, A., 1995b. No title. Mokuzai Gakkaishi 49, 735–745.

Izumi, A., Kuroda, K.I., 1997. Pyrolysis-mass spectrometry analysis of dehydrogenation lignin polymers with various syringyl/guaiacyl ratios. Rapid Commun. Mass Spectrom. 11, 1709–1715. doi:10.1002/(SICI)1097-0231(19971015)11:15<1709::AID-RCM5>3.0.CO;2-J

Jacquet, G., Pollet, B., Lapierre, C., Mhamdi, F., Rolando, C., 1995. New ether-linked ferulic acid-coniferyl alcohol dimers identified in grass straws. J. Agric. Food Chem. 43, 2746–2751.

Jiang, X.-Y., Lu, Q., Ye, X.-N., Hu, B., Dong, C.-Q., 2016. Experimental and theoretical studies on the pyrolysis mechanism of β-1-type lignin dimer model compound. BioResources 11, 6232–6243. doi:10.15376/biores.11.3.6232-6243

Joll, C.A., Couton, D., Heitz, A., Kagi, R.I., 2004. Comparison of reagents for off-line thermochemolysis of natural organic matter. Org. Geochem. 35, 47–59. doi:10.1016/j.orggeochem.2003.06.002

Jun-kai, D., Wei, J., Tian-zhi, Z., Ming, S., 1997. The effect polyunsaturated proportions thermally of isomerization and degradation of fatty acids from oils by different volume of tetramethylammonium hydroxide in assisted hydrolysis and methylation. J. Anal. Appl. Pyrolysis 42, 1–8.

Kangas, H., Liitiä, T., Rovio, S., Ohra-aho, T., Heikkinen, H., Tamminen, T., Poppius-Levlin, K., 2015. Characterization of dissolved lignins from acetic acid Lignofibre (LGF) organosolv pulping and discussion of its delignification mechanisms. Holzforschung 69, 247–256. doi:10.1515/hf-2014-0070

Karnofski, M.A., 1975. Odor generation in the kraft process. J. Chem. Educ.

Kawamoto, H., 2017. Lignin pyrolysis reactions. J. Wood Sci. 63, 117–132. doi:10.1007/s10086-016-1606-z

Kawamoto, H., Horigoshi, S., Saka, S., 2007. Effects of side-chain hydroxyl groups on pyrolytic β-ether cleavage of phenolic lignin model dimer. J. Wood Sci. 53, 268–271. doi:10.1007/s10086-006-0839-7

Kawamoto, H., Nakamura, T., Saka, S., 2008. Pyrolytic cleavage mechanisms of lignin-ether linkages : A study on p -substituted dimers and trimers. Holzforschung 62, 50–56. doi:10.1515/HF.2008.007

Kleen, M., Gellerstedt, G., 1995. Influence of inorganic species on the formation polysaccharide and lignin degradation products in the analytical pyrolysis of pulps. J. Anal. Appl. Pyrolysis 35, 15–41.

Kleen, M., Gellerstedt, G., 1991. Characterization of chemical and mechanical pulps by pyrolysis-gas chromatography/mass spectrometry. J. Anal. Appl. Pyrolysis 19, 139–152.

Kleen, M., Lindblad, G., Backa, S., 1993. Quntification of lignin and carbohydrates in Kraft pulps using analytical pyrolysis and multivariate data analysis. J. Anal. Appl. Pyrolysis 25, 209–227.

Kleen, M., Ohra-aho, T., Tamminen, T., 2003. On the interaction of HBT with pulp lignin during mediated laccase delignification - A study using fractionated pyrolysis-GC/MS. J. Anal. Appl. Pyrolysis 70, 589–600. doi:10.1016/S0165-2370(03)00028-7

Koning, S., Janssen, H.-G., Brinkman, U.A.T., 2009. Modern Methods of Sample Preparation for GC Analysis. Chromatographia 69, 33–78. doi:10.1365/s10337-008-0937-3

Kuroda, K., Ashitani, T., 2007. Thermal behavior of β-1 subunits in lignin: pyrolysis of 1, 2-diarylpropane-1, 3-diol-type lignin model compounds. J. Agric. Food Chem. 55, 2770–2778.

Kuroda, K. ichi, Nakagawa-izumi, A., 2006. Analytical pyrolysis of lignin: Products stemming from β-5 substructures. Org. Geochem. 37, 665–673. doi:10.1016/j.orggeochem.2006.01.012

Kuroda, K. ichi, Yamaguchi, A., 1995. Classification of Japanese softwood species by pyrolysis-gas chromatography. J. Anal. Appl. Pyrolysis 33, 51–59. doi:10.1016/0165-2370(94)00828-O

Kuroda, K., Suzuki, A., Kato, M., Imai, K., 1995. Analysis of rice (Oryza sativa L.) lignin by pyrolysis-gas chromatography. J. Anal. Appl. Pyrolysis 34, 1–12. doi:10.1016/0165-2370(94)00850-Z

Kuroda, K., Yamaguchi, A., Sakai, K., 1994. Analysis of Sugi wood and its lignin preparations. Mokuzai Gakkaishi 40, 987–995.

Kuroda, K.I., 2002. Electron-impact (EI) mass spectra of 1,2-dimethoxybenzenes related to the pyrolysis products of guaiacyl lignin in the presence of tetramethylammonium hydroxide (TMAH). J. Anal. Appl. Pyrolysis 64, 433–451. doi:10.1016/S0165-2370(02)00044-X

Kuroda, K.I., 2000a. Pyrolysis-trimethylsilylation analysis of lignin: Preferential formation of cinnamyl alcohol derivatives. J. Anal. Appl. Pyrolysis 56, 79–87. doi:10.1016/S0165-2370(00)00085-1

Kuroda, K.I., 2000b. Analytical pyrolysis products derived from cinnamyl alcohol-end groups in lignins. J. Anal. Appl. Pyrolysis 53, 123–134. doi:10.1016/S0165-2370(99)00067-4

Kuroda, K.I., Izumi, A., Mazumder, B.B., Ohtani, Y., Sameshima, K., 2002. Characterization of kenaf (Hibiscus cannabinus) lignin by pyrolysis-gas chromatography-mass spectrometry in the presence of tetramethylammonium hydroxide. J. Anal. Appl. Pyrolysis 64, 453–463. doi:10.1016/S0165-2370(02)00047-5

Kuroda, K.I., Nakagawa-Izumi, A., 2006. Tetramethylammonium hydroxide (TMAH) thermochemolysis of lignin: Improvement of the distribution profile of products derived from b-aryl ether subunits. J. Anal. Appl. Pyrolysis 75, 104–111. doi:10.1016/j.jaap.2005.04.011

Kuroda, K.I., Nakagawa-Izumi, A., Mazumder, B.B., Ohtani, Y., Sameshima, K., 2005. Evaluation of chemical composition of the core and bast lignins of variety Chinpi-3 kenaf (Hibiscus cannabinus L.) by pyrolysis-gas chromatography/mass spectrometry and cupric oxide oxidation. Ind. Crops Prod. 22, 223–232. doi:10.1016/j.indcrop.2005.01.002

Kuroda, K.I., Ozawa, T., Ueno, T., 2001. Characterization of sago palm (Metroxylon sagu) lignin by analytical pyrolysis. J. Agric. Food Chem. 49, 1840–1847. doi:10.1021/jf001126i

Li, J., Gellerstedt, G., 2002. Oxymercuration-demercuration kappa number : An ccurate estimation of the lignin content in chemical pulps. Nord. Pulp Pap. Res. J. 17, 410–414.

Li, J., Gellerstedt, G., 1997. The contribution to kappa number from hexeneuronic acid groups in pulp

xylan. Carbohydr. Res. 302, 213–218.

Li, J., Sevastyanova, O., Gellerstedt, G., 2002. The distribution of oxidizable structures in ECF- and TCF-bleached kraft pulps. Nord. Pulp Pap. Res. J. 17, 415–419.

Lima, C.F., Barbosa, L.C.A., Marcelo, C.R., Silvério, F.O., Colodette, J.L., 2008. Comparison between analytical pyrolysis and nitrobenzene oxidation for determination of syringyl/guaiacyl ratio in Eucalyptus spp. Lignin. BioResources 3, 701–712.

Lima, C.F., Barbosa, L.C.A., Silva, M.N.N., Colodette, J.L., Silvério, F.O., 2015. In situ determination of the syringyl/guaiacyl ratio of residual lignin in pre-bleached eucalypt kraft pulps by analytical pyrolysis. J. Anal. Appl. Pyrolysis 112, 164–172. doi:10.1016/j.jaap.2015.02.002

Lin, S.Y., Dence, C.W., 1992. Methods in Lignin Chemistry. Springer-Verlag, Nev Yourk.

Liu, C., Hu, J., Zhang, H., Xiao, R., 2016. Thermal conversion of lignin to phenols: Relevance between chemical structure and pyrolysis behaviors. Fuel 182, 864–870. doi:10.1016/j.fuel.2016.05.104

Liu, Y., Liu, Y., Lyu, G., Ji, X., Yang, G., Chen, J., Lucia, L.A., 2016. Analytical Pyrolysis Pathways of Guaiacyl Glycerol- β -guaiacyl Ether by Py-GC/MS. BioResources 11, 5816–5828.

Lopes, F.J.F., Silvério, F.O., Baffa, D.C.F., Loureiro, M.E., Barbosa, M.H.P., 2011. Determination of Sugarcane Bagasse Lignin S/G/H Ratio by Pyrolysis GC/MS. J. Wood Chem. Technol. 31, 309–323. doi:10.1080/02773813.2010.550379

Lourenço, A., Gominho, J., Marques, A.V., Pereira, H., 2013. Py-GC/MS(FID) assessed behavior of polysaccharides during kraft delignification of Eucalyptus globulus heartwood and sapwood. J. Anal. Appl. Pyrolysis 101, 142–149. doi:10.1016/j.jaap.2013.01.018

Lourenço, A., Gominho, J., Marques, A.V., Pereira, H., 2012. Reactivity of syringyl and guaiacyl lignin units and delignification kinetics in the kraft pulping of Eucalyptus globulus wood using Py-GC-MS/FID. Bioresour. Technol. 123, 296–302. doi:10.1016/j.biortech.2012.07.092

Lourenço, A., Rencoret, J., Chemetova, C., Gominho, J., Gutiérrez, A., del Río, J.C., Pereira, H., 2016. Lignin Composition and Structure Differs between Xylem, Phloem and Phellem in Quercus suber L. Front. Plant Sci. 7, 1–14. doi:10.3389/fpls.2016.01612

Łucejko, J.J., Zborowska, M., Modugno, F., Colombini, M.P., Praogonekdzyński, W., 2012. Analytical pyrolysis vs. classical wet chemical analysis to assess the decay of archaeological waterlogged wood. Anal. Chim. Acta 745, 70–77. doi:10.1016/j.aca.2012.07.046

Mamleev, V., Bourbigot, S., Le Bras, M., Yvon, J., 2009. The facts and hypotheses relating to the phenomenological model of cellulose pyrolysis. Interdependence of the steps. J. Anal. Appl. Pyrolysis 84, 1–17. doi:10.1016/j.jaap.2008.10.014

Mamleev, V., Bourbigot, S., Le Bras, M., Yvon, J., Lefebvre, J., 2006. Model-free method for evaluation of activation energies in modulated thermogravimetry and analysis of cellulose decomposition. Chem. Eng. Sci. 61, 1276–1292. doi:10.1016/j.ces.2005.07.040

Martínez, A.T., Camarero, S., Gutiérrez, A., Bocchini, P., Galletti, G.C., 2001. Studies on wheat lignin degradation by Pleurotus species using analytical pyrolysis. J. Anal. Appl. Pyrolysis 58–59, 401–411. doi:10.1016/S0165-2370(00)00116-9

Martínez, Á.T., Speranza, M., Ruiz-Dueñas, F.J., Ferreira, P., Camarero, S., Guillén, F., Martínez, M.J., Gutiérrez, A., Del Río, J.C., 2005. Biodegradation of lignocellulosics: Microbial, chemical, and enzymatic aspects of the fungal attack of lignin. Int. Microbiol. 8, 195–204. doi:im2305029 [pii]

Mazumder, B.B., Nakgawa-Izumi, A., Kuroda, K.I., Ohtani, Y., Sameshima, K., 2005. Evaluation of harvesting time effects on kenaf bast lignin by pyrolysis-gas chromatography. Ind. Crops Prod. 21, 17–24. doi:10.1016/j.indcrop.2003.12.003

Meier, D., Fortmann, I., Odermatt, J., Faix, O., 2005. Discrimination of genetically modified poplar clones by analytical pyrolysis-gas chromatography and principal component analysis. J. Anal.

Appl. Pyrolysis 74, 129–137. doi:10.1016/j.jaap.2004.12.001

Mettler, M.S., Paulsen, A.D., Vlachos, D.G., Dauenhauer, P.J., 2012. The chain length effect in pyrolysis: bridging the gap between glucose and cellulose. Green Chem. 14, 1284. doi:10.1039/c2gc35184f

Mizumoto, M., Shimokita, E., Ona, T., Seino, T., Ishida, Y., Ohtani, H., 2010. Rapid and direct characterization of total fatty acids in wood by thermochemolysis-gas chromatography-flame ionization detector/mass spectrometry with tetrabutylammonium hydroxide. J. Anal. Appl. Pyrolysis 87, 163–167. doi:10.1016/j.jaap.2009.11.004

Moldoveanu, S.C., 2010. The chemistry of the pyrolytic process., in: Moldoveanu, S.C. (Ed.), Pyrolysis of Organic Molecules with Applications to Health and Environmental Issues. Elsevier B.V., Oxford, pp. 7–48.

Mullen, C.A., Boateng, A.A., 2010. Catalytic pyrolysis-GC/MS of lignin from several sources. Fuel Process. Technol. 91, 1446–1458. doi:10.1016/j.fuproc.2010.05.022

Mussatto, S.I., 2014. Brewer ' s spent grain : a valuable feedstock for industrial applications. J. Agric. Food Chem. 94, 1264–1275. doi:10.1002/jsfa.6486

Mussatto, S.I., Dragone, G., Roberto, I.C., 2006. Brewers' spent grain: Generation, characteristics and potential applications. J. Cereal Sci. 43, 1–14. doi:10.1016/j.jcs.2005.06.001

Müller-Hagedorn, M., Bockhorn, H., Krebs, L., Müller, U., 2003. A comparative kinetic study on the pyrolysis of three different wood species. J. Anal. Appl. Pyrolysis 68–69, 231–249. doi:10.1016/S0165-2370(03)00065-2

Nakagawa-Izumi, A., Kuroda, K., 2003. Analysis of cinnamyl alcohol- and cinnamyl aldehyde end groups in lignin by trimethylsilylation/pyrolysis-gas chromatography. Bunseki Kagaku 52, 1159–1166. doi:10.2116/bunsekikagaku.52.1159

Nakamura, T., Kawamoto, H., Saka, S., 2008. Pyrolysis behavior of Japanese cedar wood lignin studied with various model dimers. J. Anal. Appl. Pyrolysis 81, 173–182. doi:10.1016/j.jaap.2007.11.002

Nanayakkara, B., Riddell, M., Harrington, J., 2016. Screening of juvenile Pinus radiata wood by means of Py-GC/MS for compression wood focussing on the ratios of p-hydroxyphenyl to guaiacyl units (H/G ratios). Holzforschung 70, 313–321. doi:10.1515/hf-2015-0068

Niemelä, K., 1988. The formation of 2-hydroxy-2-cyclopenten-1-ones from polysaccahrides dueing kraft pulping of pine wood. Carbohydr. Res. 184, 131–137.

Niemi, P., Tamminen, T., Smeds, A., Viljanen, K., Ohra-aho, T., Holopainen-Mantila, U., Faulds, C.B., Poutanen, K., Buchert, J., 2012. Characterization of lipids and lignans in brewer's spent grain and its enzymatically extracted fraction. J. Agric. Food Chem. 60, 9910–9917. doi:10.1021/jf302684x

Nierop, K.G.J., Filley, T.R., 2008. Simultaneous analysis of tannin and lignin signatures in soils by thermally assisted hydrolysis and methylation using 13C-labeled TMAH. J. Anal. Appl. Pyrolysis 83, 227–231. doi:10.1016/j.jaap.2008.07.004

Nonier, M.F., Vivas, N., Vivas De Gaulejac, N., Absalon, C., Soulie, P., Fouquet, E., 2006. Pyrolysis-gas chromatography/mass spectrometry of Quercus sp. wood: Application to structural elucidation of macromolecules and aromatic profiles of different species. J. Anal. Appl. Pyrolysis 75, 181–193. doi:10.1016/j.jaap.2005.05.006

Nunes, C.A., Lima, C.F., Barbosa, L.C.A., Colodette, J.L., Gouveia, A.F.G., Silvério, F.O., 2010. Determination of Eucalyptus spp lignin S/G ratio: A comparison between methods. Bioresour. Technol. 101, 4056–4061. doi:10.1016/j.biortech.2010.01.012

Ohara, S., Yasuta, Y., Ohi, H., 2003. Structure Elucidation of Condensed Tannins from Barks by Pyrolysis/ Gas Chromatography. Holzforschung 57, 145–149.

Ohra-aho, T., Linnekoski, J., 2015. Catalytic pyrolysis of lignin by using analytical pyrolysis-GC-MS. J. Anal. Appl. Pyrolysis 113, 186–192. doi:10.1016/j.jaap.2014.12.012

Ohra-aho, T., Sipilä, J., Tamminen, T., 2000. Analysis of lignin and model compounds by Pyrolysis-GC/MS, in: Proceedings of the Sixth EuropeanWorkshop on Lignocellulosics and Pulp. Bordeaux, France, pp. 487–490.

Oudia, A., Mészáros, E., Jakab, E., Simões, R., Queiroz, J., Ragauskas, A., Novák, L., 2009. Analytical pyrolysis study of biodelignification of cloned Eucalyptus globulus (EG) clone and Pinus pinaster Aiton kraft pulp and residual lignins. J. Anal. Appl. Pyrolysis 85, 19–29. doi:10.1016/j.jaap.2008.09.015

Oudia, A., Mészáros, E., Simões, R., Queiroz, J., Jakab, E., 2007. Pyrolysis-GC/MS and TG/MS study of mediated laccase biodelignification of Eucalyptus globulus kraft pulp. J. Anal. Appl. Pyrolysis 78, 233–242. doi:10.1016/j.jaap.2006.07.003

Patwardhan, P.R., Satrio, J.A., Brown, R.C., Shanks, B.H., 2010. Influence of inorganic salts on the primary pyrolysis products of cellulose. Bioresour. Technol. 101, 4646–4655. doi:10.1016/j.biortech.2010.01.112

Paulsen, A.D., Mettler, M.S., Dauenhauer, P.J., 2013. The role of sample dimension and temperature in cellulose pyrolysis. Energy and Fuels 27, 2126–2134. doi:10.1021/ef302117j

Pinto, P.C., Evtuguin, D. V., Neto, C.P., Silvestre, A.J.D., Amado, F.M.L., 2002. Behavior of Eucalyptus globulus lignin during kraft pulping. I. Analysis by NMR, ESI/MS, and GPC. J. Wood Chem. Technol. 22, 109–125. doi:10.1081/WCT-120013356

Ponomarenko, J., Dizhbite, T., Lauberts, M., Volperts, A., Dobele, G., Telysheva, G., 2015. Analytical pyolysis - A tool for revealing of lignin structure - antioxidant activity relationship. J. Anal. Appl. Pyrolysis 113, 360–396. doi:10.1016/j.jaap.2015.02.027

Poppius-Levlin, K., Tamminen, T., Kalliola, A., Ohra-aho, T., 2001. Characterization of residual lignins in pulps delignified by laccase/N-hydroxyacetanilide, ACS Symposium Series.

Prinsen, P., Gutiérrez, A., Rencoret, J., Nieto, L., Jiménez-Barbero, J., Burnet, A., Petit-Conil, M., Colodette, J.L., Martínez, Á.T., del Río, J.C., 2012. Morphological characteristics and composition of lipophilic extractives and lignin in Brazilian woods from different eucalypt hybrids. Ind. Crops Prod. 36, 572–583. doi:10.1016/j.indcrop.2011.11.014

Prinsen, P., Rencoret, J., Gutie, A., Liitia, T., Tamminen, T., Colodette, J.L., Mart, A.T., Jose, C., 2013. Modification of the Lignin Structure during Alkaline Deligni fi cation of Eucalyptus Wood by Kraft , Soda-AQ , and Soda-O2 Cooking. Ind. Eng. Chem. Res. 52, 15702–15712.

Qiang, L., Wen-zhi, L., Dong, Z., Xi-feng, Z., 2009. Analytical pyrolysis-gas chromatography/mass spectrometry (Py-GC/MS) of sawdust with Al/SBA-15 catalysts. J. Anal. Appl. Pyrolysis 84, 131–138. doi:10.1016/j.jaap.2009.01.002

Ralph, J., 2010. Hydroxycinnamates in lignification. Phytochem. Rev. 9, 65–83.

Ralph, J., Brunow, G., Boerjan, W., 2007. Encyclopedia of life science. John Wiley and Sons, pp. 1–10.

Ralph, J., Hatfield, R.D., 1991. Pyrolysis-GC–MS characterization of forage materials. J. Agric. Food Chem. 39, 1426–1437.

Ralph, J., Hatfield, R.D., Piquemal, J., Yahiaoui, N., Pean, M., Lapierre, C., Boudet, A.M., 1998. NMR characterization of altered lignins extracted from tobacco plants down-regulated for lignification enzymes cinnamylalcohol dehydrogenase and cinnamoyl-CoA reductase. Proc. Natl. Acad. Sci. U. S. A. 95, 12803–12808. doi:10.1073/pnas.95.22.12803

Reina, L., Galetta, A., Vinciguerra, V., Resquin, F., Menéndez, P., 2014. The relationship between Eucalyptus grandis lignin structure and kraft pulping parameters. J. Anal. Appl. Pyrolysis 107, 284–288. doi:10.1016/j.jaap.2014.03.013

Rencoret, J., del Río, J.C., Nierop, K.G.J., Gutiérrez, A., Ralph, J., 2016. Rapid Py-GC / MS assessment of the structural alterations of lignins in genetically modified plants. J. Anal. Appl. Pyrolysis 121, 155–164. doi:10.1016/j.jaap.2016.07.016

Rencoret, J., Marques, G., Ibarra, D., Li, J., Santos, J.I., Rı, C., 2008. Structural characterization of milled wood lignins from different eucalypt species. Holzforschung 62, 514–526. doi:10.1515/HF.2008.096

Rencoret, J., Prinsen, P., Gutiérrez, A., Martinez, Á.T., del Río, J.C., 2015. Isolation and structural characterization of the milled wood lignin, dioxane lignin, and cellulolytic lignin preparations from brewer's spent grain. J. Agric. Food Chem. 63, 603–613. doi:10.1021/jf505808c

Rencoret, J., Ralph, J., Marques, G., Gutiérrez, A., Martínez, Á.T., del Río, J.C., 2013. Structural characterization of lignin isolated from coconut (Cocos nucifera) coir fibers. J. Agric. Food Chem. 61, 2434–2445. doi:10.1021/jf304686x

Robertson, J.A., I'Anson, K.J.A., Treimo, J., Faulds, C.B., Brocklehurst, T.F., Eijsink, V.G.H., Waldron, K.W., 2010. Profiling brewers' spent grain for composition and microbial ecology at the site of production. LWT - Food Sci. Technol. 43, 890–896. doi:10.1016/j.lwt.2010.01.019

Rodrigues, J., Graça, J., Pereira, H., 2001. Influence of tree eccentric growth on syringyl/guaiacyl ratio in Eucalyptus globulus wood lignin assessed by analytical pyrolysis. J. Anal. Appl. Pyrolysis 58–59, 481–489. doi:10.1016/S0165-2370(00)00121-2

Rodrigues, J., Meier, D., Faix, O., Pereira, H., 1999. Determination of tree to tree variation in syringyl/guaiacyl ratio of Eucalyptus globulus wood lignin by analytical pyrolysis. J. Anal. Appl. Pyrolysis 48, 121–128. doi:10.1016/S0165-2370(98)00134-X

Ropponen, J., Räsänen, L., Rovio, S., Ohra-aho, T., Liitiä, T., Mikkonen, H., Van De Pas, D., Tamminen, T., 2011. Solvent extraction as a means of preparing homogeneous lignin fractions. Holzforschung 65, 543–549. doi:10.1515/HF.2011.089

S.Y. Lin, Dence, C.W., 1992. Methods in Lignin Chemistry. New York.

Saiz-Jimenez, C., De Leeuw, J.W., 1986. Lignin pyrolysis products: Their structures and their significance as biomarkers. Org. Geochem. 10, 869–876. doi:10.1016/S0146-6380(86)80024-9

Sarkanen, K.V., Hergert, H.L., 1971. Classification and distribution, in: Sarkanen, K.V., Ludwig, C.H. (Eds.), Lignins: Occurrence, Formation, Structure and Reactions. Wiley-Interscience, New York, pp. 43–94.

Schultz, T.P., Templeton, M.C., 1986. Proposed mechanism for the Nitrobenzene Oxidation of Lignin. Holzforschung 40, 93–97.

Selsbo, P., Ericsson, I., Kleen, M., 1997. Characterization of sulfur in wood pulps using pyrolysis-gas chromatography with sulfur-selective detection. J. Anal. Appl. Pyrolysis 43, 1–14. doi:10.1016/S0165-2370(97)00055-7

Shadkami, F., Estevez, S., Helleur, R., 2009. Analysis of catechins and condensed tannins by thermally assisted hydrolysis/methylation-GC/MS and by a novel two step methylation. J. Anal. Appl. Pyrolysis 85, 54–65. doi:10.1016/j.jaap.2008.09.001

Shadkami, F., Helleur, R., 2010. Recent applications in analytical thermochemolysis. J. Anal. Appl. Pyrolysis 89, 2–16. doi:10.1016/j.jaap.2010.05.007

Shaik, S.M., Sharratt, P.N., Tan, R.B.H., 2013. Influence of selected mineral acids and alkalis on cellulose pyrolysis pathways and anhydrosaccharide formation. J. Anal. Appl. Pyrolysis 104, 234–242. doi:10.1016/j.jaap.2013.07.010

Sheirs, J., Camino, G., Tumiatti, W., 2001. Overview of water evolution during the thermal degradation of cellulose. Eur. Polym. J. 37, 933–942.

Shen, D., Zhao, J., Xiao, R., Gu, S., 2015. Production of aromatic monomers from catalytic pyrolysis of

black-liquor lignin. J. Anal. Appl. Pyrolysis 111, 47–54. doi:10.1016/j.jaap.2014.12.013

Shen, D.K., Gu, S., Bridgwater, A. V., 2010. The thermal performance of the polysaccharides extracted from hardwood: Cellulose and hemicellulose. Carbohydr. Polym. 82, 39–45. doi:10.1016/j.carbpol.2010.04.018

Sjöberg, J., Kleen, M., Dahlman, O., 2002. Analyses of carbohydrates and lignin in the surface and inner layers of softwood pulp fibers obtained employing various alkalinen cooking processes. Nord. Pulp Pap. Res. J. 17, 296–301.

Sjöström, E., Alen, R., 1999. Analytical Methods in Wood Chemistry, Pulping, and Papermaking. Springer, Berlin.

Sobeih, K.L., Baron, M., Gonzalez-Rodriguez, J., 2008. Recent trends and developments in pyrolysis-gas chromatography. J. Chromatogr. A 1186, 51–66. doi:10.1016/j.chroma.2007.10.017

Sun, R., Lawther, J.M., Banks, W.B., 1995. The effect of alkaline nitrobenzene oxidation conditions on the yield and components of phenolic monomers in wheat straw lignin and compared to cupric(II) oxidation. Ind. Crops Prod. 4, 241–254. doi:10.1016/0926-6690(95)00038-0

Syverud, K., Leirset, I., Vaaler, D., 2003. Characterization of carbohydrates in chemical pulps by pyrolysis gas chromatography/mass spectrometry. J. Anal. Appl. Pyrolysis 67, 381–391. doi:10.1016/S0165-2370(02)00076-1

Tamminen, T., Kleen, M., Ohra-aho, T., Poppius-Levlin, K., 2003a. Chemistry of Mediated-Laccase Delignification Analyzed by Pyrolysis-GC/MS. J. Pulp Pap. Sci. 29, 319–324.

Tamminen, T., Ohra-aho, T., Hortling, B., Tenkanen, M., 2003b. Residual lignin in hydrogen peroxide-bleached softwood pulps, in: Proceedings of the 12th International Symposium onWood Pulp Chemicals, Vol. I. pp. 69–72.

Tanaka, J., Izumi, A., Suzuki, S., Ohi, H., Kuroda, K., 1997. Structural Analysis of Lignin by Pyrolysis-Gas Chromatography (IV) -Comparison with nitrobenzene oxidation for determination of decaed hardwoods and kraft-cooked hardwoods. Japan TAPPI J. 51, 358–366.

Tenkanen, M., Gellerstedt, G., Vuorinen, T., Teleman, A., Perttula, M., Li, J., Buchert, J., 1999. Determination of Hexenuronic Acid in Softwood Kraft Pulps by Three Different Methods. J. Pulp Pap. Sci. 25, 305–311.

Thiebaud, S., Borredon, M.E., Baziard, G., Senocq, F., 1997. Properties of wood esterified by fatty-acid chlorides. Bioresour. Technol. 59, 103–107.

Tsutsumi, B.Y., Kondo, R., Sakai, K., Imamura, H., 1995. The Difference of Reactivity between Syringyl Lignin and Guaiacyl Lignin in Alkaline Systems. Holzforschung 49, 423–428.

Tydén-Ericsson, I., 1973. A new pyrolyzer with improved control of pyrolysis conditions. Chromatographia 6, 353–358. doi:10.1007/BF02270569

Válková, D., Grasset, L., Amblès, A., 2009. Molecular compounds generated by ruthenium tetroxide oxidation and preparative off line thermochemolysis of lignite humic acids from South Moravia: Implications for molecular structure. Fuel 88, 2113–2121. doi:10.1016/j.fuel.2009.01.026

Wallis, A., Wearne, R., Wright, P., 1996. Chemical Analysis of Polysaccharides in Plantation Eucalyptus wood and Pulps. Appita J. 49, 258–262.

Wampler, T.P., 1999. Introduction to pyrolysis – capillary gas chromatography. J. Chromatogr. A 842, 207–220.

Wampler, T.P., 1995. Appleid pyrolysis handbook. Marcel Dekker, Inc., New York.

Watanabe, T., Kawamoto, H., Saka, S., 2009. Radical chain reactions in pyrolytic cleavage of the ether linkages of lignin model dimers and a trimer. Holzforschung 63, 424–430. doi:10.1515/HF.2009.076

Wikberg, H., Ohra-aho, T., Honkanen, M., Kanerva, H., Harlin, A., Vippola, M., Laine, C., 2016. Hydrothermal carbonization of pulp mill streams. Bioresour. Technol. 212, 236–244. doi:10.1016/j.biortech.2016.04.061

Woolfenden, E., 2012. Thermal Desorption for Gas Chromatography, in: Poole, C.F. (Ed.), Gas Chromatography. pp. 235–289. doi:10.1016/B978-0-12-385540-4.00010-9

Wu, S., Shen, D., Hu, J., Zhang, H., Xiao, R., 2016. Role of β-O-4 glycosidic bond on thermal degradation of cellulose. J. Anal. Appl. Pyrolysis 119, 147–156. doi:10.1016/j.jaap.2016.03.006

Xie, Y.M., 2004. Difference of condensed lignin structures in eucalyptus species. Nord. Pulp Pap. Res. J. 19, 18–21. doi:10.3183/NPPRJ-2004-19-01-p018-021

Xiros, C., Christakopoulos, P., 2012. Biotechnological potential of brewers spent grain and its recent applications. Waste and Biomass Valorization 3, 213–232. doi:10.1007/s12649-012-9108-8

Yang, H., Yan, R., Chen, H., Lee, D.H., Zheng, C., 2007. Characteristics of hemicellulose, cellulose and lignin pyrolysis. Fuel 86, 1781–1788. doi:10.1016/j.fuel.2006.12.013

Yang, Q., Wu, S., Lou, R., Lv, G., 2010. Analysis of wheat straw lignin by thermogravimetry and pyrolysis-gas chromatography/mass spectrometry. J. Anal. Appl. Pyrolysis 87, 65–69. doi:10.1016/j.jaap.2009.10.006

Yokoi, H., Ishida, Y., Ohtani, H., Tsuge, S., Sonoda, T., Ona, T., 1999. Characterization of within-tree variation of lignin components in Eucalyptus camaldulensis by pyrolysisgas chromatography. Analyst 124, 669–674. doi:10.1039/A809217F

Yokoi, H., Nakase, T., Goto, K., Ishida, Y., Ohtani, H., Tsuge, S., Sonoda, T., Ona, T., 2003. Rapid characterization of wood extractives in wood by thermal desorption-gas chromatography in the presence of tetramethylammonium acetate. J. Anal. Appl. Pyrolysis 67, 191–200. doi:10.1016/S0165-2370(02)00061-X

Yokoi, H., Nakase, T., Ishida, Y., Ohtani, H., Tsuge, S., Sonoda, T., Ona, T., 2001. Discriminative analysis of Eucalyptus camaldulensis grown from seeds of various origins based on lignin components measured by pyrolysis-gas chromatography. J. Anal. Appl. Pyrolysis 57, 145–152. doi:10.1016/S0165-2370(00)00137-6

Zhang, J.J., Jiang, X.Y., Ye, X.N., Chen, L., Lu, Q., Wang, X.H., Dong, C.Q., 2016. Pyrolysis mechanism of a β-O-4 type lignin dimer model compound: A joint theoretical and experimental study. J. Therm. Anal. Calorim. 123, 501–510. doi:10.1007/s10973-015-4944-y

Zhang, X., Yang, W., Dong, C., 2013. Levoglucosan formation mechanisms during cellulose pyrolysis. J. Anal. Appl. Pyrolysis 104, 19–27. doi:10.1016/j.jaap.2013.09.015

Zhou, S., Xue, Y., Sharma, A.M., Bai, X., 2016. Lignin Valorization through Thermochemical Conversion: Comparison of Hardwood, Softwood and Herbaceous Lignin. ACS Sustain. Chem. Eng. 4, 6608–6617. doi:10.1021/acssuschemeng.6b01488

Zhurinsh, A., Dobele, G., Rizhikovs, J., Zandersons, J., Grigus, K., 2013. Effect of pretreatment conditions on the analytical pyrolysis products from birch wood lignocellulose. J. Anal. Appl. Pyrolysis 103, 227–231. doi:10.1016/j.jaap.2012.12.008

Ziobro, G.C., 1990. Origin and nature of kraft colour. 1. Role of aromatics. J. Wood Chem. Technol. 10, 133–149.

I

Ohra-aho T., Tenkanen M., Tamminen T. (2005) Direct analysis of lignin and lignin-like components from softwood kraft pulp by Py-GC/MS techniques. *J. Anal. Appl. Pyrolysis* ***74,*** 123-128.

Available online at www.sciencedirect.com
SCIENCE DIRECT®
J. Anal. Appl. Pyrolysis 74 (2005) 123–128
JOURNAL of ANALYTICAL and APPLIED PYROLYSIS
www.elsevier.com/locate/jaap

Direct analysis of lignin and lignin-like components from softwood kraft pulp by Py-GC/MS techniques

Taina Ohra-aho [a,*], Maija Tenkanen [b], Tarja Tamminen [a]

[a] KCL, P.O. Box 70, FIN-02151 Espoo, Finland
[b] Department of Applied Chemistry and Microbiology, University of Helsinki, P.O. Box 27, FIN-00014, University of Helsinki, Finland

Received 2 July 2004; accepted 22 November 2004

Abstract

Analytical pyrolysis combined with gas chromatography/mass spectrometry was used to analyse the structure and quantity of aromatic components, mainly guaiacyl and hydroxyphenyl derivatives, directly from chemical pulps. The quantity of aromatic degradation products was determined using a new external calibration method. The external standard was analyzed similarly to the pulp sample, and the combined area of the degradation products formed, normalized to the sample amount, was used for calibration. The method was sensitive enough to detect aromatics from fully bleached softwood pulps at a concentration level of 0.4 wt.%.

The effect of bleaching on lignin structures in softwood pulps was studied by following the changes in guaiacyl-type degradation product distribution. The residual lignin structures that had been modified during cooking were removed during the course of bleaching. The residual lignin in fully bleached pulps therefore was found to bear features characteristic of native lignin in addition to increased oxidation. A striking enrichment of hydroxyphenyl-type aromatic pyrolysis products was observed during bleaching. It is suggested that they are derived not only from lignin but also from other pulp components.

Keywords: Analytical method; Pyrolysis; Kraft pulp; Softwood; Residual lignin; Quantitation; Gas chromatography; Mass spectrometry

1. Introduction

Pyrolysis-gas chromatography/mass spectrometry (Py-GC/MS) is a technique, which provides a method for specifically detecting lignin in pulp, without interference from other fibre components. On the other hand, only the aromatic moieties of lignin are detectable. In the case of softwood lignin, hydroxyphenyl- and guaiacyl-type phenolic compounds are detected. The method has generally been used for the qualitative recognition of lignin in pulp rather than quantitation.

A quantitative method has been reported in the literature in which the amount of each degradation product is calculated separately using the corresponding pure compounds for calibration [1]. It is quite complicated and in addition, not all the lignin degradation products are commercially available. Calibration with one monomeric internal standard underestimates the lignin content [2,3].

We have earlier developed a method based on external calibration for the determination of absolute amounts of aromatic lignin from pulps [6]. This method is now described in more detail in the experimental part below. Because not all the linkages between the lignin subunits are cleaved during pyrolysis, the standard used for external calibration needs to be structurally similar to the lignin to be quantified. Model compound studies have shown that the beta aryl ether bond is cleaved extensively in pyrolysis, but only partial cleavage of carbon–carbon bonds are reported to take place [4,5].

In addition to the quantitative determination, changes in guaiacyl and hydroxyphenyl-type aromatic structures can be followed through the bleaching sequence. In earlier studies a striking enrichment of hydroxyphenyl-type structures has been observed during bleaching [7,8]. This effect is even more pronounced when the pulp is analysed directly

* Corresponding author.
E-mail address: taina.ohra.aho@kcl.fi (T. Ohra-aho).

0165-2370/$ – see front matter © 2004 Published by Elsevier B.V.
doi:10.1016/j.jaap.2004.11.010

compared with the analysis of the corresponding isolated residual lignin [9–12]. This suggests that other fibre components in addition to lignin contribute to the formation of hydroxyphenyl degradation products.

The aim of this study was to follow the degree of delignification as well as the structural changes in the lignin and possibly other aromatic components along a light elementary chlorine free (ECF) bleaching sequence. In addition, methylated-pyrolysis and fractionated pyrolysis have been applied in order to clarify the origin of hydroxyphenyl structures as they have been suggested to contribute to the brightness reversion of fully bleached pulps.

2. Experimental

2.1. Samples

Laboratory-bleached pine (*Pinus silvestris*) kraft pulps were studied. The ECF-light bleaching sequence contained oxygen (O), chelation (Q), pressurized alkaline hydrogen peroxide (PO) and chlorine dioxide (D) stages in the order O–Q–PO–D/Q–PO. Pulp samples were analysed after each stage. Detailed information about the chemical charges and reaction parameters are reported elsewhere [13]. Kraft lignin, precipitated (pH 2.5) from black liquor from the conventional kraft cooking of pine, was used as an external standard. For the fractionated pyrolysis study, an oxygen-delignified ECF bleached spruce (*Picea abies*) kraft pulp was used [14].

2.2. The pyrolysis-gas chromatography/mass spectrometry system

A platinum foil pulse pyrolyzer (Pyrolab2000® from Pyrolab, Sweden) was connected to a GC/MS instrument (Varian 3800 GC/2000 MS). A description of the pyrolyzer has been given elsewhere [15].

2.3. Isothermal and fractionated pyrolysis

About 80 μg of the pulp sample were weighed accurately on an automatic ultra-micro balance (CAHN 29 Instruments Inc., Cerritos, USA) and transferred to the foil. The pyrolysis chamber (maintained at 150 °C) was purged with helium (18 ml/min) and the temperature rise time was set to 8 ms. Isothermal pyrolysis was performed at 580 °C for 2 s. The degradation products were led into a capillary column (J&W, DB-1701, 30 m × 0.25 mm, film 1 μm) for separation using helium as carrier gas, flow rate 0.9 ml/min. The injector temperature was 280 °C. The capillary column temperature was programmed as follows: initial temperature 100 °C, rate of increase 4 °C/min to 265 °C and held for 5 min. The different compounds were identified and quantified using an ion trap mass spectrometer (EI 70 eV). The ion trap temperature was set to 180 °C and the mass range was scanned from *m/z* 46 to 299. The products formed were identified using data from [16,17] and the commercial NIST92 library.

Table 1
Conditions used for fractionated pyrolysis

Temperature (°C)	Time (s)
40	320
12	480
4	620
2	800

The pyrolysis temperatures and times used in fractionated pyrolysis are presented in Table 1. Other conditions were the same as in the isothermal Py-GC/MS method.

2.4. Pyrolysis-methylation

Pyrolysis-methylation was performed in the presence of a 10% aqueous solution of tetramethyl ammonium hydroxide (TMAH, 10% w/w aqueous solution, Merck). About 80 μg of the pulp sample were weighed accurately and transferred to the foil. A 2–3 μl of TMAH were added and mixed gently with the sample. Pyrolysis was performed at 400 °C for 4 s. After pyrolysis, the degradation products were separated on a capillary column (J&W, DB-1, 30 m × 0.25 mm, film 1 μm) using helium as carrier gas, flow rate 1 ml/min. The injector temperature was 280 °C. The capillary column temperature was programmed as follows: initial temperature 50 °C for 5 min, rate of increase 10 °C/min to 320 °C and held for 5 min. The ion trap temperature was set to 200 °C and the mass range was scanned from *m/z* 46 to 650.

2.5. Kappa number

Kappa number was determined using the standard method SCAN-C 1. Lignin kappa was calculated by subtracting the contribution from hexenuronic acid (HexA) to the kappa number (kappa-0.085 × HexA) [18]. The hexenuronic acid content was determined by high performance liquid chromatography after enzymatic hydrolysis [19]. Lignin content (“aromatic lignin”) was calculated from the lignin kappa number by multiplying by 0.15% [20].

3. Results and discussion

3.1. External standard calibration method

Softwood pulp lignin is composed of two cinnamyl alcohol units: *p*-coumaryl alcohol and coniferyl alcohol. Sixteen guaiacyl-type pyrolysis degradation products that were formed from the coniferyl alcohol units, and 3 hydroxyphenyl-type pyrolysis degradation products that were expected to originate from *p*-coumaryl alcohol units were identified and quantified in the pulps studied. The

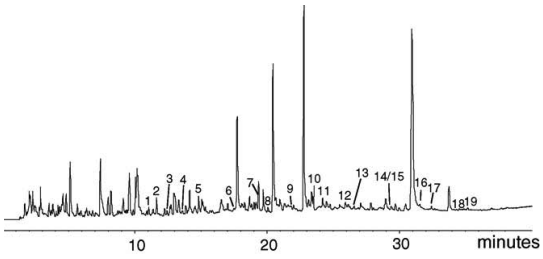

Fig. 1. Total ion current pyrogram of the unbleached pine kraft pulp. Pyrolysis was performed at 580 °C for 2 s. Numbered peaks are aromatic degradation products, the structures of which are given in Table 1.

pyrogram of the unbleached pine kraft pulp is shown in Fig. 1. The main peaks seen in the pyrogram represent the degradation products formed from polysaccharides. Aromatic degradation products are numbered in the pyrogram and the identities of these are given in Table 2. As the pyrogram illustrates, the peak intensities of the aromatic degradation products in the unbleached pulp were quite low. In order to increase the sensitivity of the quantitation method, the peak areas were integrated using specific ions *m/z*. Ions that were used for the integration are given in Table 2. The peak areas integrated using selected ions *m/z* were converted to the corresponding total peak areas using factors calculated from the pure mass spectrum of each component.

Table 2
Aromatic degradation products detected in the pulp samples

Peak number	Compound	Structure	Ions used for integration	Factor[a]
1	Phenol	H	94, 66, 65	1.5
2	Guaiacol	G	124, 109, 81	1.6
3	2-Methylphenol	H	108, 107, 77	2.2
4	4-Methylphenol	H	108, 107, 77	2.2
5	4-Methylguaiacol	G	138, 123, 67	2.0
6	4-Ethylguaiacol	G	152, 137, 122	2.2
7	4-Vinylguaiacol	G	150, 135, 107	2.1
8	Eugenol	G	164, 149, 77	3.8
9	*cis*-Isoeugenol	G	164, 149, 77	3.9
10	*trans*-Isoeugenol	G	164, 149, 77	3.5
11	Vanillin	G	152, 151, 123	2.4
12	Homovanillin	G	166, 137, 122	2.0
13	Acetoguaiacone	G	166, 151, 123	2.1
14	4-(Oxy-allyl) guaiacol	G	178, 151, 123	2.7
15	4-(Hydroxy-prop-2-enyl)guaiacol	G	180, 137, 124	3.1
16	Dihyroconifery lalcohol	G	182, 137, 122	3.1
17	*cis*-Coniferyl alcohol	G	180, 137, 124	4.0
18	*trans*-Coniferyl alcohol	G	180, 163, 137	2.7
19	Coniferaldehyde	G	178, 147, 135	5.5

H: hydroxyphenyl-type; G: guaiacyl-type.
[a] Factor used to correct the peak areas to correspond to the total peak areas.

Factors were calculated similarly as has been reported in reference study [21].

After the integration procedure, peak areas were normalized to the weighed sample amount. The quantity of aromatic products in the pulp samples was determined using a one point external standard calibration. Kraft lignin was used as an external standard because the distribution of its degradation products was similar to that for pulp lignin [12]. The method was sensitive enough to detect aromatics in the fully bleached softwood pulps at a level of 0.4 wt.%. The residual standard deviation of three parallel measurement was 5% and the concentration range was up to 0.4 wt.%.

3.2. Composition of aromatic degradation products in pulp

The distribution of hydroxyphenyl- and guaiacyl-type degradation products was followed through a light ECF bleaching sequence. Changes in the relative amounts of all aromatic degradation products are shown in Fig. 2. Strikingly, the hydroxyphenyl pyrolysis products were highly enriched during delignification and bleaching and corresponded to guaiacyl-type structures. The proportion of hydroxyphenyl structures in the fully bleached pulp was three-fold in comparison to the unbleached pulp. In wood chips the proportion of hydroxyphenyl structures was less than 1%. Enrichment in hydroxyphenyl structures has also been observed in previous studies [9–12]. However, the reason for the phenomenon has been unclear.

The hydroxyphenyl structures detected in pulps are phenol and 2- and 4-methylphenol. Thus, the substitution pattern of the degradation products differs clearly from the guaiacyl-type structures, several of which still bear residues from the propane side chains of lignin subunits. This suggests, together with the different behaviour during bleaching, that there may be sources other than lignin of the hydroxyphenyl structures. Other wood components that have been reported to form phenol, the main hydroxyphenyl structure, in pyrolysis are polysaccharides [22–23], phenolic extractives [24] and protein and amino acids [22].

The distribution of the three-hydroxyphenyl structures along the bleaching sequence is shown in Fig. 2. The result

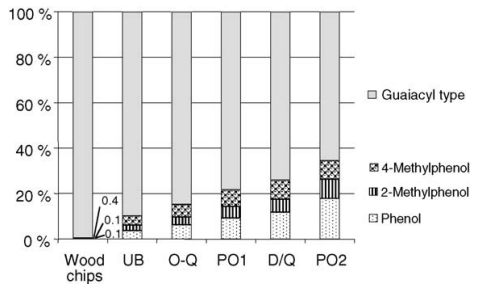

Fig. 2. Distribution between hydroxyphenyl- and guaiacyl-type degradation products during bleaching.

Table 3
Distribution of guaiacyl-type aromatic trace components (after normalization to 100%) in wood chips and pulps

Compound	Wood chips	UB	O–Q1	PO1	D/Q	PO_2
Guaiacol	3.9	13.0	10.5	10.4	8.9	10.3
4-Methylguaiacol	10.6	14.4	11.6	10.8	9.9	9.0
4-Ethylguaiacol	1.5	3.0	2.3	2.3	2.1	2.2
4-Vinylguaiacol	10.4	18.1	15.9	16.2	14.5	14.0
Eugenol	5.0	5.1	4.9	4.8	4.8	4.9
cis-Isoeugenol	2.3	3.1	3.1	3.6	3.3	4.9
trans-Isoeugenol	12.3	12.6	12.4	12.8	11.9	12.9
Vanillin	9.0	7.0	11.6	13.2	18.4	19.8
Homovanillin	5.9	6.1	7.5	8.0	13.0	16.1
Acetoguaiacone	4.8	4.3	5.5	5.3	5.9	6.0
4-(Oxy-allyl)guaiacol	2.9	1.2	1.3	n.d.	n.d.	n.d.
4-(Hydroxy-prop-2-enyl) guaiacol	5.0	4.0	4.1	4.0	4.1	n.d.
Dihyroconiferylalcohol	4.0	3.6	3.7	4.3	n.d.	n.d.
cis-Coniferyl alcohol	3.5	1.2	1.6	2.3	3.3	n.d.
trans-Coniferyl alcohol	10.0	0.6	1.3	n.d.	n.d	n.d.
Coniferaldehyde	8.8	2.8	2.8	2.0	n.d.	n.d.

shows that all hydroxyphenyl structures are enriched. The proportion of phenol increased five-fold, and that of 2-methylphenol four-fold, after the initial stage. The enrichment of 4-methylphenol was lower. The proportion of the corresponding guaiacyl structures (guaiacol and 4-methylguaiacol) simultaneously decreased (Table 3).

It is expected that all guaiacyl-type degradation products originate from lignin, reflecting the effect of bleaching on lignin structure. The distribution between guaiacyl-type structures after normalization to 100% is presented in Table 3. The main change was an increase in carbonyl-type structures due to the oxidation of lignin (vanillin, homovanillin, acetoguaiacone). No changes were observed in the proportion of the degradation products with two- and three-carbon alkyl chains. The proportion of short side chain structures (guaiacol and 4-methylguaiacol) increased during cooking as a consequence of the cleavage of the native beta aryl ether bonds, but decreased steadily during further delignification and bleaching (Table 3). This indicates that the bleaching chemicals reacted preferentially with the lignin, which had been modified during cooking, compared to the residual lignin fraction still containing beta aryl ether bonds. Native lignin structures are therefore enriched during bleaching. The result is similar to that from a study of residual lignins isolated from a fully bleached eucalypt pulp [25].

3.3. Quantity of aromatic degradation products in pine kraft pulps

The quantities of hydroxyphenyl- and guaiacyl-type structures were compared with results obtained by traditional methods. A good correlation was found between lignin values calculated from lignin kappa and the aromatic pyrolysis degradation products (Fig. 3). However, for the unbleached pulps, the quantity of aromatic pyrolysis

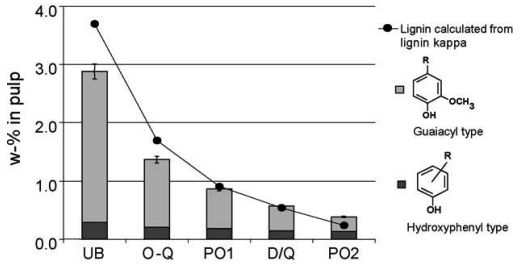

Fig. 3. Quantity of aromatic hydroxyphenyl- and guaiacyl-type degradation products in pulps determined by the Py-GC/MS external standard method. Aromatic lignin content in pulp calculated from the lignin kappa value (lignin kappa = 0.15%).

degradation products was lower than that indicated by the lignin kappa value. This is probably due to the fact that unbleached kraft pulps contain substances (also other than hexenuronic acid) that contribute to the kappa number measurement, erroneously increasing the lignin content estimated from the kappa number [26].

For the fully bleached pulp, Py-GC/MS gave higher values compared to the lignin kappa values. This result indicates that a certain fraction of residual lignin is undetectable using the kappa number measurement, as we have reported earlier [10]. This fraction is enriched during bleaching, thus giving rise to too low lignin content especially for the bleached pulps, when the calculation is based on kappa number. Thus, the pyrolysis method estimates lignin content more reliably compared to the traditional method both for unbleached and bleached pulps.

3.4. Origin of hydroxyphenyl units

The amount of guaiacyl-type structures decreased by approximately 90% during bleaching, whereas only 50% of the hydroxyphenyl structures were simultaneously removed. One aim of this study was to clarify whether this difference is due to different reactivities of the corresponding lignin subunits, or if the hydroxyphenyl structures originate to a significant extent from non-lignin material.

Pyrolysis-methylation in the presence of tetramethyl ammonium hydroxide (TMAH) was performed on unbleached and fully bleached pulp samples. The purpose of the experiment was to determine whether the hydroxyphenyl structures originated from non-aromatic structures, which during isothermal pyrolysis decomposed forming phenols. The methylated analogues of guaiacyl structures (dimethoxybenzene derivatives) and hydroxyphenyl structures (methoxylbenzene derivatives) were expected to form, if the corresponding aromatic components were already present in the starting material [27]. In this case, only methylated analogues of phenol (4-methoxy benzoic acid methyl ester) and guaiacol (3,4-dimethoxy benzoic acid methyl ester) were detected. Part of the pyrogram, detected by specific ions *m/z* 135 and 196, is shown in Fig. 4. The

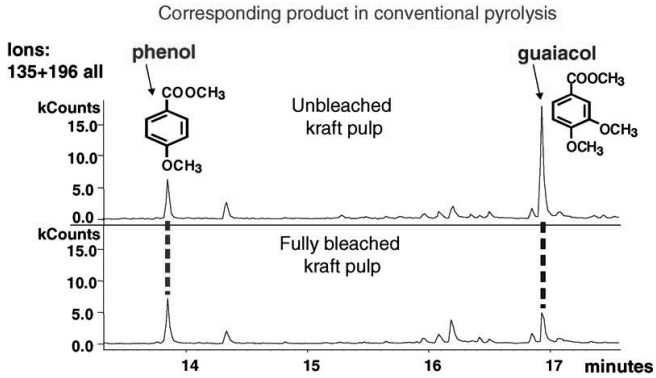

Fig. 4. Pyrolysis degradation products obtained from an unbleached and a fully bleached pulp using pyrolysis-methylation. Methylation was performed at 400 °C in the presence of TMAH.

unbleached and fully bleached pulps contained both phenol and guaiacol analogues. The yield of guaiacol, detected at ion *m/z* 196, was lower in the fully bleached pulp than in the unbleached pulp. The peak area of phenol, however, detected at ion *m/z* 135 was the same in the unbleached and fully bleached pulps, in accordance with the results obtained using isothermal pyrolysis. This test proved that the hydroxyphenyl structures originated from aromatic structures present in the pulp, and they were not secondary products formed during pyrolysis.

Another method applied to clarify the origin of the hydroxyphenyl structures was fractionated pyrolysis. The principle of this technique is that the same original sample is analyzed stepwise at increasing temperatures for different times [28]. It is therefore possible to study particular fractions of a sample. Earlier, the method has been used to study the bonding behavior of sulfur in sulfur-treated softwood pulp [29] as well the interactions between 1-hydroxybenzotriazole and softwood pulp residual lignin [30]. In the present study, fractionated pyrolysis was applied to evaluate the bonding between the hydroxyphenyl- and guaiacyl-type structures in order to determine whether they originated from the same polymer components.

The distribution of hydroxyphenyl- and guaiacyl-type structures in fully bleached pulp as a function of temperature is presented in Fig. 5. The main portion of guaiacyl structures formed at 320 °C a temperature at which no hydroxyphenyl structures were formed. Some of the guaiacyl structures and the main portion of the hydroxyphenyl structures originated at 480 °C indicating that both structures had the same origin, probably lignin. However, a high percentage of hydroxyphenyl structures formed at 620 °C, accompanied by only small quantities of guaiacyl structures. It is likely, therefore, that hydroxyphenyl structures forming at higher temperatures probably arose from some structure other than lignin.

Intact pulp polysaccharides cannot be source of the hydroxyphenyl structures, as it was shown that they are present already in the original sample in the form of aromatic structures. In addition, we have shown earlier that upon pyrolysis, pure microcrystalline cellulose only yields a small amount of phenol, but no methylphenols, which are detectable from pulp fiber [10]. On the contrary, polysaccharides modified during pulping are a probable source of the phenol derivatives, as aromatic structures are known to form from carbohydrates under pulping conditions [23]. The almost complete lack of *p*-hydroxyphenyl-type degradation products with longer residues from the phenylpropan side chain structure is a further evidence against lignin being their main source.

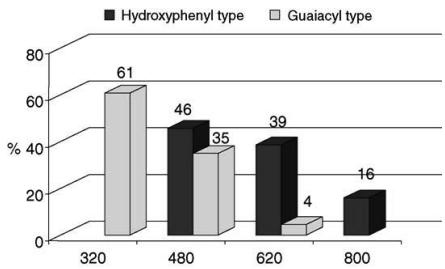

Fig. 5. Formation of guaiacyl- and hydroxyphenyl-type structures as a function of temperature in a fully bleached ECF pulp.

4. Conclusions

Analytical Py-GC/MS can be used for the characterization of residual lignin directly from softwood pulps. It is possible to determine the pulp aromatics both quantitatively and qualitatively during the bleaching sequence. For quantitative information, an external calibration method was applied. An advantage of the pyrolysis method is that the products detected are precisely known. Problems relating to lignin quantitation based on traditional methods, such as kappa number, can therefore be overcome.

Hydroxyphenyl structures were enriched during bleaching. Their main source was suggested to be aromatic structures formed from polysaccharides during pulping. It was shown that the aromatic structures were already present in the starting material, and that they were not artefacts formed during pyrolysis. Lignin in the bleached pulps was oxidized, but was otherwise strikingly similar to native lignin.

Acknowledgements

We thank Peter Vihra for performing the technical work in the pyrolysis experiments.

References

[1] A. Izumi, K.-I. Kuroda, H. Ohi, A. Yamaguchi, Mokuzai Gakkaishi 49 (1995) 735.
[2] P. Bocchini, G.D. Galletti, S. Camarero, A.T. Martinez, J. Chromatogr. A 773 (1997) 227.
[3] A.-S. Jääskeläinen, D.S. Argyropoulos, in: Proceedings of the Sixth European Workshop on Lignocellulosics and Pulp, Bordeaux, France, September 3–6, 2000, pp. 371–374.
[4] O. Faix, D. Meier, I. Fortmann, J. Anal. Appl. Pyrol. 14 (1988) 135.
[5] K.-I. Kuroda, J. Anal. Appl. Pyrol. 53 (2000) 123.
[6] T. Ohra-aho, J. Sipilä, T. Tamminen, in: Proceedings of the Sixth European Workshop on Lignocellulosics and Pulp, Bordeaux, France, September 3–6, 2000, pp. 487–490.
[7] F. Chakar, I. Lucia, A. Ragauskas, Preprints International Pulp Bleaching Conference, PPATAC 2000, pp. 123–130.
[8] L. Akim, J. Colodette, D.S. Argyropoulos, Preprints International Pulp Bleaching Conference, PPATAC 2000, pp. 103–110.
[9] T. Tamminen, M. Kleen, T. Ohra-aho, K. Poppius-Levlin, J. Pulp Paper Sci. 29 (2003) 319.
[10] T. Tamminen, T. Ohra-aho, B. Hortling, M. Tenkanen, in: Proceedings of the 12th International Symposium on Wood Pulp Chemicals, vol. I, Madison, WI, USA, June 9–12, 2003, pp. 69–72.
[11] K. Poppius-Levlin, T. Tamminen, K. Rajanen, A.-S. Jääskeläinen, L. Viikari, in: Proceedings of the 10th International Symposium on Wood Pulp Chemicals, vol. 1, Yokohama, June 7–10, 1999, p. 556.
[12] K. Poppius-Levlin, T. Tamminen, A. Kalliola, T. Ohra-aho, in: D.S. Argyropoulos (Ed.), Proceedings of the ACS Smposium Series 785, Oxidative Delignification Chemistry, Fundamentals and Catalysis, 2001, pp. 358–372 (Chapter 22).
[13] M. Tenkanen, I. Forsskåhl, T. Tamminen, M. Ranua, K. Vuorenvirta, K. Poppius-Levlin, in: Proceedings of the Seventh European Workshop on Lignocellulosics and Pulp, Turku, Finland, August 25–29, 2002, pp. 107–110.
[14] B. Hortling, T. Tamminen, A. Varhimo, in: Proceedings of the Seventh European Workshop on Lignocellulosics and Pulp, Turku, Finland, August 25–29, 2002, pp. 439–442.
[15] I. Tydén-Ericsson, Chromatographia 6 (1973) 353.
[16] J. Ralph, R.D. Hatfield, J. Agric. Food Chem. 39 (1991) 1426.
[17] O. Faix, D. Meier, I. Fortmann, Holz als Roh- und Werkstoff 48 (1990) 281.
[18] J. Li, G. Gellertedt, Carboh. Res. 302 (1997) 213.
[19] M. Tenkanen, G. Gellerstedt, T. Vuorinen, A. Teleman, M. Perttula, J. Li, J. Buchert, J. Pulp Paper Sci. 25 (1999) 306.
[20] T. Tamminen, B. Hortling, in: D.S. Argyropoulos (Ed.), Proceedings of the ACS Smposium Series 785, Oxidative Delignification Chemistry, Fundamentals and Catalysis, 2001, pp. 73–91 (Chapter 4).
[21] J. Sjöberg, M. Kleen, O. Dahlman, R. Agnemo, H. Sundvall, Nord. Pulp. Paper Res. J. 17 (2002) 295.
[22] E.B. Higman, I. Schmeeltz, W.S. Schlotzhauer, J. Agric. Food Chem. 18 (1970) 636.
[23] G.C. Ziobro, J Wood Chem. Technol. 10 (1990) 133.
[24] S. Ohara, Y. Yasuta, H. Ohi, Holzforschung 57 (2003) 145.
[25] D. Ibarra, J.C. del Rio, A. Gutierrez, I.M. Rodrigues, J. Romero, M.J. Martinez, A.T. Martinez, Proceedings of the 16th International Smposium on Analytical and Applied Pyrolysis, Alicante, Spain, May 23–27, 2004, p. 166.
[26] O. Sevastyanova, J. Li, G. Gellerstedt, Proceedings of the 11th International Symposium on Wood Pulp. Chemicals, vol. I, Nice, France, June 11–14, 2001, pp. 358.
[27] J.M. Challinor, J. Anal. Appl. Pyrol. 35 (1995) 93.
[28] I. Ericsson, R.P. Lattimer, J. Anal. Appl. Pyrol. 31 (1995) 251.
[29] P. Selsbo, I. Ericsson, M. Kleen, J. Anal. Appl. Pyrol. 43 (1997) 1.
[30] M. Kleen, T. Ohra-aho, T. Tamminen, J. Anal. Appl. Pyrol. 70 (2003) 589–600.

II

Kalliola A., Savolainen A., Ohra-aho T., Faccio G., Tamminen T. (2012) Reducing the content of VOCs of softwood kraft lignins for material applications. *BioResources, 7*, 2871-2882.

REDUCING THE CONTENT OF VOCS OF SOFTWOOD KRAFT LIGNINS FOR MATERIAL APPLICATIONS

Anna Kalliola,[a,*] Anne Savolainen,[b] Taina Ohra-aho,[a] Greta Faccio,[a] and Tarja Tamminen [a]

Three laccases, functioning in mild acidic, and one in slightly alkaline conditions, were evaluated in order to reduce low-molecular phenolic VOCs of kraft lignins, which could be used in lignin/natural fibers composites. The potential of a sulfhydryl oxidase to catalyze the oxidation of sulfur containing VOCs (thiols) was also tested in combination with the laccase-catalyzed oxidation. In addition, oxidation at alkaline pH at room temperature that may induce polymerization of phenolics in an analogous manner to the laccase-catalyzed reaction was investigated. Enzyme reactivity towards lignin was evaluated as consumption of oxygen in the reaction solution. The effect of treatments on VOC reduction was determined both by sensing (odorimetry) and chemical (TD-GC/MS, SEC) analyses. Laccases, Lcc2, and MaL from *Thielavia arenaria* and *Melanocarpus albomyces*, respectively, showed potential in reducing odors. The most promising results were obtained by oxidizing lignin with O_2 at alkaline pH. However, the odor threshold values of the main VOC compounds are extremely low, which poses a challenge to VOC reduction.

Keywords: VOC; Kraft lignin; Composite; Laccase; Sulfhydryl oxidase; Oxygen; Oxidation

Contact information: a: VTT Technical Research Centre of Finland, VTT, P.O. Box 1000, FI-02044 VTT, Finland; b: Trelleborg Industrial Products Finland Oy, Kikkerläntie 72, 38300 SASTAMALA, Finland.
**Corresponding author: anna.kalliola@vtt.fi*

INTRODUCTION

The potential of lignin to replace oil-based raw materials is being actively investigated for various material applications, such as composites. Based only on renewable resources, the Arboform® composites consist of isolated lignin, natural fibers, and natural additives, which are used in conventional thermoplastic processes such as injection molding (Naegele *et al.* 2002). However, there are several difficulties in applying lignin. One of them is the volatile organic compounds (VOCs), either present in the isolated lignin, or formed as they are processed at high temperature in thermoplastic processes. This drawback reduces the applicability of lignin-based composites, *e.g.* in the inner parts of cars.

VOCs in kraft lignin are typically lignin-originated phenolic structures, *e.g.* guaiacol (2-methoxyphenol), or reduced sulfur compounds formed in cooking. The odor threshold values of these VOCs are extremely low. For example, the odor threshold value for guaiacol in water solutions is reported to vary from 3 to 21 ppb (Fazzalari 1978; Buttery *et al.* 1988; Guth 1997). The great variation is due to different measurement techniques. For reduced sulfur compounds, dimethyl disulfide, and dimethyl trisulfide,

the threshold values are reported to be 5 and 0.2 ppb, respectively (Guth 1997; Zoeteman *et al.* 1973).

Recently, small amounts of organically modified montmorillonite (silicate clay-based) dispersed into the lignin/natural fibers system have been shown to improve the mechanical and thermal behaviors. Thermogravimetric analysis results suggested that exfoliated or intercalated layered aluminosilicates acted as a protective barrier against degradation of organic components. The thermooxidative degradation of the organic compounds (lignin, natural fibers, and additives) occurred in the temperature range of 180 to 420°C (Guigo *et al.* 2009).

Laccases catalyze the oxidation of a wide range of aromatic substrates, especially phenols, simultaneously with the reduction of molecular oxygen to water. Phenolic substrates are oxidized to phenoxyl radicals, which, depending on reaction conditions, can spontaneously polymerize via radical coupling or rearrange themselves leading to quinones, alkyl–aryl cleavage, Cα oxidation, cleavage of Cα–Cβ bonds, or aromatic ring. Mediators, acting as intermediate substrates for laccases, enable laccase to indirectly oxidize large molecules, and even nonphenolic substrates (Giardina *et al.* 2010). Polymerization of lignosulfonates by laccases with and without mediators in varying reaction conditions has been confirmed recently (Areskogh *et al.* 2010; Prasetyo *et al.* 2010). Sulfhydryl oxidases catalyze the formation of de novo disulfide bonds from free thiol groups, with the reduction of molecular oxygen to hydrogen peroxide. These enzymes have been investigated in the food industry to improve the flavor of products such as ultraheat-treated milk and aromatic beverages such as coffee, tea, chocolate, wine, and beer (Starnes *et al.* 1986; Swaisgood 1977).

The objective of this study was to evaluate different approaches aiming to reduce VOCs of softwood kraft lignins. Laccase-catalyzed oxidation was tested as a potential means to polymerize the lignin-derived low-molecular phenolics such as guaiacol. Since the solubility of lignin increases significantly as pH increases and favors laccases that are active at higher pH, a laccase with the pH optimum at 8 was evaluated in addition to three other laccases functioning in mild acidic conditions. Sulfhydryl oxidase-catalyzed oxidation was tested as a means to reduce the odor from sulfur-containing compounds, *e.g.* thiols (methyl mercaptan, CH_3SH). As a straightforward way of reducing VOCs, oxidations at alkaline pH and at room temperature were investigated. The idea of the treatment was based on the hypothesis that at ambient temperatures the reaction kinetics will be slower than at elevated temperatures, causing phenoxyl radicals to be relatively stable, which may induce polymerization of phenolics in an analogous manner to the laccase-catalyzed reaction. TD-GC/MS, is presented as a novel method to simulate and quantify the VOC formation in the temperature range of thermoplastic processing.

EXPERIMENTAL

Materials

Two softwood kraft lignins, commercial Indulin AT (Mead WestVaco), and non-commercial SE (Stora Enso) were used as raw materials.

Four laccases were tested: *Thielavia arenaria* Lcc1 (TaLcc1) and Lcc2 (TaLcc2) (Paloheimo *et al.* 2006a and b) produced as recombinant enzymes in *Trichoderma reesei*

by Roal Oy (Rajamäki, Finland), *Trametes hirsuta* (ThL) (produced in its native host by VTT), and *Melanocarpus albomyces* (MaL) (overproduced in *Trichoderma reesei* by VTT). TaLcc1, TaLcc2, and ThL are most active in mild acidic conditions, whereas MaL, in slightly alkaline conditions.

The mediator 1-hydroxybenzotriazole (HBT) was used with a dose of 5 percent with respect to lignin, in addition to ThL and TaLcc2 in two experiments. Sulfhydryl oxidase, *Aspergillus oryzae* (AoSOX1) (Faccio *et al.* 2010), produced in *Trichoderma reesei* by VTT was also tested.

Methods

Lignin dissolution

Lignin suspensions for enzyme treatments were prepared by dissolving lignin first into alkaline water, after which pH was decreased using 1 M HCl, and finally set to the target pH using 0.05 M sodium citrate buffer in the case of pH 5 and 6, and 0.05 or 0.2 M sodium phosphate buffer in the case of pH 8. In general terms, the lignin dissolution was performed according to Mattinen *et al.* (2008), however, using NaOH of higher molarities when increasing the lignin dry solids above 0.1 percent. For oxidation at alkaline pH, only a small amount of HCl was needed to decrease pH to 10 or 10.7 after dissolving lignin in NaOH.

Enzyme activity measurements

2,2'-azino-bis-(3-ethylbenzthiazoline)-6-sulphonic acid (ABTS) (Roche) was used as a substrate for laccases in spectrophotometric enzyme activity measurement at pH 5 and 6, and guaiacol (Fluka) at pH 8. Katal units were used to express the catalytic activity of the laccase preparations (nkat/mL).

One katal of laccase is that amount of laccase which converts/oxidizes a mole of substrate per second under the specified conditions. Laccases were dosed on an activity basis with respect to the lignin content (nkat/g). 1 nkatal (10^{-9} mol/s) corresponds to 0.0600 enzyme units (U, 1 μmol/min), another commonly used unit expressing the catalytic activity. AoSOX1 was dosed on protein basis in respect to the sulfur content of lignin (2.2 percent).

Treatments

At the analytical scale, the reactivity of enzymes towards the lignin was evaluated by monitoring oxygen consumption in the reaction solution. Lignin dry solids were 1, 2.5, or 5 percent. Monitoring was performed with an Oxy-10 mini sensor oxygen meter (PreSens, Germany) in a closed 1.9 mL vessel based on dynamic luminescence quenching. Parallel treatments were performed.

Selected treatments with promising enzyme dosages were repeated at a larger laboratory scale in a 2-L Parr reactor to allow the use of sensing analysis (odorimetry). Treatments were done at 5 or 10 percent lignin dry solids, and under 5 bars initial oxygen pressure at room temperature (RT) for 1 or 2 hours (Table 1).

Reference samples (pH 5, 6, and 8, samples 1, 7, 10, and 12, respectively), were prepared according to the dissolution-pH adjustment procedure at room temperature (not O_2 boosted).

Table 1. Experimental Set-up of the Oxidative Treatments Performed with and without Enzyme in 2-L Parr Reactor under 5 Bar Initial O_2 Pressure at RT. Reference samples (ref.) were not O_2 boosted.

Sample	Substrate[a]	Lignin dry solids (%)	pH	Enzyme[b]	Dosage[c] (nkat/g ; %)	HBT (%)	Treatment (h)	
1	SE	5	5	-	-	-	-	ref.
2	SE	5	5	-	-	-	2	
3	SE	5	5	ThL	100	-	2	
4	SE	5	5	ThL	100	5	2	
5	SE	5	6	TaLcc2	100	-	2	
6	SE	5	6	TaLcc2	100	5	2	
7	Ind AT	5	5	-	-	-	-	ref.
8	Ind AT	5	5	-	-	-	2	
9	Ind AT	5	5	ThL	100	-	2	
10	SE	10	8	-	-	-	-	ref.
11	SE	10	8	-	-	-	1	
12	SE	10	8	MaL	0.1	-	1	
13	SE	10	8	MaL, AoSOX1	0.1, 0.1	-	1	
14	SE	10	10.7	-	-	-	1	

[a] Lignins: SE = Stora Enso lignin, Ind AT = Indulin AT
[b] Laccases: ThL = *Trametes hirsuta*, TaLcc2 = *Thielavia arenaria* Lcc2, MaL = *Melanocarpus albomyces*, Sulfhydryl oxidase: AoSOX1 = *Aspergillus oryzae*
[c] ThL and TaLcc2 activity measurements with ABTS; doses nkat/g. MaL and AoSOX1doses on protein bases; MaL dose in respect to lignin, AoSOX1 dose in respect to sulfur in lignin.

Analyses

In the odorimetry procedure, a wet sample volume containing 5 g of lignin dry solids was placed in a small crucible and stabilized inside closed glass containers (500 mL) for 48 hours at 40ºC. Thereafter, the odor panel members (ten qualified experts) evaluated the odor intensity of each sample using a scale of 1 to 6, which was selected according to VDA-270 (1992) recommendations. The stabilized samples were also graded using numbers 0 to 10 by individual perception. The least odor-intense sample got number 0 and the most odor-intense was assigned number 10. The panel was able to evaluate a maximum 6 of the samples at a time. Three separate sessions were conducted. In general terms, the odorimetry method was a modification combining sensing analyses described by Söderhjelm and Pärssinen (1985) and Morvan *et al.* (2003).

The thermal desorption (TD) method was developed based on the earlier used method (Kleen *et al.* 2003) in order to simulate the formation of volatile degradation products at elevated temperatures prevailing in the injection molding. TD measurements were carried out with a Pyrolab pyrolyzer unit (Pyrolab2000®) connected to a Varian 3800 gas chromatography/Varian Saturn 2000 mass spectrometer. About 2.5 mg of the freeze-dried sample was weighed accurately and heated at 150 and 190ºC for 5 minutes in a pyrolysis chamber. Thereafter, volatiles were led to the gas chromatography column (J&W, DB-1701, 30 m x 0.25 mm, film 1 µm) for separation. The oven was programmed as follows: initial temperature 100°C, rate of increase 4°C/min to 265°C and held for 18 min at the final temperature. A constant carrier gas flow of 0.9 ml/L was used. The mass spectra of the products were obtained using an ion trap mass spectrometer (EI 70 eV). The scan range of m/z 46-650 was used. Sulfur and phenol compounds were tentatively

identified using commercial mass spectra library Nist05. Quantification of guaiacol was performed with an external standard calibration (guaiacol, 98 percent, Aldrich).

Average lignin molecular size classes (M_n, M_w) of the freeze-dried samples were measured by size exclusion chromatography (SEC), using PSS MCX 1000 and 100 000 columns in 0.1 M NaOH eluent (25°C) with UV detection (280 nm). The molecular size distributions and average molecular sizes were calculated in relation to polystyrene sulfonate standards, using Waters Empower 2 software.

RESULTS AND DISCUSSIONS

Laccase Reactivity towards Lignins

At analytical scale, the reactivity of laccases (ThL, TaLcc1, TaLcc2) functioning in mild acidic conditions was tested towards both kraft lignins by following the reduction of dissolved O_2 in the reaction solutions. At pH 6, ThL and TaLcc2 showed higher reactivity towards lignins, as the curves of O_2 consumption were steeper than in the case of TaLcc1 (Fig. 1a). Although the dissolution-pH adjustment procedure (Mattinen *et al*. 2008) is intended to reduce the agglomerates, lignin is mainly undissolved at pH 6, since the dissociation of guaiacyl- and syringyl-derived phenols occurs at higher pH levels (Ragnar *et al.* 2000). In order to increase the dissolution and the reactivity of lignin, the treatment was performed at pH 8 by inclusion of MaL with the respective pH optimum. At pH 8, lignin already reacted with the dissolved oxygen present in the reaction solution. However, more O_2-consuming reactions occurred in the presence of TaLcc1, TaLcc2, and MaL than in their absence (Fig. 1b). The enzyme dosing was based on guaiacol activity since lignin resembles guaiacol by its chemical structure and has similar behavior in terms of pH. Even if the activity of MaL (to guaiacol) was lowest, *e.g*. MaL 67.1 nkat/mL, TaLcc1 111.2 nkat/mL, TaLcc2 339.6 nkat/mL, it catalyzed lignin oxidation more efficiently than TaLcc1 or TaLcc2 at pH 8. Sulfhydryl oxidase (AoSOX1, 1 percent dose in respect to sulfur in lignin) was tested together with MaL.

However, the O_2 consumption did not increase when compared to MaL treatment done without AoSOX1 (Fig. 1b). From the practical point of view, a 0.1 percent dose of MaL already showed potential in treating lignin.

In addition to the laccase- (and AoSOX1) catalyzed oxidation, the oxidation of SE lignin was followed in alkaline conditions (pH 10), which causes the dissociation of the phenolic structures. Increasing pH from 8 to 10 increased O_2 consumption and indicated improved lignin reactivity when compared to MaL-catalyzed oxidation (Fig. 2).

Lignin Odor and Volatiles Formation

Based on the results obtained from the O_2 consumption measurements, selected laccase treatments and oxidation at alkaline pH were performed at higher lignin dry solids and under oxygen pressure (Table 1). The pH level for the alkaline oxidation was set to 10.7, according to experimentally determined pK_0 value of Indulin AT (at 21°C) (Norgren and Lindström 2000).

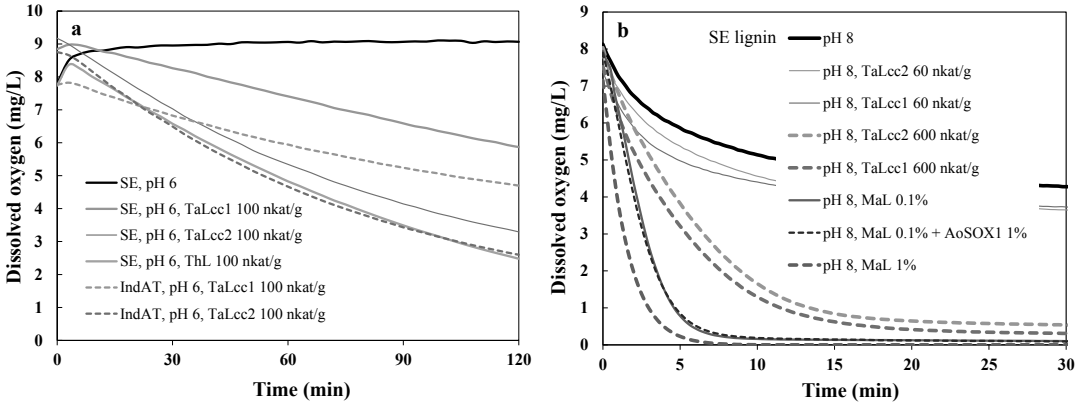

Fig. 1. a) Oxygen consumption of SE lignin and Indulin AT solution (ds. 1%) with and without laccase at pH 6. **b)** Oxygen consumption of SE lignin solution (ds. 2.5%) with and without laccase (and AoSOX1) at pH 8. 0.1% MaL dose equals to 31 nkat/g, and 1% MaL dose equals to 310 nkat/g. 1% AoSOX1 dose with respect to sulfur in lignin

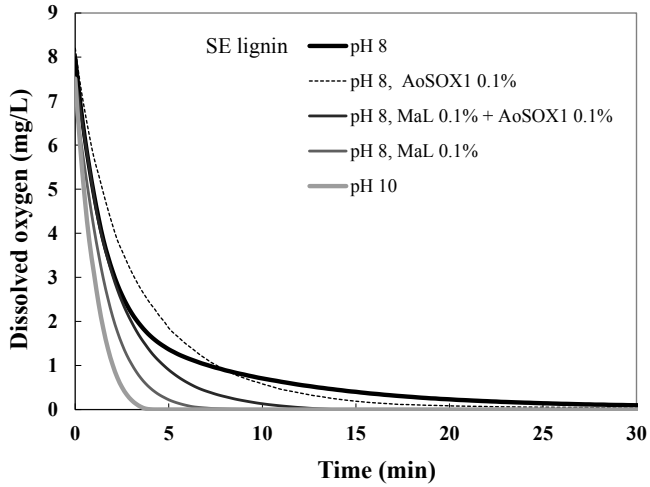

Fig. 2. Oxygen consumption of SE lignin solution (ds. 5%) with and without laccase (and AoSOX1) at pH 8, and oxidation at pH 10. 0.1% MaL dose equals to 57 nkat/g

The overall odor intensity of the lignin samples (Table 1) was evaluated by ten human sniffers (the odor panel). The odor intensity of the samples varied between 2.9 and 3.9 (4 = disturbing, 3 = clearly perceptible), and standard deviations were rather large (Fig. 3 upper panel). Although the odor of the samples differed only slightly, the oxidation by TaLcc2 and MaL+AoSOX1 and the oxidation at pH 10.7, indicated reduced VOC content, with the lowest odor intensity values *e.g.* 2.9 (Sample 5), 3.2 (Sample 13), and 3.0 (Sample 14), respectively. Grading the lignin samples using numbers from 0 to 10 (0 = the least odor intense, 10 = the most intense odor) supported the same observations (Fig. 3 lower panel).

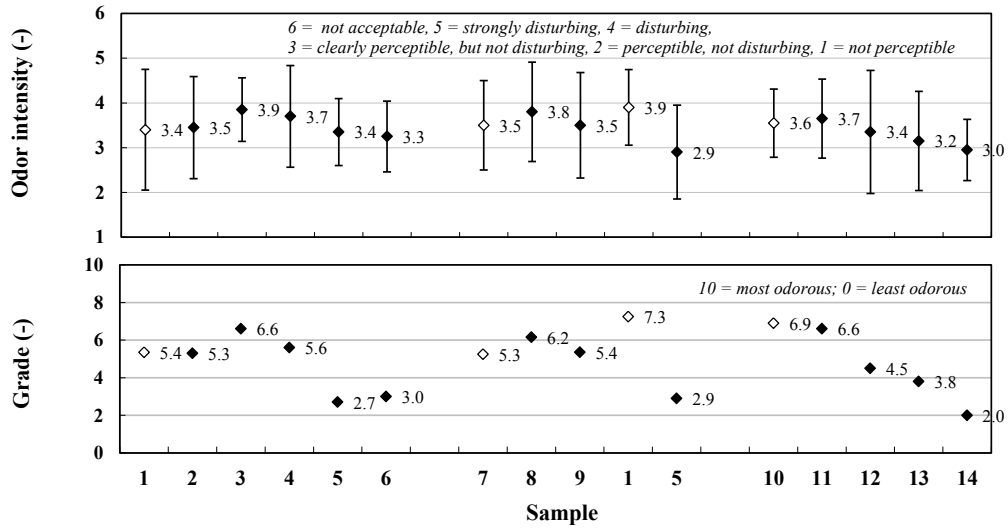

Fig. 3. Odor intensity (upper panel) and grade (lower panel) of the wet SE lignin and Indulin AT samples treated with and without laccases (and AoSOX1) at different pH level. Samples are numbered according to Table 1; open dots refer to reference samples that were not O_2 boosted. Evaluation of samples 1 and 5 was conducted in the first and second separate odor panel

Volatile degradation products of the freeze-dried lignin samples (SE lignin treated with or without MaL/MaL+AoSOX1, and at pH 10.7) were determined by TD-GC/MS at 150 and 190ºC. Lignin softening takes place typically at 150ºC, after which an increase in temperature induces depolymerization and recondensation (Bergmann *et al.* 2005). 190ºC represents the temperature of the latter range, and also resembles the temperature at thermoplastic processing.

The main part of the volatiles had already evaporated within 5 minutes at both temperatures. The most abundant degradation product of lignin was guaiacol (Fig. 4). Clearly more volatiles were formed at 190ºC than at 150ºC. In the case of reference (pH 8, ref.) and O_2 treated (pH 8, 0%) samples, the sum of main volatiles was *ca.* 5-fold more at 190ºC than at 150ºC. In the case of MaL or MaL+AoSOX1 treated lignin, it was *ca*. 3.5-fold more, and in lignin oxidized at pH 10.7 it was less than 2-fold more at 190ºC than at 150ºC.

At both temperatures, clearly less volatiles were formed as SE lignin was oxidized at pH 10.7, than treated with or without MaL/MaL+AoSOX1 at pH 8. At least three explanations for reduced formation of volatiles of alkali-oxidized lignin may exist. Firstly, in the freeze-dried alkaline sample, the low-molecular phenolics most likely existed in sodium-salt form, which hindered their volatilization. Secondly, part of the phenolics might have degraded to non-volatile structures, which is unwanted, since in composite applications the molecular size presumably correlate with strength properties. Thirdly, polymerization/radical coupling of small-molecular phenolics, *e.g.* guaiacol, could have taken place.

Also, the oxidation at pH 10.7 reduced the amount of sulfur containing VOCs. In these conditions, they might have degraded and further oxidized to sulfate. Furthermore,

the dissociation of thiols occurs at alkali pH levels, *e.g.* the pK_a value of methanethiol is 10.33 (Steward 1985), and thus the existence as sodium-salt may have hindered their volatilization.

The quantification of the main volatile, guaiacol, showed that its amounts in the SE lignin samples were still rather high when compared to the odor threshold values measured in water solutions, *i.e.* 1.3 ppm at 150ºC and 24 ppm at 190ºC (Fig. 5).

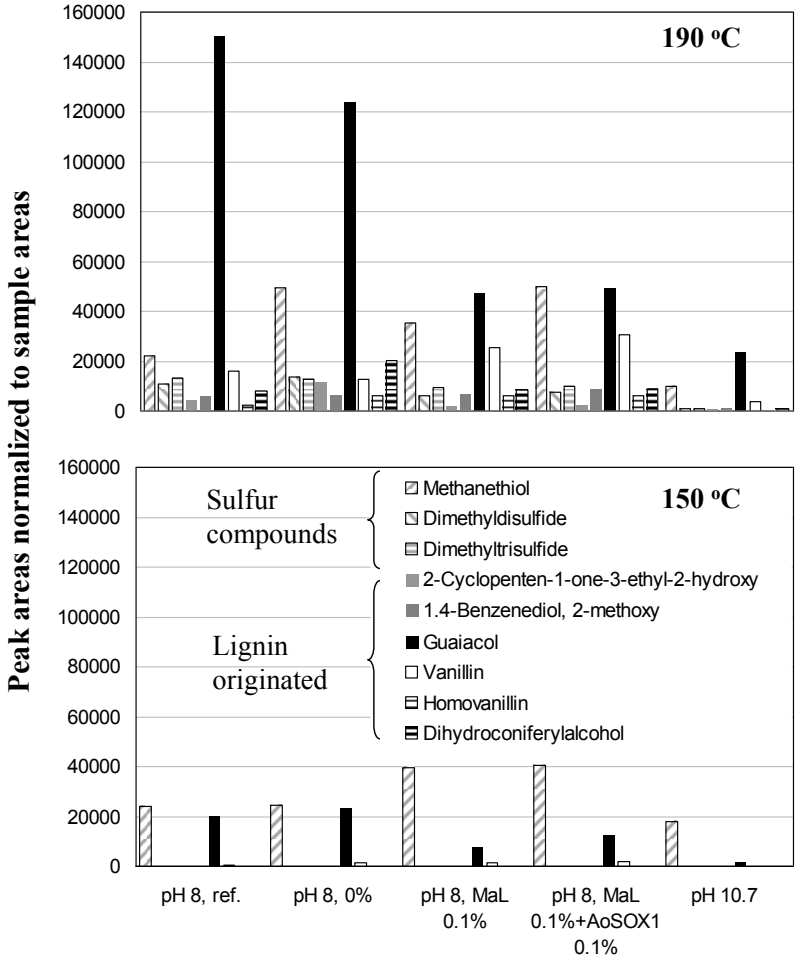

Fig. 4. Main volatiles of freeze-dried SE lignin samples at 190ºC (upper panel) and 150 ºC (lower panel). Reference sample (ref.) was not O_2 boosted

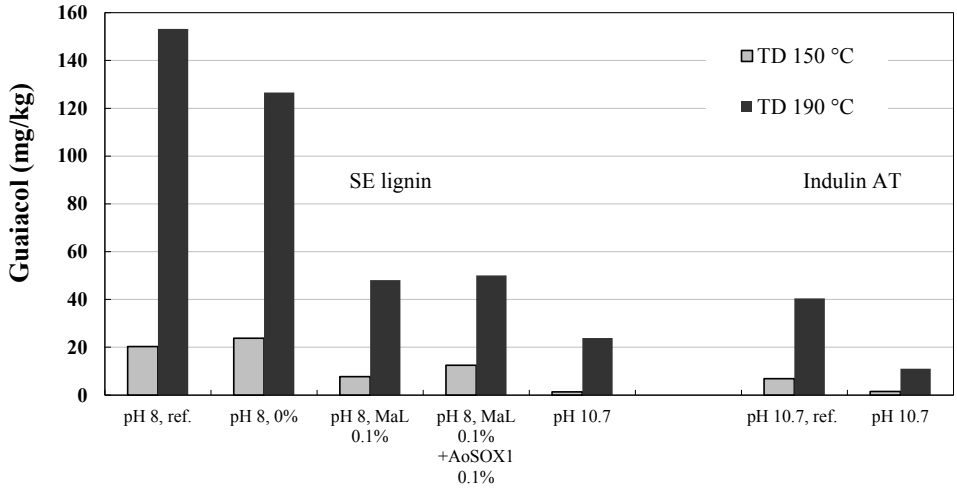

Fig. 5. Volatile guaiacol of freeze-dried SE lignin and Indulin AT samples at 150°C and 190°C. Reference samples (ref.) were not O_2 boosted

In order to investigate the importance of oxygen excess in the alkaline treatment, the pH 10.7 treatment was repeated to Indulin AT with and without oxygen boosting (5 bar initial O_2). The results clearly showed that oxygen-pressurized alkali treatment decreased the volatile guaiacol formation at 150ºC and at 190ºC, when compared to the alkaline treatment performed without O_2 boosting (Fig. 5).

Molecular Size Distribution of Lignin

The effect of the treatments on molecular size of both SE lignin and Indulin AT was analyzed using SEC. The results (molecular size distributions) indicated that the primary oxidation products, phenoxyl radicals, polymerized via radical coupling in the oxidation performed at room temperature and at pH 10.7. Also, MaL and MaL+AoSOX1 catalyzed oxidation caused minor polymerization of phenolics (Fig. 6a). Moreover, the experiments done with Indulin AT verified that at room temperature, the oxygen-pressurized alkali treatment caused lignin polymerization when compared to the alkali treatment done without O_2 boosting (Fig. 6b). However, the change in molecular size was rather small. Yet, the aim of this study was not to polymerize lignin in great extent, but to reduce the formation of low-molecular weight phenolic volatiles.

In alkaline oxygen oxidation (initially 5 bar O_2 excess) performed at elevated temperatures (90°C and 110°C), just the opposite takes place, as the Indulin AT macromolecule degrades fast, partly ending up to carbon dioxide (Kalliola *et al.* 2011). The degradation of lignin is desirable in pulp delignification, but likely unwanted in the composite applications.

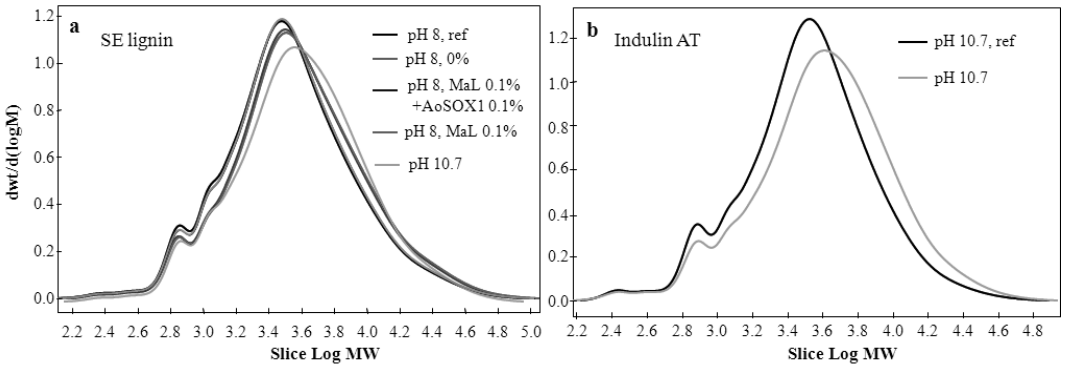

Sample	Mn	Mw	PD
SE lignin, pH 8, ref	2 250	5 150	2.3
SE lignin, pH 8, 0%	2 330	5 260	2.3
SE lignin, pH 8, MaL 0.1% + AoSOX1 0.1%	2 470	5 840	2.4
SE lignin, pH 8, MaL 0.1%	2 480	5 990	2.4
SE ligin, pH 10.7	2 570	5 980	2.3

Sample	Mn	Mw	PD
IndAT, pH 10.7, ref	2 250	4 750	2.1
IndAT, pH 10.7	2 640	6 000	2.3

Fig. 6. **a)** Molecular size distributions of freeze-dried SE lignin samples. **b)** Molecular size distributions of freeze-dried Indulin AT samples. Reference samples (ref.) were not O_2 boosted

CONCLUSIONS

1. Laccase-catalyzed oxidation and oxygen oxidation in alkaline conditions were evaluated in order to reduce VOCs of kraft lignins for composite applications. Laccases Lcc2 from *T. arenaria* and MaL from *M. albomyces* with or without sulfhydryl oxidase from *A. oryzae*, as well as the alkaline oxygen oxidation (pH 10.7), showed potential in reducing odors. The importance of the oxygen excess in the alkali treatment was highlighted by the results. The analyses performed showed no clear effect of sulfhydryl oxidase.
2. Volatile degradation products of lignin were determined by TD-GC/MS method at temperatures prevailing in the thermoplastic processing. Also, the quantification of volatile guaiacol was conducted. The analysis method developed a possibility to study the effect of application processing under varying temperature and residence time, as well as distinct volatiles formed from different lignins from each other's.
3. From the practical point of view, the most promising results were obtained by oxygen oxidizing lignin at alkaline pH. The treatment would be straightforward to apply at an industrial scale.
4. Yet, the odor threshold values of the main VOC compounds are extremely low, which makes the reduction of VOCs challenging.

ACKNOWLEDGMENTS

Tekes is acknowledged for financial support via project "VOC reduction of lignin containing materials" in the ERA-IB program. Stora Enso Corporation is thanked for providing the kraft lignin raw material. Marja Paloheimo, Roal Oy is thanked for providing Lcc1 and Lcc2 from *T. arenaria*. Mrs. Nina Vihersola and Mr. Juha Kaunisto are acknowledged for performing the experiments, Mrs. Eila Turunen for performing the TD-GC/MS and SEC analyses, Mrs. Tiina Liitiä for the determination of lignin molecular size distributions, and Mrs. Riitta-Maija Osmonen (VTT Expert Services) for arranging the sensing (odorimetry) analyses.

REFERENCES CITED

Areskogh, D., Li, J., Gellerstedt, G., and Henriksson, G. (2010). "Investigation of the molecular weight increase of commercial lignosulfonates by laccase catalysis," *Biomacromolecules* 11(4), 904-910.

Bergmann, P. C. A., Boersma, A. R., Zwart, R. W. R., and Kiel, J. H. A. (2005). "Torrefaction for biomass co-firing in existing coal-fired power stations," *Non-confidential ECN report, ECN-C--05-013*, The Netherlands.

Buttery, R., Turnbaugh, J., and Ling, L. (1988). "Contribution of volatiles to rice aroma," *J. Agric. Food Chem.* 36(5), 1006-1009.

Faccio, G., Kruus, K., Buchert, J., and Saloheimo, M. (2010). "Secreted fungal sulfhydryl oxidases: sequence analysis and characterisation of a representative flavin-dependent enzyme from *Aspergillus oryzae*," *BMC Biochemistry* 11, 31-42.

Fazzalari, F.A. (1978). *Compilation of Odor and Taste Threshold Values Data*, Amer. Society for Testing and Materials, Philadelphia.

Giardina, P., Faraco, V., Pezzella, C., Piscitelli, A., Vanhulle, S., and Sannia, G. (2010). "Review: Laccases: A never-ending story," *Cell. Mol. Life Sci.* 67, 369-385.

Guigo, N., Vincent, L., Mija, A., Naegele, H., and Sbirrazzuoli, N. (2009). " Innovative green nanocomposites based on silicate clays/lignin/natural fibres," *Composites Science and Technology* 69, 1979-1984.

Guth, H. (1997). "Quantitation and sensory studies of character impact odorants of different white wine varieties," *J. Agric. Food Chem.* 45(8), 3027-3032.

Kalliola, A., Kuitunen, S., Liitiä, T., Rovio, S., Ohra-aho, T., Vuorinen, T., and Tamminen, T. (2011). "Lignin oxidation mechanisms under oxygen delignification conditions. Part 1. Results from direct analyses," *Holzforschung* 65, 567-574.

Kleen, M., Ohra-aho, T., Tamminen, T. (2003). "On the interactions of HBT with pulp lignin during mediated laccase delignification – A study using fractionated pyrolysis-GC/MS," *J. Anal. Appl. Pyrolysis* 70, 589-600.

Mattinen, M., Suortti, T., Grosselink, R., Argyropoulos, D. S., Evtuguin, D., Suurnäkki, A., de Jong, E., and Tamminen, T. (2008). "Polymerization of different lignins by laccase," *BioResources* 3(2), 549-565.

Morvan, M., Talou, T., and Beziau, J-F. (2003). "MOS–MOSFET gas sensors array measurements versus sensory and chemical characterisation of VOC's emissions from car seat foams," *Sensors and Actuators B* 95, 212–223.

Naegele, H., Pfitzer, J., Naegele, E., Inone, E. R., Eisenreich, N., and Eckl, W. (2002). "ARBOFORM – A thermoplastic, processable material from lignin and natural fibers," In: Hu, T.Q. (ed.), *Chemical Modification, Properties, and Usage of Lignin*, Kluwer Academic/Plenum, New York.

Norgren, M. and Lindström, B. (2000). "Dissociation of phenolic groups in kraft lignin at elevated temperatures," *Holzforschung* 54(5), 519-527.

Paloheimo, M., Puranen, L., Valtakari, L., Kruus, K., Kallio, J., Mäntylä, A., Fagerström, R., Ojapalo, P., and Vehmaanperä, J. (2006a). "Novel laccase enzyme and use thereof," *Patent WO/2006/032723*.

Paloheimo, M., Valtakari, L., Puranen, L., Kruus, K., Kallio, J., Mäntylä, A., Fagerström, R., Ojapalo, P., and Vehmaanperä, J. (2006b). "Novel laccase enzymes and their uses," *Patent WO/2006/032724*.

Prasetyo, E., Kudanga, T., Østergaard, L., Rencoret, J., Gutiérrez, A., Del Río, J., Santos, J., Nieto, L., Jiménez-Barbero, J., Martínez, A., Li, J., Gellerstedt, G., Lepifre, S., Silva, C., Kim, S., Cavaco-Paulo, A., Klausen, B., Lutnaes, B., Nyanhongo, G., and Guebitz, G. (2010). "Polymerization of lignosulfonates by the laccase-HBT (1-hydroxybenzotriazole) system improves dispersibility," *Bioresource Technol.* 101, 5054-5062.

Ragnar, M., Lindgren, C. T., and Nilvebrant, N.-O. (2000). "pKa-values of guaiacyl and syringyl phenols related to lignin," *J. Wood Chem. Technol.* 20(3), 277-305.

Söderhjelm, L., and Pärssinen, M., (1985) "The use of descriptors for the characterisation of odour in packaging materials," *Paperi ja Puu – Paper och Trä* 67, 412-416.

Starnes, R. L., Katkocin, D. M., Miller, C. A., and Strobel Jr., R. J. (1986). "Microbial sulfhydryl oxidase," *US Patent US 1986/4632905, 06/738764*.

Stewart, R. (1985). "The proton: Applications to organic chemistry," In: *Vol. 46 of Organic Chemistry, A series of Monographs,*Wasserman, H. H. (ed.), Academic Press, New York.

Swaisgood, H. E. (1977). "Process of removing the cooked flavour from milk," *US Patent US 1977/4053644, 621631*.

VDA-270 (1992). "Determination of the odour characteristics of trim materials in motor vehicles".

Zoeteman, B. C. J., Piet, G. J., and van de Heuvel, R. (1973). *Threshold Odour Concentration in Water (and Air) of Chemical Substances*, Government Institute for Drinking Water Supply.

Article submitted: October 24, 2011; Peer review completed: January 13, 2012; Revised version received and accepted: May 10, 2012; Published: May 21, 2012.

III

Ohra-aho T., Ropponen J., Tamminen T. (2013) Thermochemolysis using TMAAc and TMAH reagents as means to differentiate between free acids and esters. *J. Anal. Appl. Pyrolysis* ***103***, 31-35.

Journal of Analytical and Applied Pyrolysis 103 (2013) 31–35

Contents lists available at ScienceDirect

Journal of Analytical and Applied Pyrolysis

journal homepage: www.elsevier.com/locate/jaap

Thermochemolysis using TMAAc and TMAH reagents as means to differentiate between free acids and esters

T. Ohra-aho*, J. Ropponen, T. Tamminen

VTT-Technical Research Centre of Finland, P.O. Box 1000, FI-02044 VTT, Finland

ARTICLE INFO

Article history:
Received 10 July 2012
Accepted 28 September 2012
Available online 8 October 2012

Keywords:
Thermochemolysis
Tetramethylammonium hydroxide
Tetramethylammonium acetate
Ester bond
Free acids
Py-GC/MS

ABSTRACT

The reactivity of aromatic and aliphatic esters in on-line thermochemolysis in the presence of methylation reagents was studied using model compounds. Guaiacyl and 2-nonyl palmitates were synthesised, representing aromatic and aliphatic ester bonds, respectively. These model compounds were analysed by on-line thermochemolysis using tetramethylammonium acetate (TMAAc) and tetramethylammonium hydroxide (TMAH) in order to differentiate free acids from esterified acids. The released palmitic acid with TMAH for both model compounds was close to the theoretical palmitic acid content in the model compounds, even if part of the aliphatic ester had not reacted with TMAH. The free palmitic acid content by TMAAc was one third of the theoretical value for aromatic ester and only a few percentages for aliphatic ester. The result indicated that the less basic reagent is able to hydrolyse the aromatic ester linkage to some extent, whereas the aliphatic ester remains intact. Thus, differentiation of free acids by TMAAc from the esterified acids cannot be reliably performed from matrices containing aromatic esters. It was found that transesterification due to the use of methanol as a solvent with TMAAc is an insignificant reaction in on-line thermochemolysis.

1. Introduction

The on-line derivatisation method "thermally assisted hydrolysis and methylation" in the presence of the reagent tetramethylammonium hydroxide (TMAH) was developed by Challinor [1]. The method, also called thermochemolysis, has been widely used for the characterisation of a variety of natural materials and synthetic polymers reviewed by Challinor [2] and Shadkami [3]. TMAH is a strong base and it cleaves ester and ether bonds extensively, forming more volatile methyl ester and ether derivatives [4]. TMAH is supposed to react also with the free acids present in the sample. Therefore, it can be used to determine the total fatty acid content of the sample [5–7]. Another thermochemolysis reagent, tetramethylammonium acetate (TMAAc), is more selective. It reacts only with free acid and alcohol groups. It has been used together with TMAH to differentiate between free and esterified fatty acids in wood extractives [6]. Tetraethylammonium acetate (TEAAc) is another reagent that also has been applied to give information of the free acids present in the sample. Instead of methylation, ethylated products are formed. The advantage of TEAAc is that it can be used to detect methyl esters originally present in the samples separately from the free acids [8] TMAAc and TEAAc have mainly been used together with more basic thermochemolysis reagents like TMAH and tetrabutylammonium hydroxide (TBAH) for the analysis of lipids from natural materials including humic and humin substances [9,10] as well as earlier mentioned wood extractives [6,11]. In addition, aquatic natural organic matter, which contains mainly phenolic structures, has been studied with different thermochemolysis reagents [12]. In that study, methylation reaction with TMAAc (in methanol) was explained to occur partly via transesterification. In addition to free functional groups, part of the ester bonds present in the natural organic matter was supposed to react with the methoxide ion to form methyl esters. The methoxide ion was suggested to derive from the methanol used as TMAAc solvent. The measured free acid content would thus be higher than the actual fatty acid content present in the sample. The measurement was done using off-line thermochemolysis. It is expected that transesterification does not take place in on-line thermochemolysis. Triglycerides were analysed also with TMAAc and other more basic reagents [7]. Quite high proportion of acids was in free form. Therefore, it was concluded that part of the ester bond might be cleaved at the high temperature thermochemolysis with TMAAc. Though TMAAc and TEAAc are used to determine free acid in different type of natural polymers containing both aromatic and aliphatic ester bonds, it has not been reported in literature whether TMAAc and TEAAc react differently with the two types of esters. Before using reagents with different alkalinity in the analysis of modified biopolymers containing both aliphatic and aromatic ester linkages, two model compounds, guaiacyl palmitate and 2-nonyl palmitate were synthesised, representing the aromatic ester bond between

* Corresponding author. Tel.: +358 40 570 9322; fax: +358 20 722 7026.
E-mail address: taina.ohra-aho@vtt.fi (T. Ohra-aho).

0165-2370/$ – see front matter © 2012 Elsevier B.V. All rights reserved.
http://dx.doi.org/10.1016/j.jaap.2012.09.015

phenol and fatty acid and aliphatic ester bond between aliphatic alcohol and fatty acid, respectively. These model compounds were analysed using TMAH and TMAAc in order to understand the behaviour of the reagents in the analysis of ester bonds and free acids. Even if it has been claimed that transesterification probably does not take place in on-line thermochemolysis this possibility was studied in the present study, and it was found to be negligible, as expected.

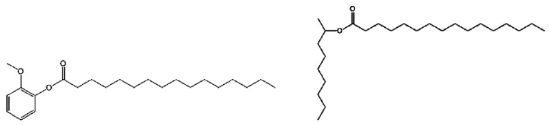

Fig. 1. Model compounds.

2. Materials and methods

2.1. The general procedure for model compound

All materials used for the synthesis were commercial and used as such unless otherwise noted. ^{1}H and ^{13}C NMR spectra were recorded on a Bruker Avance III 500 MHz NMR spectrometer and the chemical shifts were calibrated to the residual proton and carbon resonance of the deuterated solvent.

Guaiacyl palmitate: palmitic acid (7.43 g, 29.0 mmol), guaiacol (3.42 g, 27.6 mmol) and 4-dimethylaminopyridine (0.67 g, 5.52 mmol) were dissolved in dichloromethane (100 ml) and cooled to 0 °C, followed by addition of dicyclohexanecarbodiimide (6.83 g, 33.1 mmol) portion wise in a dichloromethane solution. The reaction was left to reach room temperature overnight and was then filtered to remove solids. The filtrate was evaporated and the crude product was purified by flash chromatography from heptane increasing polarity to EtOAc:heptane 5:95 to give product as a white solid. Yield was 8.32 g (83%).

^{1}H NMR (500.1 MHz, $CDCl_3$): δ 0.88 (t, J = 6.70 Hz, 3H, $-CH_3$), 1.26–1.37 (m, 22H, $-CH_2$), 1.43 (t, J = 7.11 Hz, 2H, $-CH_2$), 1.77 (t, J = 7.46 Hz, 2H, $-CH_2$), 2.58 (t, J = 7.46 Hz, 2H, $-CH_2$), 3.82 (s, 3H, $-OCH_3$), 6.93–7.21 (m, 4H, –ArH). ^{13}C NMR (125.8 MHz, $CDCl_3$): δ 14.11 ($-CH_3$), 22.67 ($-CH_2$), 25.04 ($-CH_2$), 29.06 ($-CH_2$), 29.28 ($-CH_2$), 29.35 ($-CH_2$), 29.50 ($-CH_2$), 29.61 ($-CH_2$), 29.65–29.68 (5C, $-CH_2$), 31.91 ($-CH_2$), 34.05 ($-CH_2$), 55.77 ($-OCH_3$), 112.35 (ArCH), 120,72 (ArCH), 122.82 (ArCH), 126.71 (ArCH), 139.84 (ArC), 151.14 (ArC), 171.89 (–CO).

2-*Nonyl palmitate*: palmitic acid (7.04 g, 27.4 mmol), 2-nonanol (3.77 g, 26.1 mmol) and 4-dimethylaminopyridine (0.64 g, 5.23 mmol) were dissolved in dichloromethane (100 ml) and cooled to 0 °C, followed by addition of dicyclohexanecarbodiimide (6.47 g, 31.4 mmol) portion wise from a dichloromethane solution. The reaction was left to reach room temperature overnight and was then filtered to remove solids. Filtrate was evaporated and the crude product was purified by flash chromatography from heptane increasing polarity to EtOAc:heptane 2:98 to give product as a clear oil. Yield 7.17 g (71.7%).

Yield of product was 7.17 g (72%).

^{1}H NMR (500 MHz, $CDCl_3$): δ 0.88 (t, J = 6.93 Hz, 6H, $-CH_3$), 1.19 (d, J = 6.25 Hz, 3H, CH_3), 1.25–1.34 (m, 34H, CH_2), 1.42–1.63 (m, 4H, $-CH_2$), 2.26 (t, J = 7.53 Hz, 2H, $-CH_2$), 4.89 (hex, J = 6.32 Hz, 1H, –CH). ^{13}C NMR (126 MHz, $CDCl_3$): δ 14.07 ($-CH_3$), 14.11 ($-CH_3$), 20.02 ($-CH_3$), 22.64 ($-CH_2$), 22.69 ($-CH_2$), 25.12 ($-CH_2$), 25.42 ($-CH_2$), 29.15 ($-CH_2$), 29.21 ($-CH_2$), 29.29 ($-CH_2$), 29.36 ($-CH_2$), 29.41 ($-CH_2$), 29.48 ($-CH_2$), 29.60 ($-CH_2$), 29.65–29.69 (5C, $-CH_2$), 31.78 ($-CH_2$), 31.92 ($-CH_2$), 34.77 ($-CH_2$), 35.96 ($-CH_2$), 70.71 (–CH), 173.58 (–CO).

2.2. Thermochemolysis

Thermochemolysis with TMAH (10% in aqueous solution, Merck) and TMAAc (15% in aqueous solution, TCI) was performed using a platinum foil pulse pyrolyzer (Pyrolab2000® from Pyrolab, Sweden) connected to a gas chromatograph mass spectrometer (Varian 3800 GC-Varian Saturn 2000 MS). A fused silica capillary column (J&W, DB-1701, 30 m × 0.25 mm, film thickness 1 μm) was used for the compound separation. 2–4 μl of the sample solution (model compounds diluted to methanol or dichloromethane) at concentration about 0.5 mg/ml was pipetted on the filament together with internal standard (heneicosanoic acid, Fluka purum ≥98%) and the reagent. The mixture was inserted to the pyrolyzer maintained at 175 °C and the filament was heated to temperatures between 280 and 600 °C depending on the reagent used. Pyrolysis time was 2 s. After pyrolysis, the degradation products were led into the capillary column for separation using helium as carrier gas at flow rate 1.0 ml min^{-1}. The column temperature was programmed from 80 °C (2 min) to 160 °C at 8 °C min^{-1} and extended from 160 °C to 280 °C at 5 °C min^{-1}. The final temperature was held for 5 min. The mass spectrometer was operated in EI mode (70 eV) using mass range of m/z 46–650. Acid content was calculated using internal standard calibration.

3. Results and discussion

3.1. Thermochemolysis conditions

Two model compounds guaiacyl palmitate and 2-nonyl palmitate, which contained both aromatic and aliphatic ester bonds, were synthesised. Structures of model compounds are shown in Fig. 1. These model compounds were analysed using on-line thermochemolysis with two methylation reagents TMAH and TMAAc. On-line thermochemolysis was performed in a pyrolysis unit. Therefore, short reaction time of 2 s was favoured. Both methylation reagents were used as aqueous solutions. Based on literature, thermochemolysis at pyrolysis temperature of 600 °C has given highest recovery for the fatty acids [7]. Our experience was that 400 °C and 600 °C gave basically the same yield of fatty acid. However, at high temperatures such as 600 °C, better yield for the aromatic compounds were obtained (not reported). Therefore, TMAH thermochemolysis was performed at 600 °C, whereas lower temperature was used for TMAAc thermochemolysis to avoid thermal degradation of the ester bond. Both model compounds as well as the internal standard were diluted to methanol and dichloromethane before transferring on the filament. The reason to use two solvents with different structure was to understand the effect of the solvents on the methylation reaction i.e. transesterification. If transesterification of the ester groups in the sample take place via methoxide ion formation, higher proportion of methylated products would be formed when methanol is used as a solvent in thermochemolysis by TMAAc. It was proposed that transesterification does not take place when dichloromethane is used as a solvent. The solutions were prepared for the model compounds in order to be able to transfer a suitable amount of sample on the filament and avoid overload of the detector. In TMAAc thermochemolysis, the reagent was mixed with the sample in two different ways: before or after addition of the sample on the filament. The concentration of TMAAc in the mixture was 3%. There was no difference in the results depending on how the reagent was mixed with the sample. Therefore, the results are presented as average. TMAH was always added after sample addition directly on the filament. All measurements were done at

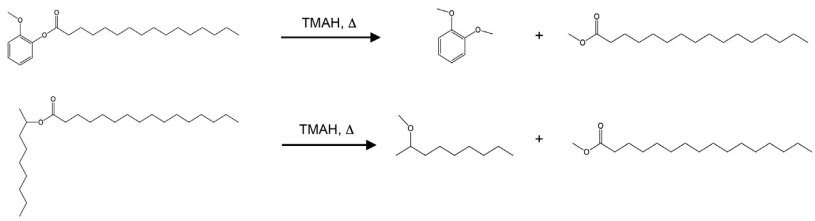

Fig. 2. Expected products formed in TMAH thermochemolysis of guaiacyl palmitate (above) and 2-nonyl palmitate (below).

least triplicate. The released palmitic acid content was calculated for the model compounds using internal standard calibration.

3.2. Thermochemolysis by TMAH and TMAAc

The expected reactions taking place in TMAH thermochemolysis of guaiacyl and 2-nonyl palmitate are shown in Fig. 2. It was expected that TMAAc does not react with ester bonds. Total ion gas chromatograms in Figs. 3 and 4 show the methylated products formed from the guaiacyl palmitate and 2-nonyl palmitate in thermochemolysis with TMAH and TMAAc. In the presence of TMAH, guaiacyl palmitate was hydrolysed and palmitic acid methyl ester and dimethoxybenzene were formed as methylation products (Fig. 3). The peak intensities of dimethoxybenzene and palmitic acid methyl ester were surprisingly high in comparison to internal standard intensity when TMAAc was used, as TMAAc is not supposed to hydrolyse esters [6]. The result indicates that part of the aromatic ester was hydrolysed in the thermochemolysis by TMAAc. In addition to methylated products, also nonmethylated guaiacol was detected probably as a thermal degradation product of guaiacyl palmitate. Nonmethylated palmitic acid was not detected, probably because the elution of fatty acids without derivatisation is poor.

Methyl palmitate was the only methylated product from 2-nonyl palmitate in the presence of TMAH (Fig. 4). Small peak of 2-nonanol was detected, but not 2-nonyl methyl ether. It has earlier been reported that all alcohol groups are not fully methylated [1]. Also small amount of the original ester 2-nonyl palmitate was found, indicating incomplete reaction of aliphatic esters in the presence of TMAH. In the thermochemolysis of 2-nonyl palmitate with TMAAc, only a small peak of methyl palmitate was found, indicating that only the free acid is reacted with TMAAc, as expected. The peak with highest abundance was the unreacted ester. In addition, a small amount of non-methylated 2-nonanol was detected. Our results regarding the thermochemolysis of aliphatic esters by TMAAc were consistent with the results reported in literature [6].

The amount of released palmitic acid was calculated for the TMAH and TMAAc thermochemolysis experiments. The palmitic acid content determined by TMAH was compared with the theoretical content. The results are shown in Figs. 5 and 6. The measured total palmitic acid content for the guaiacyl palmitate was close to the theoretical value (Fig. 5). When methanol was used as solvent, the average palmitic acid content was closer to the theoretical value than in the case of dichloromethane as solvent. However, the standard deviation was higher when methanol was used. The released palmitic acid content from the guaiacyl palmitate with TMAAc was about one third of the theoretical total content. Again higher average palmitic acid content was measured when methanol was used as solvent as compared to dichloromethane. However, the methylation of palmitic acid cannot explain to form via transesterification, because palmitic acid content was equal with both solvents. The measured free palmitic acid content was surprisingly high, as any unreacted palmitic acid after the synthesis was supposed to be removed during the purification, further verified by NMR analysis of the product. The origin of the measured high free palmitic acid content is thus concluded to be partial hydrolysis of the aromatic ester bond in the thermochemolysis by TMAAc.

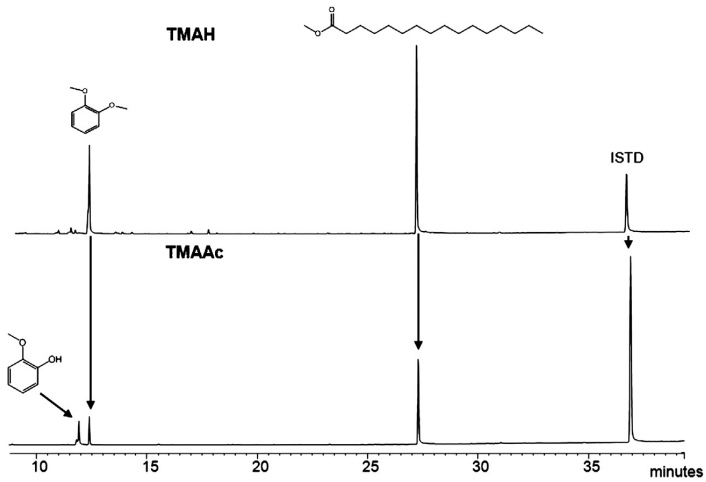

Fig. 3. Products formed from guaiacyl palmitate (in dichloromethane) by TMAH thermochemolysis (above) and TMAAc thermochemolysis (below).

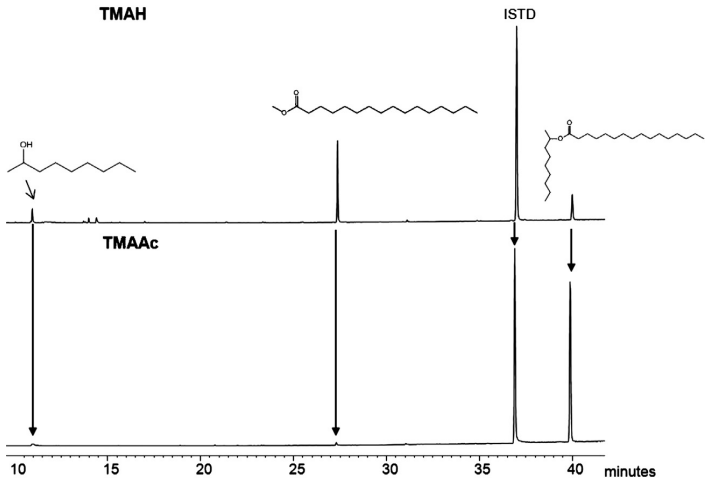

Fig. 4. Products formed from 2-nonylpalmitate (in dichloromethane) by TMAH thermochemolysis (above) and TMAAc thermochemolysis (below).

The palmitic acid content determined with TMAH from the 2-nonyl palmitate was slightly lower than the theoretical value, as part of the 2-nonyl palmitate had not reacted with TMAH (Fig. 6). A small peak of the original ester is seen in the total ion gas chromatogram, verifying the conclusion (Fig. 4). A small amount of palmitic acid was measured in the presence of TMAAc from the 2-nonyl palmitate. The palmitic acid content measured from 2-nonyl palmitate was much lower in comparison to the palmitic acid content measured from guaiacyl palmitate. In the case of 2-nonyl palmitate, TMAAc seems to react only with the free acid group, not with the ester group, as expected. The result proved that the aliphatic ester bond is more stable against less basic reagents such as TMAAc in comparison to the aromatic ester bond. Also in this case, the palmitic acid content was slightly higher when the samples were diluted in methanol rather than dichloromethane. However, the standard deviation was large when methanol was used. Due to the similar values obtained with both solvents it was proposed that transesterification due to the use of methanol as solvent with TMAAc is an insignificant reaction in on-line thermochemolysis.

The influence of pyrolysis temperature on palmitic acid yield was studied in the case of 2-nonyl palmitate, because part of the ester was not hydrolysed and methylated in the presence of TMAH. However, there were no differences in palmitic acid content at temperatures of 600, 700 and 800 °C, indicating that hydrolysis and methylation was independent on the temperature changes (Fig. 7). The influences of reaction time before pyrolysis and pyrolysis time on palmitic acid yield were not studied.

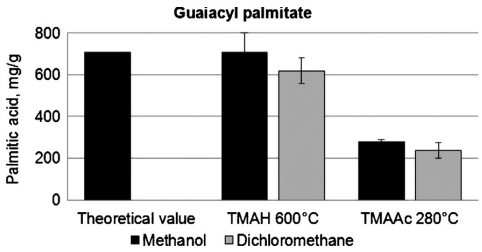

Fig. 5. Amount of palmitic acid released from guaiacyl palmitate by TMAH and TMAAc.

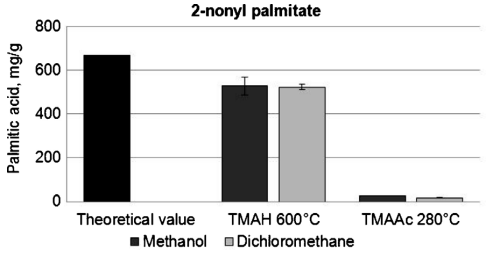

Fig. 6. Amount of palmitic acid released from 2-nonyl palmitate by TMAH and TMAAc.

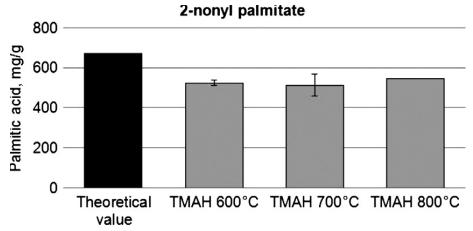

Fig. 7. Effect of temperature on palmitic acid yield from 2-nonyl palmitate (in dichloromethane) by TMAAc. One measurement was done at 800 °C.

4. Conclusions

TMAH has been used for the determination of total fatty acids content. In this study, TMAH was used to determine total palmitic acid content from model compounds that represented both aliphatic and aromatic ester bonds between alcohol and fatty acid. Palmitic acid was hydrolysed and methylated totally from the aromatic ester, whereas part of the aliphatic ester remained stable. TMAAc has earlier been used to differentiate between free and esterified acids in wood extractives. The fatty acids in wood extractives are esterified with cyclic and aliphatic alcohols. The results obtained in this study showed that the aromatic ester bond is partly hydrolysed and methylated in the presence of TMAAc, whereas the aliphatic ester bond is stable against TMAAc. It means that TMAAc can be used to distinguish between free acids and aliphatic esters

in matrices such as wood extractives, containing only aliphatic alcohols. However, it cannot used to determine free acids from samples, which contain either aromatic and aliphatic ester linkages, or only aromatic ester linkages. Transesterification in thermochemolysis in the presence of methanol has been suggested to increase the yield of methylated products. However, it was now showed that in on-line thermochemolysis, the transesterification reaction is insignificant.

Acknowledgements

The authors would like to thank Ms. Eila Turunen for performing the technical work in the Py-GC/MS experiments. The financial support from the Academy of Finland is acknowledged (Effect of fiber wall chemistry on energy demand in wood defibration, Defibre, 133276).

References

[1] J.M. Challinor, A pyrolysis-derivatisation-gas chromatography technique for the structural elucidation of some synthetic polymers, Journal of Analytical and Applied Pyrolysis 16 (1989) 323–333.
[2] J.M. Challinor, Review: the development and applications of thermally assisted hydrolysis and methylation reactions, Journal of Analytical and Applied Pyrolysis 61 (2001) 3–34.
[3] F. Shadkami, R. Hellure, Review: recent applications in analytical thermochemolysis, Journal of Analytical and Applied Pyrolysis 89 (2010) 2–16.
[4] J.M. Challinor, On the mechanism of high temperature reactions of quaternary ammonium hydroxides with polymers, Journal of Analytical and Applied Pyrolysis 29 (1994) 223–224.
[5] J.M. Challinor, Characterisation of wood extractives by pyrolysis-gas chromatography/mass spectrometry of quaternary ammonium hydroxide extracts, Journal of Analytical and Applied Pyrolysis 37 (1996) 1–13.
[6] H.-L. Hardell, N.-O. Nilvebrant, A rapid method to discriminate between free and esterified fatty acids by pyrolytic methylation using tetramethylammonium acetate or hydroxide, Journal of Analytical and Applied Pyrolysis 49 (1999) 1–14.
[7] D. Drechsel, K. Dettmer, W. Engewald, Studies of thermally assisted hydrolysis and methylation-GC–MS of fatty acids and triglycerides using different reagents and injection systems, Chromatographia 57 (2003) S-283–S-289.
[8] L. Grasset, C. Guignard, A. Amblès, Free and esterified aliphatic carboxylic acids in humin and humic acids from a peat sample as revealed by pyrolysis with tetramethylammonium hydroxide or tetramethylammonium acetate, Organic Geochemistry 33 (2002) 181–188.
[9] C. Guignard, L. Lemée, A. Amblès, Lipid constituents of peat humic acids and humin. Distinction from directly extractable bitumen components using TMAH and TEAAc thermochemolysis, Organic Geochemistry 36 (2005) 287–297.
[10] D. Válková, L. Grasset, A. Amblès, Molecular compounds generated by ruthenium tetroxide oxidation and preparative off line thermochemolysis of lignite humic acids from South Moravia: implications for molecular structure, Fuel 88 (2009) 2113–2121.
[11] M. Mizumoto, E. Shimokita, T. Ona, T. Seino, Y. Ishida, H. Ohtani, Rapid and direct characterization of total fatty acids in wood by thermochemolysis-gas chromatography–flame ionization detector/mass spectrometry with tetrabutylammonium hydroxide, Journal of Analytical and Applied Pyrolysis 87 (2010) 163–167.
[12] C.A. Joll, D. Couton, A. Heitz, R.I. Kagi, Comparison of reagents for off-line thermochemolysis of natural organic matter, Organic Geochemistry 32 (2004) 47–59.

IV

Ohra-aho T., Gomes F.J.B., Colodette J.L., Tamminen T. (2013) S/G ratio and lignin structure among Eucalyptus hybrids determined by Py-GC/MS and nitrobenzene oxidation. *J. Anal. Appl. Pyrolysis* ***101***, 166-171.

Journal of Analytical and Applied Pyrolysis 101 (2013) 166–171

Contents lists available at SciVerse ScienceDirect

Journal of Analytical and Applied Pyrolysis

journal homepage: www.elsevier.com/locate/jaap

S/G ratio and lignin structure among Eucalyptus hybrids determined by Py-GC/MS and nitrobenzene oxidation

T. Ohra-aho[a,*], F.J.B. Gomes[b], J.L. Colodette[b], T. Tamminen[a]

[a] VTT-Technical Research Centre of Finland, P.O. Box 1000, FI-02044 VTT, Finland
[b] Department of Forest Engineering, Federal University of Viçosa, 36570-000 Viçosa, Brazil

ARTICLE INFO

Article history:
Received 7 September 2012
Accepted 24 January 2013
Available online 1 February 2013

Keywords:
Eucalypt
Wood
Lignin
S/G ratio
Py-GC/MS
Nitrobenzene oxidation

ABSTRACT

The ratio among syringyl (S) and guaiacyl (G) lignin substructures is increasingly used as criteria in the selection of Eucalyptus species to pulping processes. The S/G distribution of several Brazilian Eucalyptus species and their crossings was determined by analytical pyrolysis-GC/MS (Py-GC/MS) and alkaline nitrobenzene oxidation directly from wood fibers. The ratio varied among the Eucalyptus hybrids. In Py-GC/MS, the S/G ratio is calculated by summing up the proportions of S and G type lignin pyrolysis products with various 1–3 carbon containing side chain structures. Py-GC/MS revealed that the distribution of the lignin side chain structures varied among the species. Similar trends were seen both in the G and in the S series. The result was verified with principal component analysis (PCA), which also revealed that similar side chains structures in the G and S units are correlated with each other. That PCA result confirmed that all G and S type degradation products should be included in the calculation of S/G ratios instead of selected products. S/G ratios determined by Py-GC/MS and alkaline nitrobenzene oxidation were close to each other, but not equal. Lower values were obtained by Py-GC/MS. The differences between the two methods are probably related the degradation mechanism of lignin with Py-GC/MS and nitrobenzene oxidation methods. Based on these results, it is not possible to say which of the methods is more reliable. However, both methods can well be used to compare the S/G ratios of lignin among samples.

1. Introduction

Lignin is a highly heterogeneous polymer composed of hydroxycinnamyl alcohols, including coniferyl, sinapyl and *p*-coumaryl alcohol building blocks. The structure of lignin varies depending on the plant species, cell type and environmental factors. Lignin units are linked by a variety of ether and carbon–carbon bonds that are usually classified into condensed linkages, such as biphenyl, biphenyl ethers and non-condensed linkages, including alkyl-aryl ether linkages (β-O-4) [1]. In hardwood species like Eucalyptus spp, lignin is mainly composed of guaiacyl (G) and syringyl (S) moieties. Several studies have shown that the structure of lignin, particularly S/G ratio, affects the processability of the wood, *e.g.* delignification [2–4]. Furthermore, the S/G ratio determined both with alkaline nitrobenzene and with permanganate oxidation methods has been found to correlate with the proportion of the condensed structures of lignin. The higher the S/G ratio less condensed structures has been determined from the wood [5].

Analytical pyrolysis combined with gas chromatography–mass spectrometry (GC/MS) has been increasingly used to determine lignin structure from wood fibers, because time consuming sample preparation is not needed. In addition, the phenolic lignin pyrolysis products have been identified and reported [6–8]. The technique has increasingly been used for the estimation of the S/G ratio of lignin [2,4,9–15]. Another method commonly used for the same purpose is the nitrobenzene oxidation method [9–17]. In the alkaline nitrobenzene oxidation, lignin is oxidatively cleaved to form aromatic carbonyl compounds, *i.e.* syringaldehyde and vanillin as main products [18]. Due to the lacking reactivity of nitrobenzene oxidation against condensed structures, the yield of the carbonyl compounds is approximately 50% of the lignin. Due to the high proportion of condensed guaiacyl units, only about 30% of them are converted to vanillin. On the contrary, the conversion of syringyl units to syringaldehyde may be as high as 90% due to the low proportion of condensation in this case. Therefore, the obtained S/G ratio by alkaline nitrobenzene oxidation is expected to be higher than the actual proportion of guaiacyl and syringyl units in lignins [1,17].

In pyrolysis, lignin is thermally degraded to a mixture of phenols by heating samples in an inert atmosphere. The formed products retain the structural information of the original polymer. However, it has been difficult to find direct relationship among the phenolic pyrolysis degradation products and the original lignin structure. It is proposed that the phenols formed result from the cleavage of

* Corresponding author. Tel.: +358 40 570 9322; fax: +358 20 722 7026.
E-mail address: taina.ohra-aho@vtt.fi (T. Ohra-aho).

0165-2370/$ – see front matter © 2013 Elsevier B.V. All rights reserved.
http://dx.doi.org/10.1016/j.jaap.2013.01.015

the β-O-4 and some condensed linkages such as β-5 [19–22]. However, the yield of the pyrolysis products is expected to be highly dependent on the number of condensed structures present in lignin [9,10,12,23]. Thus, also Py-GC/MS overestimates the syringyl units in lignin similarly to nitrobenzene oxidation. A correction equation has been developed in order to compensate for the effect of condensation and thus reduce the yield of S units with relation to G units [10]. The yield of the monomeric pyrolysis degradation products for the different Japanese hardwood species has been reported to vary from 12.2 to 26.1% of Klason lignin [14]. For hardwood type synthetic dehydrogenation polymers the pyrolysis yield varied from 10 to 20% [12]. The pyrolysis yields were thus much lower than that reported for the nitrobenzene oxidation yields of vanillin and syringaldehyde [12,14]. S/G ratios by Py-GC/MS and alkaline nitrobenzene oxidation have been compared [9,11–14]. The ratios for wood samples are close to each other, but not equal [11,13,14]. In several studies poor chromatographic separation of carbohydrate derivatives from lignin derivatives has caused problems in integration of lignin derivatives [11,13,14]. To overcome this problem, selected lignin pyrolysis degradation products have been used for the S/G ratio calculation by Py-GC/MS [11,13]. That, however, may lead to false information about the S/G ratios. Good correlation among Py-GC/MS and nitrobenzene oxidation methods has been obtained for the isolated lignins [12]. In isolated lignin samples, the cellulosic fiber matrix is not present, which in wood samples may affect the result. The problem related to overlapping carbohydrate derivatives is also overcome. However, the isolation process may change the lignin structure and also the isolation increases the analysis time.

Eucalyptus wood is fast growing plant material that is increasingly used for pulp production in temperate zones. S/G ratio of lignin is one of the most important parameters used to evaluate the performance of Eucalyptus wood. Thus, reliable and fast methods for the determination of S/G ratios of lignin directly from wood samples without any need of lignin isolation are needed. In this study, a large number of wood samples from several Eucalyptus species including *E. grandis*, *E. urophylla*, *E. globulus*, *E. dunnii*, *E. camaldulensis* and their crossings were subjected to Py-GC/MS analysis. The aim of the study was to determine possible differences in the structure of lignin and S/G ratio among Eucalyptus hybrids by Py-GC/MS. Especially the effect of the change of species in Eucalyptus crossings on lignin structure was studied. In addition, Py-GC/MS was compared with alkaline nitrobenzene oxidation, aiming at clarifying the potential of the two methods for the estimation of the S/G ratio in lignin. The aim was also to understand the reasons behind the observed differences among the S/G ratios obtained with Py-GC/MS and alkaline nitrobenzene oxidation.

2. Material and methods

2.1. Sample preparation

Eighteen 7-year-old Eucalyptus hybrids, including a number of double/triple/fourth crossings among *E. grandis*, *E. urophylla*, *E. globulus*, *E. dunnii* and *E. camaldulensis* species obtained from Brazil were used as raw materials of this study. Detailed list of the Eucalyptus hybrids is presented in Table 1.

For the chemical analyses, wood chips were prepared with a laboratory chipper (a Chogokukikai model). The chips were well mixed (260 m^3 rotary mixers) and screened according to SCAN-CN 40:94 procedures [24]. For the S/G ratio determination with alkaline nitrobenzene oxidation, the chips were grinded in a Wiley type mill (40 mesh screen) to 40–60 mesh and extractives were removed (mixture of ethanol/toluene 1:2 followed first by ethanol and secondly by hot water) according to TAPPI T264cm-97 standard procedure [25]. Lignin composition and S/G ratio was measured by Py-GC/MS for the Wiley milled chips without extractives removal.

Table 1
Samples.

No.	Eucalyptus hybrids	Short code
1	*E. urophylla* (IP) × *E. grandis* (IP)	IP
2	*E. urophylla* (Flores IP) × *E. urophylla* (Timor)	U1×U2
3	*E. urophylla* (Flores IP) × *E. camaldulensis* (VM2)	U1×C2
4	*E. urophylla* (Flores IP) × [*E. urophylla* (R) × *E. globulus* (R)]	U1×UGL
5	*E. grandis* (Coffs Harbour) × [*E. urophylla* (R) × *E. globulus* (R)]	G1×UGL
6	*E. dunni* (R) × [*E. urophylla* (R) × *E. globulus* (R)]	D1×UGL
7	*E. camaldulensis* (VM1) × [*E. urophylla* (R) × *E. globulus* (R)]	C1×UGL
8	[*E. dunnii* (R) × *E. grandis* (R)] × [*E. urophylla* (R) × *E. globulus* (R)]	DG×UGL
9	[*E. dunnii* (R) × *E. grandis* (R)] × *E. urophylla* (Timor)	DG×U2
10	[*E. dunnii* (R) × *E. grandis* (R)] × *E. camaldulensis* (VM1)	DG×C1
11	[*E. dunnii* (R) × *E. grandis* (R)] × *E. globulus* (R) (Dad, pollen)	DG×GL2
12	*E. dunni* (KR) × *E. globulus* (R) (Dad, pollen)	D2×GL2
13	*E. grandis* (Coffs Harbour) × *E. globulus* (R) (Dad, pollen)	G1×GL2
14	*E. urophylla* (Timor) × *E. globulus* (R) (Mom, stigma)	U2×GL1
15	*E. urophylla* (Timor) × *E. camaldulensis* (VM1)	U2×C1
16	*E. camaldulensis* (VM1) × *E. camaldulensis* (VM1)	C1×C2
17	*E. dunni* (R) × *E. dunni* (KR)	D1×D2
18	*VCP – E. grandis* (VCP) × *E. urophylla* (VCP)	VCP

2.2. Determination of the S/G ratio by nitrobenzene oxidation/HPLC

The determination of the S/G ratio of each extractive-free wood sample was obtained by the nitrobenzene oxidation according to Lin and Dence [17]. Approximately 0.2 g (oven dryed) of each wood sample together with NaOH aqueous solution (7 mL; 2 mol L^{-1}) and nitrobenzene (0.5 mL) was loaded into a stainless steel reactor and heated up to 170 °C for 2.5 h, with analyses repeated twice. The oxidized material was then extracted with chloroform (6× 30 mL). After the first extraction, HCl was added (2.5 mL; 4 mol L^{-1}) to the aqueous phase. The combined organic phases were evaporated. The sample was transferred to a 50 mL volumetric flask and the volume completed with acetonitrile/water solution (1:1, v/v). Following, the solution was filtered in a regenerated cellulose membrane, pore size 0.45 μm, analyzed by high performance liquid chromatography (HPLC) in a Shimadzu CBM-10A apparatus equipped with a UV-VIS detector SPD-10AV, operating at 280 nm wavelength, LC-10AD pump and Rheodyne injector with a 20 mL loop and a Lichrosorb RP-18 (250 mm × 4 mm, 5 μm) reverse phase analytical column. The mobile phase was composed of acetonitrile/water (1:6, v/v) and the pH was adjusted to 2.6 with trifluoroacetic acid (TFA) buffer. The column temperature was kept at 40 °C, and mobile phase flow of 1.5 mL/min was used. Vanillin and syringaldehyde standards (Aldrich, Milwaukee, WI, USA) were used for quantification of derivatives of guaiacyl and syringyl units, respectively. Calibration curves using vanillin and syringaldehyde standards were obtained in the concentrations of 0.375, 0.75, 1.125, and 1.5 mmol L^{-1} for vanillin, and 0.825, 1.65, 2.475, and 3.3 mmol L^{-1} for syringaldehyde. The solutions were prepared in an acetonitrile/water mixture (1:1, v/v), at pH 2.6. The equation used for vanillin and syringaldehyde were $y = 5{,}669{,}520x - 84{,}175$ ($R^2 = 0.9993$, %RSD = 1.35) and $y = 3{,}056{,}620x + 75{,}181$ ($R^2 = 0.9996$, %RSD = 2.05), respectively. The partial least square method was used to fit the data.

2.3. Py-GC/MS

Py-GC/MS measurements were performed with a filament pulse pyrolyzer (Pyrola2000, PyrolAB, Sweden), which was connected to a GC/MS instrument (Varian 3800 GC/2000 MS). About 100 μg of the sample was weighed accurately on an automatic ultra-micro balance (CHAN 29 Instruments Inc. Cerritos, USA) and placed directly on the filament, which contained a small cavity. Pyrolysis chamber maintained at 175 °C was purged with Helium 18 mL/min in order to lead the pyrolysis products into the gas chromatography injector, which contained split liner (Restek, 3.4 mm × 5.0 mm × 54 mm). A split injector maintained at 280 °C using a split ratio of 1:18 was used. Temperature rise time to final pyrolysis temperature 580 °C was set to 8 ms and total pyrolysis time was 2 s. Pyrolysis products were separated using a capillary column (J&W, DB-1701, 30 m × 0.25 mm, film 1 μm), using the following temperature program: initial temperature 100 °C, rate of increase 4 °C/min to 265 °C and held for 10 min. Helium was used as a carrier gas, using constant flow rate of 0.9 mL/L. Ion trap mass spectrometer was used for the compound detection with the mass scan range of m/z 46–399 (EI 70 eV). The ion trap and transfer line temperature was set to 180 °C and 250 °C, respectively. The peak areas of lignin pyrolysis products were integrated and normalized to the weight of the sample. Co-eluted compounds numbered as 14/15, 23/24 and 25/26 were integrated using selected main ions (122 + 137 + 166 + /167 + 182, 123 + 151 + 178/124 + 137 + 180, 181 + 208/167 + 210) and the peaks areas were corrected back to the total peak area using factors, which were calculated for the pure mass spectra of the compound (2/2.5, 2.7/3.1, 4.5/5.3). Average of at least two parallel measurements was calculated and the peak areas of guaiacyl and syringyl lignin pyrolysis products were normalized to 100%. The pyrolysis products formed were identified using data from the literature [6–8] and commercial NIST05 library.

2.4. Data analysis

All guaiacyl and syringyl type lignin pyrolysis products integrated and normalized to 100% separately were subjected for data analysis. Multivariate data analysis using principle component analysis (PCA) was carried out with SIMCA-P 8.1 (Umetrics AB, Umeå, Sweden). PCA was used in order to better observe the variations in such a large data set. PCA is designed for visualization of similarities and differences among samples. It shows the underlying structure in data and presents it in two or three-dimensional figures so that the major trends and dominant patterns can be overviewed. At the beginning data with all variables are centered and scaled to unit variances. A principal component model (PC) is obtained, in which the first principal component (PC1) is a line in a K-dimensional space (K = number of variables) that describes the largest variance in the data set. In general, one principal component is not sufficient to model the variation in the data set adequately. Therefore, a second component (PC2) is calculated. The PC2 is orthogonal to the PC1 and it reflects the second largest source of variation in data [26]. Two principal components were thus calculated for the data set, because third component did not improve the model. The obtained score and loading plot shows the projection of the observations (Eucalyptus crossings) and variables (guaiacyl and syringyl lignin derivatives) to a plane, respectively.

3. Results and discussion

3.1. Lignin structure in Eucalyptus hybrids

Similar type of profiles (pyrograms) was obtained for all Eucalyptus crossings. As an example, the pyrograms of Eucalyptus clones *E. urophylla* (IP) × *E. grandis* (IP) and [*E. dunnii* (R) × *E. grandis* (R)] × *E. globulus* (R) (Dad, pollen) are shown in Fig. 1. Totally 37 lignin pyrolysis derivatives, including 3 *p*-hydroxyphenyl, 17 guaiacyl and 17 syringyl substructures (Tables 3 and 4), were identified. After the peak areas were integrated, relative contents were calculated. The unmarked peaks in the pyrograms were mainly pentose and hexose carbohydrate units originating from both cellulose and hemicelluloses, which were not taken into account in the calculations. Both lignin derivatives as well carbohydrate derivatives were well separated from each other, only exceptions were peaks 14/15, 23/24 and 25/26, which were co-eluted.

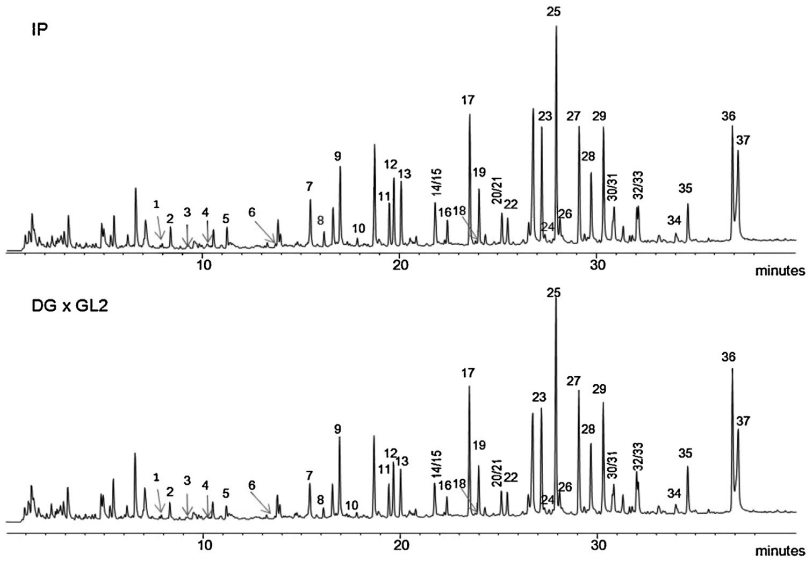

Fig. 1. Pyrograms of Eucalyptus hybrids IP (*E. urophylla* (IP) × *E. grandis* (IP)) and DG×GL2 ([*E. dunnii* (R) × *E. grandis* (R)] × *E. globulus* (R) (Dad, pollen)) obtained at 580 °C. Peak identities of guaiacyl and syringyl lignin pyrolysis derivatives are shown in Tables 3 and 4. Peaks 1, 3 and 4 refer to phenol, 2-methyl- and 4-methylphenol, respectively.

Table 2
Proportion of *p*-hydroxyphenyl, guaiacyl and syringyl lignin pyrolysis derivatives and S/G ratios determined with py-GC/MS and alkaline nitrobenzene oxidation method.

	H%	G%	S%	S/G ratio	
				Py-GC/MS	Nitrobenzene oxidation[b]
IP	0.5	29.4	70.1	2.4	2.8
U1×U2	0.5	28.8	70.7	2.5[a]	3.0
U1×C2	0.5	28.2	71.4	2.5[a]	3.1
U1×UGL	0.3	24.8	74.8	3.0	3.3
G1×UGL	0.5	27.3	72.1	2.6[a]	3.1
D1×UGL	0.4	25.1	74.5	3.0[a]	3.9
C1×UGL	0.4	28.6	71.0	2.5	3.3
DG×UGL	0.3	28.7	70.9	2.5	3.3
DG×U2	0.5	29.1	70.4	2.4[a]	2.7
DG×C1	0.5	30.1	68.5	2.2	2.9
DG×GL2	0.4	25.6	74.0	2.9	3.0
D2×GL2	0.4	24.8	74.8	3.0	3.7
G1×GL2	0.5	27.0	72.5	2.7	3.6
U2×GL1	0.4	25.3	74.4	2.9	4.0
U2×C1	0.5	28.2	71.3	2.5	2.8
C1×C2	0.5	24.6	74.9	3.0[a]	3.2
D1×D2	0.3	24.3	75.4	3.1	3.9
VCP	0.5	34.5	64.9	1.9[a]	3.0

[a] Average of three parallel measurements.
[b] Average of two parallel measurements.

As shown in Table 2, the main lignin pyrolysis derivatives in hardwoods are syringyl and guaiacyl type substructures. The proportion of *p*-hydroxyphenyl structures represented less than 1% of all lignin derivatives determined. The *p*-hydroxyphenyl type products probably originate at least partly from non-lignin material [10,27], even if in these samples the proportion of *p*-hydroxyphenyl structures correlated with the proportion of the guaiacyl structures. Due to the low proportion of *p*-hydroxyphenyl derivatives, only guaiacyl and syringyl units were compared in the structural evaluation of the Eucalyptus hybrids. The range of guaiacyl units varied from 24.3 to 34.5% and syringyl units from 64.9 to 75.4% of the identified lignin structures (Table 2).

The same side chain structures were detected both in guaiacyl and in syringyl units (Tables 3 and 4). Thus, it was possible to compare the distribution of guaiacyl and syringyl side chain structures separately after normalization of the peak areas to 100% (Tables 3 and 4). Basically similar changes in both series (G and S) among different hybrids were observed. The main part of the oxygen rich degradation products is expected to originate as a result of β-O-4 bond cleavage [20,21]. Low content of oxygen rich degradation products has been seen for example in lignin after Kraft cooking, which is known to cleave the β-O-4 bonds, supporting the interpretation hypothesis [27]. The proportion of oxygen rich degradation products in both series (G and S) slightly changed among Eucalyptus hybrids. This suggests that the frequency of β-O-4 type ether linkages varies in these clones.

The overall variation in lignin structure among Eucalyptus hybrids was minor. However, some differences were seen. Change of one crossing to another altered the distribution pattern of lignin derivatives. That variation was seen for example comparing lignin pyrolysis products among the crossings U1×U2, U1×C2, U1×UGL as well crossings U1×UGL, G1×UGL, D1×UGL, C1×UGL, and DG×UGL and crossings DG×UGL, DG×U2, DG×C1, DG×GL2 among each other (Tables 3 and 4).

Due to the difficulties to observe the variation in such a large data set, multivariate analysis using PCA was used. Two principal components that describe the variance of the data were calculated. Same data as illustrated in Tables 3 and 4 were subjected to PC analysis. The first principle component described the highest variance (44%) and the second component the second highest variance (27%)

Table 3
Distribution of guaiacyl lignin units in different Eucalyptus crossings after normalization to 100%. Proportions of side chain structures with and without oxygen were calculated separately.

Peak no.	Compound	IP	U1×U2	U1×C2	U1×UGL	G1×UGL	D1×UGL	C1×UGL	DG×UGL	DG×U2	DG×C1	DG×GL2	D2×GL2	G1×GL2	U2×GL1	U2×C1	C1×C2	D1×D2	VCP
2	G	3.8	3.9	3.5	2.9	4.1	3.1	4.9	2.7	3.7	4.9	3.2	3.3	3.8	3.3	3.6	4.2	2.4	3.3
5	G-CH_3	3.5	4.0	3.1	3.3	3.6	3.3	3.6	3.2	3.8	3.7	2.9	3.0	3.4	3.7	3.4	4.1	3.4	3.7
6	G-CH_2—CH_3	0.5	0.6	0.5	0.4	0.5	0.3	0.5	0.3	0.5	0.6	0.3	0.4	0.4	0.4	0.4	0.5	0.3	0.5
7	G-CH=CH_2	9.1	9.9	8.8	8.9	10.2	9.8	9.3	8.0	9.8	9.5	8.7	9.5	9.2	9.1	9.1	10.7	9.7	10.1
8	G-CH_2—CH=CH_2	2.3	2.3	2.1	2.2	2.3	2.3	2.0	2.2	2.5	2.2	2.3	2.4	2.3	2.3	2.2	2.1	2.5	2.4
10	G-CH=CH—CH_3 *cis*	1.4	1.5	1.3	1.3	1.4	1.5	1.2	1.2	1.5	1.3	1.2	1.5	1.4	1.4	1.3	1.3	1.5	1.5
11	G-CH=CH—CH_3 *trans*	7.4	7.9	6.5	7.1	8.0	8.1	6.5	6.9	8.1	6.9	7.2	7.7	7.9	8.1	7.3	7.7	8.7	7.9
13	G-CHO	11.3	9.8	11.1	11.4	10.3	10.7	9.0	11.4	10.7	9.5	10.6	11.9	10.1	9.8	9.3	9.3	11.6	10.9
14	G-CH_2CHO	9.7	9.2	9.6	9.7	9.2	9.4	7.1	9.9	9.5	7.9	9.5	10.3	8.6	8.7	8.4	7.9	10.8	10.1
16	G-CO—CH_3	4.2	3.8	4.2	4.3	4.1	4.0	3.7	4.0	4.0	3.8	3.9	4.7	4.0	3.7	3.6	3.9	3.9	4.0
18	G-CH_2—CO—CH_3	1.3	1.4	1.2	1.1	1.5	1.1	1.5	1.0	1.1	1.3	1.1	1.2	1.3	1.3	1.3	1.3	1.0	1.1
20	G-CO—CH=CH_2	6.0	5.7	6.0	6.4	5.3	6.3	4.7	6.7	6.2	5.1	6.2	6.3	5.5	5.8	5.6	5.3	7.6	6.3
21	G-CHOH—CH=CH_2	2.5	2.7	2.2	2.3	2.4	2.4	2.1	2.5	2.6	2.2	2.1	2.3	2.3	2.5	2.5	2.4	2.7	2.7
24	G-CH_2—CH_2—CH_2OH	1.7	1.7	1.6	1.5	1.5	1.5	1.9	1.7	1.8	2.0	1.5	1.4	1.5	1.4	1.5	1.7	1.8	1.8
26	G-CH=CH—CH_2OH *cis*	2.8	2.9	3.4	3.2	2.9	2.7	3.1	3.8	3.0	3.1	3.7	3.0	3.0	3.0	3.4	3.1	2.7	2.9
29	G-CH=CH—CH_2OH *trans*	22.4	22.6	25.2	24.3	23.3	24.0	30.0	23.9	20.9	26.6	26.8	21.6	25.6	26.2	28.2	25.3	19.9	20.1
31	G-CH=CH—CHO	10.3	9.7	9.6	9.6	9.3	9.3	8.9	10.5	10.4	9.3	8.8	9.7	9.6	9.3	8.7	9.3	9.5	10.7

Table 4
Distribution of syringyl lignin units separately in different Eucalyptus crossings after normalization to 100%. Proportions of side chain structures with and without oxygen were calculated separately.

Peak no.	Compound	IP	U1×U2	U1×C2	U1×UGL	G1×UGL	D1×UGL	C1×UGL	DG×UGL	DG×U2	DG×C1	DG×GL2	D2×GL2	G1×GL2	U2×GL1	U2×C1	C1×C2	D1×D2	VCP
9	S	6.4	6.4	6.2	6.1	7.5	5.6	8.3	5.3	6.3	8.1	5.9	6.0	6.8	6.2	6.7	7.2	4.5	5.5
12	S-CH_3	5.1	5.5	4.5	4.9	5.2	4.9	5.4	5.0	5.7	5.3	4.4	4.6	5.3	5.4	5.6	5.6	4.8	5.0
15	S-CH_2—CH_3	1.2	1.4	1.2	1.1	1.3	1.0	1.2	1.0	1.3	1.4	1.0	1.1	1.2	1.2	1.3	1.3	1.0	1.2
17	S-CH=CH_2	9.8	10.4	9.6	9.2	10.6	9.4	10.5	8.8	10.3	10.8	9.5	9.4	10.2	9.9	10.5	11.0	8.7	9.9
19	S-CH_2—CH=CH_2	3.9	4.0	3.8	3.7	4.1	3.9	3.6	3.8	4.2	4.0	3.6	4.0	3.9	3.9	3.9	4.0	4.0	4.1
22	S-CH=CH—CH_3 *cis*	2.1	2.3	1.9	2.0	2.2	2.1	1.6	2.0	2.2	1.9	1.9	2.2	2.0	2.1	1.9	1.9	2.2	2.3
23	S-CH=CH—CH_3 *trans*	7.8	8.7	7.6	7.7	8.7	8.1	7.9	7.3	8.7	8.6	7.6	8.0	8.3	8.4	8.4	8.5	7.9	8.4
25	S-CHO	15.8	14.3	16.2	17.6	15.1	16.5	13.8	17.7	15.4	13.7	16.1	17.2	15.0	14.9	14.0	13.8	18.4	15.9
27	S-CH_2—CHO	9.3	8.8	9.5	10.0	9.0	9.7	7.5	10.2	9.3	7.8	10.2	10.0	9.0	9.1	9.1	8.3	11.3	9.3
28	S-CO—CH_3	5.5	5.0	5.6	5.9	5.3	5.6	5.1	5.9	5.7	5.0	5.5	5.8	5.7	5.1	5.2	5.3	5.4	5.0
30	S-CH_2—CO—CH_3	1.8	1.9	1.6	1.6	2.1	1.5	2.1	1.4	1.7	2.0	1.6	1.7	1.9	1.8	1.9	2.1	1.3	1.4
32	S-CO—CH=CH_2	4.4	4.5	4.9	5.1	3.9	5.1	3.6	5.4	4.9	4.1	5.2	4.8	4.3	4.6	4.9	4.5	6.1	5.1
33	S-CHOH—CH=CH_2	4.3	4.6	3.9	3.9	4.3	4.0	3.8	4.0	4.3	4.1	3.7	3.8	4.2	4.6	4.5	4.4	4.3	4.5
34	S-CH_2—CH_2—CH_2OH	1.0	1.0	1.0	1.0	1.0	0.9	1.1	1.0	1.0	1.1	1.0	0.9	1.0	1.0	1.0	1.0	0.9	1.1
35	S-CH=CH—CH_2OH *cis*	3.2	3.2	3.7	3.4	3.1	3.4	3.5	3.5	3.0	3.5	3.9	3.1	3.5	3.5	3.8	3.3	3.5	3.3
36	S-CH=CH—CH_2OH *trans*	8.5	9.3	10.2	8.7	8.4	9.3	12.6	8.1	7.0	10.0	10.2	8.7	9.1	9.8	9.5	9.4	6.9	8.0
37	S-CH=CH—CHO	9.8	8.9	8.5	8.3	8.2	9.0	8.3	9.5	9.0	8.6	8.5	8.8	8.7	8.5	7.9	8.3	8.8	9.9

Fig. 2. PCA of the pyrolysis data for Eucalyptus hybrids. The score plot of the two principle components shows how the samples are related to each other.

of the data. Fig. 2 shows a score plot, which illustrates the distribution of Eucalyptus samples based on the pyrolysis data shown in the loading plot in Fig. 3.

No grouping was observed among the hybrids. However, PCA confirmed the finding that when one crossing was replaced by another, the distribution of lignin derived pyrolysis products was also changed. That indicated also differences in the lignin original structures among different Eucalyptus hybrids. In the first principle component direction, Eucalyptus hybrids with high content of carbonyl group in side chain were grouped on the right side of the score plot whereas those hybrids with high amount of short side chain structures were placed on the left side of the loading plot. In the second component direction, Eucalyptus hybrids were divided based on the lignin structural units with three carbon atoms in side chain. Lignin structural units with alcohol group in side chain were placed in the upper part of the plot, whereas the reduced structures were placed in the lower part. Although there was no clear grouping of the Eucalyptus hybrids based on the syringyl and guaiacyl type phenolic compounds of lignin, the results clearly proved that lignin structure differs among the different Eucalyptus hybrids. Similar finding has been reported elsewhere [15,28].

The loading plot (Fig. 3) also shows that guaiacyl and syringyl units with equal side chain structures were grouped together. In

Fig. 3. Loading plot describes which guaiacyl (G) and syringyl (S) lignin structural units are important for the classification of samples seen in the Score plot.

PCA it means that structures close to each others have a positive correlation. This indicates that they both originate from similar linkage types in lignin.

3.2. S/G ratio

For the S/G ratio determination with Py-GC/MS, all guaiacyl and syringyl type phenolic compounds shown in Tables 3 and 4 were taken for the calculation, because in PCA (Fig. 3) a positive relation was found among guaiacyl and syringyl type phenolic compounds with similar side chains. The S/G ratios obtained by Py-GC/MS were compared with nitrobenzene oxidation. They varied among the Eucalyptus clones from 1.9 to 3.1 and from 2.7 to 4.0, respectively (Table 2). The average percentage error for Py-GC/MS measurements was 6% and for nitrobenzene oxidation the error varied in the range of 4–5%. The S/G values obtained for Py-GC/MS were thus lower than by nitrobenzene oxidation. Similar results have been obtained earlier [13,14]. The suggested reason for the lower S/G ratio determined by Py-GC/MS in contrast to nitrobenzene oxidation is that in nitrobenzene oxidation only β-O-4 linkages are cleaved, while in Py-GC/MS other linkages in lignin are cleaved as well to some extent. The difference in S/G ratio among the two methods was not constant, varying from 0.1 to 1.1 depending on sample. One cause for the deviation is probably the fact that the structure of lignin is different in Eucalyptus hybrids, which may affect the yield of the degradation products in both Py-GC/MS and alkaline nitrobenzene methods. More information about the lignin linkages and the degradation mechanisms of both methods would be needed to clarify the differences obtained among the methods. Based on our results it is difficult to evaluate which method is more reliable or more accurate. Both methods can well be applied to follow the S/G ratios among sample series, *e.g.* in the process line.

4. Conclusions

The distribution of lignin-derived pyrolysis products, obtained by the Py-GC/MS method, varied among the studied Eucalyptus crossings. This indicates that the lignin structures differ among the samples. Principal component analysis showed that the same side chain structures in the guaiacyl and syringyl series correlated with each other. This motivated to use all detectable G and S type degradation products in the calculation of S/G ratio. The S/G ratios determined with pyrolysis and with nitrobenzene oxidation were close to each other. However the discrepancy between the methods varied among the Eucalyptus hybrids, probably due to differences in their lignin structures that affect the result of both methods. Both methods can thus be used to evaluate S/G ratio but neither of them provides universally correct values.

Acknowledgements

The authors thank Ms. Eila Turunen for performing the technical work in the Py-GC/MS experiments. The Financial support from the Academy of Finland and Brazilian CNPq are gratefully acknowledged (*Effect of fiber wall chemistry on energy demand in wood defibration*, Defibre, 133276).

References

[1] K.V. Sarkanen, H.L. Hergert, Classification and distribution, in: K.V. Sarkanen, C.H. Ludwig (Eds.), Lignins: Occurrence, Formation, Structure and Reactions, Wiley-Interscience, New York, 1971, pp. 43–94.
[2] J.C. Del Rio, A. Gutiérrez, J. Romero, M.J. Martínez, A.T. Martínez, Identification of residual lignin markers in eucalypt Kraft pulps by py-GC/MS, Journal of Analytical and Applied Pyrolysis 58–59 (2001) 425–439.
[3] F.J. González-Vila, G. Almendros, J.C. del Rio, F. Martín, A. Gutierrez, J. Romeo, Ease of delignification assessment of wood from different Eucalyptus species by pyrolysis (TMAH)-GC/MS and CP/MAS ^{13}C-NMR spectrometry, Journal of Analytical and Applied Pyrolysis 49 (1999) 295–305.
[4] J.C. Del Rio, A. Gutiérrez, M. Hernando, P. Ladín, J. Romero, A.T. Martínez, Determining the influence of eucalypt lignin composition in paper pulp yield using Py-GC/MS, Journal of Analytical and Applied Pyrolysis 74 (2005) 110–115.
[5] Y. Xie, Difference of condensed lignin structures in Eucalyptus species, Nordic Pulp and Paper Research Journal 19 (2004) 18–21.
[6] O. Faix, D. Meier, I. Fortmann, Thermal degradation products of wood, Holz als Roh- und Werkstoff 48 (1990) 281–285.
[7] O. Faix, D. Meier, I. Fortmann, Thermal degradation products of wood, Holz als Roh- und Werkstoff 48 (1990) 351–354.
[8] J. Ralph, R.D. Hatfield, Pyrolysis-GC–MS characterization of forage materials, Journal of Agricultural and Food Chemistry 39 (1991) 1426–1437.
[9] D.J. Gardner, T.P. Schultz, G.D. McGinnis, The pyrolytic behaviour of selected lignin preparations, Journal of Wood Chemistry and Technology 5 (1985) 85–110.
[10] J.H. Böttcher, Untersuchungen zur Charakterisierung von Holz und Holzkomponenten mittels konventioneller Analysentechniken und der FTIR-Spekroskopie unter Anwendung von multivariaten statistischen Verfahren, Doctoral Thesis, University of Hamburg, Fachbereich Biologie, Hamburg, 1993.
[11] C.F. Lima, L.C.A. Barbosa, C.R. Marcelo, F.O. Silvério, J.L. Colodette, Comparison between analytical pyrolysis and nitrobenzene oxidation for determination of syringyl/guaiacyl ratio in Eucalyptus spp. lignin, Bioresources 3 (2008) 707–712.
[12] A. Izumi, K. Kuroda, Pyrolysis-gas chromatography analysis of dehydrogenation polymers with various syringyl to guaiacyl ratios, Mokuzai Gakkaishi 43 (1997) 194–202.
[13] C.A. Nunes, C.F. Lima, L.C.A. Barbosa, J.L. Colodette, A.F.G. Gouveia, F.O. Silvério, Determination of *Eucalyptus* spp. lignin S/G ratio: a comparison between methods, Bioresource Technology 101 (2010) 4056–4061.
[14] A. Izumi, K. Kuroda, H. Ohi, A. Yamaguchi, Structural analysis of lignin by pyrolysis-gas chromatography (III) – comparative studies of pyrolysis–gas chromatography and nitrobenzene oxidation for the determination method of lignin composition in hardwood, Japan TAPPI Journal 49 (1995) 1339–1346.
[15] H. Yokoi, T. Nakase, Y. Ishida, H. Ohtani, S. Tsuge, T. Sonoda, T. Ona, Discriminative analysis of *Eucalyptus camaldullenis* grown from seeds of various origins based on lignin components measured by pyrolysis-gas chromatography, Journal of Analytical and Applied Pyrolysis 57 (2001) 145–152.
[16] Y. Watanabe, K. Kitao, Pyrolytic gas-liquid chromatography of lignin, Wood Research 38 (1966) 40–46.
[17] S.Y. Lin, C.W. Dence, Methods in Lignin Chemistry, Springer-Verlag, New York, 1992.
[18] T.P. Schultz, M.C. Templeton, Proposed mechanisms for nitrobenzene oxidation of lignin, Holzforschung 40 (1986) 93–97.
[19] M. Klein, P. Virk, Energy Laboratory Report No. MIT-EL 81-005, Massachusetts Institute of Technology, Cambridge, MA, 1981.
[20] R. Brežný, V. Mihalov, V. Kováčik, Low temperature thermolysis of lignins, Holzforschung 37 (1983) 199–204.
[21] K.J. Kuroda, Analytical pyrolysis products derived from cinnamyl alcohol-end groups in lignins, Journal of Analytical and Applied Pyrolysis 53 (2000) 123–134.
[22] K. Kuroda, A. Nakagawa-Izumi, Analytical pyrolysis of lignin: products stemming from β-5 substructures, Organic Geochemistry 37 (2006) 665–673.
[23] K. Kuroda, A. Yamaguchi, K. Sakai, Analysis of Sugi wood and its lignin preparations, Mokuzai Gakkaishi 40 (1994) 987–995.
[24] Scandinavian Pulp, Paper and Board Testing Committee, SCAN-Test Methods, Scandinavian Pulp, Paper and Board, Stockholm, Sweden, 2004.
[25] Technical Association of the Pulp and Paper Industry (TAPPI), TAPPI Test Methods 2000–2001, TAPPI, Atlanta, USA, 2000.
[26] L. Eriksson, E. Johansson, N. Kettaneh-Wold, S. Wold, Introduction to Multi- and Megavariate Data Analysis Using Projection Methods (PCA & PLS), Umetrics, Sweden, 1999, pp. 43–68.
[27] T. Ohra-aho, M. Tenkanen, T. Tamminen, Direct analysis of lignin and lignin-like components from softwood Kraft pulp by different pyrolysis-GC/MS techniques, Journal of Analytical and Applied Pyrolysis 74 (2005) 123–128.
[28] P. Prinsen, A. Gutiérrez, J. Rencoret, L. Nieto, J. Jiménez-Barbero, A. Burnet, M. Petit-Conil, J.L. Colodette, Á.T. Martínez, J.C. del Rio, Morphological characteristics and composition of lipophilic extractives and lignin in Brazilian woods from different eucalypt hybrids, Industrial Crops and Products 36 (2012) 572–583.

V

Ohra-aho T., Niemi P., Aura A.-M., Orlandi M., Poutanen K., Buchert J., Tamminen T. (2016) Structure of brever's spent grain lignin and its interactions with gut microbiota *in vitro*. *J. Agric. Food Chem.* **64**, 812-820.

JOURNAL OF AGRICULTURAL AND FOOD CHEMISTRY

Article

pubs.acs.org/JAFC

Structure of Brewer's Spent Grain Lignin and Its Interactions with Gut Microbiota in Vitro

Taina Ohra-aho,*[,†] Piritta Niemi,[†] Anna-Marja Aura,[†] Marco Orlandi,[§] Kaisa Poutanen,[†] Johanna Buchert,[#] and Tarja Tamminen[†]

[†]VTT Technical Research Centre of Finland Ltd., P.O. Box 1000, FI-02044 VTT, Espoo, Finland

[§]Department of Environmental and Earth Sciences, University of Milano—Bicocca, Piazza della Scienza 1, Milan, I-20126 Italy

[#]Natural Resources Institute Finland, Viikinkaari 4, FI-00790 Helsinki, Finland

ABSTRACT: Lignin is part of dietary fiber, but its conversion in the gastrointestinal tract is not well understood. The aim of this work was to obtain structural information on brewer's spent grain (BSG) lignin and to understand the behavior of the polymeric part of lignin exposed to fecal microbiota. The original BSG and different lignin fractions were characterized by pyrolysis-GC/MS with and without methylation. Methylation pyrolysis proved that the ratio between guaiacyl and syringyl units was similar in all lignin samples, but the ratio between *p*-coumaric and ferulic acids varied by the isolation method. Combined pyrolysis results indicated higher acylation of γ-OH groups in syringyl than in guaiacyl lignin units. The polymeric lignin structure in the alkali-soluble fraction after enzymatic hydrolysis was slightly altered in the in vitro colon fermentation, whereas lignin in the insoluble residue after enzymatic treatments remained intact.

KEYWORDS: *brewer's spent grain, lignin, Py-GC/MS, TMAH/Py, in vitro fermentation, colon microbiota*

INTRODUCTION

Brewer's spent grain (BSG) is the most abundant byproduct generated in the brewing of beer.[1] It is composed of the insoluble parts of malts, which are not dissolved in mashing, namely, the husks, bran, and residues of endosperm. BSG is rich in cell wall polysaccharides (arabinoxylan and cellulose), protein, and lignin.[2] A lower amount of lipids is also present. BSG is a food grade material and currently used for ruminant feed.[3] However, as it is rich in protein and dietary fiber, it could be used in more valuable applications as well, such as a dietary component in human food.

Although lignin is included in our everyday diet as a part of plant cell walls, the metabolism of lignin in humans or other animals is not well-known. Instead, it is generally assumed that lignin is an inert material in the gastrointestinal tract and not fermented or metabolized by the colon microbiota. However, there are some indications of lignin degradation by goats.[4] In addition, lignin has been shown to be a precursor of the mammalian lignans, enterodiol and enterolactone, in rats,[5] suggesting that nonruminants could also be able to degrade lignin. More recently, partial lignin degradation by human fecal microbiota has been shown.[6,7] Mono- and dimeric phenolic metabolites were released and metabolized from BSG and its enzymatically extracted fractions through microbial conversions in an in vitro colon model.

Being a polymeric material, lignin is not absorbed in the gastrointestinal tract but remains in the gut lumen, where it may interact with other components of the digested food or affect microbial conversion activities, as has been shown for isolated condensed tannins, which inhibited dietary fiber fermentation by colon microbiota.[8] Nevertheless, potential health effects have been proposed to arise from lignin. The mammalian lignans, enterodiol and enterolactone, produced from lignin[5] may help protect against cancer and cardiovascular disease.[9,10] Furthermore, lignin-rich dietary fiber is capable of adsorbing carcinogenic compounds in the colon,[11] thus preventing the carcinogens from being absorbed into circulation and thus lowering the risk of cancer.[12]

The structure of BSG lignin has been recently characterized from different lignin fractions, those being "milled-wood" lignin, dioxane lignin, and celluolytic lignin, isolated from BSG.[13] In the present paper, lignin fractions isolated previously by sequential enzymatic hydrolyses[7,12] were characterized by analytical pyrolysis coupled with gas chromatography and mass spectrometer (Py-GC/MS) with and without tetramethylammonium hydroxide (TMAH). The results were compared with two other isolation methods, acidolysis and enzymatic hydrolysis followed by mild acidolysis, to learn more about the BSG lignin structure and fractionation. Structural analysis of the initial BSG was performed as reference, because the enzymatic and chemical fractionations may have changed the original lignin structure. The characterization data were further utilized when the conversion of the BSG lignin fractions by fecal microbiota was studied using an in vitro colon model. Release of lignin-related small phenolic metabolites in the fermentation of BSG lignin has been reported earlier.[6,7] In the current study, the aim was to understand the behavior of the polymeric part of lignin exposed to fecal microbiota.

Received: November 21, 2015
Revised: January 10, 2016
Accepted: January 11, 2016
Published: January 11, 2016

DOI: 10.1021/acs.jafc.5b05535
J. Agric. Food Chem. 2016, 64, 812−820

MATERIALS AND METHODS

Materials. BSG was obtained from Sinebrychoff brewery (Kerava, Finland) and stored at −20 °C.[14] The main components were carbohydrates (42.2%), mainly arabinoxylan (22.2%) and glucan (17.1%), protein (22.8%), lignin (19.3%), lipids (11.0%), and ash (4.7%).

Preparation of Lignin Fractions. BSG was fractionated with enzymatic methods as described previously.[7,14] In brief, Masuko milled BSG was treated sequentially with carbohydrate- and protein-degrading enzymes. Two different fractions were obtained by a three-step hydrolysis: one by precipitation of protease- and alkali-soluble material (denoted protease-alkaline extracted fraction, P-AEF) and one as the insoluble residue after the hydrolyses (INS). For acidolysis (AL) and enzymatic mild acidolysis (EMAL) lignin isolation, BSG was dried and milled with a Retch S100 ball mill (400 rpm for 10 h) to very fine powder (Figure 1). The extractives

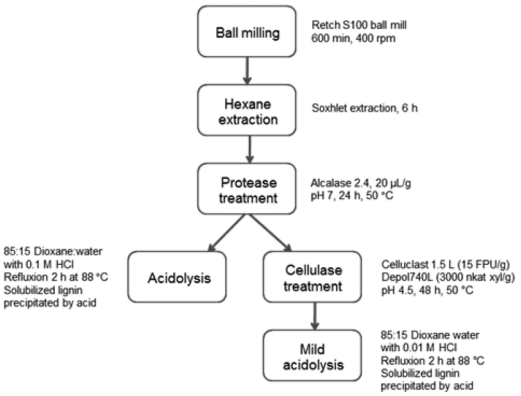

Figure 1. Scheme for the BSG fractionation methods acidolysis and enzymatic mild acidolysis.

were removed with hexane in a Soxhlet for 6 h. Proteolysis was carried out for the hexane-extracted material with Alcalase 2.4 L (20 µL/g of dry material) at 50 °C and pH 7 for 24 h. Acidolysis was performed by refluxing the material in 85:15 dioxane/water solutions with 0.1 M HCl at 88 °C for 2 h under nitrogen atmosphere according to the method of Gellerstedt et al.[15] The solids were separated by filtration, and the dissolved lignin was precipitated from the filtrate with 0.01 M HCl at 4 °C overnight. Isolation of EMAL was performed according to the method of Guerra et al.,[16] with some modifications as follows: The extractive-free and protease-treated BSG was first treated with Depol740 (3000 nkat/g solid material) and Celluclast 1.5 (15 FPU/g solid material at pH 4.5, 50 °C for 48 h. After carbohydrate digestion, it was further treated with 0.01 M HCl in 85:15 dioxane/water solutions at 88 °C for 2 h under argon nitrogen atmosphere. The dissolved lignin was precipitated as described above.

In Vitro Colon Model. Fermentation of lignin fractions P-AEF and INS in the in vitro colon model was performed according to the method of Barry et al.[17] with some modifications described by Niemi et al.[6] and Aura et al.[7] The fermentation experiments were performed in triplicate, but samples for Py-GC/MS analysis were taken from one batch. A time course from 0 to 24 h was followed using the same inoculum for all of the substrates. Incubation was performed at 37 °C in tightly closed bottles and in magnetic stirring (250 rpm). Fecal backgrounds were incubated without addition of the supplements. Fermentation of P-AEF and INS was performed in different fecal controls, FC1 and FC2, respectively.

For Py-GC/MS analyses, 1 mL of the fermented samples (P-AEF-FC1, INS-FC2, FC1, and FC2) of 0 and 24 h time points was thawed; 0.5 mL of water (pH 2.5) and 25 µL of 6 M HCl were added to lower the pH to near 2.5. Samples were centrifuged (14000 rpm/10 min) to remove the liquid fraction, and thereafter the solid fractions were washed twice with water (pH 2.5). The solid fractions were stored at −20 °C until analyzed.

Py-GC/MS measurements without and with tetramethylammonium hydroxide (TMAH) were performed with a filament pulse pyrolyzer (Pyrola2000, PyrolAB, Sweden), which was connected to a GC/MS instrument (Varian 3800 GC/2000 MS, Palo Alot, CA, USA). About 50−100 µg of the solid samples was weighed accurately on an automatic ultramicro balance (CHAN 29 Instruments Inc., Cerritos, CA, USA) and transferred to the filament. A equal volume of samples obtained from in vitro colon fermentation was pipetted on filament. For methylation pyrolysis, a 10% TMAH aqueous solution (2 µL) was added and mixed with the sample. The pyrolysis chamber maintained at 175 °C was purged with helium at 18 mL/min to lead the degradation products into the gas chromatography injector, maintained at 280 °C. The temperature rise time to final pyrolysis temperature 600 °C was set to 8 ms, and the total pyrolysis time was 2 s. Pyrolysis products were separated on a 30 m × 0.25 mm i.d., 1 µm film thickness, fused silica capillary column of DB-1701 (J&W Scientific, Folsom, CA, USA) using the following temperature program for direct pyrolysis: initial temperature 80 °C held for 1 min, rate of increase of 4 °C/min to 265 °C and held for 17.75 min. For TMAH/Py: initial temperature 80 °C held for 2 min, rate of increase of 8 °C/min to 160 °C and extended from 160 to 280 °C at 5 °C/min. A constant carrier gas flow of 1.0 mL/min was used. An ion trap mass spectrometer was used for compound detection with the mass scan range of m/z 46−650 (EI 70 eV). The ion trap temperature was set to 180 °C. The degradation products formed were identified using data from the literature[18−21] and commercial NIST05 library. The peak areas of carbohydrate, lignin, *p*-coumaryl acid, ferulic acid, and protein pyrolysis degradation products were integrated and normalized to the weight of the sample. Peak molar areas were calculated for all pyrolysis products before normalization to 100%. Two parallel measurements were carried out for the lignin samples and three measurements for the fermentation samples. The results are given as average. Average standard deviations for the Py-GC/MS and Py/TMAH measurements were 15 and 17%, respectively. Due to the high amount of interfering components formed from the fecal controls, only the largest peaks were integrated from the total ion chromatograms obtained from the pyrolysis in the presence of TMAH.

Principal Component Analysis (PCA). Py-GC/MS and TMAH/Py data were separately subjected to PCA. Multivariate data analysis was carried out with SIMCA-13 (Umetrics AB, Umeå, Sweden), according to the method of Ohra-aho et al.[22] Two principal components were calculated for both data sets. The most important variables, lignin degradation products with predictivity >0.5, were included in the model. The changes in P-AEF and INS during fermentation in an in vitro colon model in comparison to fecal controls were evaluated using score plots.

RESULTS AND DISCUSSION

The isolation of two lignin-rich fractions, soluble (P-AEF) and insoluble fraction (INS), from BSG using enzymatic hydrolysis has been described before.[7,14] Acidolysis (AL) and enzymatic mild acidolysis (EMAL) were applied to produce purer lignin samples for comparison.

Lignin yields in the P-AEF, INS, AL, and EMAL fractions were 14, 39, 21, and 5.8% on the theoretical lignin in BSG, respectively. On athe basis of the composition analyses, the P-AEF and the INS both contained about 40% of lignin. P-AEF contained a similar proportion of protein (45%) as lignin and less carbohydrate (6.7%), whereas INS contained more carbohydrates (39%) but less protein (6.6%). Both fractions contained also about 10% of ash.[7,14] For AL and EMAL, composition analyses were not performed due to inadequate amounts of material, but an estimation was obtained from the Py-GC/MS results (Figure 2). Residual lipids were not included. For comparison, the composition of all samples was

DOI: 10.1021/acs.jafc.5b05535
J. Agric. Food Chem. 2016, 64, 812−820

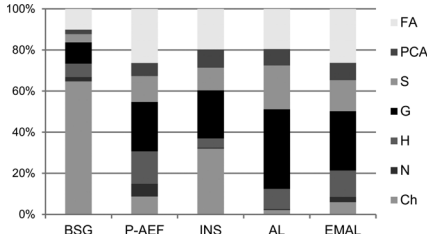

Figure 2. Contents of carbohydrates (Ch), nitrogen-containing aromatic structures from protein (N), *p*-hydroxyphenyl type structures from protein and lignin (H), syringyl (S) and guaiacyl (G) structures from lignin, 4-vinylphenol from *p*-coumaric acid (*p*-CA), and 4-vinylguaicol from ferulic acid, determined by Py-GC/MS.

evaluated semiquantitatively by Py-GC/MS. The purest lignin was obtained with AL. The AL fraction contained about 60% of lignin and a low amount of protein and carbohydrate impurities (about 10 and 2%, respectively). Protein content was reduced by a protease treatment prior to AL. In the extraction of lignin with AL, 63% of the hexane-extracted and protease-treated material was dissolved, but only 7% was recovered by precipitation, resulting in a very low yield. Fifty-six percent of the material could not be precipitated with acidic water. Also, on the basis of the brown color of the filtrate and the mass balance, part of the dissolved lignin had remained in the soluble phase. Similar problems with poor precipitation of BSG lignin have been described previously[14] and hypothesized to be due to linkages between lignin and the water-soluble peptides and oligosaccharides formed in the protease treatment. Carbohydrate and protein removal in EMAL was not as complete as in AL, but slightly better than in enzymatically hydrolyzed P-AEF. The EMAL fraction contained about 45% of lignin, which was lower than in AL but slightly higher than in P-AEF and INS. However, the yield of the EMAL fraction was low. This means that lignin was poorly soluble with diluted acid water and indicates that lignin was attached to carbohydrates via other than ester bonds. Protein and carbohydrate removal from BSG to obtain a pure lignin fraction was not totally complete by any of the methods applied, in accordance with previous literature.[13] Although lignin content was enriched after each isolation stage in comparison to the original BSG, the yields of lignin were low due to poor precipitation in P-AEF and AL and poor solubility of lignin in EMAL. Because fractions represented only part of the BSG lignin, the original BSG was analyzed similarly to the fractions, and the results were compared.

Lignin Composition Determined by Py-GC/MS. As examples, the total ion chromatograms of original BSG and P-AEF obtained by Py-GC/MS at 600 °C are shown in Figure 3. Identified aromatic pyrolysis degradation products of lignin, protein, and ferulic and *p*-coumaric acids are marked in the chromatogram with numbers. The corresponding peak identities are shown in Table 1. Peak identities of degradation products of protein (numbers) and carbohydrates (letters) are listed below Figure 3. The highest peaks in the original BSG originate from arabinoxylan (b, c, e, h) and glucan (d, f, g, k). These carbohydrate-derived peaks are almost absent in the P-AEF chromatogram, in accordance with its composition.[14] 4-Vinylphenol (7) and 4-vinylguaiacol (8) mainly originate from *p*-coumaric and ferulic acid via decarboxylation during

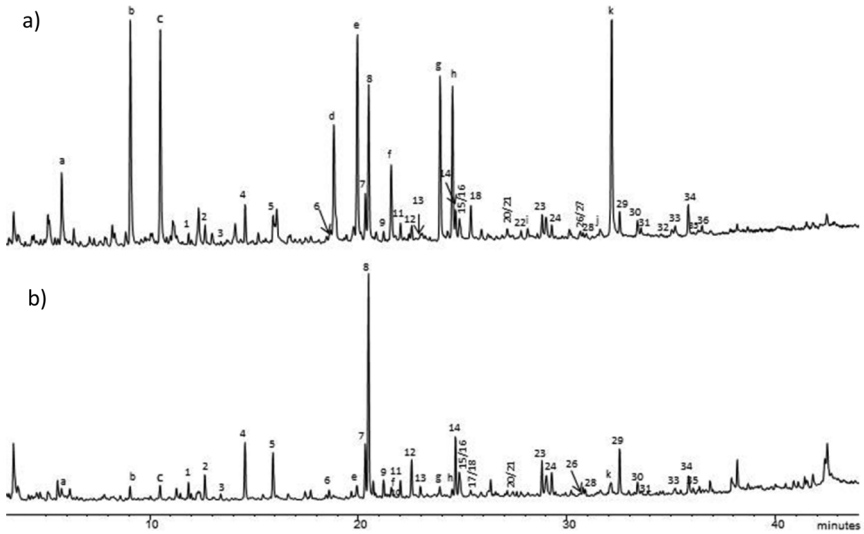

Figure 3. Total ion chromatograms of (a) BSG and (b) P-AEF (protease-alkaline extracted fraction) obtained at 600 °C. Peak identities of pyrolysis degradation products of guaiacyl and syringyl type lignin and ferulic and *p*-coumaric acids are shown in Table 1. Peak identities of *p*-hydroxyphenyl (H) type degradation products, catechols, and protein (prot): 1, phenol (H); 2, 2-methylphenol (H); 4, 4-methylphenol (H); 10, catechol; 12, indole (prot); 16, methylindole (prot); 17, hydroquinone; 19, 4-hydroxybenzaldehyde (H). Carbohydrate derivatives: a, 2-furaldehyde; b, unidentified pentose product from xylan; c, 1,5-anhydro-4-deoxypent-1-en-3-ulose; d, 5-hydoxymethyl-2-tetrahydrofuraldehyde-3-one; e, 1,5-anhydroarabinofuranose; f, 5-hydroxymethyl-2-furaldehyde; g, 1,4-dideoxy-D-glycero-hex-1-enopyranose-3-ulose; h, 1,4-anhydroxylopyranose; i, 1,6-anhydrogalactopyranose; j, 1,4-anhydroglucopyranose; k, 1,6-anhydroglucopyranose.

DOI: 10.1021/acs.jafc.5b05535
J. Agric. Food Chem. 2016, 64, 812−820

Table 1. Relative Molar Abundance of Aromatic Degradation Products of Guaiacyl (G) and Syringyl (S) Type Lignin Units and *p*-Coumaric and Ferulic Acid Formed in Py-GC/MS from the Original BSG and Lignin-rich Enzymatically and Chemically Isolated Fractions of BSG

peak	compound	M_w	orig	BSG	P-AEF	INS	AL	EMAL
7	4-vinylphenol	120	H/*p*-CA	8.0	8.8	13.8	8.5	10.0
2	guaiacol	124	G	4.4	5.0	5.8	7.0	5.3
5	4-methylguaiacol	138	G	4.9	7.6	3.6	9.1	6.1
6	4-ethylguaiacol	152	G	1.2	1.7	0.8	2.1	2.2
8	4-vinylguaiacol	150	G/FA	36.6	36.2	30.3	20.8	31.4
9	eugenol	164	G	1.8	2.3	1.4	2.0	2.5
13	*cis*-isoeugenol	164	G	1.1	1.4	0.8	1.5	1.8
14	*trans*-isoeugenol	164	G	4.9	7.7	4.1	6.6	9.0
18	vanillin	152	G	7.2	1.0	4.1	2.0	1.5
21	homovanillin	166	G	1.5	0.0	2.2	2.5	0.7
22	acetoguaiacone	166	G	1.6	0.7	1.3	0.8	0.6
25	guaiacylacetone	180	G	0.6	1.0	0.8	3.2	3.1
26	4-(oxyallyl)guaiacol	178	G	0.7	0.1	0.6	0.6	0.4
27	4-(1-hydroxyprop-2-enyl)guaiacol	180	G	0.3	0.0	0.6	0.5	0.1
31	*cis*-coniferyl alcohol	180	G	1.6	0.8	1.9	0.6	0.3
34	*trans*-coniferyl alcohol	180	G	4.1	3.8	5.8	1.6	0.9
35	coniferaldehyde	178	G	1.7	0.0	2.0	1.3	0.0
11	syringol	154	S	2.1	2.3	2.9	3.5	2.2
15	methylsyringol	168	S	2.3	3.7	1.8	4.8	3.0
20	4-ethylsyringol	182	S	0.1	0.5	0.2	0.9	0.7
23	4-vinylsyringol	180	S	3.2	4.7	3.1	6.6	6.1
24	4-allylsyringol	194	S	1.5	2.0	1.2	1.8	1.9
28	*cis*-propenylsyringol	194	S	1.0	1.5	0.7	1.4	1.5
29	*trans*-propenylsyringol	194	S	3.4	5.7	2.9	4.8	5.3
30	syringaldehyde	182	S	2.3	0.3	1.5	1.1	0.6
32	homosyringaldehyde	196	S	0.2	0.0	0.6	0.5	0.0
33	acetosyringone	196	S	1.5	1.0	1.3	1.4	0.9
36	syringylacetone	210	S	0.2	0.4	0.3	2.0	1.6
37	4-(oxyallyl)syringol	208	S	0.0	0.0	0.2	0.4	0.4
38	4-(1-hydroxyprop-2-enyl)syringol	210	S	0.0	0.0	0.2	0.1	0.0
39	*cis*-sinapyl alcohol	210	S	0.0	0.0	0.2	0.0	0.0
40	*trans*-sinapyl alcohol	210	S	0.0	0.0	1.7	0.0	0.0
41	sinapaldehyde	208	S	0.0	0.0	1.1	0.0	0.0
	S/G			0.5	0.7	0.6	0.7	0.7

pyrolysis[23−25] but also partially from lignin. The presence of *p*-coumaric and ferulic acid in BSG has been verified previously.[26] In pyrolysis, protein has been found to form phenol (1), 4-methylphenol (4), indole (14), and methylindole (16) as the main degradation products and 4-vinylphenol (7) as a minor product.[13,27] Both guaiacyl (G) and syringyl (S) units with various side chains were detected, confirming the presence of lignin. Also, *p*-hydroxyphenyl type degradation units (H) were present, but most of those are expected to originate from proteins and *p*-coumaric acid. Lignans, which were found in small quantities (<0.01%) in BSG,[14] degrade in pyrolysis to similar guaicyl and syringyl structures as lignin.[28,29] However, the effect of lignans on the yields of guaicyl and syringyl units can be regarded as insignificant due to their low amount.

All of the degradation products mentioned above were found in BSG and its fractions, but only the phenolic compounds released in pyrolysis from the guaiacyl and syringyl type lignin units as well as ferulic and *p*-coumaric acids were included for the structural characterization (Table 1). *p*-Hydroxyphenyl-type pyrolysis degradation products were excluded because they cannot be specified as lignin degradation products.[13,27] 4-Vinylguaiacol and 4-vinylphenol were the most abundant aromatic pyrolysis degradation products in all samples, indicating high contents of ferulic and *p*-coumaric acids. Higher proportions of guaiacyl type than syringyl type lignin derivatives were formed from the original BSG and the fractions, indicating that BSG lignin is rich in guaiacyl type units. This is in agreement with previous findings.[13] In the present study, the S/G ratio varied between 0.5 and 0.7, being lowest in the original BSG.

The most abundant pyrolysis products in BSG were guaiacyl type degradation products guaiacol, 4-methylguaiacol, *trans*-isoeugenol, vanillin, and *trans*-coniferyl alcohol. A slightly lower proportion of corresponding syringyl type degradation products syringol, 4-methylsyringol, *trans*-propenylsyringol, and syringaldehyde was detected. This composition was close to that detected for the INS fraction. In comparison to the other fractions, INS contained the highest proportion of oxygen-containing side-chain structures, that is, vanillin, syringaldehyde, homovanillin, homosyringaldehyde, *cis*- and *trans*-coniferyl alcohol, coniferaldehyde, *cis*- and *trans*-sinapyl alcohol, and sinapaldehyde. These degradation products are released from native lignin structures with high content of *β*-*O*-4 bonds.[30] Especially the oxygen-containing syringyl units with

DOI: 10.1021/acs.jafc.5b05535
J. Agric. Food Chem. 2016, 64, 812−820

Table 2. Relative Molar Abundance of Aromatic Degradation Products of Guaiacyl (G) and Syringyl (S) Type Lignin Units and *p*-Coumaric and Ferulic Acid Formed in Py/TMAH from the Original BSG and Lignin-rich Enzymatically and Chemically Isolated Fractions of BSG

compound	orig	M_w	BSG	P-AEF	INS	AL	EMAL
1,2-dimethoxybenzene	G	138	0.0	0.0	0.0	0.2	0.0
3,4-dimethoxytoluene	G	152	0.0	0.0	0.0	0.2	0.7
3,4-dimethoxybenzeneethylene	G	164	0.0	1.0	0.3	0.6	1.2
3,4-dimethoxybenzene methanol methyl ether	G	182	0.0	0.0	0.0	0.5	0.0
1,2-dimethoxy-4-propenylbenzene	G	178	0.0	0.0	0.0	0.4	0.3
3,4-dimethoxybenzaldehyde	G	166	0.0	1.5	0.7	0.9	1.2
3,4-dimethoxybenzoic acid methyl ester	G	196	4.5	4.6	4.5	4.6	5.3
3,4-dimethoxybenzeneacetic acid methyl ester	G	210	0.0	0.4	0.5	0.6	0.3
cis-1-(3,4-trimethoxyphenyl)-2-methoxyethene	G	194	8.6	8.7	8.4	5.6	10.3
trans-1-(3,4-trimethoxyphenyl)-2-methoxyethene	G	194	5.9	4.7	4.7	3.1	5.3
cis-1-(3,4-dimethoxyphenyl)-2-methoxyprop-1-ene	G	208	0.0	1.0	1.0	0.9	1.4
trans-1-(3,4-dimethoxyphenyl)-2-methoxyprop-1-ene	G	208	0.0	0.6	0.9	0.7	0.6
1-(3,4-dimethoxyphenyl)-1-methoxyprop-1-ene	G	208	0.0	1.0	1.2	0.9	1.5
erythro-4-(1,2,3-trimethoxypropyl)-1,2-dimethoxybenzene	G	270	3.7	3.7	4.0	5.1	6.1
threo-4-(1,2,3-trimethoxypropyl)-1,2-dimethoxybenzene	G	270	5.8	4.0	3.9	4.7	5.1
1,2,3-trimethoxybenzene	S	168	0.0	2.7	0.6	0.5	4.0
3,4,5-trimethoxybenzaldehyde	S	196	0.0	0.6	0.4	0.8	0.6
3,4,5-trimethoxybenzoic acid methyl ester	S	226	5.3	5.8	4.1	8.0	6.1
cis--1-(3,4,5-trimethoxyphenyl)-2-methoxyethene	S	224	17.1	6.6	6.8	7.3	10.1
trans-1-(3,4,5-trimethoxyphenyl)-2-methoxyethene	S	224	0.0	3.7	3.5	3.3	0.0
erythro-4-(1,2,3-trimethoxypropyl)-1,2,3-trimethoxybenzene	S	300	4.0	5.0	3.7	5.2	5.1
threo-4-(1,2,3-trimethoxypropyl)-1,2,3-trimethoxybenzene	S	300	6.8	4.4	3.6	4.3	4.5
trans-3-(4-methoxypenyl)-3-propenoic acid methyl ester	*p*-CA	192	11.4	11.1	20.1	24.1	11.1
cis-3-(3,4-dimethoxyphenyl)-3-propenoic acid methyl ester	FA	222	1.5	0.8	1.6	0.5	0.6
trans-3-(3,4-dimethoxyphenyl)-3-propenoic acid methyl ester	FA	222	25.5	28.1	25.5	17.0	18.6
S/G			1.2	0.9	0.8	1.1	0.8
p-CA/FA			0.4	0.4	0.4	0.7	1.4

three carbon atoms in the side chain were less abundant in the other fractions. Recently it has been reported that a small amount of γ-OH groups are acylated in BSG lignin mainly in syringyl units.[13] Similar structures have been observed also for other plant materials such as kenaf bast[31] and coconuts coir fibers.[32] In pyrolysis, acetyl groups have been reported to be eliminated together with the attached hydroxyl group, leading to the formation of double-bond structures in the side chains.[33] This happens also in the case of acylation by *p*-coumaric acid.[13,34] The total absence of sinapyl alcohol-type degradation products in the BSG samples thus suggests that the γ-OH groups in syringyl units are more acylated than guaiacyl units. This was observed especially for P-AEF, AL, and EMAL samples.

Methylation pyrolysis with tetramethylammonium hydroxide (Py/TMAH) provides more precise information about the content of *p*-coumaric and ferulic acid as well as lignin structure. In the presence of TMAH decarboxylation is avoided by the formation of methyl esters from the free acid groups. Due to the high alkalinity of the TMAH, ester groups in the sample are hydrolyzed and exchanged into their respective fatty acid methyl esters. In addition, more information is obtained of the hydroxyl groups present in the side chains due to the formation of methyl ethers with hydroxyl groups.[35,36] The most abundant aromatic degradation products in BSG and its fractions were ferulic and *p*-coumaric acid, as detected also by Py-GC/MS. Using this method, the distinction between the cinnamic acids and lignin-derived pyrolysis degradation products can be made. The proportion of ferulic acid was highest in the original BSG, P-AEF, and INS, but clearly lower in AL and EMAL fractions (Table 2). AL contained the lowest amount of carbohydrates (Figure 2), indicating that acidolysis treatment efficiently removed ferulate-linked polysaccharides. Ferulic acids have been reported to act as cross-links between polysaccharides and lignin, forming ester bonds with polysaccharides and ether bonds with lignin.[34,37] Acidolysis may also to some extent cleave the ether bonds between lignin units.[38] EMAL treatment has also been found to release carbohydrate[37] and ferulate residues, but to a lesser extent due to the milder acidolysis conditions used. The proportion of *p*-coumaric acid was the same as in BSG, P-AEF, and EMAL but lower than in INS and AL. *p*-Coumaric acid has been reported to acylate the γ-carbon of the lignin side chain.[34] Recently it has been found that *p*-coumarates are present in condensed lignin in high amounts.[13] On this basis, it seems that lignin in INS and AL is enriched with condensed lignin. Clearly higher content of syringyl units typically formed from lignin subunits containing β-*O*-4 bonds[39] were measured for all samples by Py/TMAH than by Py-GC/MS. As a result, also somewhat higher S/G ratios of 0.8−1.2 were obtained by Py/TMAH in comparison to Py-GC/MS, especially in the case of BSG and AL. The Py/TMAH analysis confirmed that acylation of γ-OH groups in the syringyl structures leads to underestimation of the content of native type syringyl structures in Py-GC/MS. Thus, Py/TMAH should be used for the determination of S/G ratios of acylated lignins.

Fermentation of the Lignin Fractions in the in Vitro Colon Model. Release of lignin-related small phenolic

DOI: 10.1021/acs.jafc.5b05535
J. Agric. Food Chem. 2016, 64, 812−820

Table 3. Relative Molar Abundance of Aromatic Degradation Products Formed from Lignin and *p*-Coumaric and Ferulic Acid in Py-GC/MS before and after Fermentation of Lignin-rich Fractions of P-AEF, INS, and Controls FC1 and FC2 in in Vitro Colon Model

			P-AEF-FC1		FC1		INS-FC2		FC2	
compound	orig	M_w	0 h	24 h	0 h	24 h	0 h	24 h	0 h	24 h
4-vinylphenol	*p*-CA	120	11.2	10.3	23.5	17.5	14.8	14.9	22.0	11.1
guaiacol	G	124	5.5	5.7	4.8	5.5	5.5	5.0	5.1	5.1
4-methylguaiacol	G	138	6.7	8.2	5.8	7.0	7.3	7.1	6.7	7.3
4-ethylguaiacol	G	152	2.2	2.4	1.6	2.4	1.6	1.9	2.2	2.1
4-vinylguaiacol	FA	150	30.4	27.1	29.9	28.3	34.3	32.1	35.7	37.0
eugenol	G	164	2.0	2.8	1.5	1.9	1.7	2.0	1.6	2.2
cis-isoeugenol	G	164	1.3	1.4	0.8	1.1	1.0	1.1	0.8	1.3
trans-isoeugenol	G	164	9.3	10.7	6.3	7.6	7.5	8.4	5.8	8.5
vanillin	G	152	1.4	1.1	1.6	1.4	1.9	1.7	1.8	2.7
homovanillin	G	166	0.0	0.0	0.0	0.0	0.6	0.0	0.2	0.0
acetoguaiacone	G	166	0.8	0.8	0.9	0.8	0.8	0.9	0.3	1.0
guaiacylacetone	G	180	1.7	1.1	1.5	1.3	1.1	0.7	1.1	0.6
cis-coniferyl alcohol	G	180	0.8	0.6	0.4	0.0	0.9	1.0	0.5	1.2
trans-coniferyl alacohol	G	180	1.7	2.3	1.5	2.3	2.8	4.0	1.8	5.0
coniferaldehyde	G	178	0.0	0.0	0.0	0.0	0.6	0.0	0.0	0.0
syringol	S	154	3.1	3.0	2.6	3.0	2.6	2.6	2.0	1.9
4-methylsyringol	S	168	4.2	4.6	3.4	4.2	3.5	3.8	2.8	3.0
4-ethylsyringol	S	182	0.8	0.8	0.6	0.8	0.5	0.4	0.4	0.3
4-vinylsyringol	S	180	5.5	5.2	5.7	5.5	3.6	3.4	3.8	3.4
4-allylsyringol	S	194	2.0	2.1	1.3	1.7	1.3	1.6	1.1	1.2
cis-propenylsyringol	S	194	1.5	1.6	0.7	1.3	1.0	1.2	0.0	0.9
trans-propenylsyringol	S	194	5.6	6.5	3.4	4.4	3.5	4.3	2.8	3.0
syringaldehyde	S	182	0.8	0.4	0.9	0.6	0.6	0.6	0.8	0.6
acetosyringone	S	196	0.8	0.8	0.6	0.6	0.7	0.8	0.3	0.5
syringylacetone	S	210	0.8	0.5	0.9	0.7	0.4	0.3	0.3	0.2
S/G ratio			0.6	0.5	0.5	0.6	0.4	0.5	0.4	0.3

metabolites in the fermentation of P-AEF and INS has been reported earlier.[6,7] In this study, the same samples as in the present study were utilized to monitor the changes in the polymeric part of the lignin. The same pyrolysis degradation products that were determined for the original samples were monitored also from the samples after fermentation. Additionally, possible new types of pyrolysis products were searched for.

The same lignin pyrolysis products were detected for all samples, even including the fecal controls (Table 3). This indicates that the microbiota had already been exposed to lignin-containing food. There were no signs of formation of new lignin-based pyrolysis products from polymeric lignin after incubation with fecal microbiota. New demethylated guaiacyl units were expected to be formed from the polymeric lignin, as numerous demethylated lignin-based low molecular weight metabolites have been detected for both P-AEF[6] and INS.[7] A small amount of a catechol (not quantified due to the low amount), but not 4-methylcatechol, was detected in INS by Py-GC/MS. Due to its low concentration, the catechol compound was not detectable anymore from the fecal samples with INS. The fecal microbiota could not demethylate the polymeric lignin, but was probably capable of altering the monomeric phenolic compounds released from lignin during fermentation.[6,7] This indicates that extracellular enzymes hydrolyze lignin to smaller phenolic units, which are further metabolized by microbial inoculum. Large lignin molecules cannot be extensively metabolized by the microbial inoculum.

The distributions of guaiacyl- and syringyl-type pyrolysis products and ferulic and *p*-coumaric acid before and after fermentation of P-AEF and INS were compared with the fecal controls (Table 3). Guaiacyl units were enriched in fermentation, but clearly more in the fecal controls than in the actual samples. Variations in the syringyl units were lower. The S/G ratio was similar before and after fermentation for all samples.

Due to difficulties in monitoring the changes in BSG lignin caused by the microbiota, the Py-GC/MS data were subjected to PCA. Two principal components of the data were able to describe 90% of the total variance. The first component described the highest variance (62%) and the second component the second highest variance (28%) of the data. The obtained score plot is the map of the samples (Figure 4), which are explained by the lignin degradation products (Table 3).

Distribution of the samples in different positions in score plot suggests that the samples and controls slightly differed from each other. Samples before (0 h) and after (24 h) fermentation were placed in different positions of the score plot, indicating that some changes in lignin structure took place during fermentation. In the first component direction, the main changes were observed in P-AEF and its control. The distance between samples before and after fermentation was the same for both samples (P-AEF-FC1 and FC1), indicating that similar changes occurred between lignin structures of P-AEF and the respective control. However, the second component showed higher variation in P-AEF-FC1 than in the respective control (FC1), suggesting that the microbiota was able to alter the P-AEF lignin structure to a some extent. This result is consistent

DOI: 10.1021/acs.jafc.5b05535
J. Agric. Food Chem. 2016, 64, 812−820

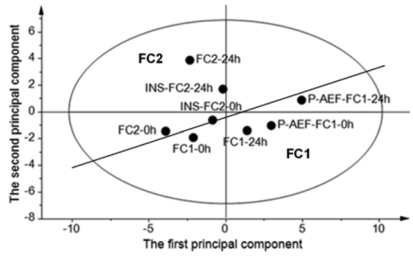

Figure 4. PCA of the pyrolysis data for lignin-rich fractions of BSG (soluble P-AEF and insoluble INS fractions after the enzymatic hydrolysis) and fecal controls (FC1 and FC2) before (0 h) and after (24 h) fermentation in the in vitro colon model. The score plot of the two principal components shows how the samples are related to each other on the basis of the Py-GC/MS data presented in Table 3.

with previous research showing the release of low molecular weight lignin-related compounds from P-AEF,[6] as the structure of the remaining, polymeric P-AEF lignin was changed in the colon model. The observed changes in INS-FC2 were smaller than in the respective control FC2. INS was enriched with recalcitrant cell wall polysaccharides[7] that were most probably cross-linked to lignin via ferulates. It contained also a high proportion of *p*-coumarates that were assumed to acylate the γ-OH of the lignin side chain and especially condensed lignin structures.[13] These properties create structural limitations for enzymatic degradation of the matrix, which may have hindered the microbial conversion of lignin in INS fraction.

Py/TMAH was used to confirm the results obtained by Py-GC/MS, especially the ratio of *p*-coumaric and ferulic acid. Only fermented lignin-rich fractions were analyzed. There were no significant changes in *p*-CA/FA or S/G ratios during fermentation (Table 4). Small changes were seen in the lignin composition before and after fermentation for both P-AEF and INS. The changes were similar to those seen in Py-GC/MS. Also, TMAH/Py results before and after fermentation of BSG lignin-rich fractions were evaluated using PCA. Two principal components of the data were able to describe 96% of the total variance. The first component described the highest variance (74%) and the second component the second highest variance (22%) of the data seen in score plot (Figure 5). On the basis of

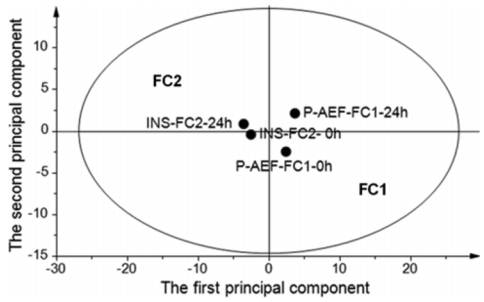

Figure 5. PCA of the pyrolysis data for lignin-rich fractions of BSG (soluble P-AEF and insoluble INS fractions after the enzymatic hydrolysis) before (0 h) and after (24 h) fermentation in the in vitro colon model. The score plot of the two principal components shows how the samples are related to each other on the basis of the TMAH/Py data presented in Table 4.

the PCA results, there were some changes in lignin composition of the P-AEF as samples before and after fermentation were placed in different positions, whereas lignin in INS seemed to be unaffected by microbiota, indicated by the same position of samples in the score plot before and after fermentation.

In conclusion, lignin fractions (P-AEF, INS, AL, and EMAL) isolated from BSG with different methods varied from one another in terms of yield, purity, and lignin structure. Yield of fractions remained low in EMAL due to poor solubility of lignin, whereas in P-AEF and AL lignin was solubilized, but it

Table 4. Relative Molar Abundance of Aromatic Degradation Products Formed from Lignin and *p*-Coumaric Acid and Ferulic Acid in Py/TMAH before and after Fermentation of Lignin-rich Fractions P-AEF and INS in the in Vitro Colon Model

compound	orig	M_w	P-AEF-FC1 0 h	P-AEF-FC1 24 h	INS-FC2 0 h	INS-FC2 24 h
1,2-dimethoxybenzene	G	138	1.0	2.2	0.0	0.0
1,2-dimethoxytoluene	G	152	5.1	5.8	0.0	0.0
3,4-dimethoxybenzaldehyde	G	166	11.5	12.8	11.4	10.7
3,4-dimethoxybenzoic acid methyl ester	G	196	11.5	8.8	4.2	3.1
3,4-dimethoxybenzeneacetic acid methyl ester	G	210	1.2	1.0	0.8	0.6
cis-1-(3,4-dimethoxyphenyl)-2-methoxyethene	G	194	0.5	0.7	0.0	0.0
trans-1-(3,4-dimethoxyphenyl)-2-methoxyethene	G	194	0.8	0.6	1.6	2.4
1-(3,4-dimethoxyphenyl)-1-methoxyprop-1-ene	G	208	1.8	3.2	2.7	3.1
erythro-4-(1,2-dimethoxypropyl)-1,2-dimethoxybenzene	G	270	1.9	1.3	1.1	1.0
3,4,5-trimethoxybenzaldehyde	S	196	7.1	7.3	5.9	5.5
3,4,5-trimethoxybenzoic acid methyl ester	S	226	11.7	13.6	6.4	7.5
cis-1-(3,4,5-trimethoxyphenyl)-2-methoxyethene	S	224	0.0	0.0	1.7	2.5
erythro-4-(1,2-dimethoxypropyl)-1,2,3-trimethoxybenzene	S	300	1.0	1.4	0.6	0.9
trans-3-(4-methoxyphenyl)-3-propenoic acid methyl ester	*p*-CA	192	11.5	10.8	25.4	25.1
cis-3-(3,4-dimethoxyphenyl)-3-propenoic acid methyl ester	FA	222	2.2	2.1	2.7	2.9
trans-3-(3,4-dimethoxyphenyl)-3-propenoic acid methyl ester	FA	222	31.3	28.6	35.5	34.8
S/G			0.6	0.6	0.7	0.8
p-CA/FA			0.3	0.4	0.7	0.7

DOI: 10.1021/acs.jafc.5b05535
J. Agric. Food Chem. 2016, 64, 812−820

was poorly precipitable. Due to the complexity of BSG structure, removal of protein and carbohydrates from lignin fractions was not totally complete by any of the methods applied. Acylation of the γ-OH group was suggested to be the reason for the lack of sinapyl alcohol detection in Py-GC/MS, as such structures degrade via formation of unsaturated side chain and loss of oxygen. More precise information on lignin structure and S/G ratios in this sense was obtained with Py/TMAH, which showed that the original BSG and all isolated lignins contained high amounts of both syringyl- and guaiacyl-type degradation products probably derived from β-O-4-linked lignin. In vitro colon model fermentation showed that the structure of more soluble P-AEF was slightly altered by microbial conversions, whereas lignin in the more recalcitrant INS remained intact.

AUTHOR INFORMATION

Corresponding Author

*(T.O.) Phone: +358 40 570 9322. Fax: +358 20 722 7026. E-mail: taina.ohra-aho@vtt.fi.

Funding

Financial supports from the Academy of Finland (Project *Lignin Fiber*, 133091) and COST Action FP0602 (*Biotechnology for Lignocellulose Biorefineries*) are gratefully acknowledged

Notes

The authors declare no competing financial interest.

ACKNOWLEDGMENTS

We thank Luca Zoia and Eeva-Liisa Tolppa for guidance with preparation of AL and EMAL samples and Eila Turunen for performing the technical work in the Py-GC/MS experiments of lignin fractions.

REFERENCES

(1) Xiros, C.; Christakopoulos, P. Biotechnological potential of brewers spent grain and its recent applications. *Waste Biomass Valorization* **2012**, *3*, 213−232.

(2) Robertson, J. A.; I'Anson, K. J. A.; Treimo, J.; Faulds, C. B.; Brocklehurst, T. F.; Eijsink, V. G. H.; Waldron, K. W. Profiling brewers' spent grain for composition and microbial ecology at the site of production. *LWT−Food Sci. Technol.* **2010**, *43*, 890−896.

(3) Musatto, S. I.; Dragone, G.; Roberto, I. C. A review. Brewers' spent grain: generation, characteristics and potential applications. *J. Cereal Sci.* **2006**, *43*, 1−14.

(4) Silanikove, N.; Brosh, A. Lignocellulose degradation and subsequent metabolism of lignin fermentation products by the desert black Bedouin goat fed on wheat straw as a single-component diet. Br. *Br. J. Nutr.* **1989**, *62*, 509.

(5) Begum, A. N.; Nicolle, C.; Mila, I.; Lapierre, C.; Nagano, K.; Fukushima, K.; Heinonen, S.; Adlercreutz, H.; Rémésy, C.; Scalbert, A. Dietary lignins are precursors of mammalian lignans in rats. *J. Nutr.* **2004**, *134*, 120−127.

(6) Niemi, P.; Aura, A.-M.; Maukkonen, J.; Smeds, A.; Mattila, I.; Niemelä, K.; Tamminen, T.; Faulds, C. B.; Buchert, J.; Poutanen, K. Interactions of a lignin-rich fraction from brewer's spent grain with gut microbiota in vitro. *J. Agric. Food Chem.* **2013**, *61*, 6754−6762.

(7) Aura, A.-M.; Niemi, P.; Mattila, I.; Niemelä, K.; Smeds, A.; Tamminen, T.; Faulds, C. B.; Buchert, J.; Poutanen, K. Release of small phenolic compounds from brewer's spent grain and its lignin fractions by human intestinal microbiota in vitro. *J. Agric. Food Chem.* **2013**, *61*, 9744−9753.

(8) Aura, A.-M.; Mattila, I.; Hyötyläinen, T.; Gopalacharyulu, P.; Cheynier, V.; Souquet, J.; Bes, M.; Le Bourvellec, C.; Guyot, S.; Orešič, M. Characterization of microbial metabolism of Syrah grape products in an in vitro colon model using targeted and non-targeted analytical approaches. *Eur. J. Nutr.* **2013**, *52*, 833−846.

(9) Pietinen, P.; Stumpf, K.; Männistö, S.; Kataja, V.; Uusitupa, M.; Adlercreutz, H. Serum enterolactone and risk of breast cancer: a case-control study in eastern Finland. *Cancer Epidemiol. Biomarkers Prev.* **2001**, *10*, 339−344.

(10) Vanharanta, M.; Voutilainen, S.; Lakka, T. A.; van der Lee, M.; Adlercreutz, H.; Salonen, J. T. Risk of acute coronary events according to serum concentrations of enterolactone: a prospective population-based case-control study. *Lancet* **1999**, *354*, 2112−2115.

(11) Funk, C.; Braune, A.; Grabber, J. H.; Steinhart, H.; Bunzel, M. Model studies of lignified fiber fermentation by human fecal microbiota and its impact on heterocyclic aromatic amine adsorption. *Mutat. Res., Fundam. Mol. Mech. Mutagen.* **2007**, *624*, 41−48.

(12) Vitaglione, P.; Napolitano, A.; Fogliano, V. Cereal dietary fibre: a natural functional ingredient to deliver phenolic compounds into the gut. *Trends Food Sci. Technol.* **2008**, *19*, 451−463.

(13) Rencoret, J.; Prinsen, P.; Gutiérrez, A.; Martínez, Á. T.; del Río, J. C. Isolation and structural characterisation of the milled wood lignin, dioxane lignin, and cellulolytic lignin preparations from brewer's spent grain. *J. Agric. Food Chem.* **2015**, *63*, 603−613.

(14) Niemi, P.; Tamminen, T.; Smeds, A.; Viljanen, K.; Ohra-aho, T.; Holopainen-Mantila, U.; Faulds, C. B.; Poutanen, K.; Buchert, J. Characterisation of lipids and lignans in brewer's spent grain and its enzymatically extracted fraction. *J. Agric. Food Chem.* **2012**, *60*, 9910−9917.

(15) Gellerstedt, G.; Pranda, J.; Lindfors, E. L. Structural and molecular properties of residual birch kraft lignin. *J. Wood Chem. Technol.* **1994**, *14*, 467−482.

(16) Guerra, A.; Filpponen, I.; Lucia, L. A.; Saquing, C.; Baumberger, S.; Argyropoulos, D. S. Toward a better understanding of the lignin isolation process from wood. *J. Agric. Food Chem.* **2006**, *54*, 5939−5947.

(17) Barry, J.-L.; Hoebler, C.; MacFarlane, G. T.; MacFarlane, S.; Mathers, J. C.; Reed, K. A.; Mortensen, P. B.; Nordgaard, I.; Rowland, I. R.; Rumney, C. J. Estimation of the fermentability of dietary fibre in vitro: a European inerlaboratory study. *Br. J. Nutr.* **1995**, *74*, 303−322.

(18) Faix, O.; Meier, D.; Fortmann, I. Thermal degradation products of wood. *Holz Roh-Werkst.* **1990**, *48*, 351−354.

(19) Ralph, J.; Hatfield, R. D. Pyrolysis-GC-MS characterization of forage materials. *J. Agric. Food Chem.* **1991**, *39*, 1426−1437.

(20) Hardell, H.-L.; Nilvebrant, N.-O. Analytical pyrolysis of spruce milled wood lignins in the presence of tetramethylammonium hydroxide. *Nord. Pulp Pap. Res. J.* **1996**, *11*, 121−126.

(21) Kuroda, K-i. Electron-impact (EI) mass spectra of 1,2-dimethoxybenzenes related to the pyrolysis products of guaiacyl lignin in the presences of tetramethylammonium hydroxide (TMAH). *J. Anal. Appl. Pyrolysis* **2002**, *64*, 433−451.

(22) Ohra-aho, T.; Gomes, F.; Colodette, J.; Tamminen, T. S/G ratio and lignin structure among *Eucalyptus* hybrids determined by Py-GC−MS and nitrobenzene oxidation. *J. Anal. Appl. Pyrolysis* **2013**, *101*, 166−171.

(23) Kuroda, K-i.; Suzuki, A.; Kato, M.; Imai, K. Analysis of rice (*Oryza sativa* L.) lignin in pyrolysis-gas chromatography. *J. Anal. Appl. Pyrolysis* **1995**, *34*, 1−12.

(24) Blokker, P.; Boelen, P.; Broekman, R.; Rozema, J. The occurrence of *p*-coumaric acid and ferulic acid in fossil plant materials and their use as UV-proxy. *Plant Ecol.* **2006**, *182*, 197−207.

(25) del Río, J. C.; Gutiérrez, A.; Rodríguez, I. M.; Ibarra, D.; Martínez, A. T. Composition of non-woody plant lignins and cinnamic acids by Py-GC/MS, Py/TMAH and FT-IR. *J. Anal. Appl. Pyrolysis* **2007**, *79*, 39−46.

(26) Hernanz, D.; Nuñez, V.; Sancho, A. I.; Faulds, C. B.; Williamson, G.; Bartolomé, B.; Gómez-Cordovés, C. Hydroxycinnamic acids and ferulic acid dehydrodimers in barley and processed barley. *J. Agric. Food Chem.* **2001**, *49*, 4884−4888.

(27) Kleen, M.; Ohra-aho, T.; Tamminen, T. On the interaction of HBT with pulp lignin during mediated laccase delignification a study

DOI: 10.1021/acs.jafc.5b05535
J. Agric. Food Chem. 2016, 64, 812−820

using fractionated pyrolysis-GC/MS. *J. Anal. Appl. Pyrolysis* **2003**, *70*, 589−600.
(28) Nakagawa-izumi, A.; Kuroda, K.-I.; Ozawa, T. Thermochemolytic behavior of b−b lignin structures in the presence of tetramethylammonium hydroxide (TMAH). *Org. Geochem.* **2004**, *35*, 763−774.
(29) Kuroda, K.-I.; Nakagawa-izumi, A. Analytical pyrolysis of lignin: products stemming fromb-5 substructures. *Org. Geochem.* **2006**, *37*, 665−673.
(30) Kuroda, K-i. Analytical pyrolysis products derived from cinnamyl alcohol-end groups in lignins. *J. Anal. Appl. Pyrolysis* **2000**, *53*, 123−134.
(31) Ralph, J.; Lu, F. The DFRC method for lignin analysis. 6. A simple modification for identifying natural acetates on lignins. *J. Agric. Food Chem.* **1998**, *46*, 4616−4619.
(32) Rencorent, J.; Ralph, J.; Marques, G.; Gutiérrez, A.; Martínez, Á. T.; del Río, J. C. Structural characterization of lignin isolated from coconut (*Cocos nucifera*) coir fibers. *J. Agric. Food Chem.* **2013**, *61*, 2434−2445.
(33) Moldoveanu, S. C. The chemistry of the pyrolytic process. In *Pyrolysis of Organic Molecules with Applications to Health and Environmental Issues*, 1st ed.; Elsevier: Oxford, UK, 2010; Vol. 28, pp 7−48.
(34) Ralph, J. Hydroxycinnamates in lignification. *Phytochem. Rev.* **2010**, *9*, 65−83.
(35) Challinor, J. M. A pyrolysis-derivatisation-gas chromatography technique for the structural elucidation of some synthetic polymers. *J. Anal. Appl. Pyrolysis* **1989**, *16*, 323−333.
(36) del Rıo, J. C.; Martin, F.; Gonzalez-Vila, F. J. Thermally assisted hydrolysis and alkylation as a novel pyrolytic approach for the structural characterization of natural biopolymers and geomacromolecules. *TrAC, Trends Anal. Chem.* **1996**, *15*, 70−79.
(37) Jacquet, G.; Pollet, B.; Lapierre, C.; Mhamdi, F.; Rolando, C. New ether-linked ferulic acid-coniferyl alcohol dimers identified in grass straws. *J. Agric. Food Chem.* **1995**, *43*, 2746−2751.
(38) Jääskeläinen, A. S.; Sun, Y.; Argyropoulos, D. S.; Tamminen, T.; Hortling, H. The effect of isolation method on the chemical structre of residual lignin. *Wood Sci. Technol.* **2003**, *37*, 91−102.
(39) Kuroda, K.-I.; Nakagawa-izumi, A. Tetramethylammonium hydroxide (TMAH) thermochemolysis of lignin: Improvement of the distribution profile of products derived from b-aryl ether subunits. *J. Anal. Appl. Pyrolysis* **2006**, *75*, 104−111.

DOI: 10.1021/acs.jafc.5b05535
J. Agric. Food Chem. 2016, 64, 812−820

VI

Ohra-aho T., Gomes F.J.B., Colodette J.L., Tamminen T. Carbohydrate composition in Eucalyptus wood and pulps – comparison between Py-GC/MS and acid hydrolysis. Accepted for publication to *J.Anal Appl. Pyrolysis.*

Carbohydrate composition in Eucalyptus wood and pulps - comparison between Py-GC/MS and acid hydrolysis

[1]T. Ohra-aho*, [2]F.J.B. Gomes, [2]J.L. Colodette, [1]T. Tamminen

[1]*VTT-Technical Research Centre of Finland, P.O. Box 1000, FI-02044 VTT, Finland*

[2] *Department of Forest Engineering, Federal University of Viçosa, 36570-000,Viçosa, Brazil*

**Corresponding author: Tel. +358 40 570 9322; fax.: +358 20 722 7026; E-mail address: taina.ohra-aho@vtt.fi*

Abstract

In analytical pyrolysis, carbohydrates are degraded into stable anhydrosugars, which are analyzed by GC/MS. The benefit of Py-GC/MS is that fiber composition including carbohydrates, lignin and its S/G ratio can be determined simultaneously from fiber-based materials without need of extensive pretreatment, contrary to the traditional method. In this study, the relative carbohydrate composition of various *Eucalyptus* species was determined by Py-GC/MS. In addition, pulps produced from the same species by soda-AQ and soda-O_2 processes were analyzed similarly. The results were compared with those obtained by acid hydrolysis followed by HPLC. This comparison showed that the relative carbohydrate composition determined by Py-GC/MS for the wood samples differed from the values obtained by acid hydrolysis. Significantly better correlation between the two methods was observed for the pulp samples cooked to varying kappa number levels. Fractionated pyrolysis was applied in order to find explanation to the observed difference in the degradation behavior of carbohydrates in wood and pulp samples. Due to the close association of lignin and carbohydrates, the thermal behavior of lignin was followed as well. The results showed that the thermal behavior of xylan and cellulose differed in the wood samples, but were almost equal in the pulp samples. Thermal degradation of xylan was similar with lignin in both sample types. Similar thermal behavior between the components is a prerequisite for reliable Py-GC/MS analysis. Therefore, this method cannot be recommended for the comparison of carbohydrate compositions between different wood raw materials. However, it is applicable to pulp samples and may find application in research for profiling carbohydrate compositional changes with processing methods and conditions.

Keywords: Eucalyptus wood, pulp, carbohydrate composition, Py-GC/MS, acid hydrolysis, fractionated pyrolysis

1 Introduction

Eucalyptus wood is increasingly used for pulp production especially in tropical zones due to its fast growth rate. Chemical composition of wood varies between different wood species and clones as well as habitat and age of the wood. Characterisation of wood fibre components, i.e. lignin, cellulose and hemicelluloses, is important in order to understand wood behaviour during chemical and mechanical treatments as well as quality of final pulp products [1]. Traditional way to determine carbohydrate composition together with lignin content from fibre-based material is acid hydrolysis. After acid hydrolysis with sulphuric acid, carbohydrate monomers can be determined by High Performance Liquid Chromatography (HPLC). From the same solution, acid-soluble lignin can be determined by UV-Vis spectrometer. The total amount of lignin is the sum of acid insoluble material, so-called Klason lignin, and the acid-soluble lignin [2]. Analytical pyrolysis combined with gas chromatography and mass spectrometry (Py-GC/MS) provides a method for simultaneous determination of lignin and carbohydrates from fibre-based materials from small sample amounts [3–7]. Additional benefit of the method is that pre-treatment like extractives removal from the studied material is not needed [8]. Before acid hydrolysis, extractives removal is essential, due to the possible condensation reactions of lignin and extractives.

Eucalyptus wood polysaccharides comprise mainly of cellulose and xylan, but minor amount of glucomannan is present as well. In comparison to cellulose, hemicelluloses have lower molecular weight and may be branched. Hardwood xylans contain 4-O-methylglucuronic acid side groups and are highly substituted by O-acetyl groups. In addition, xylan is linked with lignin [9-10]. Xylan, similarly to other hemicelluloses, is thermally less stable than cellulose. The side groups present in xylan also lower the thermal stability [11]. In pyrolysis, hemicelluloses together with cellulose are degraded to a significant degree to anhydrosugars, such as 1,6-anhydromannopyranose, 1,6-anhydrogalactopyranose, 1,6-anhydroglucopyranose (levoglucosan), 1,5-anhydroarabinofuranose and 1,4-anhydroxylopyranose. Also significant amounts of pyrans, furans, light oxygenates and

gases are formed [4,11–13]. Their yields are highly dependent on the lignocellulosic material, pyrolysis temperature [11], and present of trace amounts of metals, especially in the case of pulp samples [14–16]. Due to the incomplete formation of anhydrosugars, Py-GC/MS is typically used for qualitative analysis rather than quantitation. However, the relative carbohydrate composition determined from Kraft pulps by Py-GC/MS has been found to correlate well with the results obtained by traditional wet chemical methods [15–17], but information is lacking about the applicability of Py-GC/MS for the analysis of wood feedstocks in a similar manner as pulps.

The aim of this study was to evaluate the applicability of Py-GC/MS for the determination of the relative carbohydrate composition of *Eucalyptus* wood species. The lignin composition and S/G ratio of these samples has been determined earlier by the same method [18]. The hypothesis was thus that further analysis of the same pyrolysis runs of *Eucalyptus* wood species would provide information also about the polysaccharide component of the samples. Thus, Py-GC/MS could be used as an optional method for the determination of lignin and carbohydrate composition together with the S/G ratio. For the method evaluation, two types of eucalypt pulps from different cooking stages were subjected to the same method comparison as the wood samples. Finally, the thermal behaviour of the polysaccharide components in the wood and pulp matrices was studied using fractionated pyrolysis by increasing the pyrolysis temperature stepwise [19].

2 Material and methods

2.1 Sample preparation

Eighteen 7-year-old *Eucalyptus* species, including a number of double/triple/fourth crossings among *E. grandis, E. urophylla, E. globulus, E. dunnii* and *E. camaldulensis* were obtained from the Brazilian Network of *Eucalyptus* Genome Research – Genolyptus. Detailed list of the eucalypt hybrids is presented in the **Table 1**. For the carbohydrate analysis by acid hydrolysis, wood chips were screened, refined and extracted as described in [18]. For Py-GC/MS analysis, the eucalypt

chips were Wiley milled, but extractives were not removed.

Soda-O_2 and soda-AQ pulps of eucalypt hybrid G1xUGL (*E. grandis* (Coffs Harbour) x [*E. urophylla* (R) x *E. globulus* (R)]) at different degrees of delignification (kappa values 50, 35 and 15) were prepared in a Brazilian pulp mill laboratory, using an M&K digester (USA). Before Py-GC/MS analysis, the pulps were washed with calcium rich tap water to replace alkaline metals to calcium ions according to a method described elsewhere [15], and thereafter dried and Wiley milled.

2.2 Acid hydrolysis

Carbohydrate composition was determined by HPLC with Pulse Amperometric Detection (HPAEC-PAD) after pre-treatment (30°C, 1 h) of the materials with 72% H_2SO_4 followed by hydrolysis with 3% H_2SO_4 in an autoclave (120°C, 1 h). HPAEC-PAD was carried out by Dionex ICS-3000 system equipped with a CarboPac PA1 (250 x 4mm) analytical column. The monosaccharides were separated isocratically with 0.001 M NaOH (45 min, flow rate 1 mL/min) according to Wallis et al. [20]. For the comparison with Py-GC/MS data, the relative carbohydrate content was calculated by normalization to 100 %. The mean deviation percentages of the two parallel measurements of wood samples for the glucose, xylose, mannose, galactose and arabinose were 4 %, 2 %, 6 %, 3 % and 4 %, respectively. The mean distribution percentage of the parallel measurements of pulp samples for the xylose and glucose were 0.8 % and 0.1 %, respectively.

2.3. Py-GC/MS

Both isothermal and fractionated Py-GC/MS measurements were performed with a filament pulse pyrolyzer (Pyrola2000, PyrolAB, Sweden), which was connected to a GC/MS instrument (Varian 3800 GC/2000 MS). The detailed description of the isothermal pyrolysis at 580°C for 2s is described elsewhere [18]. The conditions used for the fractionated pyrolysis were based on our previous study [21], with some modification of temperatures and time. Fractionated pyrolysis was

performed at temperatures of 320, 450, 580 and 800 °C for 44, 16, 4, and 2 s, respectively. Both in the isothermal and the fractionated pyrolysis GC/MS conditions were the same. In the case of isothermal and fractionated pyrolysis, 70-100 μg of the sample was weighed accurately and transferred on the filament. After that, the pyrolysis degradation products were led with carrier gas into a gas chromatography capillary column for separation (J&W, DB-1701, 30 m x 0.25 mm, film 1 μm). The degradation products were detected using ion trap mass spectrometry with the mass scan range of m/z 46-399 (EI 70 eV). Carbohydrate pyrolysis products were identified using data from the literature [4,22]. The identities of carbohydrate degradation products used for the calculation are shown in Table 2. The anhydrosugars were integrated form total ion chromatograms, except for 1,6-anhydrogalactopyranose (g). Due to the low content of 1,6-anhydrogalactopyranose (g) the peak area was integrated using selected main ion 60. Its peak area was converted to the total peak area using factor 4.2 (calculated from the mass spectrum of the pure compound). The relative monosaccharide composition was calculated after the normalization of peak areas of anhydrosugars to 100 %. Anhydrosugars 1,5-anhydroarabinofuranose (c) and 1,6-anhydrogalactopyranose (g) were used to calculate arabinose and galactose, respectively. Two degradation products 1,5-anhydro-4-deoxypent-1-en-3-ulose (a) and 1,4-anhydroxylopyranose (f) were used to determine xylose, whereas glucose was determined in two ways using only 1,6-anhydroglucopyranose (i) (method A) or using four main degradation products of cellulose 1,6-anhydroglucopyranose (i), 5-hydroxymethyl-2-tetrahydofuraldehyde-3-one (b), 5-hydroxymethyl-2-furaldehyde (d) and 1.4-dideoxy-D-*glycero*-hex-1-enopyranos-3-ulose (e) (method B). Average of two and three parallel measurements was calculated for the Eucalypt hybrids and pulps, respectively. In case of wood samples, the mean error percentages of xylose, arabinose and galactose were 8 %, 20 %, and 40 %, respectively. The mean error percentage of glucose was 6 % when the content was calculated using only 1,6-anhydroglucopyranose (method A) and 4 % when the four main degradation products of cellulose (1,6-anhydroglucopyranose, 5-hydroxymethyl-2-tetrahydofuraldehyde-3-one, 5-

hydroxymethyl-2-furaldehyde and 1.4-dideoxy-D-*glycero*-hex-1-enopyranos-3-ulose) were included to the glucose content calculation (method B). Mannose was not detected. For the pulps, the average standard deviation percentage of xylose was 4 %. For glucose, the average standard deviations were 2 % and 0.4 % using only one degradation product (method A) and the four main cellulose degradation products (method B), respectively. Lignin degradation products were integrated from the fractionated pyrolysis data according to our previous publications [18,21].

3. Results and discussion

The pyrogram profiles of the eucalypt hybrids were all alike. As an example, the pyrograms of eucalypt hybrid G1xUGL (*E. grandis* (Coffs Harbour) x [*E. urophylla* (R) x *E. globulus* (R)]) wood and Kraft pulp from the same wood species are shown in **Fig. 1** and identities of degradation product of cellulose and hemicelluloses are shown in **Table 2**. The main degradation products of cellulose are marked in the pyrogram with letters b, d, e and i and main degradation products of hemicelluloses with letters a, c, f, g and h. For the pulps, increasing intensity of cellulose products (b, d, e, i) were observed directly from the pyrograms as a function of the progress of cooking. Only xylose of all hemicelluloses was present in the final pulps. The most abundant unmarked peaks in the wood samples were lignin pyrolysis degradation products. Their intensity was decreased radically during cooking. Lignin composition and S/G ratio of the same samples have been presented in our previous paper [18].

3.1 Carbohydrate composition in eucalypt hybrids

The comparison among Py-GC/MS and acid hydrolysis methods for the carbohydrate composition analysis of *Eucalyptus* woods is shown in **Fig. 2**. When only 1,6-anhydroglucopyranose was used for the calculation of the relative glucose content (method A) glucose and xylose varied between 51.3–64.1 % and 33.0–46.5 %, respectively. The corresponding values obtained by acid hydrolysis

were 74.1–78.6 % and 16.7–22.6 %. The contents were also calculated using 1,6-anhydroglucopyranose together with three other pyrolysis degradation product of cellulose (method B): 5-hydroxymethyl-2-tetrahydofuraldehyde-3-one (b), 5-hydroxymethyl-2-furaldehyde (d) and 1.4-dideoxy-D-*glycero*-hex-1-enopyranos-3-ulose (e). The values 67.9–78.2% for glucose and 19.4–30.6% for xylose obtained by this calculation method were closer to the acid hydrolysis values. The range on glucose and xylose content among the *Eucalyptus* species was same with both Py-GC/MS methods (A and B). This indicates that the changes on carbohydrate composition among samples can be followed either including only 1,6-anhydroglucopyranose (method A) or alternatively including all four main cellulose pyrolysis derivatives (method B). The latter method can be used only when the sample contains low amount of galactoglucomannan or glucomannan [5], such as eucalypt wood. **Fig. 3** shows that the correlation between the Py-GC/MS and acid hydrolysis methods is poor for glucose and xylose in the case of wood samples. The same was detected also for the minor constituent's arabinose and galactose (not shown).

3.2 Carbohydrate composition in eucalypt pulps

Similar Py-GC/MS conditions as used in the present study have earlier been used to determine the relative carbohydrate composition from pulp samples. The correlation between Py-GC/MS and acid hydrolysis for the pulps has been reported to be good [15–17]. Thus, the method seems to work for pulps better than for wood samples. In order to confirm that hypothesis, two different types of pulps, soda-AQ and soda-O_2, were cooked to different stages from the same raw material (*E. grandis (Coffs Harbour) x [E. urophylla (R) x E. globulus (R)]* and analyzed by Py-GC/MS and acid hydrolysis. Only the relative contents of glucose and xylose were followed, as the other hemicelluloses were mainly dissolved during cooking. The Py-GC/MS results were calculated using the two methods, method A and method B, described above for the wood samples. When only 1,6-anhydroglucopyranose was included to the relative carbohydrate composition (method A), both xylose and glucose contents were closer to the values obtained by acid hydrolysis compared to

method B (**Fig. 4**), in accordance with the earlier studies [9] but opposite to what was detected for the wood samples. In addition, good correlation among Py-GC/MS and acid hydrolysis results was seen (**Fig. 4**). This result is consistent with earlier reports [15–17]. The correlation was even better when the different types of pulps (soda-AQ and soda-O_2) were followed separately. Based on the result, Py-GC/MS seems to be suitable for the comparison of carbohydrate compositions between pulps originating from the same process type. The correlation between Py-GC/MS and acid hydrolysis was better by method B, but the absolute values were closer by using only 1,6-anhydroglucopyranose (method A).

The differences observed for the wood and pulp samples indicate that the degradation behavior of cellulose and hemicelluloses are different for the two types of samples. Possible reasons for this are differences in xylan structure due to cooking, such as release of acetyl and uronic acid groups. Delignification during cooking affects also xylan as it is partially linked with lignin. In the pulp samples analysed, lignin has mainly been dissolved [9]. In order to clarify the influence of cooking and lignin content to the thermal degradation behavior of carbohydrates in pyrolysis, two eucalypt hybrids and one pulp samples were analyzed by using fractionated pyrolysis.

3.3 Thermal degradation behavior of carbohydrates

Eucalypt hybrid G1xUGL and soda-O_2 pulp (kappa 15), cooked from the same raw material were selected for the fractionated pyrolysis. The second Eucalypt hybrid C1xUGL was selected due to the high difference of glucose and xylose contents among the methods. The fractionated pyrolysis results of the carbohydrates were calculated only by method B (including all cellulose-related degradation products). Because carbohydrates are linked with lignin both in wood and pulp [10], the degradation behavior of lignin was followed by fractionated pyrolysis together with carbohydrates.

In the case of wood samples, the degradation products of xylan were determined at two temperatures 320 and 450 °C. Slightly higher proportion was detected at 450 °C (**Table 3**). Galactose was released at the same temperatures as xylose, but the proportions varied slightly

among the samples (C1xUGL and G1xUGL). Arabinose was released completely at 320 °C. Main part of glucose was released at 450 °C, but small proportion also at other temperatures 320, 580 and 800 °C. Degradation of cellulose at higher temperatures than hemicelluloses is in accordance with the results reported in the literature [11-12]. Thermal behavior of xylan was similar among wood species (G1xUGL and C1xUGL), but different in comparison to the pulp. About 99 % of xylan was released at 450 °C from the pulp and only minor part at lower temperatures. Release of acetyl and methylglucuronic acid side groups has been reported to be occur at lower temperature than the degradation of the xylan backbone [11]. Cooking releases side groups of xylan [9], which can partly explain the higher thermal stability of pulp than wood xylan. The higher thermal stability of pulp than wood xylan has earlier been verified by thermogravimetric analysis [23]. The linear pulp xylan may also interact with the cellulose surfaces, which may stabilize it further.

Lignin degrades from wood species (G1xUGL and C1xUGL) clearly at two different temperatures 320 °C and 450 °C, the higher temperature being dominant. In the case of pulp, the highest proportion of lignin, about 90 %, was released at 450 °C and clearly lower proportion, 6 % and 4 %, in the other temperatures 320 °C and 580°C, respectively. Thus, the thermal degradation behavior of lignin follows closely the behavior of xylan both in the wood and pulp samples. Also the thermal behavior of cellulose was rather similar among the wood and pulp samples. The thermal degradation behavior of all fiber components was thus close to each other in the pulp samples, but not in the wood samples, which explains the observed inconsistencies in case of wood samples.

4. Conclusions

Py-GC/MS is not recommended for the comparison between eucalypt wood samples, as the relative carbohydrate contents by Py-GC/MS were not found to correlate with the results obtained by acid hydrolysis followed by HPLC. This was shown by fractionated pyrolysis to be due to differences in the thermal degradation behaviors of the carbohydrate components in wood. However, the two

methods gave comparable results for the relative carbohydrate composition when analyzing pulp samples, in accordance with the detected similar thermal degradation behaviors of the fiber components in the case of pulps.

ACKNOWLEDGMENTS

Ms. Eila Turunen is thanked for performing the technical work in the Py-GC/MS experiments. Financial support from the Academy of Finland and Brazilian CNPq are gratefully acknowledged (Effect of fiber wall chemistry on energy demand in wood defibration, Defibre, 133276). We thank Suzano Papel e Celulose (Brazil) for providing the pulp samples from the alkaline cooking experiments.

REFERENCES

[1] H. Sixta, Handbook of pulp, WILEY-VCH Verlag GmbH & Co. KGaA, Weinheinm, 2008.

[2] TAPPI, Technical Association of the Pilp and Paper Industry, TAPPI Test Methods, 2000-2001, TAPPI, Atlanta, USA, 2000.

[3] O. Faix, D. Meier, I. Fortmann, Thermal degradation products of wood: Gas chromatographic separation and mass spectrometric characterization of monomeric lignin derived products, Holz Als Roh- Und Werkst. 48 (1990) 281–285.

[4] O. Faix, I. Fortmann, J. Bremer, D. Meier, Thermal degradation products of wood: Gas chromatographic separation and mass spectrometric characterization of polysaccharide derived products, Holz Als Roh- Und Werkst. 49 (1991) 213–219.

[5] M. Kleen, G. Gellerstedt, Characterization of chemical and mechanical pulps by pyrolysis-gas chromatography/mass spectrometry, J. Anal. Appl. Pyrolysis. 19 (1991) 139–152.

[6] J.C. del Río, A. Gutiérrez, M.J. Martínez, A.T. Martínez, Py-GC/MS study of Eucalyptus globulus wood treated with different fungi, J. Anal. Appl. Pyrolysis. 58–59 (2001) 441–452. doi:10.1016/S0165-2370(00)00184-4.

[7] A. Lourenço, J. Gominho, A.V. Marques, H. Pereira, Py-GC/MS(FID) assessed behavior of polysaccharides during kraft delignification of Eucalyptus globulus heartwood and sapwood,

J. Anal. Appl. Pyrolysis. 101 (2013) 142–149. doi:10.1016/j.jaap.2013.01.018.

[8] L.C.A. Barbosa, C.R. Maltha, V.L. Silva, J.L. Colodette, Determination of the syringyl/guaiacyl ratio in eucalyptus wood by pyrolysis-gas chromatography/mass spectrometry (Py-GC/MS), Quim. Nova. 31 (2008) 2035–2041. doi:10.1590/S0100-40422008000800023.

[9] P.C. Pinto, D. V. Evtuguin, C.P. Neto, A.J.D. Silvestre, F.M.L. Amado, Behavior of Eucalyptus globulus lignin during kraft pulping. I. Analysis by NMR, ESI/MS, and GPC, J. Wood Chem. Technol. 22 (2002) 109–125. doi:10.1081/WCT-120013356.

[10] J. Li, R. Martin-sampedro, C. Pedrazzi, G. Gellerstedt, Fractionation and characterization of lignin-carbohydrate complexes (LCCs) from eucalyptus fibers, Holzforschung. 65 (2011) 43–50. doi:10.1515/HF.2011.013.

[11] D.K. Shen, S. Gu, A. V. Bridgwater, The thermal performance of the polysaccharides extracted from hardwood: Cellulose and hemicellulose, Carbohydr. Polym. 82 (2010) 39–45. doi:10.1016/j.carbpol.2010.04.018.

[12] H. Yang, R. Yan, H. Chen, D.H. Lee, C. Zheng, Characteristics of hemicellulose, cellulose and lignin pyrolysis, Fuel. 86 (2007) 1781–1788. doi:10.1016/j.fuel.2006.12.013.

[13] S. Wu, D. Shen, J. Hu, H. Zhang, R. Xiao, Role of β-O-4 glycosidic bond on thermal degradation of cellulose, J. Anal. Appl. Pyrolysis. 119 (2016) 147–156. doi:10.1016/j.jaap.2016.03.006.

[14] J. Kelly, M. Mackey, R.J. Helleur, Quantitative analysis of saccharides in wood pulps by quartz-tube pulse pyrolysis-polar phase gas chromatography, J. Anal. Appl. Pyrolysis. 19 (1991) 150–117.

[15] M. Kleen, G. Lindblad, S. Backa, Quntification of lignin and carbohydrates in Kraft pulps using analytical pyrolysis and multivariate data analysis, J. Anal. Appl. Pyrolysis. 25 (1993) 209–227.

[16] K. Syverud, I. Leirset, D. Vaaler, Characterization of carbohydrates in chemical pulps by pyrolysis gas chromatography/mass spectrometry, J. Anal. Appl. Pyrolysis. 67 (2003) 381–391. doi:10.1016/S0165-2370(02)00076-1.

[17] J. Kelly, R. Helleur, Quantitative analysis of the major saccharides in sulfite-treated wood pulps by pyrolysis-gas chromatography: the effect of metal ions, J. Anal. Appl. Pyrolysis. 23 (1992) 153–163.

[18] T. Ohra-aho, F.J.B. Gomes, J.L. Colodette, T. Tamminen, S/G ratio and lignin structure among Eucalyptus hybrids determined by Py-GC/MS and nitrobenzene oxidation, J. Anal. Appl. Pyrolysis. 101 (2013) 166–171. doi:10.1016/j.jaap.2013.01.015.

[19] P. Selsbo, I. Ericsson, M. Kleen, Characterization of sulfur in wood pulps using pyrolysis-gas chromatography with sulfur-selective detection, J. Anal. Appl. Pyrolysis. 43 (1997) 1–14. doi:10.1016/S0165-2370(97)00055-7.

[20] A. Wallis, R. Wearne, P. Wright, Chemical Analysis of Polysaccharides in Plantation Eucalyptus Wood and Pulps, Apitta J. 49 (1996) 258–262.

[21] T. Ohra-aho, M. Tenkanen, T. Tamminen, Direct analysis of lignin and lignin-like components from softwood kraft pulp by Py-GC/MS techniques, J. Anal. Appl. Pyrolysis. 74 (2005) 123–128. doi:10.1016/j.jaap.2004.11.010.

[22] O. Faix, I. Fortmann, J. Bremer, D. Meier, Thermal degradation products of wood: A collection of electron-impact (EI) mass spectra of polysaccharide derived products, Holz Als Roh- Und Werkst. 49 (1991) 299–304.

[23] A. Oudia, E. Mészáros, R. Simões, J. Queiroz, E. Jakab, Pyrolysis-GC/MS and TG/MS study of mediated laccase biodelignification of Eucalyptus globulus kraft pulp, J. Anal. Appl. Pyrolysis. 78 (2007) 233–242. doi:10.1016/j.jaap.2006.07.003.

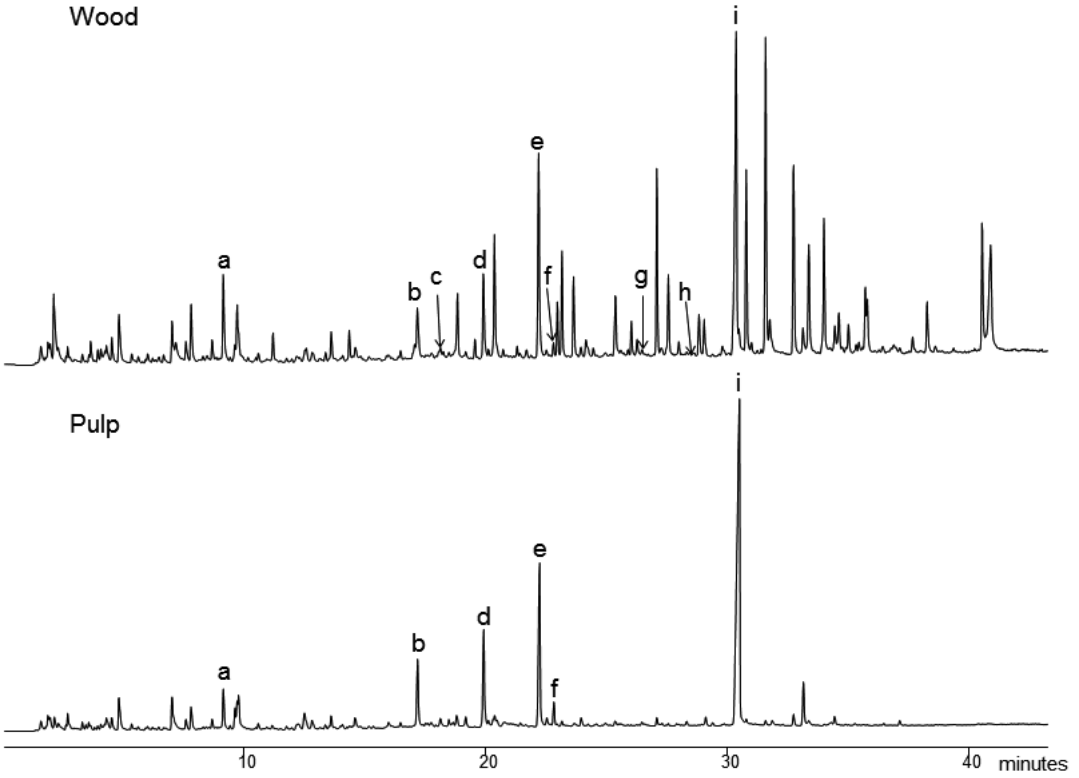

Fig. 1. Pyrograms of eucalypt hybrid G1xUGL (*E. grandis* (Coffs Harbour) x [*E. urophylla* (R) x *E. globulus* (R)]) wood and soda-O_2 pulp cooked from G1xUGL (kappa 15) obtained at 580 °C. Carbohydrate-related degradation products marked in the pyrogram are given in Table 2.

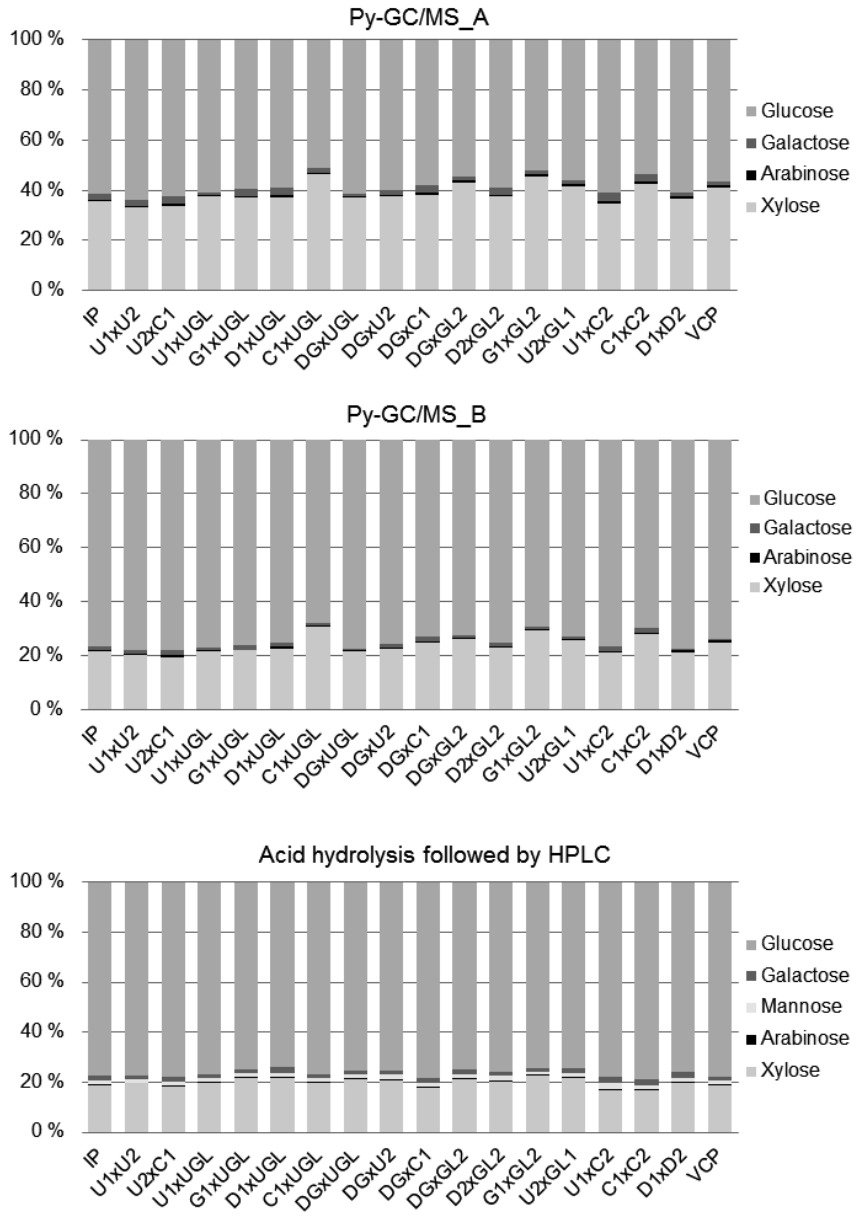

Fig. 2. Carbohydrate composition (after normalization to 100%) determined by Py-GC/MS and acid hydrolysis followed by HPLC. Py-GC/MS results has been calculated two ways A) relative glucose content calculated including only 1,6-anhydroglucopyranose B) relative glucose content calculated including 5-hydroxymethyl-2-tetrahydofuraldehyde-3-one; 5-hydroxymethyl-2-furaldehyde; 1.4-dideoxy-D-glycero-hex-1-enopyranos-3-ulose and 1,6-anhydroglucopyranose

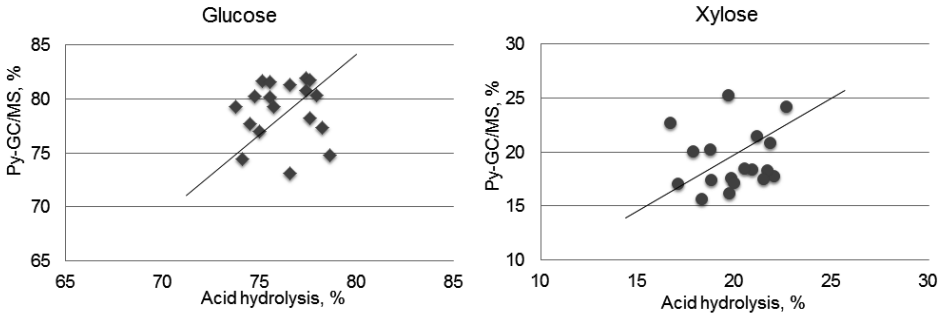

Fig. 3. Comparison of relative glucose and xylose content between Py-GC/MS and acid hydrolysis followed by HPLC from eucalypt hybrids. Relative glucose content has been calculated using method B (see Fig. 2.)

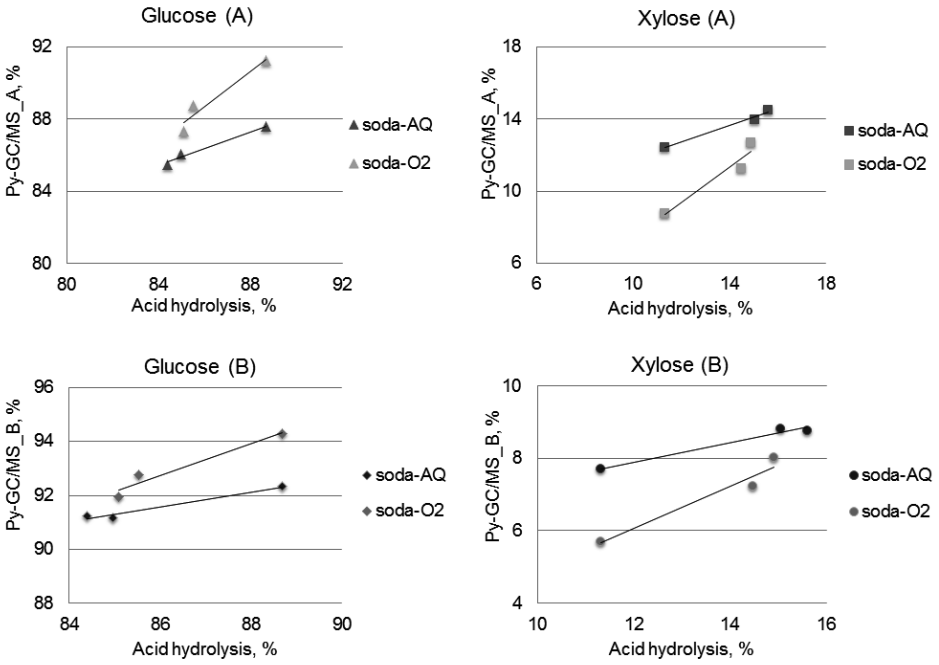

Fig. 4. Comparison of relative glucose and xylose content between Py-GC/MS and acid hydrolysis followed by HPLC from different cooking stages of soda-AQ and soda-O_2 pulps. Raw material was the same for both pulps (*E. grandis* (Coffs Harbour) x [*E. urophylla* (R) x *E. globulus* (R)]. Py-GC/MS results have been calculated using method A and B (see Fig 2.).

Table 1. Sample names and short codes

No	Eucalyptus hybrids	Short code
1	*E. urophylla (IP) x E. grandis (IP)*	IP
2	*E. urophylla (Flores IP) x E. urophylla (Timor)*	U1xU2
3	*E. urophylla (Flores IP) x E. camaldulensis(VM2)*	U1xC2
4	*E. urophylla (Flores IP) X [E. urophylla (R) x E. globulus (R)]*	U1xUGL
5	*E. grandis (Coffs Harbour) x [E. urophylla (R) x E. globulus (R)]*	G1xUGL
6	*E. dunni (R) x [E. urophylla (R) x E. globulus (R)]?*	D1xUGL
7	*E. camaldulensis (VM1) x [E. urophylla (R) x E. globulus (R)]*	C1xUGL
8	*[E. dunnii (R) x E. grandis (R)] x [E. urophylla (R) x E. globulus (R)]*	DGxUGL
9	*[E. dunnii (R) x E. grandis (R)] x E. urophylla (Timor)*	DGxU2
10	*[E. dunnii (R) x E. grandis (R)] x E. camaldulensis (VM1)*	DGxC1
11	*[E. dunnii (R) x E. grandis (R)] x E. globulus (R) (Dad, pollen)*	DGxGL2
12	*E. dunni (KR) x E. globulus (R)(Dad, pollen)*	D2xGL2
13	*E. grandis (Coffs Harbour) x E. globulus (R) (Dad, pollen)*	G1xGL2
14	*E. urophylla (Timor) x E. globulus (R)(Mom, stigma)*	U2xGL1
15	*E. urophylla (Timor) x E. camaldulensis (VM1)*	U2xC1
16	*E. camaldulensis (VM1) x E. camaldulensis (VM1)*	C1xC2
17	*E. dunni (R) x E. dunni (KR)*	D1xD2
18	*VCP - E. grandis (VCP) x E. urophylla (VCP)*	VCP

Table 2. Pyrolysis degradation products of carbohydrates. Compound letter refer the letters in **Fig. 1**

Marker	MW	Compound name	Anhydrosugar
a	114	4-hydroxy-5,6-dihydro-(2H)-pyran-2-one	xylose
b	144	5-hydroxymethyl-2-tetrahydofuraldehyde-3-one	glucose
c	132	1,5-anhydroarabinofuranose	arabinose
d	126	5-hydroxymethyl-2-furaldehyde	glucose
e	144	1.4-Dideoxy-D-glycero-hex-1-enopyranos-3-ulose	glucose
f	132	1,4-Anhydroxylopyranose	xylose
g	162	1,6-anhydrogalactopyranose	galactose
h	162	1,6-anhydromannopyranose	mannose
i	162	1,6-anhydroglucopyranose	glucose

Table 3. Thermal behavior of carbohydrates and lignin in eucalypt hybrids (C1xUGL and G1xUGL) and soda-O_2 pulp of G1xUGL (κ=15) determined by fractionated pyrolysis. Results presented as relative amount (%, after normalization to 100%) of degradation products released from carbohydrates and lignin as a function of temperature.

	C1xUGL				G1xUGL				soda-O_2 pulp of G1xUGL			
Tem., °C	320	450	580	800	320	450	580	800	320	450	580	800
Time, s	44	16	4	2	44	16	4	2	44	16	4	2
Xylose	42.9	57.1	0.0	0.0	44.1	55.9	0.0	0.0	1.3	98.7	0.0	0.0
Arabinose	100.0	0.0	0.0	0.0	100.0	0.0	0.0	0.0				
Galactose	55.4	44.6	0.0	0.0	43.3	56.7	0.0	0.0				
Glucose	2.2	97.1	0.6	0.1	2.3	97.4	0.3	<0.1	0.1	99.4	0.4	0.1
Lignin	28.2	71.1	0.7	0.1	24.2	74.7	1.0	0.1	5.9	89.8	4.2	0.2

Aalto-DD 230/2017
VTT SCIENCE 168

ISBN 978-952-60-7733-8 (printed)
ISBN 978-952-60-7734-5 (pdf)
ISSN-L 1799-4934
ISSN 1799-4934 (printed)
ISSN 1799-4942 (pdf)

978-951-38-8595-3 (printed)
978-951-38-8594-6 (pdf)
2242-119X
2242-119X (printed)
2242-1203 (pdf)

Aalto University
School of Chemical Engineering
Department of Bioproducts and Biosystems
www.aalto.fi

BUSINESS + ECONOMY

ART + DESIGN + ARCHITECTURE

SCIENCE + TECHNOLOGY

CROSSOVER

DOCTORAL DISSERTATIONS